TITLE SYNTHESIS AND STRUCTURAL STUDIES OF SOME METAL COMPLEXES OF TETRAAZA MACROCYCLIC LIGANDS

AUTHOR Philip John BAILLIE

DEGREE Ph.D

AWARDING BODY University of North London

DATE 1993

THESIS NUMBER DX180675

# SYNTHESIS AND STRUCTURAL STUDIES OF SOME METAL COMPLEXES OF TETRAAZA MACROCYCLIC LIGANDS

PHILIP JOHN BAILLIE

A thesis submitted in partial fulfilment of the requirements of the University of North London for the degree of Doctor of Philosophy

THIS RESEARCH PROGRAMME WAS CARRIED OUT IN COLLABORATION WITH JAMES COOK UNIVERSITY OF NORTH QUEENSLAND

SEPTEMBER 1993

# SYNTHESIS AND STRUCTURAL STUDIES OF SOME METAL COMPLEXES OF TETRAAZA MACROCYCLIC LIGANDS

## ABSTRACT

A series of dibenzo macrocyclic tetraamine ligands with 14-, 15-, 16-, 17- and 19-membered inner great rings ($L^{14}$ to $L^{19}$) has been synthesized to investigate the effect of ring size variation on their complexation behaviour with the metal-ions, Ni(II), Zn(II) and Cd(II).

The structures of $L^{16}$ and $L^{17}$ have been determined and are discussed in Chapter 2. A comparative study of ligand conformations and hole-sizes across a series of four macrocycles is presented. The variation of features of the $^{1}H$ and $^{13}C$ NMR spectra implies a comparatively high conformational rigidity in $L^{15}$. The $^{15}N$ NMR spectra of $L^{15}$ and $L^{17}$ indicate $^{1}H$-$^{15}N$ spin-spin coupling for the anilino, but not for the benzylamino donors, showing that the intramolecular H-bonding of the anilino protons observed in the solid state is partially retained in solution.

A comparative discussion of a range of Ni(II) complexes of the ligands is presented in Chapter 3. *X*-Ray crystallographic studies have been carried out on $[NiL^{17}Cl_2]$ and on the thiocyanate complexes of $L^{15}$, $L^{16}$ and $L^{17}$ which are compared with that of $L^{14}$. An inverse correlation between the in-plane and axial bond lengths around the Ni-atoms holds up to $L^{16}$. Complexes of $L^{16}$ and $L^{17}$ with nickel(II) nitrate have been prepared and the crystal structure of that of $L^{16}$ contains two complexes, $[NiL^{16}(NO_3)_2]$ and $[NiL^{16}(NO_3)(H_2O)]NO_3$. Cyclic voltametry shows that the formation of the Ni(III) species is facilitated by the smaller ligands; the oxidation of $[NiL^{17}Cl_2]$ is non-reversible and probably ligand-based. The visible spectra of the chloride and thiocyanate complexes have been assigned in terms of weak tetragonal-field splitting which is significant only for $L^{14}$ and $L^{15}$, the larger ligands giving essentially octahedral complexes.

A range of Cd(II) and Zn(II) complexes of $L^{16}$ and $L^{17}$ have been prepared and are discussed in Chapter 4. Crystal structure analyses of Cd(II) complexes of $L^{16}$ and $L^{17}$ have been performed. $[CdL^{16}Br]_2[CdBr_4]$ exhibits two five-co-ordinate complexes with significant differences in ligand conformation and in displacements of the Cd-atom from the donor plane. The influence of the $[CdBr_4]^{2-}$ ion on these conformations is considered. $[CdL^{17}Br_2]$ contains the Cd-atom virtually in the place of the macrocyclic donors with two axially co-ordinated Br-atoms.

The formation constants of the Zn(II) and Cd(II) complexes of the ligands have been determined in the collaborating establishment and the contribution of structural features to the thermodynamic stability of the complexes is discussed in Chapter 5. Although hole size effects predominate in the Ni(II) complexes, they are complicated by changes in co-ordination geometry across the ligand series for the Zn(II) and Cd(II) complexes.

## PREFACE

The results and conclusions presented in this thesis represent original work by the candidate unless specific reference is made to the contrary. No part of the original work has been used in submission for any other academic award.

The work described was carried out in the School of Applied Chemistry at the University of North London and (in part) at the Istituto di Chimica Generale ed Inorganica, Università di Pavia, Pavia, Italy. Collaborative work has been performed at James Cook University of North Queensland, Townsville, Australia.

# SYNTHESIS AND STRUCTURAL STUDIES OF SOME METAL COMPLEXES OF TETRAAZA MACROCYCLIC LIGANDS

## ABSTRACT

A series of dibenzo macrocyclic tetraamine ligands with 14-, 15-, 16-, 17- and 19-membered inner great rings ($L^{14}$ to $L^{19}$) has been synthesized to investigate the effect of ring size variation on their complexation behaviour with the metal-ions, Ni(II), Zn(II) and Cd(II).

The structures of $L^{16}$ and $L^{17}$ have been determined and are discussed in Chapter 2. A comparative study of ligand conformations and hole-sizes across a series of four macrocycles is presented. The variation of features of the $^{1}H$ and $^{13}C$ NMR spectra implies a comparatively high conformational rigidity in $L^{15}$. The $^{15}N$ NMR spectra of $L^{15}$ and $L^{17}$ indicate $^{1}H$-$^{15}N$ spin-spin coupling for the anilino, but not for the benzylamino donors, showing that the intramolecular H-bonding of the anilino protons observed in the solid state is partially retained in solution.

A comparative discussion of a range of Ni(II) complexes of the ligands is presented in Chapter 3. X-Ray crystallographic studies have been carried out on $[NiL^{17}Cl_2]$ and on the thiocyanate complexes of $L^{15}$, $L^{16}$ and $L^{17}$ which are compared with that of $L^{14}$. An inverse correlation between the in-plane and axial bond lengths around the Ni-atoms holds up to $L^{16}$. Complexes of $L^{16}$ and $L^{17}$ with nickel(II) nitrate have been prepared and the crystal structure of that of $L^{16}$ contains two complexes, $[NiL^{16}(NO_3)_2]$ and $[NiL^{16}(NO_3)(H_2O)]NO_3$. Cyclic voltametry shows that the formation of the Ni(III) species is facilitated by the smaller ligands; the oxidation of $[NiL^{17}Cl_2]$ is non-reversible and probably ligand-based. The visible spectra of the chloride and thiocyanate complexes have been assigned in terms of weak tetragonal-field splitting which is significant only for $L^{14}$ and $L^{15}$, the larger ligands giving essentially octahedral complexes.

A range of Cd(II) and Zn(II) complexes of $L^{16}$ and $L^{17}$ have been prepared and are discussed in Chapter 4. Crystal structure analyses of Cd(II) complexes of $L^{16}$ and $L^{17}$ have been performed. $[CdL^{16}Br]_2[CdBr_4]$ exhibits two five-co-ordinate complexes with significant differences in ligand conformation and in displacements of the Cd-atom from the donor plane. The influence of the $[CdBr_4]^{2-}$ ion on these conformations is considered. $[CdL^{17}Br_2]$ contains the Cd-atom virtually in the place of the macrocyclic donors with two axially co-ordinated Br-atoms.

The formation constants of the Zn(II) and Cd(II) complexes of the ligands have been determined in the collaborating establishment and the contribution of structural features to the thermodynamic stability of the complexes is discussed in Chapter 5. Although hole size effects predominate in the Ni(II) complexes, they are complicated by changes in co-ordination geometry across the ligand series for the Zn(II) and Cd(II) complexes.

## ACKNOWLEDGMENTS

During the course of this work, assistance and encouragement has been given by the following, to whom I acknowledge a debt of gratitude;

Dr. Peter Tasker of I.C.I. Specialties, my original Director of Studies, for his continued enthusiastic interest as an advisor, for many useful discussions and enjoyable visits to Blackley and Doboross, and for twice arranging financial support for study visits to Italy,

Professor Mary McPartlin (who took over as Director of Studies half way through the research programme), for teaching me crystallography, and for providing invaluable advice during the preparation of this thesis,

Professor Len Lindoy of James Cook University of North Queensland, for many helpful discussions during his visits to the U.K., and to his colleagues (in particular, Tony Leong for undertaking the potentiometric studies)

Professor Luigi Fabbrizzi of the University of Pavia, Italy, for the use of his laboratories for the electrochemical studies and for the hospitality he and his colleagues (particularly Dr. Antonio Poggi) extended to me during my visits to Italy in 1986 and 1990,

Alan Bashall, Dr. Harry Powell and Dr. Gráinne Conole for their help in collecting diffraction data and for advice in overcoming problems encountered in crystal structure solutions,

John Crowder, for obtaining the NMR spectra,

Nick Choi, for collecting the data and determining the structures of three of the nickel complexes.

I would also like to thank my employer, the University of North London, for financial assistance and leave of absence to attend many U.K. Macrocyles Group meetings and International Symposia on Macrocyclic Chemistry.

CONTENTS

## Chapter One

### 1. Introduction

This work is an investigation into some aspects of the co-ordination chemistry of a homologous series of macrocyclic tetraamines (1.i) with a selection of divalent metal-ions with a view to furthering the understanding of factors involved in the metal-ion selectivity of macrocyclic ligands.[1]

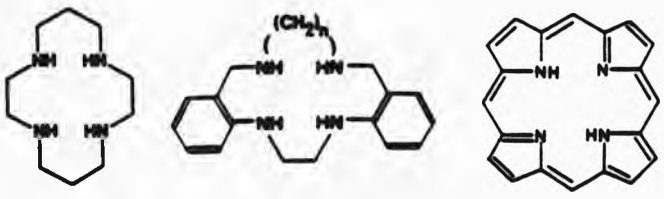


(1.ii) (1.i) (1.iii)

These ligands may be regarded as related to the archetypal alicyclic tetraamines of the type represented by cyclam (1.ii) and its homologues and isomers. It was anticipated that the effect of the presence of fused benzo substituents in (1.i) would be to restrict the flexibility of the ligands to an extent intermediate between that of (1.ii) and the more rigid macrocycles exemplified by the porphyrins (1.iii). In conjunction with this, the 'lop-sided' variation of macrocyclic ring atomicity induced by increasing the alkyl chain length between the benzylic amine functions was expected to affect the metal-ion selectivity across the series of ligands.

At this point, it is worth giving a definition of macrocyclic ligands and noting some of the reasons for the growth of interest, in the last twenty years or so, in these systems. Following that, some concepts pertinent to the study of the ligands under investigation will briefly be discussed.

## 1.1 Macrocyclic ligands

A macrocyclic ligand may be defined as a cyclic multidentate ligand which contains a minimum of three donor atoms incorporated into or attached to the ring and which has at least nine atoms in the ring.[2] Variation of the ring atomicity, donor type and number, type and extent of ring substitution, degree of unsaturation, together with the distribution of donors, substituents, and multiple bonds gives rise to a virtually limitless range of macrocyclic ligands. The co-ordination chemistry of such ligands has now become a major sub-division of co-ordination chemistry.[3]

## 1.2 Applications of macrocyclic ligands

Macrocycles have been employed in a wide range of roles and the following examples illustrate this diversity.

### 1.2.1 Models for biological processes

Naturally occurring macrocyclic complexes play important roles in living systems;[4] in oxygen absorption and transport, the haem proteins contain iron porphyrin complexes (1.iv); in photosynthesis, chlorophyll contains a partially reduced porphyrin complex of magnesium (1.v); and the natural antibiotic macrolides e.g. nonactin (1.vi), selectively transport alkali metal ions across cell membranes. The understanding of these and other natural systems has been a major factor in the growth of interest in synthetic macrocycles and their co-ordination chemistry. By using such synthetic systems, the structural complexity common in natural systems may be reduced so as to simplify the investigation of structure - property relationships; desired features can be incorporated in the model compounds, whilst undesirable complicating features may be excluded.

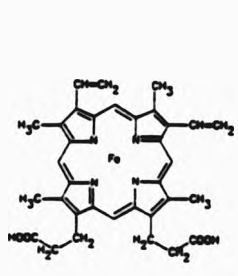

(1.iv)

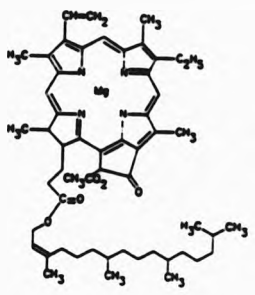

(1.v)

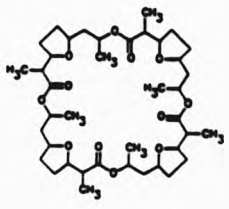

(1.vi)

### 1.2.2 Metal separation

Solvent extraction of metal complexes is an important technique in certain industries for the recovery of metals. This method is becoming increasingly attractive as a result of dwindling world supplies of high grade ores and increasing energy costs as well as environmental concern associated with smelting processes. Many metals may be efficiently won from low grade ores by solvent extraction, especially if the complexing/extracting agents are selective in their action. Investigations have been made into the suitability of macrocyclic ligands for this application.[5] The high cost of macrocyclic ligands will usually prohibit their use as extractants for base metals from primary ores, but their study can reveal features useful in the design of novel extractants and analytical reagents.[6]

### 1.2.3 Further applications

The high resistance to degradation, the intense colours, and the ease of preparation of copper complexes of the synthetic phthalocyanines (1.vii) has led to their use as pigments and dyes. Medical applications include heavy metal detoxification, tomography, and as

chemotherapeutic agents in the treatment of cancers. For these purposes, selective complexes of high stability are required so that complexes of potentially dangerous metals are excreted intact.

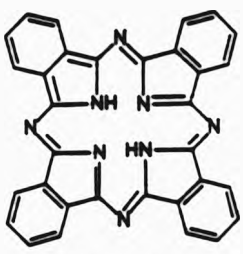


(1.vii)

## 1.3 The Macrocyclic Effect

The term 'macrocyclic effect' was coined in response to the observation that the stability constant for the copper(II) complex of the $N_4$-macrocycle, meso-5,5,7,12,12,14-hexamethyl-1,4,8,11-tetraaza-cyclotetradecane (1.viii), is $10^4$ times higher than that of an open chain analogue, 3,7-diazanonane-1,9-diamine (1.ix).[7,8]

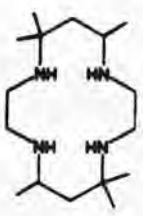


(1.viii)

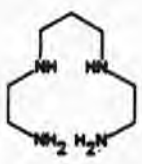


(1.ix)

This enhanced stability was greater than expected from the presence of an additional chelate ring. The effect may be regarded as a reflection of the Gibbs free energy term for the metathetical reaction,

$$ML + L' \rightleftharpoons ML' + L$$

where L is a non-cyclic ligand and L' is a macrocyclic ligand. Reibnegger and Rode have suggested that a large contribution to the macrocyclic effect arises from the high energy requirement to arrange the open-chain analogue from its linear conformation to one appropriate for complexation; such a requirement is absent for macrocyclic ligands.[9] Such enhanced stability may have contributions from both enthalpic and entropic terms. The macrocyclic effect in this respect may be considered an extension of the chelate effect.[10] An increase in the size of a chelate ring from five-membered is usually accompanied by a decrease in complex stability, which has been interpreted in terms of steric strain resulting in an unfavorable enthalpic contribution.[11] Entropy effects on the decrease of stability with increasing ring size are considered to become significant only for rings greater than seven-membered. In addition, Hancock and Martell have observed that the complex destabilization that occurs with increase in chelate ring size is more pronounced for larger than for smaller metal ions.[12]

Enhanced complex stability is expected if the ligand adopts a conformation which closely matches that which occurs in a corresponding complex. Such 'pre-organization'[13] of the ligand may account for the unusual stability variations along some series of related ligands. As well as pre-organization, related terms such as 'pre-straining',[14] 'pre-orienting'[15] and 'multi-juxtapositional fixedness'[16] have also been used to describe various aspects of 'molecular organization'. Lehn has defined this as,

> "...any combination of characteristics that lends some element of order to a particular chemical process or property, given that in a more primitive system, that

element of order would not exist."[17]

Busch identified five structural factors that, either singly or in combination, may contribute to the molecular organization reflected in the chemical and physical properties of a complexation system. These factors are topology, shape (or geometry), relative size of complexation components, rigidity and 'complementarity' (compatibility between the complexing species).[18]

### 1.4 Ligand design

Ligand design may be facilitated by consideration of an n-dimensional matrix, each dimension representing a particular systematic variation in ligand structure. Such variations may include for example: chelate ring size, degree of unsaturation and extent of substitution on the ligand backbone. The amount of work involved in synthesizing all the members of even a small ligand matrix can be daunting. But by selecting a particular variation (one of the matrix rows), perhaps one which may be produced by the use of cognate reactions, the properties of 'missing' elements of the matrix may be inferred and particular ligand syntheses can be targeted to fill in at least some of the gaps. The purpose of the present project was to investigate the effect on metal complexation of the variation of one structural feature, namely variation of the alkyl chain length, n, in the tetraaza macrocycles of type (1.i). A variation in steric strain might be expected as the macrocyclic ring size is varied. However, the build-up of such strain may be relieved by changes in the co-ordination geometry around the metal, e.g. by a change from planar to tetrahedral, as exhibited by the tropocoronands (1.x).[19] The increase in length of both alkyl chains in (1.x) induces a gradual variation in co-ordination geometry from square-planar to tetrahedral.

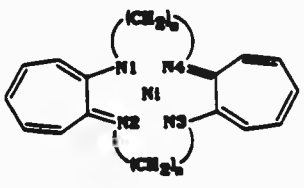


(1.x)

For the ligand series investigated in the present study, it appeared possible that the monotonic variation in ring size might promote a catastrophic change in the co-ordination geometry of individual complexes. Such a change has been termed a 'structural dislocation' and may form the basis for discrimination between different metal ions.[20,21] This concept will be discussed further in §1.8.2.1 in connection with the zinc(II) and cadmium(II) complexes.

The additional rigidity imposed by the fused benzo substituents in (1.i) over that of the corresponding saturated macrocycles of the cyclam type (1.ii) has the effect of reducing the tendency of the ligand to pucker and adapt its conformation to suit a variety of metal co-ordination requirements and metal sizes. A further effect is to change the nature of two of the secondary amine donors to weaker anilino nitrogens; the lone pair is partially delocalised into the aromatic system.

A more obvious mechanism for metal-ion discrimination by macrocyclic systems involves the fit of the metal into the macrocyclic cavity. However, it is noted that the relative importance of such 'size-match' selectivity has been the subject of much debate.[12]

## 1.5 The Macrocyclic Cavity

Of fundamental importance in determining the properties of a

macrocyclic complex is the size of the cavity available to the metal.[1] If the metal is to effectively co-ordinate to all the donors of the ligand, it must lie in or near to this cavity. To a large extent the size of the hole is determined by the ring atomicity. For a series of cyclam type ligands, the natural hole size in the least strained free ligand in conformations suitable for co-ordination to a metal ion has been calculated using molecular mechanics.[22] The hole size was shown to increase by 0.10-0.15 Å for each additional atom incorporated into the ring. On complexation, contraction or expansion of the hole to fit metals which are either too small or too large for the natural cavity of the ligand, tends to minimize the differences between the natural hole sizes of the ligands. The degree to which this natural hole size variation is altered is influenced by the rigidity of the ligand. Ligand rigidity is maximized in fully unsaturated obligate planar systems such as the porphyrin ring (as occurs in haem) or the synthetic phthalocyanine macrocycles (1.vii). The introduction of saturation into an unsaturated ligand backbone will increase the tendency for it to pucker and fold on co-ordination such that the ring may better adapt to the spatial requirements of the metal-ion.

A simple procedure for estimating macrocycle hole size from X-ray crystallographic data has been devised.[23] Figure 1.1 shows an idealized macrocyclic ligand with five donor atoms each separated by ethane bridging groups. The ligand hole size radius, $R_H$, is defined as the mean of the distances, $R_{n,i}$, of each donor atom, i, from the centroid, C. The radius of the bonding cavity, $R_A$, available to the metal is then defined as the mean of $(R_{n,i} - R_{d,i})$. For secondary amine nitrogen donors, $R_d$ has been calculated from X-ray data to be 0.72 Å.[23] In reality, the actual bonding cavity will rarely be

circular, especially in a mixed-donor system, but the (probably irregular) cavity may still be defined in this way.

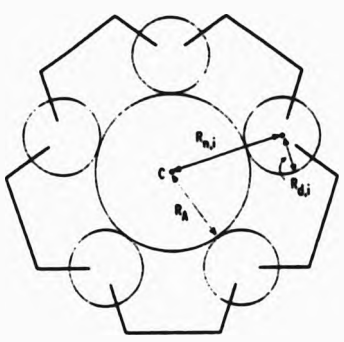


FIGURE 1.1 Hole size and bonding cavity radii in macrocyclic ligands.

Although other factors may also be important, for a series of related macrocyclic ligands, additional stability will normally be expected for a macrocyclic ligand whose bonding cavity radius most closely matches the appropriate radius of the metal. This seems to be the case for a series of 14- to 17-membered $N_2O_2$ donor ligands (1.xi) where the best fit of high-spin nickel(II) to the macrocyclic cavity occurs at the 16-membered complex,[23] which also exhibits the highest formation constant.[24] X-ray structure determinations have been carried out for [Ni(1.xi, N = 14)$Cl_2$],[25] [Ni(1.xi, N = 15)$Cl_2$],[26] [Ni(1.xi, N = 15)$(NCS)_2$],[27] and [Ni(1.xi, N = 16)$Br_2$].[28,29] The bonding cavity radii calculated for these structures are included in Figure 1.2.

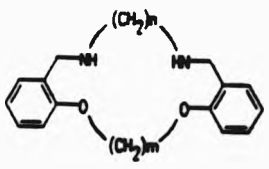


(1.xi)

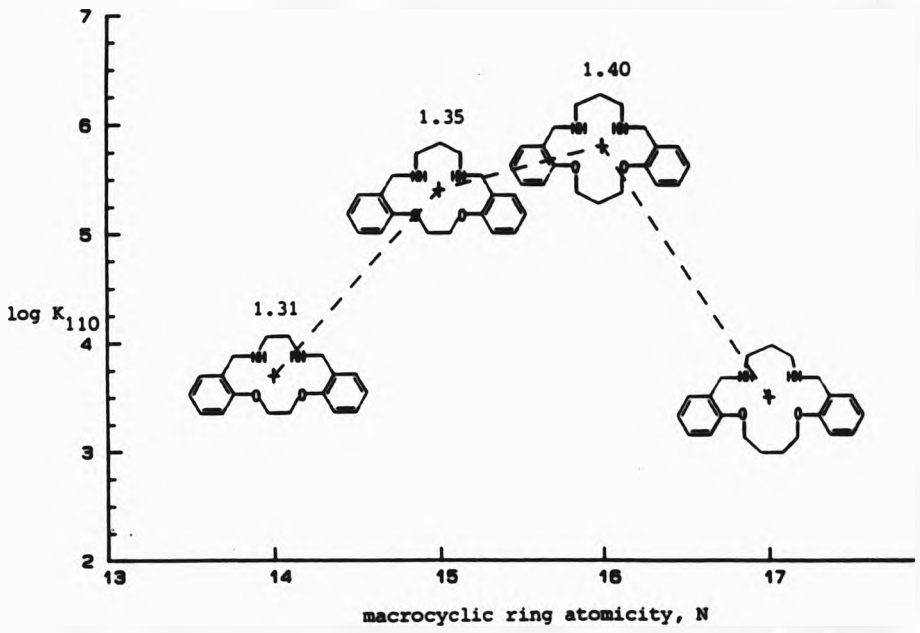


FIGURE 1.2 The variation of formation constants (log $K_{110}$) with macrocyclic ring atomicity (N) for the high-spin nickel(II) complexes of $N_2O_2$ ligands of type (1.xi).

## 1.6 Ligand basicity

The basicity of an amine is determined by the availability of its lone pair of electrons. Solvation of the amine involving hydrogen bond formation from the lone pair to protic solvent molecules is one of the major factors reducing its basicity. Along a series of closely related macrocycles, the differences in mode or extent of solvation are likely to be slight, but the effect on the relative basicities of the ligands can not be entirely neglected. For polyamines, the ease with which successive protonations are achieved depends largely on electrostatic repulsions of the positive charges.[30] This is more

marked for the less flexible cyclic polyamines.

The stepwise protonation constants for a cyclic tetraamine may be defined using the following equilibria:

$$H + L = LH, \qquad K_{011} = [LH]/[L][H]$$

$$H + LH = LH_2, \qquad K_{012} = [LH_2]/[LH][H]$$

$$H + LH_2 = LH_3, \qquad K_{013} = [LH_3]/[LH_2][H]$$

$$H + LH_3 = LH_4, \qquad K_{014} = [LH_4]/[LH_3][H]$$

where the charges have been omitted for clarity and the equilibrium constants are in the conventional form $K_{MLH}$ where M, L and H are the stoicheiometric coefficients of the metal (for protonation constants only, M = 0), ligand, and hydrogen ions in the product, respectively. The potentiometric determination of protonation constants depends upon the measurement of the total hydrogen ion concentration throughout the course of an acid-base titration. Successful computer refinement of estimates of the equilibrium constants leads to a model of the system which matches the experimental results.[31] A 'species' in solution, such as LH, may consist of several LH species with the proton bound to a different basic site in each. Of course, this does not matter when all the potential donor sites are equivalent. It should be noted that such measurements of macroscopic equilibria can provide no information about microscopic equilibria; the exact location of the hydrogen on a ligand containing more than one possible protonation site is unknown.[31] However, when the equilibrium constants are fairly well separated, it is often possible to identify the predominant species by reference to analogous single-site systems.

### 1.7 Kinetic and Thermodynamic Stability

The ease with which a particular complex ion is able to exchange one or more of the ligands in its co-ordination sphere determines its

lability. Those complexes for which such ligand exchange reactions are rapid are called labile, whilst those which exchange their ligands slowly (or not at all) are referred to as inert. The terms stable and unstable normally refer to the thermodynamically controlled equilibrium position for the complexation reaction. The stability constant, $K_{110}$, for the reaction:

$$M + L \rightleftharpoons ML$$

may be defined as [ML]/[M][L].

### 1.8 Metal complexes

The metals selected for the investigation of the complexation behaviour of the ligands were restricted to nickel(II), cadmium(II), and zinc(II), so that a more thorough study of the structural changes associated with the increase in macrocyclic ring size was possible within the scale of the project. The reasons for selecting these particular metals are outlined in the following sections.

#### 1.8.1 Nickel(II) complexes

A significant body of work has accumulated on nickel(II) complexes of macrocyclic ligands.[1] Complexes of this $d^8$ transition metal ion with multidentate ligands providing medium-sized chelate rings have spectroscopic and electrochemical properties amenable to study, which reflect the structures of these complexes. The predominantly covalent bonding in Ni(II) complexes with this type of neutral quadridentate macrocyclic ligand and simple axial ligands tends to impose a tetragonally distorted co-ordination geometry, with the macrocycle disposed in a near-planar arrangement around the metal.[32] If strong ligands are co-ordinated in axial positions, the resulting (high-spin) complex is formed, with the classical $d^2sp^3$ hybridisation scheme.

Tetragonal distortion arises from differences between the in-plane and axial ligand field strengths and, in the extreme, square planar (low-spin) complexes are formed, with $dsp^2$ hybridization around the metal-ion. In solution, the following spin-state equilibrium may be established and is occasionally measureable.[33]

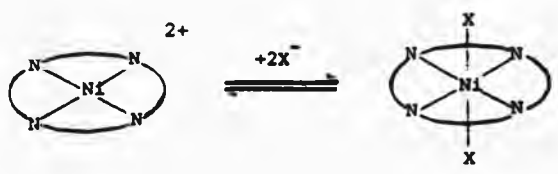


low-spin high-spin

The way in which the macrocycle co-ordinates to the metal may be affected by the nature of the non-macrocyclic ligands. The ligand (1.xii) has been shown to co-ordinate to nickel(II) in $[Ni(1.xii)Cl_2]$ such that the chloro ligands are trans-axial,[34] whereas in $[Ni(1.xii)(NCS)_2]$, the thiocyanato ligands are cis- and the macrocycle is co-ordinated in a folded configuration.[35]

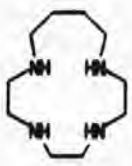


(1.xii)

Oxidation of nickel(II) to the less stable nickel(III) may be achieved electrochemically or with strong oxidizing agents (such as nitrosonium tetrafluoroborate) and saturated tetraaza macrocyclic ligands have been found to facilitate this oxidation.[36] In the present work, it is anticipated that macrocyclic ring size will have a considerable influence on the stabilization of the smaller nickel(III) species (Pauling covalent radius 2.30 Å [37]). The electron is removed on oxidation from an essentially metallic antibonding orbital which is

raised in energy by very strong in-plane interactions with these ligands.[38] In the present work, the introduction of weakly basic anilino nitrogen atoms producing a weaker donor set, was expected to reduce the effectiveness of the ligand to stabilize the higher oxidation state. Consequently the potential for the Ni(III) - Ni(II) couple would be increased (become more positive).

It was also thought that the situation might be complicated by the possibility of the formation of nickel(II) - ligand radical species in which the unpaired electron is delocalized over the co-ordinated ligand, rather than centred on the metal and that further complications may arise from competitive co-ordination of the solvent and counter-ion, as well as from the existence of spin-state equilibria in the $d^7$ nickel(III) species. Analysis of their visible spectra is expected to provide information on the degree of tetragonal distortion of the complexes.[39]

1.8.2 Zinc(II) and cadmium(II) complexes

In contrast to the well-defined stereochemical requirements of nickel(II), the post-transition $d^{10}$ metals, zinc(II) and cadmium(II) exhibit co-ordination geometries that are stereochemically less demanding. The bonding in such complexes is less covalent than in those of nickel(II). The absence of any ligand field stabilization effect in complexes of Zn(II) and Cd(II), because of their filled d-shells, allows the stereochemistry to be determined more by electrostatic forces and metal size. The larger Cd(II) is more often associated with higher co-ordination numbers (six or seven) than the smaller Zn(II) (four or five). The presence of such ionic character in the bonding of Zn(II) and Cd(II) complexes makes it difficult to define a consistent octahedral covalent radius for these metals.

Although Pauling assigns values to the tetrahedral covalent radii for Zn(II) and Cd(II), 1.31 and 1.48 Å respectively, no octahedral radii are given.[37] Thus, assessment of a goodness-of-fit parameter for these metals in macrocyclic complexes has to be more empirical and the metal radius used may not be widely applicable.

1.8.2.1 Structural dislocation and dislocation discrimination

A concept which may prove more useful in the interpretation of the trends in thermodynamic stability across the ligand series is that of structural dislocation. A couple of examples will serve to illustrate this concept and the related concept of dislocation discrimininationfor some homologous series of ligands.

The Zn(II) complexes of the $N_3S_2$ ligands (1.xiii) show (Figure 1.3) a clear dislocation in the co-ordination of the zinc.

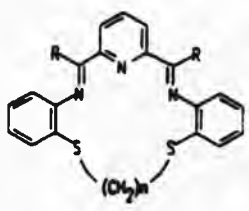


(1.xiii)

In the 15- and 16-membered ligand complexes, the zinc is co-ordinated to all three nitrogen donors and to both sulphur donors in a distorted pentagonal bipyramidal arrangement.[40] The Zn-S distances are 2.5 to 2.7 Å for $[Zn(1.xiii, R = H, n = 2)(ClO_4)_2]$ and 2.6 to 2.8 Å for $[Zn(1.xiii, R = H, n = 3)(H_2O)_2]^{2+}$. The incorporation of an extra methylene unit in (1.xiii) is accompanied by a change in the metal co-ordination mode in $[Zn(1.xiii, R = Me, n = 4)I_2]$.[41] Here, the zinc adopts a pseudo-square pyramidal geometry and is bonded only to the three nitrogen donors of the macrocycle: the sulphur atoms are

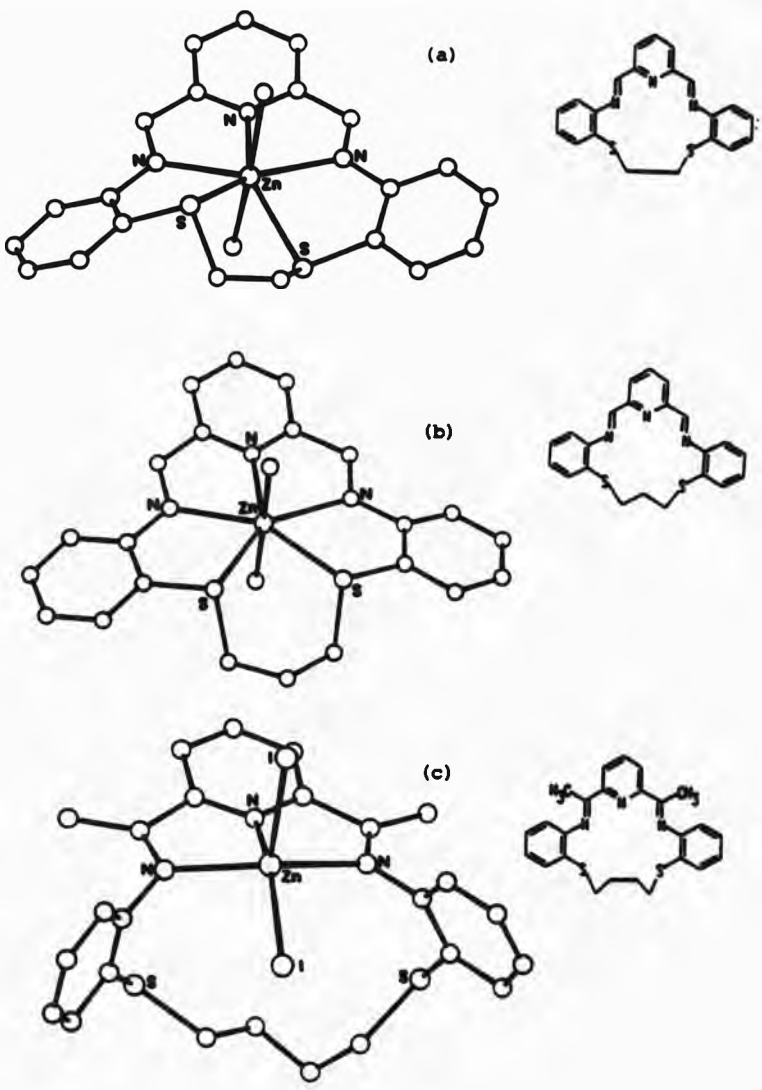


FIGURE 1.3 The structures of (a) [Zn(1.xiii, R = H, n = 2)$(ClO_4)_2$], (b) [Zn(1.xiii, R = H, n = 3)$(H_2O)_2]^{2+}$ (Ref. 40) and (c) [Zn(1.xiii, R = Me, n = 4)$I_2$] (Ref. 41). For clarity, only the co-ordinated oxygen atoms of the perchlorato ligands are drawn in (a).

not co-ordinated and are each about 4.3 Å from the metal. The implication for discrimination is that in the cadmium(II) complexes of these ligands, any changes in the co-ordination environment around the metal occurs at a different point in the ligand series. For example, the cadmium may be bonded to all five donors of (1.xiii, n = 4). Stability constants are not available - potentiometric determination is ruled out because of the ease with which iminolysis occurs.[41] Unfortunately, no structures of cadmium(II) complexes of (1.xiii) have been reported.

Figure 1.4 shows the variation in stability constants across a series of three $N_3O_2$ ligands (1.xiv) and the crystal structures of zinc(II) and cadmium(II) complexes of the 17-membered ligand (1.xiv, m = n = 2) show different co-ordination modes (Figure 1.5).[20]

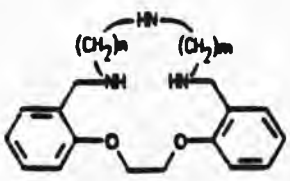


(1.xiv)

The zinc atom is co-ordinated only to the three nitrogen donors of the macrocycle, whereas the cadmium atom is bonded to all five donors. NMR studies indicated that the 18- and 19-membered ligands (1.xiv, n = 2, m = 3) and (1.xiv, n = m = 3) exhibit essentially the same co-ordination mode with zinc(II) and hence the formation constants show no apparent dislocation.[42] The drop in stability constant of the cadmium(II) complex on passing from the 18- to the 19-membered ligand has been interpreted in terms of a change in metal co-ordination geometry from one in which the metal is bonded to all five macrocyclic donors to one in which the ether oxygen atoms are

FIGURE 1.4 Formation constants (log $K_{110}$) for zinc(II) complexes of two series of dibenzo substituted macrocyclic ligands, (1.xi) and (1.xiv) and for the cadmium(II) complexes of (1.xiv). [95% MeOH, I = 0.1 mol $dm^{-3}$, 25°C, (1.xi) from Ref. 43 ($Me_4NCl$), (1.xiv) from Ref. 20 ($Et_4NCl$).]

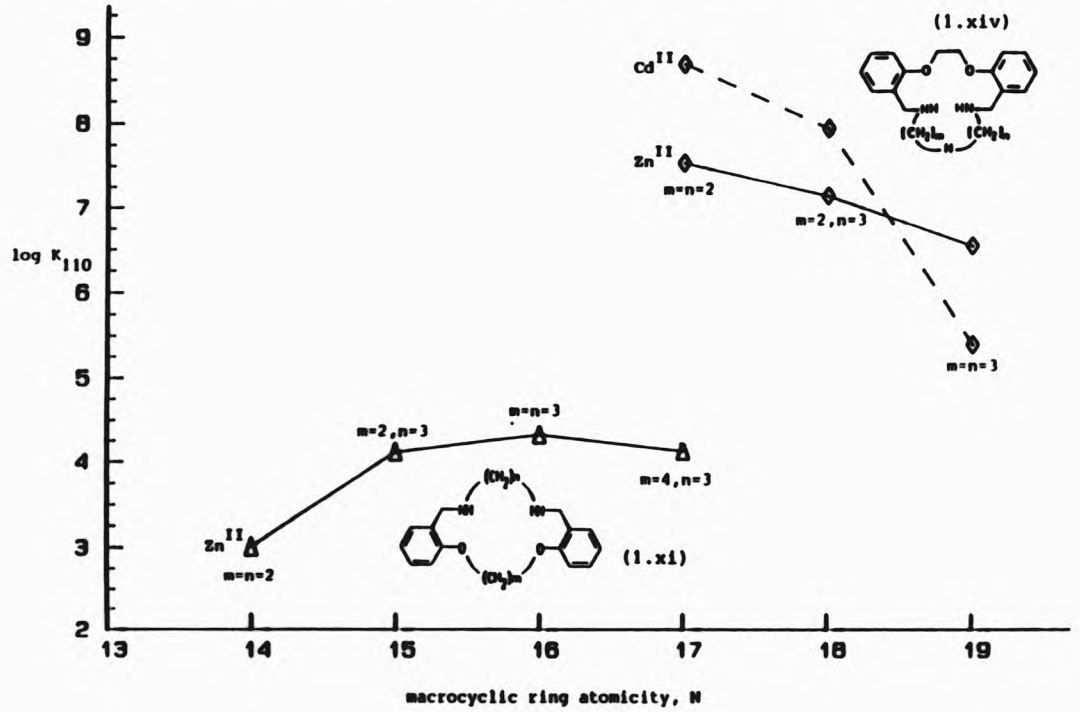

again not co-ordinated.[20]

The $N_2O_2$ ligands (1.xi) form only weak complexes with zinc(II) (Figure 1.4) and the variation in log $K_{110}$ over the series is small (no dislocation is apparent).[43] NMR studies indicate that the ether oxygen donors do not co-ordinate at least in solution and the X-ray structure of the zinc(II) complex of the closely related N,N'-dimethylated ligand (1.xv) (Figure 1.5) lends support to this view.[43]

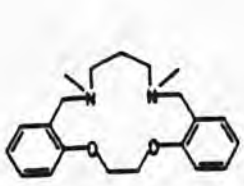

(1.xv)

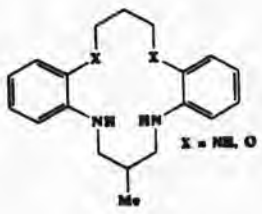


(1.xvi)

The formation constants of zinc(II) complexes of the ligands (1.xvi, X = NH) and (1.xvi, X = O) are very low (log $K_{110}$ = 3.8 and < 3.0, respectively) as is that of the cadmium(II) complex of (1.xvi, X = NH) (log $K_{110}$ = 3.0), demonstrating that the co-ordinating power of anilino donors is of the same order as that of the weak phenoxy ether donors.[44] Structural evidence for the weak co-ordinative ability of anilino donors is provided by the open-chain ligand (1.xvii).[45]

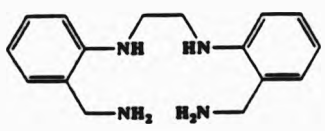


(1.xvii)

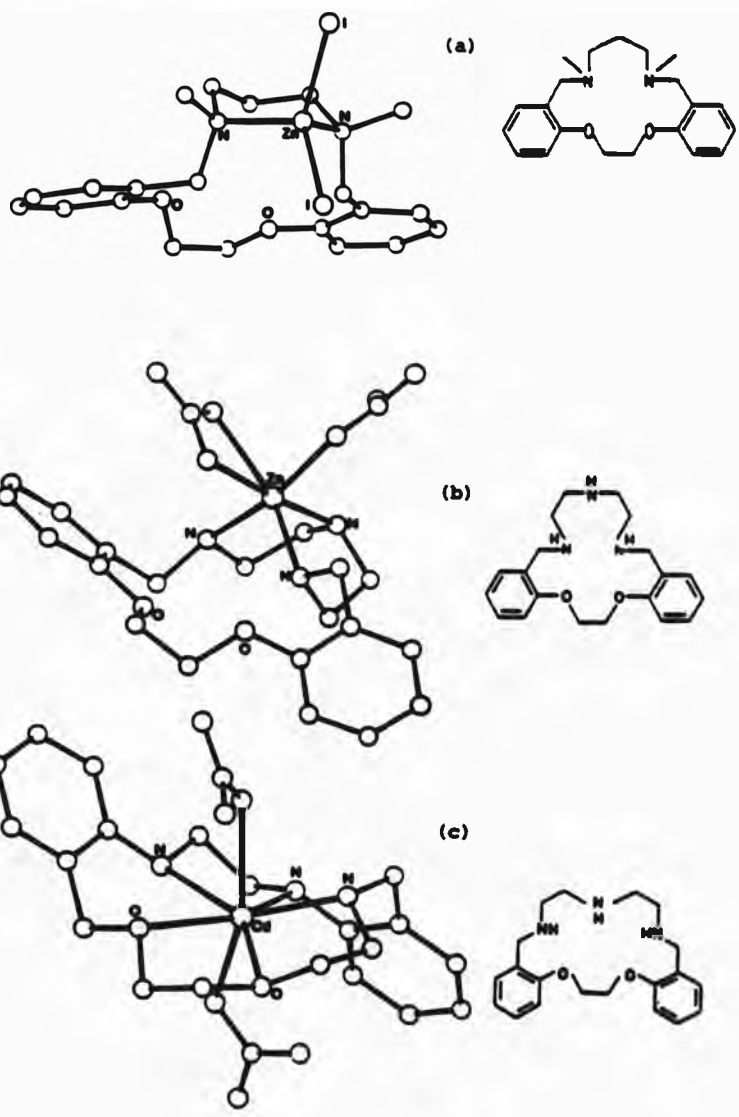


FIGURE 1.5 The structures of (a) $[Zn(1.xv)I_2]$ (Ref. 43), (b) $[Zn(1.xiv, m = n = 2)(NO_3)_2]$ (Ref. 20) showing the non-co-ordination of the ether oxygen atoms and (c) $[Cd(1.xiv, m = n = 2)(NO_3)_2]$ (Ref. 20) in which the metal is bonded to all five macrocyclic donor atoms.

This ligand has been shown to co-ordinate to cadmium(II) to give a five-co-ordinate complex with one of the anilino donors not co-ordinated (Figure 1.6).

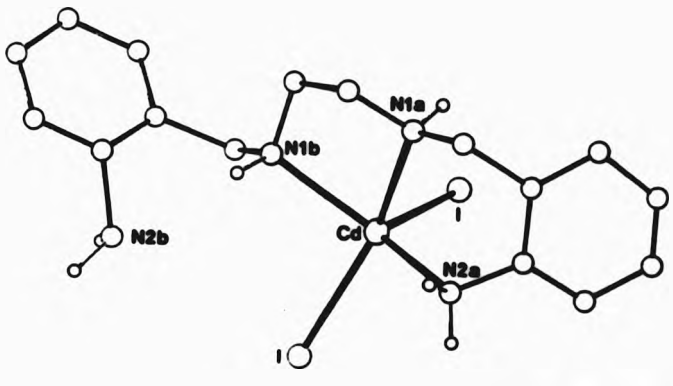


FIGURE 1.6 The structure of $[Cd(1.xvii)I_2]$ showing the non-co-ordination of one of the primary anilino donor atoms.[45]

## 1.9 Hydrogen bonding

In the context of the work presented in this thesis, it is pertinent to review briefly hydrogen bond formation. Significant hydrogen bonding between A-H and X will occur only when A and X are strongly electronegative. Typical hydrogen donor groups include -O-H and >N-H. A hydrogen acceptor group must have a region of high electron density, such as the one unshared electron pair on an amine nitrogen atom or the two on an alcohol or water oxygen atom.[46,47,48] It is diagnostic of strong hydrogen bonds that A...X is equal to or less than the sum of the van der Waals radii of A and X and that the angle A-H-X is near to 180°. For weak (usually longer) bonds, considerable deviations from 180° are often found. In large molecules, such as the tetraaza macrocycles used in this project, stereochemical considerations affecting A and X may prevent A, H and X from achieving

collinearity.

It is a matter of contention whether hydrogen bonds tend to form only along the direction of the lone pair(s) of the acceptor atom or whether they can adopt any orientation relative to the lone pairs. Taylor and Kennard concluded from a study of 196 O-H...O< bonds that the former is probably not necessary and deviations from lone pair directionality are common.[49]

1.10 Ligand configuration

In a complex of a cyclic ligand containing four secondary amine donors, linked by bridging groups (a,b,c,d), co-ordinated at the corners of a quadrilateral, the hydrogen atoms attached to each nitrogen will be orientated approximately axially.

(1.xviii)

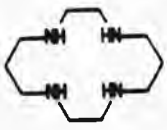

(1.ii)

(1.xix)

Except when a = b = c = d, as in e.g. 1,4,7,10-tetraazacyclododecane (1.xviii), each tetrahedral nitrogen atom, when co-ordinated, is an asymmetric centre and the number of distinct non-enantiomeric combinations of the donor atoms depends upon the symmetry of the distribution of the bridging groups. To a large extent, the macrocycle conformation will depend on the combination of chiral configurations present. For ligands in which a = c and b = d, such as 1,4,8,11-tetraazacyclotetradecane (1.ii, cyclam), five forms are possible;[50] but if a = c and b = d, such as occurs in 1,4,8,11-tetraazacyclopentadecane (1.xix), a further form of II can

exist.[51] These forms and their point group symmetries are shown in Figure 1.7. The ligands under investigation conform to this last type (a = c and b = d).

FIGURE 1.7 Diastereoisomers and point group symmetries for complexes of tetraaza macrocycles. The number of possible configurations depends on the symmetry of the distribution of the bridging groups a, b, c and d. The Roman numerals correspond to the designations proposed by Bosnich et al. for complexes of cyclam.[50]
* Designation proposed by Hay and Tarafder.[51]

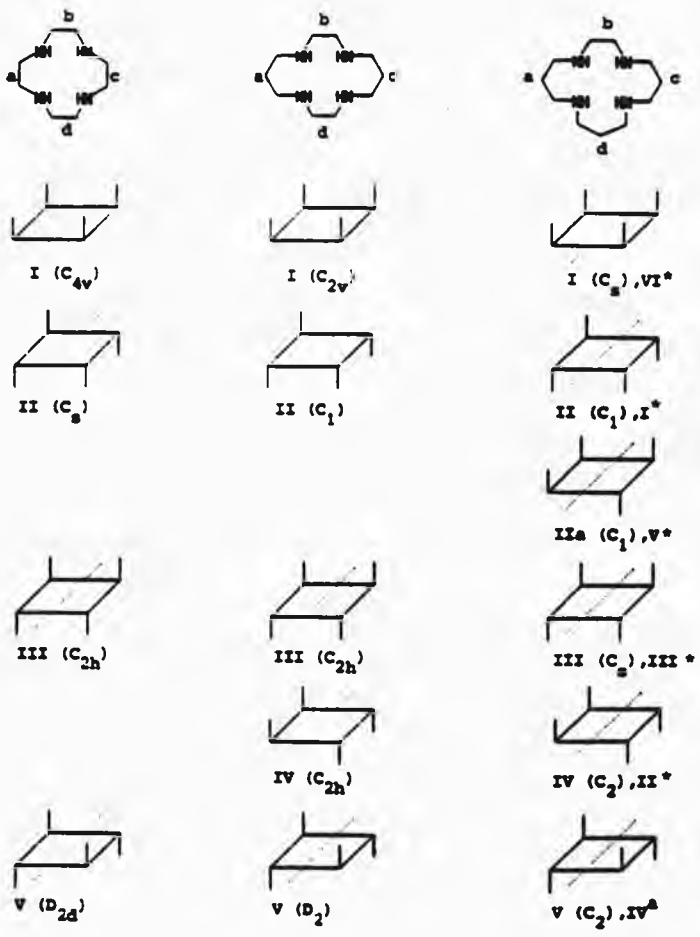

## Chapter Two

### 2. The Tetraaza Macrocyclic Ligands

The tetraaza macrocyclic ligands studied in this work (2.1, R = H, m = 2) form a homologous series by variation of only one of the inter-donor polymethylene bridges. The notation chosen for the ligands, for example: $L^{14}$, $L^{15Bu}$ etc., although apparently idiosyncratic, has the advantage of enabling ready identification of the ligand without constant reference to an explanatory chart. Instead of arbitrary labels ($L^1$, $L^2$ etc.) the superscript is used to convey the macrocyclic ring atomicity and the nature of any alkyl substituent, R.

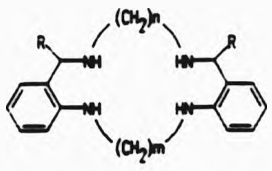


(2.1)

Two of the smaller unsubstituted ligands, $L^{14}$ and $L^{15}$, were first reported in 1984 and 1982 respectively, in work investigating the effect of changing the donor set from $N_4$ to $N_2O_2$ and $N_2S_2$ on the size of the bonding cavity available to nickel(II).[25,52] The main aim of the present work was to extend the series of $N_4$ ligands to include $L^{16}$ and $L^{17}$ and to investigate any trends in their properties which may affect their complexation behaviour. The sixteen-membered ligand, $L^{16}$ has been reported earlier in connection with the formation constants of its zinc(II) and cadmium(II) complexes,[53,54] but no details of its synthesis or spectroscopic properties were available. The larger ligands, $L^{17}$ and $L^{19}$ have been produced during the course of this work.

## 2.1 Preparation of ligands

The ligands employed in this work were prepared according to the synthetic route outlined in Figure 2.1. Details of the syntheses of the ligands and precursors are given in Chapter Six. The reaction of two molecules of methyl 2-aminobenzoate (methyl anthranilate) with 1,2-dibromoethane yields the $C_2$-bridged diester (Ia). Reduction of the ester functions gives the $C_2$-dialcohol (Ib), which is then oxidised to the $C_2$-dialdehyde (Ic). Under suitable reaction conditions, condensation of the appropriate diamine with (Ic) (step D in Figure 2.1) yields a range of 1:1 (aldehyde:amine) macrocyclic diimines ($P^N$).

The fourteen- to sixteen-membered precursor diimine macrocycles, $P^{14}$, $P^{15}$ and $P^{16}$ had been reported by Green et al. in 1971.[55] The melting points, infrared and NMR spectra of the precursors and the diimines, $P^{14}$, $P^{15}$ and $P^{16}$, obtained in the present work compared favourably with those reported. In 1980, the series of $N_4$ diimines was extended by Tasker and co-workers to include $P^{17}$ and $P^{19}$,[56] but synthetic details were not available. Infrared and NMR spectra obtained for these compounds in this work are consistent with those expected.

The synthesis of $P^{18}$ was not attempted during the course of the present work for the following reason. In a footnote to Reference 56, it was noted that reaction of 1,6-diaminohexane with (Ic) (to yield $P^{18}$) "appears to proceed similarly to that with 1,2-diaminoethane [yielding $P^{14}$], but is still under study." Subsequent attempts to prepare $P^{18}$ have been unsuccessful.[57] It may be that polymers and/or cyclic oligomers are produced preferentially to $P^{18}$. The nature of the products of the condensation (step D) is affected by solvent and

FIGURE 2.1 Reaction scheme for the synthesis of the tetraaza macrocycles, $L^{14}$ to $L^{19}$. (A) 1,2-dibromoethane, $Na_2CO_3$, 130°C, 30 h, 53%; (B) $LiAlH_4$, tetrahydrofuran, reflux, 1 h, 77%; (C) $MnO_2$, $Et_2O$, reflux, 1 h, 51%; (D) $NH_2(CH_2)_nNH_2$; $P^{14}$, (n=2), MeOH, reflux, 6 h, 87%; $P^{15}$, (n = 3), MeOH:$CH_2Cl_2$ (5:1), reflux, 3 h, 82%; $P^{16}$, (n = 4), MeOH:$CH_2Cl_2$ (5:1), reflux, 5 h, 59%; $P^{17}$, (n = 5), EtOH, reflux, 4 h, 87%; $P^{19}$, (n = 7), EtOH, reflux, 4 h, 64%; (E) $LiAlH_4$, $Et_2O$, reflux, 3.5-8 h, 56-93%.

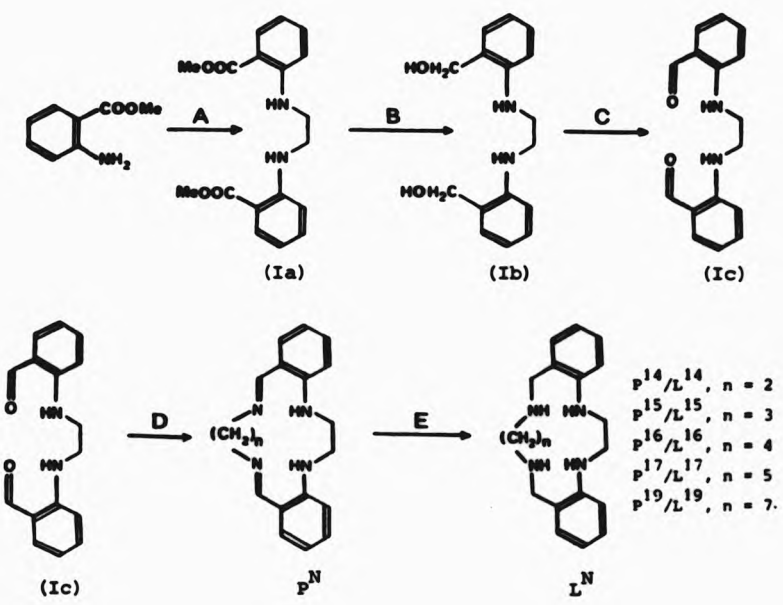

temperature. This has been demonstrated by the preparation of the 2:2 (aldehyde:amine) twenty-eight-membered macrocycle (2.ii), which can also be obtained from $P^{14}$ by prolonged heating in acidified methanol.[58]

(2.ii)

Attempts to prepare $P^{19}$ were not always successful; a presumably oligomeric product was often obtained, which defied reduction under the same conditions as $P^{19}$ itself. It may be that, as well as the nineteen-membered ring, the condensation of 1,7-diaminoheptane with the dialdehyde (Ic) affords oligomeric products typified by (2.ii). However, the reasons for the non-reduction of these oligomers have not been investigated.

Reduction of the imine functions (step E in Figure 2.1) had been previously achieved in most cases using sodium tetrahydridoborate, $NaBH_4$, under relatively forcing conditions.[58,59,60] In the present study, a suspension of lithium tetrahydridoaluminate, $LiAlH_4$, in diethyl ether was preferred as the reducing agent. This gave faster reaction times, four to six hours rather than nine hours, and a simpler work-up than the borohydride reductions. Satisfactory microanalyses (C, H and N) were obtained for $L^{14}$ to $L^{17}$. No microanalytical data was obtained for the viscous oil $L^{19}$, but infrared, NMR and mass spectral data are consistent with those

expected.

## 2.2 Crystal structures

The crystal structures of $L^{16}$ and $L^{17}$ have been determined during the course of this work. Details of the crystal data and structure solutions are given in Chapter Six and tables of fractional atomic coordinates, thermal parameters, bond lengths and interbond angles for $L^{16}$ and $L^{17}$ are given in the Appendix (Tables A1.1 to A2.5). The crystal structure analyses confirm the macrocyclic nature and the constitution of the free ligands.

In the discussion following, the structures of $L^{16}$ and $L^{17}$ will be compared with the reported structures of $L^{14}$ and the C-alkylated homologues of $L^{15}$; $L^{15Et}$ (2.i, R = Et, m = 2, n = 3) and $L^{15Bu}$ (2.i, R = Bu, m = 2, n = 3).[25,44,59,61] For $L^{15}$ itself, despite many attempts, no crystals suitable for crystallographic study have been produced. Some clues to the structure of this ligand may be found in the structures of $L^{15Et}$, $L^{15Bu}$ and their common precursor, $P^{15}$. With this in mind, it is worth considering briefly the previously reported structures of the precursor diimines, $P^{14}$, $P^{15}$ and $P^{16}$.[56,62]

Of these diimines, $P^{14}$ (Figure 2.2) has been shown to be relatively flat compared to the other two. The phenylene rings are inclined to opposite sides of the $N_4$ mean plane giving a step-shaped molecule. However, $P^{15}$ and $P^{16}$ both exhibit a pronounced folded or saddle-shaped conformation, i.e. with both phenylene rings inclined to the same side of the $N_4$ plane. It has been postulated that the distortion of the molecule from planarity arises in order to minimise the interaction between the two secondary amine hydrogen atoms,[62] but this interaction could be equally well minimised if the phenylene

$P^{14}$

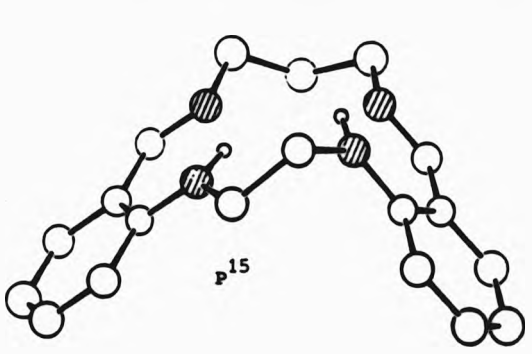

$P^{15}$

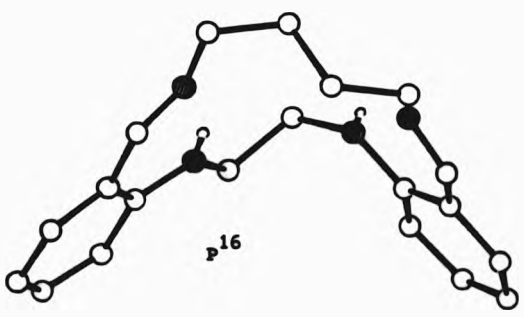

$P^{16}$

FIGURE 2.2 The structures of the diimines $P^{14}$, $P^{15}$ (Ref. 56) and $P^{16}$ (Ref. 62).

rings were displaced each to either side of the $N_4$ plane. It is noticeable that the $C_3$-bridge in $P^{15}$ adopts the 'chair' conformation and this virtual mirror symmetry is continued in the saddle arrangement of the molecule. The conformation of this bridge is likely to be a major factor contributing to the overall shape of the molecule.

### 2.2.1 The structure of $L^{14}$

The ligand $L^{14}$ (Figure 2.3) was shown to be relatively flat (but puckered) with a virtual two-fold rotation axis between the mid-points of the $C_2$-bridges, dividing the molecule into two halves, a and b. The fused benzo rings are inclined to opposite sides of the $N_4$ mean plane giving an overall step-shape to the ligand similar to that seen in $P^{14}$. One important feature of this structure is the presence of two intramolecular hydrogen bonds across the a- and b-halves of the macrocyclic cavity, indicated by dashed lines in Figure 2.3. Each hydrogen bond involves the anilino hydrogen atom and the lone-pair of the benzylamine nitrogen atom (see §2.2.3.3).

### 2.2.2 The structures of $L^{15}$, $L^{15Et}$ and $L^{15Bu}$

Although the structure of $L^{15}$ is not known, it may be envisaged that it is similar to that of $P^{15}$ (Figure 2.2). However, the reported crystal structures of $L^{15Et}$ and $L^{15Bu}$ (Figure 2.3),[44,59] both produced from $P^{15}$, exhibit different conformations. The ligand $L^{15Et}$ retains the chair conformation and the saddle arrangement observed for $P^{15}$. The isomer obtained is meso- with respect to the pair of ethyl substituted chiral carbon atoms (R,S) and to the pair of chiral benzylamino nitrogen atoms N(1a) (R) and N(1b) (S) so that the pairs of ethyl chains and secondary amine hydrogen atoms lie on the opposite

FIGURE 2.3 The structures of $L^{14}$ (Ref. 25) and of $L^{15Et}$ and $L^{15Bu}$ (Ref. 44) showing the conformations of the $-CH_2CH_2CH_2-$ bridges in the fifteen-membered ligands. The absolute configurations of the benzylamine nitrogen atoms and the asymmetric carbon atoms are indicated with the Cahn-Ingold-Prelog notation. The hydrogen bonds are represented by dashed lines. For $L^{15Bu}$, the molecule drawn is at -x,-y,-z.

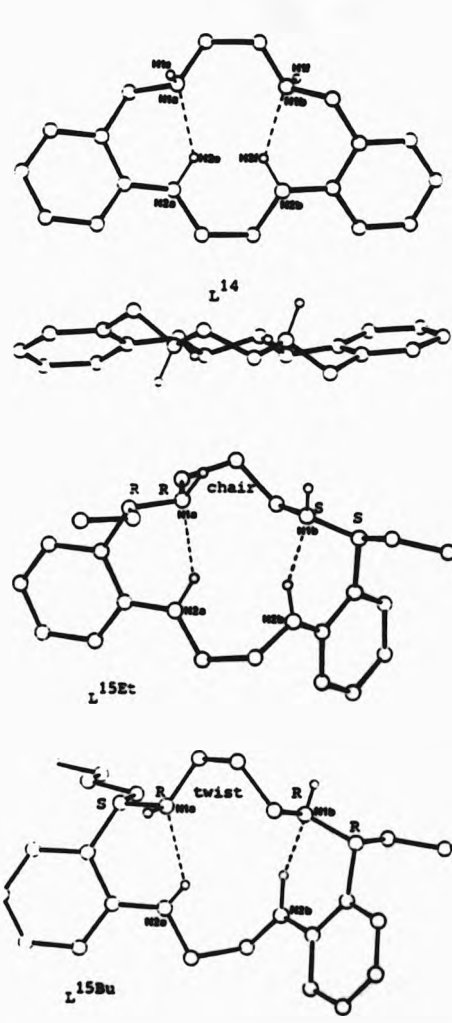

side of the $N_4$ plane to the phenylene rings. A different conformation is observed in $L^{15Bu}$. This molecule exhibits the $C_3$-bridge in the 'twist' conformation and the ligand is step-shaped. Here, although the butyl substituted carbon atoms are meso- (S,R) the benzylamino nitrogen atoms are racemic (R,R). It can be seen that the intramolecular hydrogen bonds are present in both ligands.

### 2.2.3 The structures of $L^{16}$ and $L^{17}$

The structures of $L^{16}$ and $L^{17}$ are shown in Figures 2.4 and 2.5, respectively. It is advantageous to discuss aspects of these two ligands together and to compare them with those of the fourteen- and fifteen-membered ligands described above.

#### 2.2.3.1 Amine hybridization

The secondary amines in all the ligands are of two distinct chemical types: benzylamino [labelled N(1)] and anilino [labelled N(2)]. The differences between these two types of potential donor atoms derive from the nature of the hybridization around the nitrogen atoms. The lone pair of the anilino nitrogen atoms will be delocalized to some extent and conjugated with the $\pi$-electron system of the phenylene ring, giving some $sp^2$ character to the atom. One effect of this conjugation will be a shortening of the N(2)-C(2) bonds compared to all the other C-N bonds in the ligand. Indeed, the mean of the C(2)-N(2) bond lengths in all five ligands is 1.389(8) Å, whereas the mean of all the other C-N bond lengths (30 bonds) is 1.464(8) Å. In $L^{16}$, the C(2)-N(2) bond lengths are 1.399(8) and 1.375(8) Å in the a- and b-halves, respectively and for $L^{17}$, the corresponding bond lengths are 1.392(6) and 1.399(6) Å. A further effect of the increased $sp^2$ character of the anilino nitrogen atoms is manifested in the C-N-C

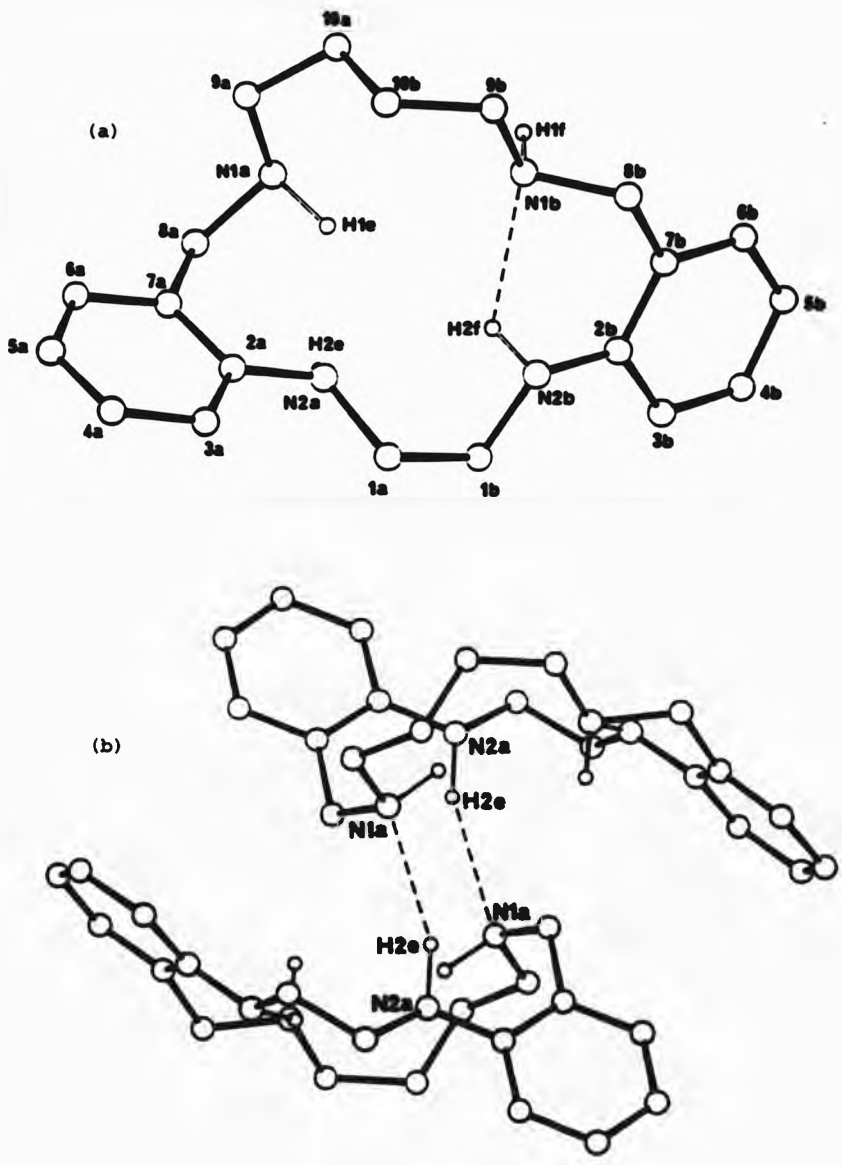


FIGURE 2.4 Two views of the structure of $L^{16}$ showing, (a) the intramolecular hydrogen bond (dashed lines) and (b) the intermolecularly hydrogen bonded dimeric unit.

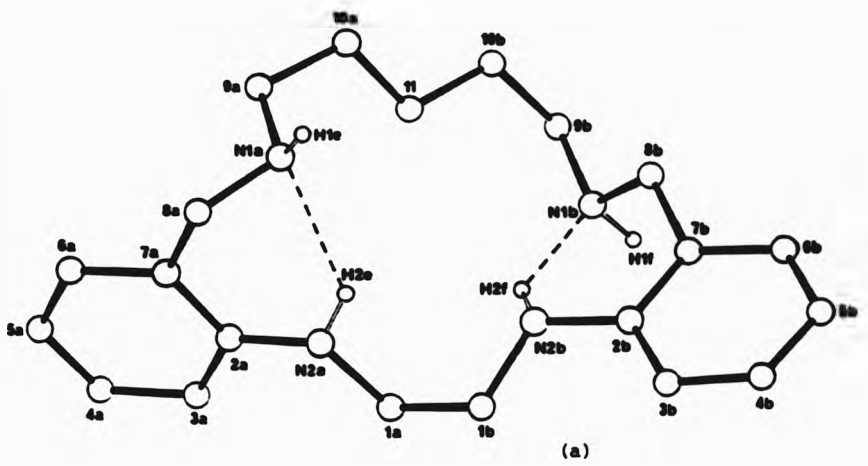


(a)

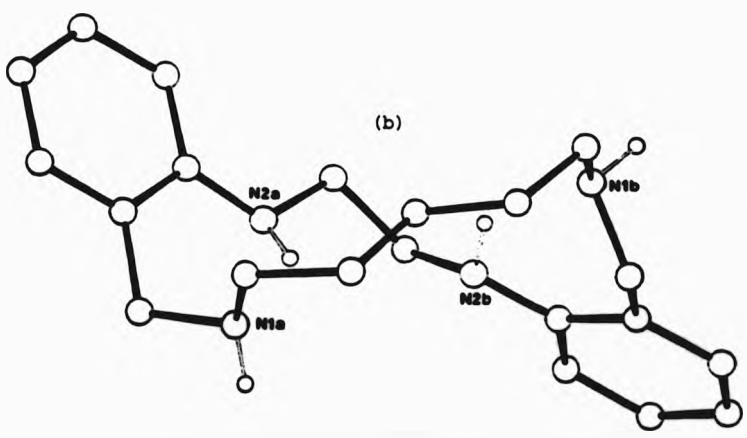


FIGURE 2.5 The structure of $L^{17}$ showing (a) the ligand cavity with the intramolecular hydrogen bonds (as dashed lines) and (b) the zig-zag conformation of the $-CH_2(CH_2)_3CH_2-$ chain and the twisted appearance of the ligand.

interbond angles. The C(2)-N(2)-C(1) angles in the five ligands range from 117 to 121°, consistent with a flattening of the anilino groups compared with the more pyramidal benzylamine functions. For the latter amines, the angles C(8)-N(1)-C(9) range from 108 to 113°, which are near to the ideal tetrahedral angle.

2.2.3.2 Co-planarity of the nitrogen atoms

The co-planarity of the four nitrogen atoms in each ligand may be described in two ways. As well as the deviation of the nitrogen atoms from their least-squares plane (Table 2.1), the dihedral angle ($\varphi$) between the plane defined by N(1a), N(2a) and CEN (CEN is the centroid of the four nitrogen atoms) and that defined by N(1b), N(2b) and CEN provides a convenient measure of this co-planarity.

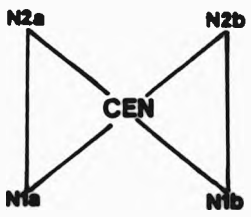


For $L^{14}$ and $L^{15Et}$, the dihedral angle $\varphi$ is 13° and 16°, respectively and the deviations of the nitrogen atoms are less than 0.16 Å for $L^{14}$ and about 0.2 Å for $L^{15Et}$. For $L^{15Bu}$, $\varphi$ is at a minimum (1°) corresponding to the much greater co-planarity of the $N_4$ set in this molecule (deviations are of the order of 0.01 Å). The structure of $L^{16}$ is twisted such that $\varphi$ is 25° and the four nitrogen atoms are not co-planar, but are disposed at the vertices of an oblate tetrahedron with deviations from their mean plane of ca. 0.3 Å. A much greater

TABLE 2.1 Deviations ( Å) from least-squares plane of nitrogen atoms in the free ligands.

| ligand | N(1a) | N(1b) | N(2a) | N(2b) |
|---|---|---|---|---|
| $L^{14}$(a) | 0.156 | -0.159 | -0.152 | 0.155 |
| $L^{15Et}$(b) | 0.185 | -0.185 | -0.202 | 0.202 |
| $L^{15Bu}$(b) | 0.011 | -0.011 | -0.013 | 0.013 |
| $L^{16}$ | 0.263 | -0.274 | -0.337 | 0.348 |
| $L^{17}$ | 0.301 | -0.405 | -0.670 | 0.774 |

(a) Calculated from data in Ref. 25; (b) calculated from data in Ref. 61.

TABLE 2.2 Intramolecular hydrogen bonding in the free ligands: interatomic distances ( Å) and angles (°) at the hydrogen atoms.(a)

| ligand | N(1)...N(2) | N(1)...H | N(2)-H...N(1) |
|---|---|---|---|
| $L^{14}$(b) | 2.83 | 2.01 | 137 |
| | 2.78 | 1.99 | 134 |
| $L^{15Et}$(c) | 2.82 | 1.99 | 140 |
| | 2.82 | 2.00 | 135 |
| $L^{15Bu}$(c) | 2.80 | 2.20 | 120 |
| | 2.87 | 2.05 | 130 |
| $L^{16}$ | 3.09 | 2.83 | 93(d) |
| | 2.87 | 2.24 | 125 |
| $L^{17}$ | 2.89 | 2.27 | 135 |
| | 2.87 | 2.04 | 137 |

(a) For each ligand, the first and second rows refer to the a- and b-halves of each molecule, respectively; (b) calculated from Ref. 25; (c) calculated from Ref. 61; (d) this angle and the longer distances are not consistent with the mode of hydrogen bonding that occurs in each of the other ligands (see text).

tetrahedral distortion is evident in $L^{17}$, with $\varphi = 56°$ and deviations of the nitrogen atoms of up to 0.77 Å.

2.2.3.3 Hydrogen bonding in the free ligands

The structures of $L^{14}$, $L^{15Et}$ and $L^{15Bu}$ all exhibit a pattern of intramolecular hydrogen bonding such that each anilino hydrogen atom is associated with the lone pair of the proximal benzylamino nitrogen atom, forming a cyclic six-membered hydrogen bonded unit in each chemically equivalent half of the molecule. These hydrogen bonds are indicated in the Figures by dashed lines and the geometry is summarized in Table 2.2. The N...N distances (2.78 to 2.89 Å) all lie within the van der Waals contact distance of 3.07 Å.[63] The N...H distances are between 1.99 and 2.20 Å and the angles at the hydrogen atom range from 120 to 140°. The same pattern is observed for $L^{17}$ with similar distances and angles. In $L^{16}$, however, only one of this type of intramolecular hydrogen bond is present, that across the b-half of the molecule, N(2b)-H(2f)...N(1b). In the a-half, the anilino hydrogen, H(2e), is directed towards the benzylamino nitrogen, N(1a), of a neighbouring molecule at equivalent position 1-x,-y,-z forming a centrosymmetric hydrogen bonded dimeric unit (N...N 3.51 Å, N...H 2.50 Å, N-H...N 155°). In contrast to the mode of hydrogen bonding in the other four compounds, in $L^{16}$ the hydrogen attached to the benzylamino nitrogen, H(1e), points into the ring and appears to be hydrogen bonded to the anilino nitrogen atom, N(2a). The distance N(1a)...N(2a) in $L^{16}$, 3.09 Å, is noticeably greater than corresponding distances in the other four ligands and in the b-half of $L^{16}$ (2.87 Å) and would seem to indicate a weaker hydrogen bond. Here, N(2a)...H(1e) = 2.18 Å and the angle at the hydrogen atom is 132°. This difference in the pattern of intramolecular hydrogen

bonding in the a-half of $L^{16}$ may be associated with a slight disorder of the corresponding phenylene ring. Figure 2.6 shows the thermal ellipsoids of the unsubstituted carbon atoms of both phenylene rings.

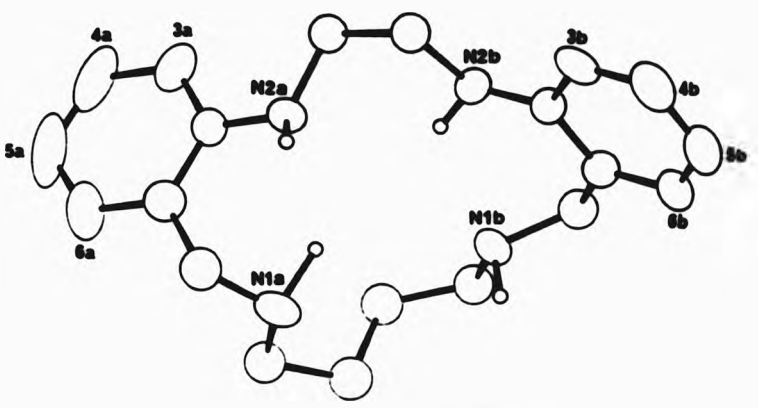


FIGURE 2.6 Thermal ellipsoid plot of $L^{16}$. The unsubstituted carbon atoms of the phenylene rings in the a-half of the molecule show a greater degree of ellipsoidal distortion than those in the b-half. Only the b-half contains an intramolecular hydrogen bond.

One of the anisotropic thermal parameters, $U_{11}$, (Table A1.3) of each of the unsubstituted phenylene carbon atoms of the a-ring is much larger than that for each corresponding atom of the b-ring. In some cases this value is more than double that of the corresponding atoms in the b-half [e.g. C(5a), $U_{11}$ = 0.200(12) $Å^2$, C(5b), $U_{11}$ = 0.079(6) $Å^2$].

The distinction between strong and weak hydrogen bonds is generally less pronounced for the N-H...N system than for the O-H...O.[64] The N...N distances for the intramolecular hydrogen bonds in all the ligands, although short (2.78 to 2.89 Å) do not necessarily mean that they are very strong. The small range of N...N

distances and absence of any trend indicate a lack of dependence of hydrogen bond strength on macrocyclic ring size; this distance is principally determined by the geometry of the phenylene ring substitution.

2.2.3.4 Phenylene ring geometry

The mean values of the C-C bond lengths in the phenylene rings of $L^{16}$ and $L^{17}$ are 1.388(11) and 1.386(8) Å, respectively. It is noteworthy that in each ring, the longest bond is that which also constitutes part of the macrocyclic inner great ring, namely C(2)-C(7). For $L^{16}$, these bond lengths are 1.401(9) and 1.415(9) Å and for $L^{17}$, 1.412(7) and 1.409(8) Å. For $L^{16}$, the deviations of the atoms of the phenylene rings from their respective mean planes are less than 0.01 Å, except for C(5a) (0.013 Å). For $L^{17}$, these deviations are less than 0.01 Å in the a-ring and less than 0.02 Å in the b-ring.

The closest non-bonding contact distance in the structure of $L^{16}$ is 1.92 Å between H(2f) and C(1b) and in $L^{17}$, 1.90 Å between H(8b) and N(1b).

2.2.4 Comparison of torsion angles in the ligands

The conformations of the macrocyclic inner great ring of the ligands (either free or complexed) may be precisely defined by the sequence of interbond torsion angles. A comparative study of these angles allows a qualitative assessment of the relative ligand strain in the series of ligands and complexes. A brief explanation of this structural parameter will be useful for the following discussion.

Consider the bond sequence in the four-atom fragment of a linear alkane, $-C_a-C_b-C_c-C_d-$. When viewed along the bond $C_b-C_c$, a torsion angle of X° represents a clockwise rotation, through X°, of the bond, $C_c-C_d$, from $C_a-C_b$. The sign of this angle does not depend upon the direction of the bond sequence. Torsion angles of 0, 60, 120 and 180° are classified as cis (c), gauche (g), anticlinal (ac) and anti (a), respectively. For $sp^3$ hybridized atoms, torsion angles of 60 and 180° are associated with the minimization of repulsions between further substituents on $C_b$ and $C_c$. Conversely, cis and anticlinal conformations are associated with maximum repulsions. Deviations of up to 30° from these angles may occur and, in the following discussion, a deviation of >20° is denoted by an asterisk. It needs to be noted that c = -c and a = -a, but neither g = -g nor ac = -ac and even slight deviations from 0 or 180° can change the sign of cis and anti torsion angles. In all the complexes and ligands, -N(2)-C(2)-C(7)-C(8)- is necessarily cis (with variations of up to 7°) since the bond forms part of a phenylene ring. This angle is otherwise disregarded in the following discussion. {As all the crystal structures considered here are centrosymmetric, pairs of enantiomeric species are present and the signs of the torsion angles in one enantiomer are reversed in the other. For ease of comparison, it was necessary to ensure that enantiomers of the same hand were chosen. In some cases this has required inversion of the species from that given in published work. For the step-shaped complexes corresponding to diastereoisomer V,

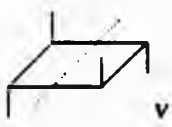

V

the enantiomer selected was that giving the S,S,S,S configuration sequence to the chiral amines. The hand of the remainder of the complexes was chosen such that the C(2a)-C(7a)-C(8a)-N(1a) torsion angle [-C(7a)-C(8a)- for brevity] is -g rather than g.}

$L^{14}$ has a step-shaped conformation with torsion angles of a or -a and g or -g [except for -C(2)-C(7)-] with no deformations greater than 14° (Table 2.3). Increasing the ring atomicity from 14 to 15, the ligands $L^{15Et}$ and $L^{15Bu}$ both have non-symmetric conformations with -C(1b)-N(2b)- gauche rather than anti and -C(7b)-C(8b)- g rather than -g. Deformations of more than 20° are apparent for -N(1b)-C(9b)- in both ligands, for -C(1b)-N(2b)- in $L^{15Bu}$, and for -C(9b)-C(10)- in $L^{15Et}$. The sequence of angles -C(8a)-N(1a)-C(9a)-C(10)- is -g,a,-g in $L^{15Et}$, but a,a,g in $L^{15Bu}$. In $L^{15Et}$ both hydrogen atoms on N(1a) and N(1b) are directed to the same side of the macrocyclic donor plane. This is not the case for $L^{15Bu}$. Although both butyl substituents are on the same side of the plane, the amine hydrogen atoms are on opposite sides. The conformation of $L^{16}$ is essentially the same as that of $L^{14}$ in the region of the ligand from C(8a) through the $C_2$-bridge to C(8b) with a maximum deformation of 12° from ideal angles. The signs of -C(7a)-C(8a)- and -C(7b)-C(8b)- are the same, indicating that the ligand is formally step-shaped. As in $L^{15Bu}$, one of the torsion angles -C(8)-N(1)- adopts the g conformation (rather than both a, as in $L^{14}$). The sequence from N(1a) through the $C_4$-bridge to N(1b) is a,-g,ac,-g,-a. Although the torsion angle, -C(10a)-C(10b)-, is designated as ac, implying eclipsed hydrogen atoms on C(10a) and C(10b), [H(10a) and H(10d)] the strain is relieved to some extent by the deformation of this angle from 120° to 138°. Despite the step-shaped appearance of $L^{17}$ (Figure 2.5), the torsion angles which define this conformation show it to be formally

TABLE 2.3 Endocyclic torsion angles (°) in the inner great ring of the $N_4$ macrocyclic ligands.(a,b)

| ligand or complex | Sequence of Torsion Angles | | | | | | | | |
|---|---|---|---|---|---|---|---|---|---|
| | ---1---- | N2---- | 2---- | 7---- | 8---- | N1---- | 9---- | | |
| $L^{14}$(c) | 62 | 170 | 175 | -2 | -53 | -178 | -162 | 70 | |
| | | 174 | 166 | 0 | -55 | 179 | -168 | | |
| | g | a | a | -c | -g | -a | -a | g | |
| | | a | a | -c | -g | a | -a | | |
| | ---1---- | N2---- | 2---- | 7---- | 8---- | N1---- | 9---- | 10 (d) | |
| $L^{15Et}$(e) | 69 | 174 | 179 | 2 | -50 | -67 | -170 | -65 | |
| | | 77 | -174 | 0 | 50 | 67 | 154 | 86 | |
| | g | a | a | c | -g | -g | -a | -g | |
| | | g | -a | c | g | g | a* | g* | |
| $L^{15Bu}$(f) | 63 | 166 | -176 | -3 | -52 | -174 | 166 | 60 | |
| | | 82 | 176 | -5 | 50 | 64 | 154 | 54 | |
| | g | a | -a | -c | -g | -a | a | g | |
| | | g* | a | -c | g | g | a* | g | |
| | ---1---- | N2---- | 2---- | 7---- | 8---- | N1---- | 9---- | 10---- | |
| $L^{16}$ | 69 | 177 | -169 | -2 | -63 | -69 | 162 | -78 | 138 |
| | | -169 | 168 | 5 | -57 | 180 | -166 | -72 | |
| | g | a | -a | -c | -g | -g | a | -g | ac |
| | | -a | a | c | -g | a | -a | -g | |
| | ---1---- | N2---- | 2---- | 7---- | 8---- | N1---- | 9---- | 10---- | 11 |
| $L^{17}$(g) | 71 | 175 | 180 | -1 | -56 | -68 | 168 | -66 | -175 |
| | | 163 | -161 | -4 | 51 | 180 | 64 | 54 | -179 |
| | g | a | a | -c | -g | -g | a | -g | -a |
| | | a | -a | -c | g | a | g | g | -a |

(a) For each compound, the first and second rows represent the torsion angles in the a- and b-halves of the macrocycle, respectively. The third and fourth rows show the corresponding designations [a = anti, 180±30°; g = gauche, 60±30°; ac = anticlinal, 120±30°; c = cis, 0±30°; * = deformation >20°]. (b) Carbon atoms are denoted by numerals only. (c) Calculated from Ref. 25. (d) This atom is labelled 9(c) in Refs. 38 and 44. (e) Hand reversed from that in Ref. 44. (f) Ref. 44. (g) Hand reversed from that given in Appendix.

saddle-shaped; -C(7a)-C(8a)- and -C(7b)-C(8b)- are of opposite sign. The apparent step-shape, with the phenylene rings disposed to either side of the $N_4$-plane, is associated with the torsion angle -N(1b)-C(9b)- being gauche instead of (as it is in the other ligands) anti. The sequence of torsion angles through the pentamethylene bridge has already been mentioned and gives this area of the molecule the extended zig-zag conformation associated with linear alkanes. Such an extended conformation is an important contributory factor in determining the large hole size of $L^{17}$.

2.2.5 Hole sizes of the free ligands

Using the same procedure developed for the complexes (described in §1.5), the hole sizes for the free ligands have been calculated and are plotted in Figure 2.7. Even though the ligands are not suitably oriented for complexation, the hole sizes increase almost linearly (0.1 Å for each additional methylene group) up to $L^{16}$, but $L^{17}$ exhibits a more dramatic increase (almost 0.2 Å). It is interesting to compare the distance between the benzylamino nitrogen atoms, N(1a)...N(1b), as the number of intervening methylene groups is increased. In $L^{14}$ this distance is 2.90 Å. No data is available for $L^{15}$, but the different conformations of the $C_3$-bridge in $L^{15Et}$ (chair) and $L^{15Bu}$ (twist) give rise to distances of 3.27 and 3.79 Å, respectively. In $L^{16}$, the distance is about the same as that in $L^{15Bu}$, 3.76 Å. The extended conformation of the $C_5$-bridge in $L^{17}$ increases the N(1a)...N(1b) distance to 5.38 Å, half as much again as that in $L^{16}$. This increasing distance is the main contributory factor in the dramatic increase of hole size in the free ligands on passing from $L^{16}$ to $L^{17}$. The significance of this will become more apparent in the discussions of the hole sizes of the nickel(II), zinc(II) and

cadmium(II) complexes in Chapter Five.

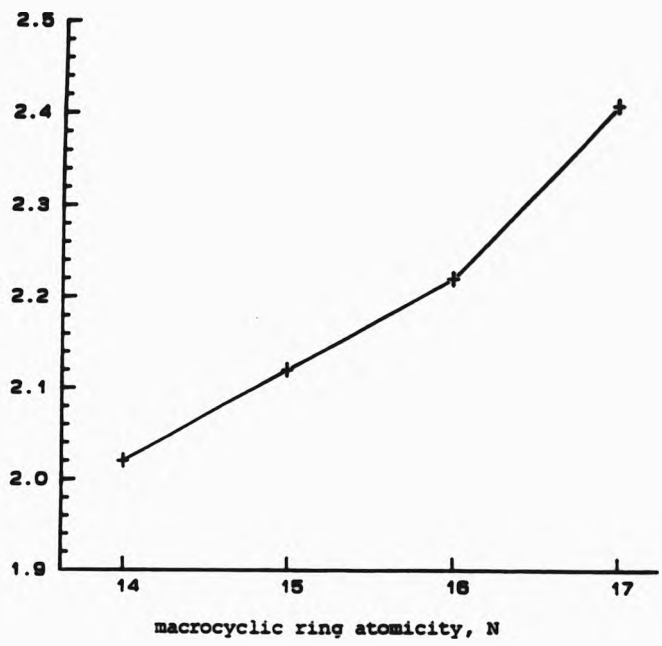


FIGURE 2.7 The variation of macrocyclic hole size, $R_H$/ Å, with macrocyclic ring atomicity, N, for the free ligands. $R_H$ is calculated according to the method in Ref. 23 from X-ray structure determinations. $L^{14}$ from Ref. 25, for N = 15, the hole size is the mean of those calculated for $L^{15Et}$ (2.10 Å) and $L^{15Bu}$ (2.14 Å) from Ref. 44.

## 2.3 NMR spectra

Elucidation of the solution structure of the ligands has now been attempted using multinuclear and two-dimensional NMR spectroscopy. The number and the multiplicity of the observed signals in the $^{1}H$, $^{13}C$ and $^{15}N$ NMR spectra indicate that, in solution, corresponding nuclei in the a- and b-halves of the macrocycles exhibit chemical shift

equivalence by way of a two-fold rotation axis or a mirror plane through the mid-point of the alkyl bridges.[65] Motional averaging of the alkyl groups contributes to this equivalence as the molecules have some degree of flexibility, but the shapes and intensity ratios of some $CH_2$ multiplets display effects due to signal overlap and, for $L^{15}$, non-first order behaviour resulting from chemical shift non-equivalence of the hydrogen atoms attached to C(1a) and C(1b) (see below).[65]

The $^1H$ NMR spectrum of a dilute solution of $L^{16}$ showed little change from that of the saturated solution, even in the chemical shifts of the amine hydrogen atoms (<0.1 p.p.m.), showing that the dependence of chemical shift on concentration is only slight.

2.3.1 $^1H$ NMR spectra

The $^1H$ NMR spectrum of $L^{14}$ (Figure 2.8) includes two broad peaks at $\delta$ = 1.2 and 6.82 p.p.m., each integrating for two protons. These collapse on deuteriation, so are ascribed to amino hydrogen resonances. On the basis of their chemical shifts, the more downfield signal is assigned to the anilino hydrogen atoms. The chemical shifts for RNHR and ArNHR are variable but are expected to lie in the range $\delta$ = 1-5 and 3-6 p.p.m. respectively.[66] The non-bonding electrons of the nitrogen atom are delocalized into the aromatic system causing deshielding of the anilino hydrogen. The variation in chemical shifts through the ligand series is slight. Table 2.4 lists the chemical shifts and assignments of the signals from the non-aromatic protons in $L^{14}$ to $L^{17}$. Three signals arising from the methylene protons, H(1), H(8) and H(9) appear as sharp singlets, each integrating for four protons. Green, Smith and Tasker have assigned the $^1H$ NMR spectrum of the diimines $P^{14}$, $P^{15}$ and $P^{16}$, which contain one less methylene group

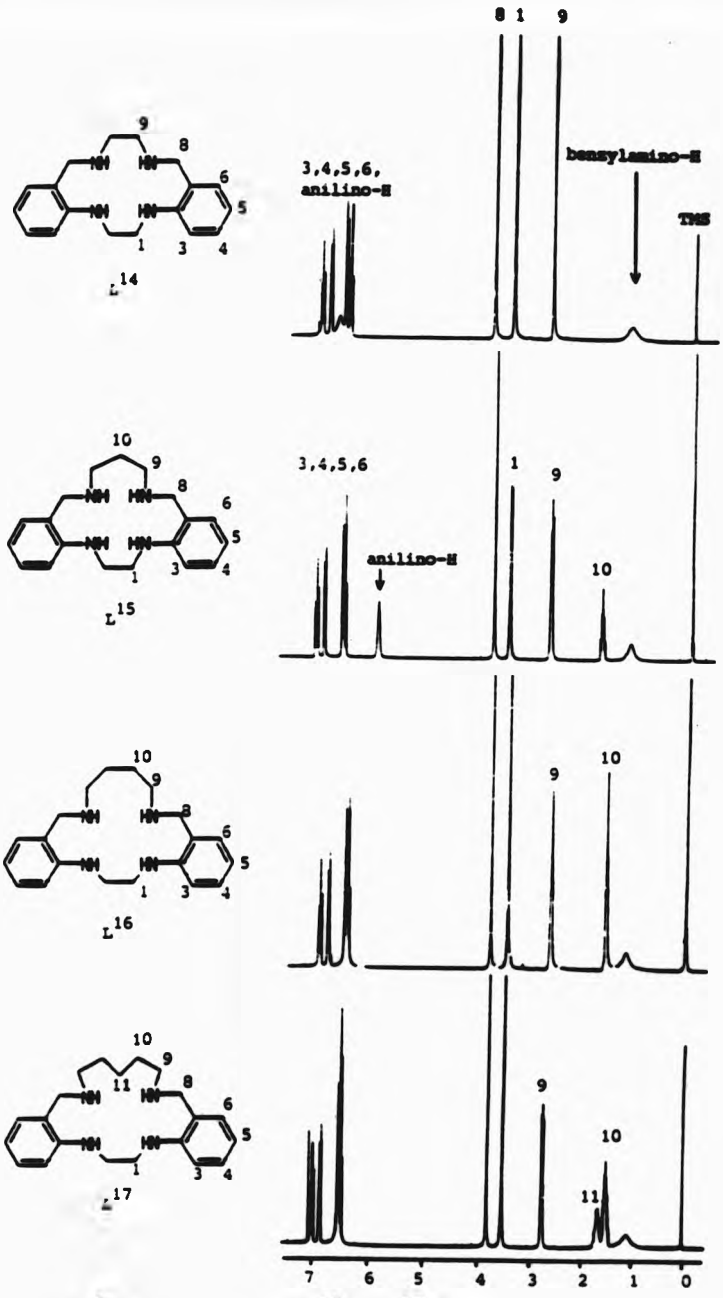


FIGURE 2.8 The $^{1}H$ NMR spectra of $L^{14}$ to $L^{17}$ at 250.133 MHz as saturated solutions in $CDCl_3$, relative to TMS ( $\delta$ = 0 p.p.m.), T = 300 K. The atom numbering scheme used for the crystal structure determinations is retained.

TABLE 2.4 $^{1}$H NMR shifts(a) ($\delta$/ p.p.m.) of methylene and amine protons in the macrocycles.(b)

| ligand | methylene | | | | | -NH- | |
|---|---|---|---|---|---|---|---|
| | H(1) | H(8) | H(9) | H(10) | H(11) | RNHR | ArNHR |
| $L^{14}$ | 3.44 | 3.81 | 2.71 | - | - | 1.12 | 6.82 |
| $L^{15}$ | 3.45 | 3.75 | 2.70 | 1.71 | - | 1.17 | 5.97 |
| $L^{16}$ | 3.44 | 3.77 | 2.63 | 1.56 | - | 1.21 | 6.64 |
| $L^{17}$ | 3.46 | 3.75 | 2.70 | 1.46 | 1.60 | 1.05 | 6.64 |
| $L^{17}$(c) | 3.32 | 3.62 | 2.56 | 1.39 | 1.51 | 1.95 | 6.78 |

(a) At 250.133 MHz, as saturated solutions in $CDCl_3$, T = 300 K, with respect to TMS ($\delta$ = 0 p.p.m.); (b) the atom numbering scheme is illustrated in Figure 2.8; (c) in dimethylsulphoxide-$d_6$.

TABLE 2.5 $^{1}$H NMR shifts(a) of aromatic protons in ligands $L^{14}$ to $L^{17}$.(b)

| ligand | H(3) | H(4) | H(5) | H(6) |
|---|---|---|---|---|
| $L^{14}$ | 6.71(d) | 7.17(td) | 6.62(td) | 7.28(dd) |
| $L^{15}$ | 6.67(ov) | 7.18(td) | 6.64(ov) | 7.03(dd) |
| $L^{16}$ | 6.67(dd) | 7.16(td) | 6.61(td) | 7.00(dd) |
| $L^{17}$ | 6.66(ov) | 7.17(td) | 6.61(ov) | 7.01(dd) |

(a) At 250.133 MHz, as saturated solutions in $CDCl_3$, T = 300 K, with respect to TMS ($\delta$ = 0 p.p.m.), d = doublet, td = triplet of doublets, dd = doublet of doublets, ov = overlapping; (b) the atom numbering scheme is illustrated in Figure 2.8. For each proton, the shift given is the mean of all the observable peaks in the multiplet.

than the corresponding tetraamines.[55] By comparison with these, the most downfield methylene signal in the spectrum of $L^{14}$ ($\delta$ = 3.81 p.p.m.) is assigned to the benzyl methylene hydrogen atoms, H(8), which suffer the combined deshielding effects of both the aromatic ring and the amine group; notwithstanding that the modified Shoolery rules in Reference 66 predict a shift of 3.5 p.p.m. for hydrogen atoms in this environment. Accepting this assignment for the moment, the two upfield signals must be due to the protons H(1) and H(9). These can readily be identified by consideration of the spectra of the larger ligands. On increasing the number of atoms in the benzylamino bridge, the H(1) signal for each ligand remains fairly constant at between 3.44 and 3.46 p.p.m. and that corresponding to H(9) (at 2.63 to 2.71 p.p.m.) splits because of spin-spin coupling to its neighbours.

The signals from the aromatic protons in $L^{14}$ to $L^{17}$ (Table 2.5) are sufficiently well resolved to see effects of three and four bond coupling of ca. 7-8 Hz and ca. 1 Hz, respectively, although the coupling constants are not readily determined, because of slight broadening of signals and, in $L^{15}$ and $L^{17}$, to overlap of signals from H(3) and H(5). By combining the substituent effects for the most appropriate groups ($-NHCH_3$ and $-CH_2NH_2$) the "doublets" arising from H(3) and H(6) are easily distinguished with expected shifts of around 6.5 and 7.0 p.p.m. respectively and the "triplets" arising from H(4) and H(5) expected at 7.0 and 6.7 p.p.m. respectively.[66] This pattern is in surprisingly good agreement with the observed chemical shifts considering the approximate match of substituents. The assignments were confirmed for $L^{15}$ and $L^{17}$ by a $^{13}C$ INADEQUATE experiment (see §2.3.2) in conjunction with the C-H COSY plots.

The spectrum of $L^{15}$ (Figures 2.8 and 2.9) shows two features which differentiate it from the other ligands. The peaks assigned to the NH protons appear at 1.17 and 5.97 p.p.m., the latter being less broad and more upfield than the corresponding signal in $L^{14}$, $L^{16}$ and $L^{17}$. The two signals of the methylene protons, H(9) and H(10), are readily assigned on the basis of their multiplicity and integration; the signal arising from the unique methylene group, H(9), is split into a distorted quintet which integrates for two protons and that from H(10) is split into a distorted triplet integrating for four protons. In contrast to that in the other ligands, the H(1) signal is not a singlet, but, when expanded (inset in Figure 2.9) can be seen to have a complex band shape. It appears as two peaks separated by 5.2 Hz containing two further peaks of lower intensity separated by 1.2 Hz and two low intensity peaks appearing as little more than shoulders on the outside of the multiplet. This signal collapses to a singlet on deuteriation indicating that the observed splitting is, at least in part, due to coupling to the anilino-NH protons. This spin-spin coupling of the H(1) protons is clearly demonstrated in the homonuclear $^1H$ COSY contour plot in Figure 2.9. Similar coupling (Figure 2.10) between NH and $CH_2$ has been observed in a $N_4S_2$ ligand (2.iii) containing two pyrido nitrogen atoms.[67]

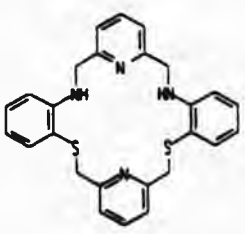


(2.iii)

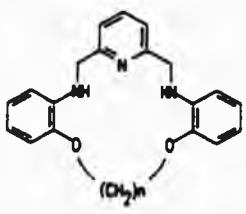


(2.iv)

In this ligand, a coupling constant of ca. 5.7 Hz can be clearly seen

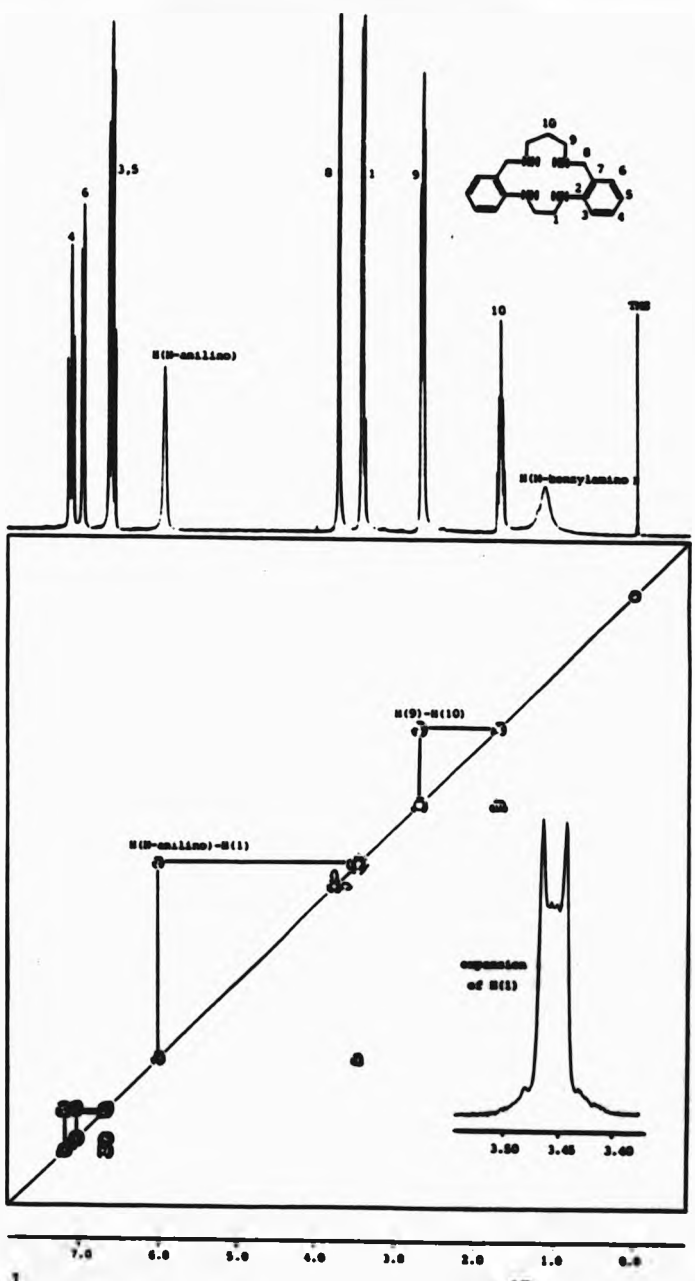


FIGURE 2.9 $^{1}$H COSY contour plot and 1-D spectrum of $L^{15}$ showing the spin-spin coupling between the anilino protons and the four H(1) protons. Inset is an expansion of the signal from H(1), the appearance of which is complicated by mutual coupling of the four methylene protons.

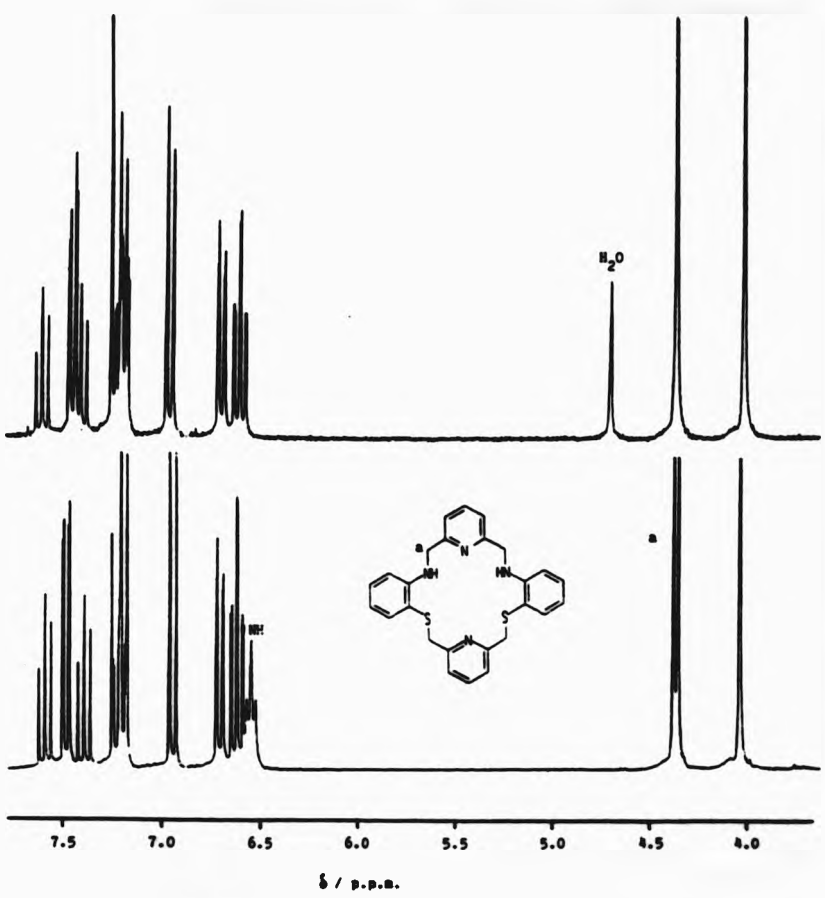


FIGURE 2.10 The $^1H$ NMR spectra of (2.iii) (a) with and (b) without the addition of $D_2O$. The spin-spin coupling of the protons at 'a' with the anilino protons is clearly apparent from the splitting of both peaks. The effect is more marked here than in the spectrum of $L^{15}$. Spectra reproduced with permission from Ref. 67.

in the signals from both proton types ($CH_2$ doublet, NH triplet), but the $CH_2$ signal is not complicated by coupling to other $CH_2$ groups. The $^1H$ NMR spectra (at 250 MHz in $CDCl_3$) of a homologous series of $O_2N_3$ ligands (2.iv, n = 2, 3, 4 and 6) have been reported.[68] The signal (ca. 4.5 p.p.m.) due to the aminomethylene protons is seen as a singlet when n = 2 and 4, but as a doublet when n = 3 and 6. Furthermore, the NH signal is split into a triplet when n = 6, but otherwise appears as a singlet. It seems that the observation of this type of coupling, governed as it is by the relative rate of exchange of the amine hydrogen atom, is a sensitive indicator of enhanced conformational rigidity. Irradiation of $L^{15}$ at the midpoint of the anilino-NH signal also brings about collapse of the H(1) signal to a structureless singlet and not to a split peak which would be expected if the four protons, H(1), were non-equivalent and mutually coupled. A further effect arising from this double resonance experiment is that the signal from the benzylamino-NH protons suffers a loss of intensity. That coupling to the anilino-NH protons occurs at all indicates that the NH protons are exchanging relatively slowly; this would be expected if the intramolecular hydrogen bond was comparatively strong, or, more likely, if the gross conformation of the ligand was exchanging slowly. As the number of methylene units bridging the benzylamino nitrogen atoms is increased, the decrease in rigidity will allow gross changes in conformation to occur more rapidly. The methylene protons, H(1), will be observed to be equivalent if either a symmetry element exists between them, or if molecular motion around the C(1a)-C(1b) bond (approximating to a symmetry operation) is rapid on the NMR timescale.[69] The non-equivalence of the protons H(1), in $L^{15}$, whether geminal or vicinal, is observable in the spectrum. This may be explained by a consideration of the interconversion of the

ligands between the step and saddle conformations which requires the inversion of one of the benzylamine nitrogen atoms with concomitant breaking and reforming of its intramolecular hydrogen bond. If it is assumed that for $L^{15}$, the barrier to this interconversion is high, both isomers or the predominant (lowest energy) one would be observable. It can be seen that differences in the two-fold symmetry of the ligands in the step and saddle arrangements will lead to chemical shift non-equivalence of the methylene protons of the bridging alkyl chains. In the saddle conformation, the environment on one side of the macrocyclic donor plane is different to that on the other side, whereas the environments are comparable in the step conformation. Figure 2.11 shows the saddle-shaped precursor diimine $P^{15}$ in which the potential mirror symmetry is broken by the $C_2$-bridge between the anilino nitrogen atoms.

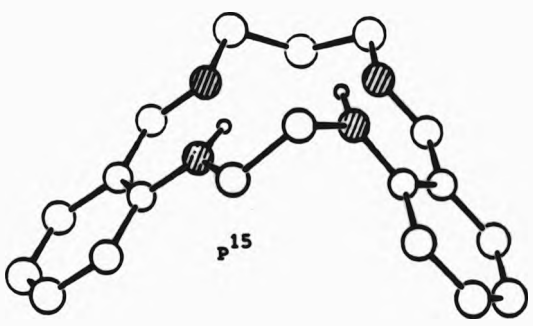


FIGURE 2.11 The saddle-shaped structure of the diimine, $P^{15}$. The pseudo-mirror plane breaks down at the ethylene bridge (redrawn from Ref. 44).

The pseudo-mirror plane symmetry of the ligand with the $C_3$-bridge in the 'chair' conformation would be expected to impart a geminal non-equivalence to the protons H(1) even if the dynamic process of the inversion of their gauche conformation is rapid. Inversion of the gauche conformation of the $C_2$-bridge can occur without concomitant inversion of the anilino nitrogen atoms and does not require hydrogen bond breaking; the lone pair is delocalized giving a more flattened amine with considerable $sp^2$ character. Of course, the molecules are not completely rigid in solution, the conformational equilibria will average out to some extent the differences in environment, but the effects of non-equivalence may be observable if a predominance of one conformation is present. The spin-spin coupling of the H(1) protons to the anilino-H has been demonstrated, but the complex appearance of the H(1) peak indicates that some other factor is present, which is lost on deuteriation and on decoupling by irradiation of the anilino protons. The addition of $D_2O$ to the NMR solution of $L^{15}$, by providing molecules capable of hydrogen bonding to the benzylamino lone pairs, reduces the energy barrier to the conformation changes described above, so that the H(1) protons become equivalent by motional averaging via more rapid benzylamino nitrogen inversion and a single peak is observed.

2.3.2 $^{13}C$ NMR spectra of the ligands and precursors

The $^{13}C$ NMR spectra of the non-cyclic precursors are unremarkable, but serve as a useful starting point for the assignment of the spectra of the macrocycles. The assignments for the non-aromatic resonances are given in Table 2.6 with the ranges expected for each type of carbon atom.[70] The bridging methylene carbons of the ubiquitous $C_2$-bridge show only a small shift variation (41.6-42.2 p.p.m.) despite major,

TABLE 2.6 $^{13}C$ NMR resonances ($\delta$/ p.p.m.) and assignments for non-aromatic carbon atoms of methyl 2-aminobenzoate (MAB) and intermediates in the synthesis of the ligands.(a,b)

| compound | carbon atom type | | |
|---|---|---|---|
| | $OCH_3$(42-58) | COO(167-176) | $NCH_2$(37-62) |
| MAB | 51.4 | 168.7 | - |
| Ia | 51.5 | 169.1 | 42.2 |
| | | $CH_2OH$(40-70) | |
| Ib | - | 64.7 | 42.1 |
| | | CHO(196-207) | |
| Ic | - | 194.1 | 41.6 |

(a) At 20.12 MHz in $CDCl_3$ relative to TMS ( $\delta$ = 0 p.p.m.);
(b) numbers in parentheses after each atom type are the expected ranges based on the correlation chart in Ref. 70.

TABLE 2.7 $^{13}C$ NMR shifts(a) ($\delta$/ p.p.m.) of the non-aromatic carbon atoms in the di-imine precursors.(b)

| compound | methylene | | | | imine |
|---|---|---|---|---|---|
| | C(1) | C(9) | C(10) | C(11) | C(8) |
| $P^{14}$ | 41.9 | 61.0 | - | - | 163.4 |
| $P^{15}$ | 40.4 | 62.9 | 33.5 | - | 164.0 |
| $P^{16}$ | 41.2 | 60.6 | 27.5 | - | 164.2 |
| $P^{17}$ | 42.1 | 60.5 | 30.9 | 24.2 | 164.0 |

(a) At 20.12 MHz in $CDCl_3$ relative to TMS ( $\delta$ = 0 p.p.m.);
(b) see Figure 2.8 for the atom numbering scheme.

but remote, structural differences in the molecules. This observation aided the assignment of the methylene signals in the spectra of the macrocycles. Assignment of the methylene carbon signals of the diimines is simplified somewhat due to the incremental nature of the ring expansion (Table 2.7). For each ligand, a heteronuclear $^{1}H$-$^{13}C$ COSY was obtained and from the cross-peaks and the assignments of the methylene proton signals, the corresponding signals in the $^{13}C$ NMR spectrum were assigned. Such a $^{1}H$-$^{13}C$ COSY plot (for $L^{17}$) is illustrated in Figure 2.12. The shifts are near constant for each atom as extra carbon atoms are inserted in the alkyl bridge, the more so for those atoms remote from the site of the insertion. For those molecules with an odd number of atoms in the alkyl chain, the signal corresponding to the (unique) apical atom is readily assigned from its lower intensity. The imine signal in the precursor diimines may be confidently assigned because of its large downfield shift. In a similar manner, the signals for the methylene groups bridging the amine donors in the tetraamines were assigned (Table 2.8).

It was still not possible to assign with confidence the unsubstituted phenylene $^{13}C$ signals. As with the aromatic proton signals, estimates of the chemical shifts for the aromatic carbon signals of the ligands were obtained by combining the the substituent effects of the most appropriate groups ($-NHCH_3$ and $-CH_2NHCH_2Ph$) from Reference 70. These are included in Table 2.9. The agreement between the calculated and observed chemical shift values is remarkably good; for $L^{14}$ for example, the greatest difference is only 1.5 p.p.m. [for C(2)].

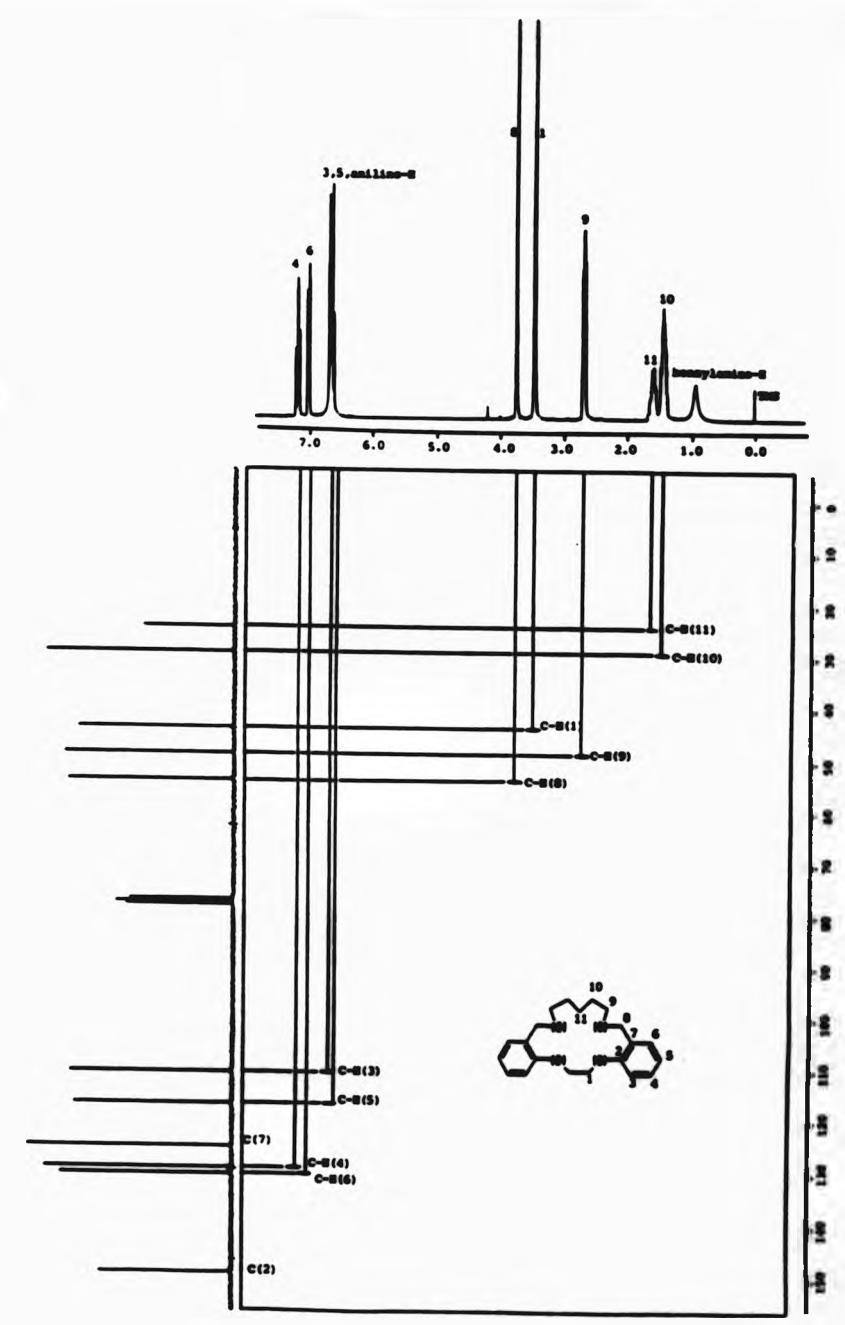


FIGURE 2.12 $^{13}C$-$^{1}H$ COSY of $L^{17}$.

The connectivity of the carbon atoms in $L^{15}$ and $L^{17}$ was established with the use of an $^{13}C$ INADEQUATE (incredible natural abundance double quantum experiment).[71] This technique detects signals due to homonuclear one-bond coupling. In natural abundance samples, only a very small proportion of the $^{13}C$ nuclei will have $^{13}C$ neighbours and the number of molecules with three connected $^{13}C$ nuclei will be negligible.

TABLE 2.8 $^{13}C$ NMR shifts(a) ($\delta$/ p.p.m.) of methylene carbon atoms in the ligands.(b)

| ligand | C(1) | C(9) | C(8) | C(10) | C(11) | C(12) |
|---|---|---|---|---|---|---|
| $L^{14}$ | 42.17 | 53.64 | 48.85 | - | - | - |
| $L^{15}$ | 41.68 | 54.25 | 48.08 | 29.93 | - | - |
| $L^{16}$ | 42.94 | 53.52 | 47.81 | 27.40 | - | - |
| $L^{17}$ | 43.47 | 53.59 | 48.42 | 29.05 | 24.15 | - |
| $L^{19}$ | 44.3 | 53.8 | 48.2 | 28.8 | 26.1 | 27.5 |

(a) At 62.896 MHz (20.12 MHz for $L^{19}$) in $CDCl_3$ relative to TMS ($\delta$ = 0 p.p.m.), T = 300 K; (b) see Figure 2.8 for the atom numbering scheme.

The INADEQUATE responses are all due to isolated pairs of nuclei. This is a very insensitive technique requiring large amounts of sample, high solubility and a long data acquisition time. The spectrum reproduced in Figure 2.13 was acquired over sixty-five hours using a saturated solution of $L^{15}$ in $CDCl_3$. Despite the low signal to noise ratio, every possible direct C-C connection is apparent. Starting from previously assigned signals, e.g. the methylenes

TABLE 2.9 $^{13}C$ NMR shifts(a) ($\delta$/ p.p.m.) for aromatic carbons in the precursors and ligands.(b)

| compound | C(2) | C(3) | C(4) | C(5) | C(6) | C(7) |
|---|---|---|---|---|---|---|
| MAB(c) | 150.8 | 116.2 | 134.2 | 116.8 | 131.3 | 110.7 |
| Ia | 151.0 | 111.2 | 134.7 | 115.0 | 131.9 | 110.5 |
| Ib | 147.4 | 110.9 | 129.4 | 116.9 | 129.7 | 124.4 |
| Ic | 150.5 | 110.7 | 136.9 | 115.5 | 135.9 | 118.9 |
| $P^{14}$ | 149.8 | 111.1 | 131.2 | 115.0 | 133.7 | 118.6 |
| $P^{15}$ | 148.9 | 110.1 | 131.1 | 114.7 | 134.0 | 117.9 |
| $P^{16}$ | 148.9 | 109.7 | 131.1 | 114.5 | 134.0 | 117.7 |
| $P^{17}$ | 149.1 | 109.7 | 131.1 | 114.5 | 133.9 | 117.7 |
| $L^{14}$ | 148.40 | 110.69 | 128.53 | 116.32 | 129.58 | 124.16 |
| $L^{15}$ | 147.58 | 109.99 | 128.52 | 116.46 | 129.74 | 124.20 |
| $L^{16}$ | 148.36 | 110.02 | 128.36 | 115.96 | 129.65 | 123.86 |
| $L^{17}$ | 148.60 | 109.99 | 128.40 | 116.06 | 129.62 | 124.32 |
| $L^{19}$ | 148.8 | 110.5 | 128.5 | 116.3 | 129.6 | 124.3 |
|  | 149.9 | 111.8 | 127.4 | 115.6 | 128.6 | 124.0(d) |

(a) At 20.12 MHz for all except $L^{14}$ to $L^{17}$ (62.896 MHz) as saturated solutions in $CDCl_3$ relative to TMS ( $\delta$ = 0 p.p.m.); (b) the atom numbering scheme is as given in Figure 2.8 with the addition of C(2) for the anilino and C(7) for the benzyl-substituted carbon atoms; (c) MAB = methyl 2-aminobenzoate; (d) values calculated for the ligands from the combined substituent effects of $-NHCH_3$ and $-CH_2NHCH_2Ph$ given in Ref. 70.

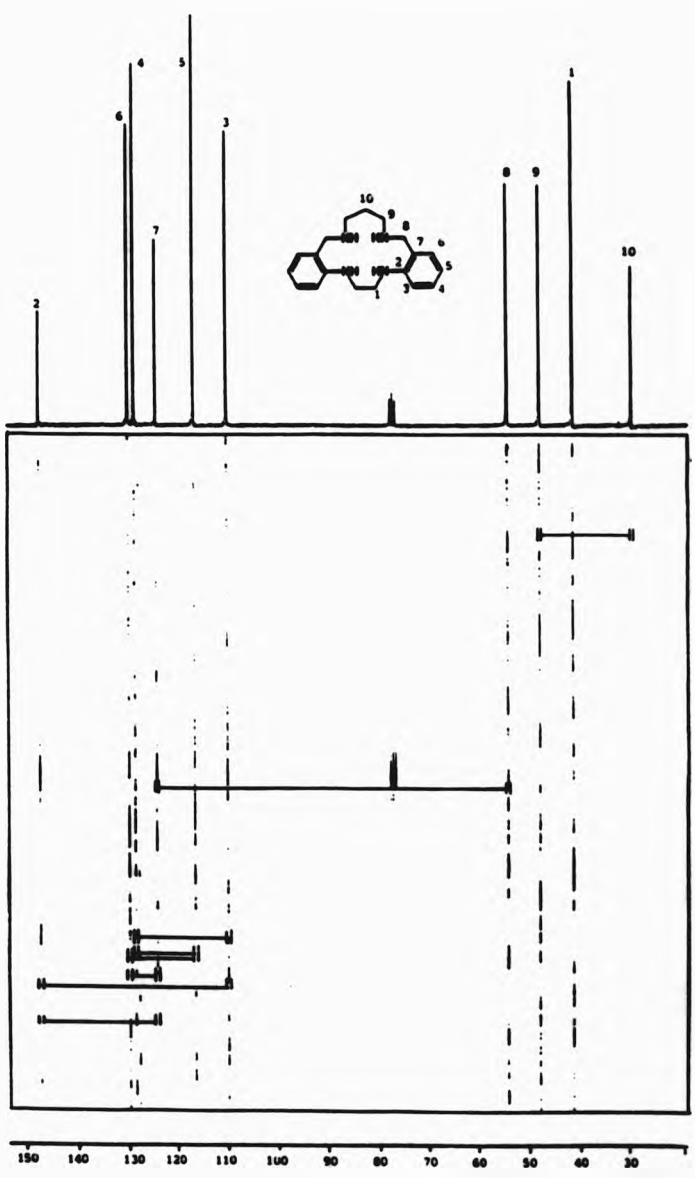


FIGURE 2.13 Plot of $^{13}C$ INADEQUATE responses for $L^{15}$.

assigned from the COSY experiments and the anilino substituted aromatic carbon, it is possible to determine the connectivity of the molecule. This was especially useful for the unsubstituted aromatic carbon atoms. Figure 2.14 shows an expansion of the $^{13}C$ INADEQUATE plot in the region of the aromatic signals for $L^{17}$. Starting with the substituted carbon atoms C(2) and C(7) which, of course, give no cross-peak on the $^{1}H$-$^{13}C$ COSY plots of the ligands (Figure 2.12) the connectivity of the aromatic carbon atoms can be readily traced.

As the ring size is increased, a small but significant downfield trend in the signals for the carbon atoms of the $C_2$-bridge is apparent. Ignoring $L^{15}$ for the moment, as the ring size is increased, the plot of macrocyclic ring atomicity against the chemical shift of C(1) is surprisingly linear (Figure 2.15) with an incremental downfield shift of ca. 0.4 p.p.m. per additional methylene unit. The lop-sided expansion of the ring coupled with the restricted conformations imposed by the two intramolecular hydrogen bonds has the effect of deforming the bond between the two carbon atoms, C(1a)-C(1b), and producing the small downfield shift. The chemical shift of C(1) in $L^{15}$ does not follow this linear trend, but falls lower than expected. The chemical shifts of carbon-13 atoms are particularly sensitive to conformational differences.[72] This anomalous shift may be a consequence of the predominance of the saddle conformation of $L^{15}$.

Comparable systems to the above are limited, since a continuous range of ring sizes is required with the hydrogen bonding pattern and one-sided ring expansion being present. However, Figure 2.15 illustrates the same effect for a series of $O_2N_3$ ligands (2.iv) bearing a fused pyrido substituent and two fused phenylene rings.[68]

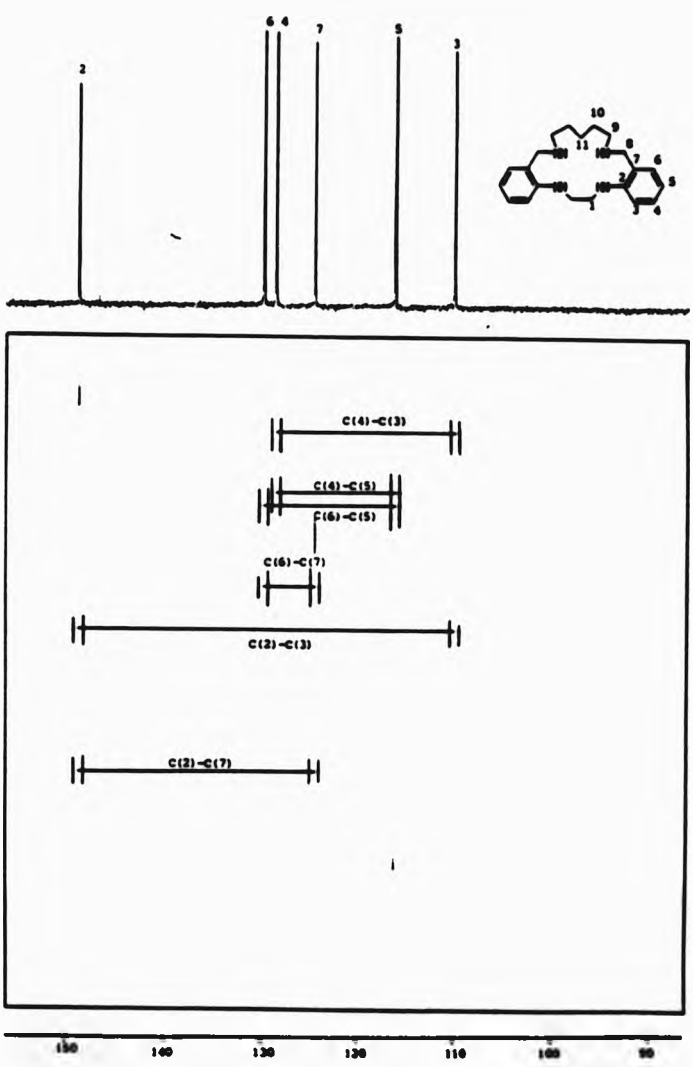


FIGURE 2.14 Expansion of the aromatic carbon atom region of the plot of $^{13}C$ INADEQUATE responses for $L^{17}$.

The sixteen-membered ligand incorporating the $C_3$-bridge between the phenoxy-ether oxygens shows a similar distinct discontinuity in the plot of ring-size versus chemical shift of the (equivalent) methylene carbon atoms attached to the 2- and 6-positions of the pyrido ring.

FIGURE 2.15 The variation of $^{13}C$ chemical shift of $C^{\alpha}$ with macrocyclic ring atomicity for the ligands $L^{14}$ to $L^{19}$ and for the series of ligands (2.iv) (from Ref. 68).

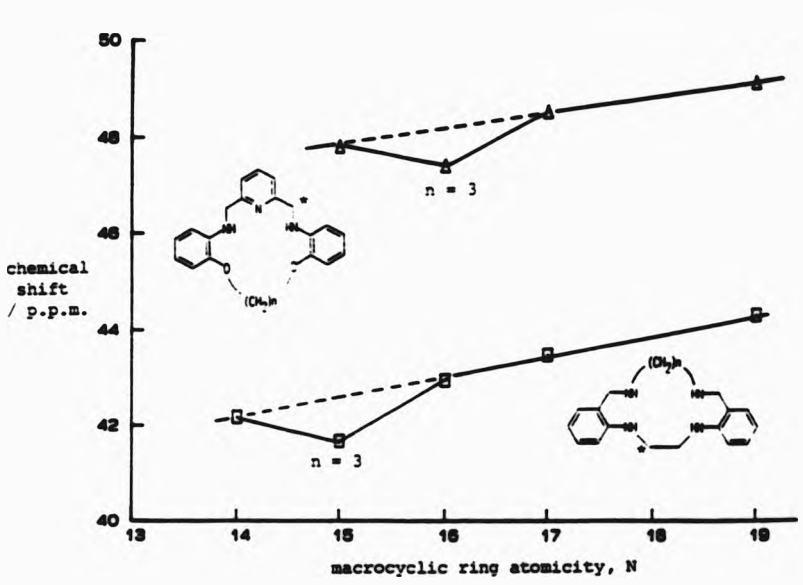


Otherwise, the plot is again linear for the fifteen-, seventeen- and nineteen-membered macrocycles with a downfield shift of ca. 0.3 p.p.m. per additional methylene unit. The similarity between these plots is remarkable, considering the differences in structure between the two ligand series and in each series indicates an anomalous behaviour of the $C_3$-bridged compounds.

A plot of the $^{13}C$ NMR shift of C(1) versus the endocyclic torsion angle N(1a)-C(1a)-C(1b)-N(1b), calculated from the X-ray crystal structure determinations of $L^{14}$, $L^{16}$ and $L^{17}$ is presented in Figure 2.16.

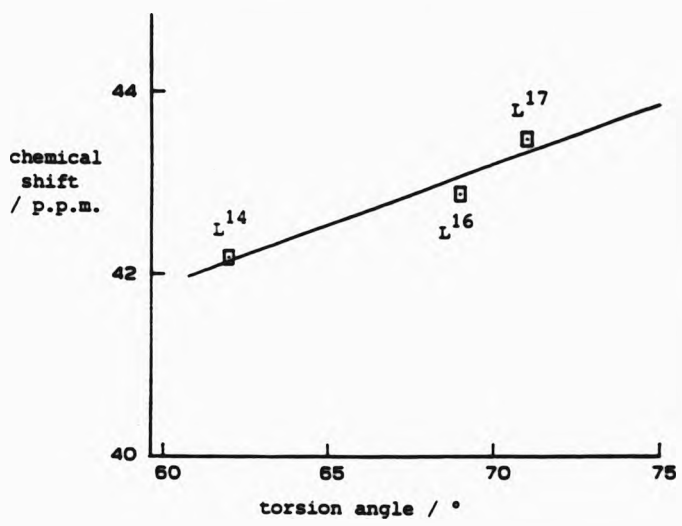


FIGURE 2.16 The increase in the endocyclic torsion angle -C(1a)-C(1b)- with increasing macrocyclic ring atomicity for the structures of the free ligands $L^{14}$, $L^{16}$ and $L^{17}$.

Admittedly, caution must be exercised in relating data from solid state studies to those from solution studies because intermolecular forces and rates of dynamic processes are not the same. Nevertheless, deformation of this torsion angle from 60° will increase the interaction between the vicinal $CH_2$ hydrogen atoms. The perturbation of the C-H bonds involved will cause the charge to drift towards carbon and an increased shielding will arise,[70] The limited data in Figure 2.16 do indeed show such a trend.

2.3.3 $^{15}N$ NMR spectra of $L^{15}$ and $L^{17}$

$^{15}N$ NMR spectra have been recorded in $CDCl_3$ at 25.35 MHz for $L^{15}$ and $L^{17}$, the most soluble of the present ligands. The use of liquid ammonia as the reference signal (at 0 p.p.m.) is inconvenient and, instead, external referencing was employed [using nitromethane as a 1:1 (v/v) mixture with $CDCl_3$ containing $[Cr(pd)_3]$ (0.033 mol $dm^{-3}$)]. The chemical shift of the nitrogen nucleus in this reference is 379.6 p.p.m. with respect to ammonia.[73]

The $^{15}N\{^1H\}$ spectrum of $L^{15}$ shows two sharp signals at $\delta$ = 38.0 and 60.4 p.p.m. assigned to the benzylamino and anilino nitrogens, respectively. For $L^{17}$, the corresponding signals occur at $\delta$ = 35.8 and 63.7 p.p.m. (cf. secondary aliphatic amine $(CH_3CH_2CH_2)_2NH$, $\delta$ = 38.0 p.p.m. and secondary aromatic amine $C_6H_5.CH_3NH$, $\delta$ = 52.8).[74] The proton-coupled spectra (Figure 2.17) suffer from a poor signal to noise ratio because the component peaks of split signals are necessarily of reduced intensity. Nevertheless, they each show a distinct doublet for the anilino nitrogen, with $^1J_{NH}$ = 84 Hz for $L^{15}$ and 85 Hz for $L^{17}$. These values are in the middle of the range of expected one-bond coupling constants for ArNHR (75-95 Hz). Values for $^1J_{NH}$ occur in the regions ca. 75, ca. 90 and ca. 135 Hz for pyramidal, trigonal and linear bonding to nitrogen respectively.[74] In fact, an equation has been developed which relates the coupling constant to the s character of the hybridization around the nitrogen atom.[75]

$$\text{percent s} = 0.43\,^1J_{NH} - 6$$

Applying this to the 85 Hz coupling constant mentioned above, yields an s character of about 31% which is consistent with the expected $sp^2$ hybridization. The signal arising from the benzylamino nitrogen atoms appears as a 'noisy' broad signal. Although three and four bond

coupling constants may be present, they can not readily be distinguished from the noise.

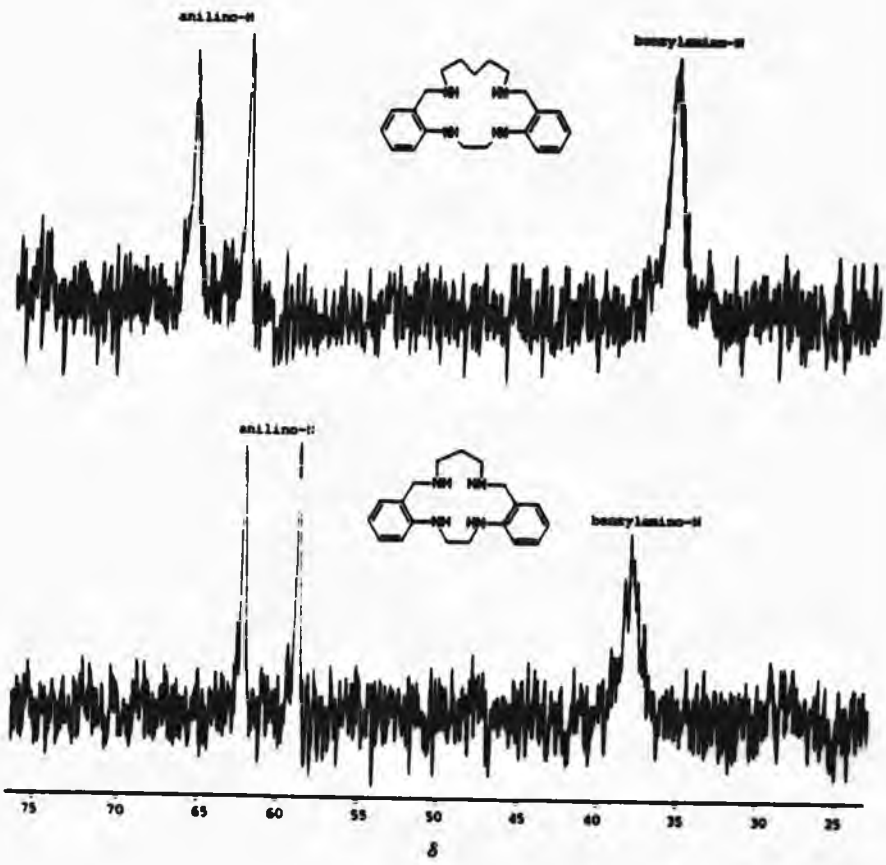


FIGURE 2.17 Proton coupled $^{15}N$ NMR spectra of $L^{15}$ and $L^{17}$ showing the $^{15}N$-$^{1}H$ splitting of the anilino nitrogen peak in each case.

The $^{1}H$-$^{15}N$ COSY spectrum (Figure 2.18) shows a response solely for the anilino nitrogen, reinforcing the view that the hydrogen bonded proton is undergoing slow exchange; it remains bonded to the anilino nitrogen for a sufficiently long time for the coupling to be resolved, but that

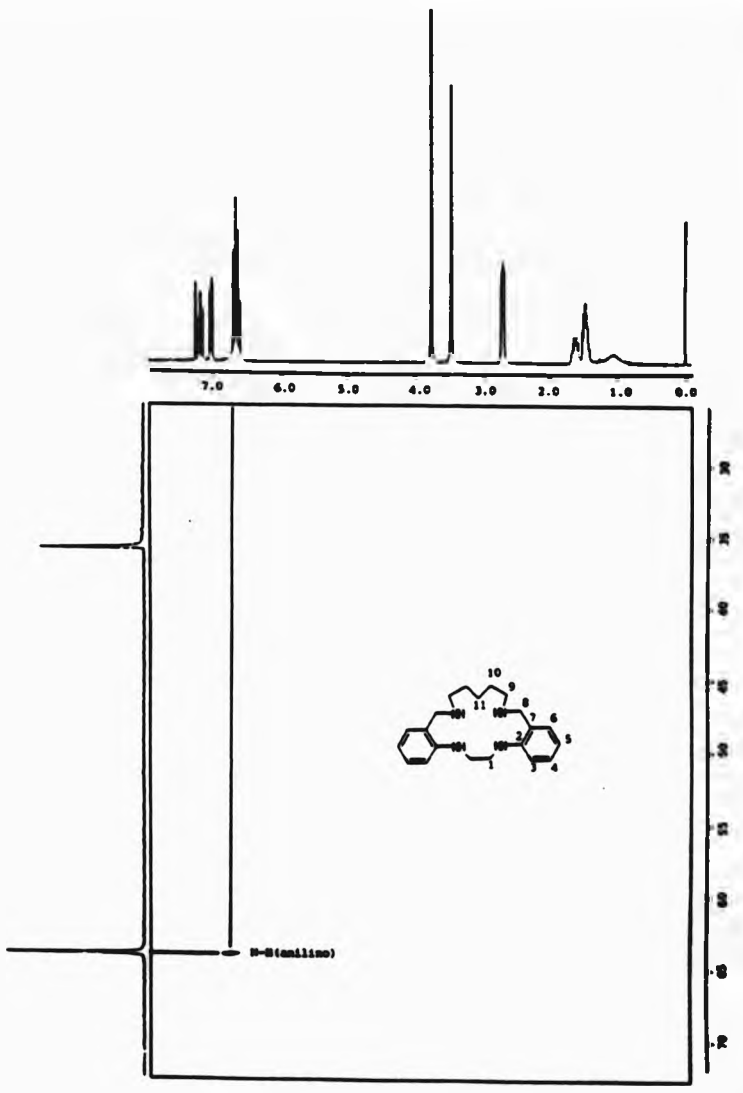


FIGURE 2.18 $^{1}H$-$^{15}N$ COSY plot for $L^{15}$.

attached to the benzylamino nitrogen is undergoing relatively rapid exchange.

## 2.4 Infrared spectra

The principle peaks in the infrared spectra of the ligands are summarized in Table 2.10.

TABLE 2.10 Selected bands in the infrared spectra of the tetraaza macrocycles.(a)

| $\nu$ / $cm^{-1}$ | | | | | assignment |
|---|---|---|---|---|---|
| $L^{14}$ | $L^{15}$ | $L^{16}$ | $L^{17}$ | $L^{19}$ | |
| 3039w | 3040w<br>3017w | 3040 | 3040<br>3018w | 3043<br>3014w | aromatic C-H stretch |
| | | 2940 | 2934 | | |
| 2888w | 2902 | 2923 | 2904 | 2927s | alkyl C-H |
| 2868w | 2851 | | 2840s | 2852s | stretch |
| 2824s | 2819s<br>2806s | 2818s | 2830(sh) | 2826(sh) | |
| 1606s | 1607s | 1606s | 1606s | 1606s | aromatic skeletal |
| 1584 | 1585s | 1588s | 1585s | 1588s | in-plane ring |
| 1511s | 1504s | 1522s | 1512s | 1517s | vibrations |
| 1470 | 1485 | | 1476 | | alkyl C-H |
| 1449s | 1459s | 1463s | 1462s<br>1448s | 1460s | deformations |
| 757s | | | | | aromatic C-H |
| 746s | 743s | 749s | 748s | 747s | out-of-plane |
| 731s | 726s | 719 | 722s | | deformations |

(a) As KBr discs for $L^{14}$ to $L^{17}$ and as a liquid film between KBr plates for $L^{19}$.

All the spectra exhibit the characteristic absorptions expected for the aromatic rings; the three skeletal in-plane ring vibrations at around 1606-1607, 1584-1588 and 1504-1522 $cm^{-1}$, the aromatic C-H stretch as a weak absorption at around 3040 $cm^{-1}$ accompanied by a

second peak at 3014-3018 $cm^{-1}$ for $L^{15}$, $L^{17}$ and $L^{19}$, and the C-H out-of-plane deformations (characteristic of a 1,2-disubstituted benzene) manifested as one or more peaks at around 760 $cm^{-1}$.[5] Medium to strong peaks between 719 and 731 $cm^{-1}$ may be due to $CH_2$-rocking vibrations, although they are usually weak.[66]

The C-H stretching region of $L^{14}$ shows one prominent band at 2824 $cm^{-1}$ consistent with all the methylene groups being bonded to nitrogen atoms.[77] As the number of methylene units is increased, further bands arise between 2940 and 2840 $cm^{-1}$. There is no discernible gradation in the relative intensities of these bands, but the peak at 2826 $cm^{-1}$ in the spectrum of $L^{19}$ appears as a shoulder on the peak at 2852 $cm^{-1}$ and that at 2927 $cm^{-1}$ is the strongest. One to three peaks between 1441 and 1485 $cm^{-1}$ may be due to C-H deformations, even though they are stronger than expected. Other bands which are common to the series of ligands are assigned in Table 2.10. The N-H stretching vibrations of the ligands are reproduced in Figure 2.19. The N-H stretching vibrations of secondary amines give an absorption band between 3450 and 3300 $cm^{-1}$, with dialkyl amines absorbing between 3350 and 3310 $cm^{-1}$ and alkyl-aryl amines, between 3450 and 3400 $cm^{-1}$.[77] Intra- and intermolecular hydrogen bonding gives rise to complicated N-H stretching bands. Owing to intramolecular association, the frequency of the N-H stretching vibration is diminished, and the band becomes broader to an extent depending on the strength of the hydrogen bond. In the solid and liquid states, further intermolecular association may occur, causing these bands to broaden and their frequencies to decrease; the liquid $L^{19}$, gives a broad featureless band at 3275 $cm^{-1}$.

FIGURE 2.19 N-H stretching region of the infrared spectra of the ligands. For each ligand, the major aryl C-H stretch at ca. 3040 $cm^{-1}$ is included. The transmission scale is arbitrary.

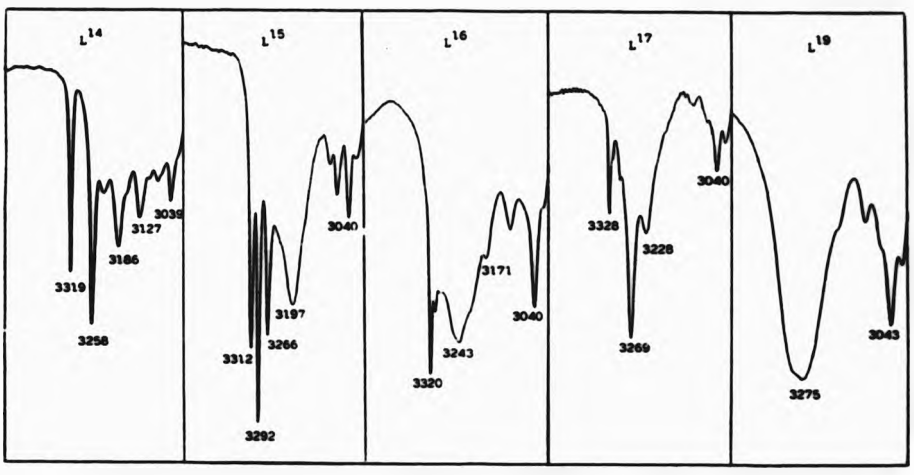


## 2.5 Mass spectra

Owing to the low volatility of the ligands, the electron impact mass spectra of $L^{15}$, $L^{16}$, $L^{17}$ and $L^{19}$ were obtained at maximum instrument temperature (ca. 350-400°C). For $L^{14}$, the data are taken from Reference 58. Each ligand exhibits a molecular ion with relative abundance decreasing with increasing alkyl chain length; $L^{16}$ and $L^{17}$ have more or less equal relative abundances. The $(M+H)^+$ peak is observed for $L^{15}$. Table 2.11 lists the fragment-ion peaks common to all the ligands and Table 2.12 lists those associated with homologous series. All the spectra contain several pairs of peaks at mass values which, when added together, equal the mass of the molecular ion.

TABLE 2.11 Mass spectral peaks peculiar to each ligand and their relationship to the molecular ion.

| assignment | m/z(% relative abundance) | | | | |
|---|---|---|---|---|---|
| | $L^{14}$ | $L^{15}$ | $L^{16}$ | $L^{17}$ | $L^{19}$ |
| M+1 | - | 311(23) | - | - | - |
| M | 296(52) | 310(63) | 324(20) | 338(23) | 366(14) |
| M-106 | - | 204(11) | 218(2) | 232(9) | 260(20) |
| M-118 | - | 192(9) | 206(3) | 220(6) | 248(10) |
| M-120 | 176(48) | 190(38) | 204(7) | 218(29) | 246(45) |
| M-130 | - | 180(12) | 194(1) | 208(1) | 236(4) |
| M-132 | - | 178(9) | - | - | 234(10) |
| M-135 | - | - | 189(10) | 203(18) | - |
| M-147 | 149(61) | - | - | - | - |
| M-149 | 147(67) | 161(61) | 175(8) | 189(22) | 217(5) |
| M-236 | - | - | - | 104(10) | 130(17) |
| M-252 | - | 58(7) | 72(12) | 86(55) | 112(17) |
| M-254 | - | - | 70(20) | - | - |

TABLE 2.12 Mass spectral peaks common to each ligand.

| m/z | % relative abundance | | | | |
|---|---|---|---|---|---|
| | $L^{14}$ | $L^{15}$ | $L^{16}$ | $L^{17}$ | $L^{19}$ |
| 252 | - | 8 | <1 | <1 | - |
| 237 | - | - | 2 | 4 | 3 |
| 236 | 11 | 23 | 1 | - | 4 |
| 149 | 61 | - | 1 | 2 | 4 |
| 147 | 67 | 61 | 12 | 25 | 24 |
| 132 | 54 | 25 | 17 | 31 | 21 |
| 130 | - | 27 | 10 | 19 | 17 |
| 120 | 91 | 60 | 79 | 96 | 76 |
| 118 | 100 | 100 | 100 | 100 | 100 |
| 106 | 89 | 53 | 53 | 94 | 88 |
| 91 | 80 | 51 | 16 | 17 | 19 |

The fragmentation pattern of amines is dominated by alpha-cleavage:[77] in the case of the present compounds, for $L^{14}$,

The cleavage of one bond in a cyclic structure produces only an isomeric ion; cleavage of at least two bonds is necessary to produce a fragment ion. Two-bond cleavage results in the formation of an odd-electron ion and a neutral molecule, whereas three-bond cleavage includes a hydrogen transfer and produces an even-electron ion and a radical. The molecular ion is an odd-electron ion. An odd-electron ion which may be formulated to contain an even number of nitrogen atoms has an even mass/charge ratio, m/z, and conversely an even-electron ion containing an even number of nitrogens has an odd m/z. Competition for the charge may result in the appearance of both fragment ions. Figure 2.20 shows the possible alpha-cleavage sites in $L^{14}$ (a, c, e and g) together with sites b, d, f and h, the cleavage of which would produce the mesomerically stabilized quinonoid ions.

FIGURE 2.20 Cleavage sites in the ligands (a) $L^{14}$ and (b) $L^{N}$ (N = 15 to 17).

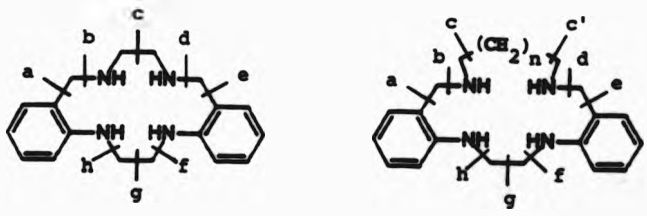

Taking these as the most likely cleavage sites, the fragmentation scheme in Figure 2.21 may be postulated. However, the existence of alternative cleavage sites and the possibility of (possibly cyclic) rearrangements of primary and subsequent fragments, together with the charge competition, precludes an unambiguous assignment of structure for the decomposition products. Accordingly, the fragment-ion structures depicted in Figure 2.21 are not the only structures possible, but are intended to show the probable origins of the fragments. For some of the fragment-ions, one of the heterocyclic isomers possible is also shown. The fragment ion peaks in the spectrum of $L^{14}$ at m/z, 149 and 147, more or less half the molecular ion, must arise from even-electron ions (as they contain an even number of nitrogen atoms and an odd m/z). This indicates that a three-bond cleavage mechanism is occurring to give both $C_9H_{11}N_2^+$ (147) and $C_9H_{13}N_2^+$ (149). Conversely, the peak at m/z 148 indicates that a two-bond cleavage mechanism also occurs giving the odd-electron ion, $C_9H_{12}N_2^{\dagger}$. The loss of hydrogen from $C_9H_{13}N_2^+$ to give $C_9H_{11}N_2^+$ is also possible. By postulating one or two small neutral losses from these initial fragments, the fragmentation scheme in Figure 2.21 accounts for the peaks in the spectrum of $L^{14}$.

The base peak, at m/z 118, is probably due to an indole type heterocycle. The peaks at m/z 91 and m/z 65 in all the spectra are due to the benzylium or, more probably, the tropylium ion. Benzyl compounds are known to afford $C_7H_7^+$ and its decomposition product, $C_5H_5^+$ (m/z 65).[66]

A similar scheme (Figure 2.22) accounts for the majority of the peaks in the spectra of $L^{15}$ to $L^{19}$. Homologous series of peaks are present at M-120 and M-149 for each ligand. In contrast to that of

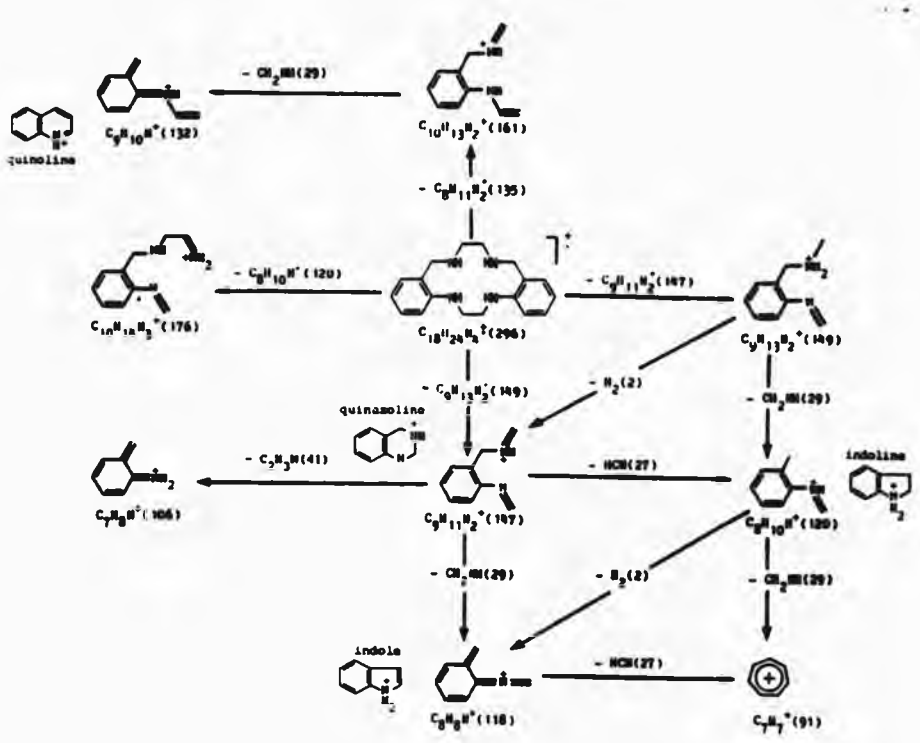


FIGURE 2.21 A suggested fragmentation scheme accounting for the major peaks in the electron impact mass spectrum of L[14]. For each fragment, the structure drawn is intended only to indicate the probable origin of the fragment based on the combinations of cleavage sites in Figure 2.20. The possibility of cyclic rearrangement is highlighted, where appropriate, by the inclusion of alternative structures based on common heterocycles.

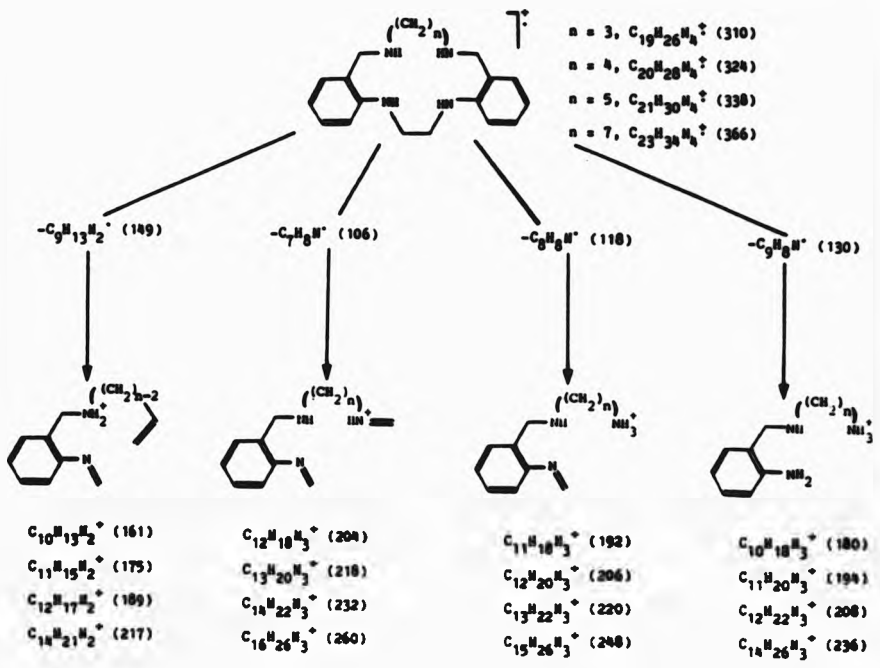


FIGURE 2.22 The larger mass spectral fragments observed in the electron impact mass spectra of the ligands $L^{15}$, $L^{16}$, $L^{17}$ and $L^{19}$. As they form homologous series, these fragments are formulated to retain the polymethylene bridge between the benzylamino nitrogen atoms. The formulae under each fragment structure correspond to the ligands in the order above, where n = 3, 4, 5 and 7, respectively. The structures drawn are intended only to show the origin of the peak; for each one, a number of isomeric structures is possible.

$L^{14}$, the spectra of the remaining ligands do not exhibit the peak at M-147. Other series of peaks not present in the spectrum of $L^{14}$, including M-106, M-118 and M-130, indicating further initial fragmentations, are listed in Table 2.11. The inclusion of longer alkyl chains into the ligands introduces an extra site for alpha cleavage (c' in Figure 2.20), and expulsion of a (possibly cyclized) amine as the initial fragmentation is evident from the peak at m/z, 252 in $L^{15}$ (very weak in $L^{16}$ and $L^{17}$) and a moderate peak at m/z, 237 for $L^{16}$, $L^{17}$ and $L^{19}$. These fragments are best formulated so as to retain the $C_2$-bridge between the anilino nitrogen atoms and both of the phenylene rings.

## 2.6 Ligand basicities

Protonation constants for the ligands $L^{14}$ to $L^{17}$ were obtained (by Professor L. F. Lindoy's group at James Cook University of North Queensland, Australia) from titration of the free base (in acidified 95% methanol:water containing tetraethylammonium perchlorate) with tetraethylammonium hydroxide ($[H^+]$ ca. 0.004 mol $dm^{-3}$) as described elsewhere.[68] The results are summarized in Table 2.13 together with those for a selection of related ligands. Smooth titration curves were obtained for $L^{14}$ to $L^{16}$, but a discontinuity in the curve for $L^{17}$, presumably arising from precipitation of $LH^+$, was detected at higher pH (ca. pH 9) precluding the accurate determination of log $K_{011}$.

Micheloni, Paoletti, and co-workers studied the thermodynamics of the stepwise protonation of a range of cyclam-type ligands.[30,81,83] They rationalized the protonation steps in terms of the breaking of intramolecular hydrogen bonds, which reduce the availability of the lone pair, and eversion of the protonated amine with accompanying

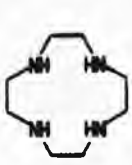

1

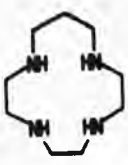

2

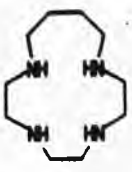

3

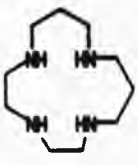

4

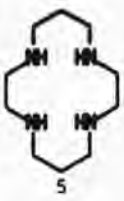

5

6

7

8

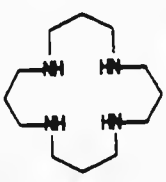

9

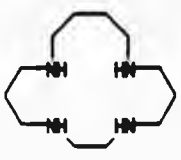

10

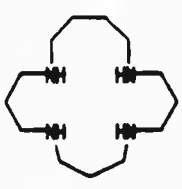

11

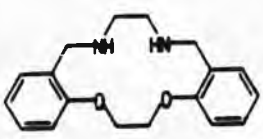

14

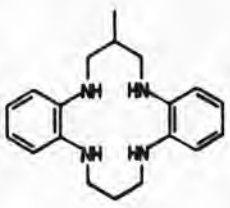

12

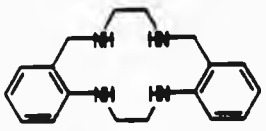

18

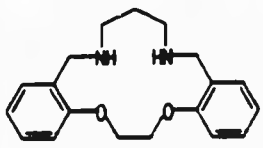

15

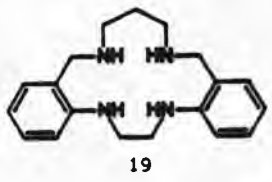

19

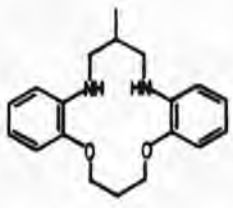

13

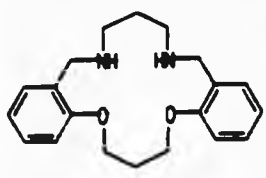

16

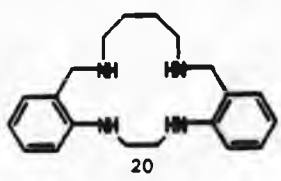

20

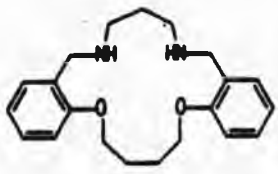

17

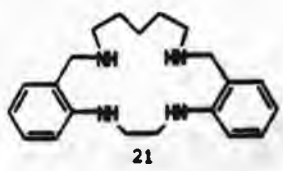

21

TABLE 2.13 Ligand protonation constants for selected 12- to 17-membered macrocyclic ligands containing $N_4$ and $N_2O_2$ donor sets.(a,b)

| ligand | (c) | log $K_{011}$ | log $K_{012}$ | log $K_{013}$ | log $K_{014}$ |
|---|---|---|---|---|---|
| 1 (d) | 2222 | 10.51 | 9.49 | 1.6 | 0.8 |
| 2 (d) | 2223 | 10.90 | 9.91 | 1.6 | 0.9 |
| 3 (e) | 2224 | 10.92 | 9.40 | 4.62 | - |
| 4 (f) | 2233 | 10.93 | 9.86 | 4.01 | - |
| 5 (g) | 2323 | 11.58 | 10.62 | 1.61 | 2.42 |
| 6 (g) | 2333 | 11.08 | 10.38 | 5.28 | 3.60 |
| 7 (e) | 2225 | 9.83 | 8.95 | 5.40 | 1.6 |
| 8 (h) | 2324 | 11.04 | 10.47 | 3.98 | 3.41 |
| 9 (f) | 3333 | 10.64 | 9.49 | 7.06 | 5.30 |
| 9 (i) | 3333 | 10.85 | 9.80 | 7.21 | 5.69 |
| 10 (h) | 2343 | 10.73 | 9.85 | 6.83 | 3.96 |
| 11 (h) | 3334 | 11.20 | 10.13 | 7.96 | 6.30 |
| 12 (j) | 2323 | 4.19 | 3.10 | - | - |
| 13 (j) | 2323 | 4.28 | 1.83 | - | - |
| 14 (k) | 2323 | 9.19 | 5.40 | - | - |
| 15 (k) | 2333 | 9.81 | 6.82 | - | - |
| 16 (k) | 3333 | 10.07 | 7.09 | - | - |
| 17 (k) | 4333 | 9.63 | 8.10 | - | - |
| 18 (k) | 2323 | 9.45 | 3.85 | 1.19 | - |
| 19 (k) | 2333 | 9.72 | 4.97 | 2.01 | - |
| 20 (k) | 2343 | 9.93 | 7.02 | 1.71 | - |
| 21 (j,l) | 2353 | 9.28 | 7.92 | 1.95 | - |

(a) $K_{011} = [LH]/[L][H]$, $K_{012} = [LH_2]/[LH][H]$, $K_{013} = [LH_3]/[LH_2][H]$, $K_{014} = [LH_4]/[LH_3][H]$; (b) See key to ligands opposite; (c) inter-donor bridge atomicity;

(d) $H_2O$, I = 0.2 mol $dm^{-3}$ ($NaClO_4$), 35°C, Ref. 78;

(e) $H_2O$, I = 0.1 mol $dm^{-3}$ ($NaNO_3$), 25°C, Ref. 79;

(f) $H_2O$, I = 0.1 mol $dm^{-3}$ ($NaNO_3$), 25°C, Ref. 80;

(g) $H_2O$, I = 0.5 mol $dm^{-3}$ ($KNO_3$), 25°C, Ref. 30;

(h) $H_2O$, I = 0.5 mol $dm^{-3}$ ($KNO_3$), 25°C, Ref. 81;

(i) $H_2O$, I = 0.5 mol $dm^{-3}$ ($KNO_3$), 25°C, Ref. 82;

(j) 95% MeOH, I = 0.1 mol $dm^{-3}$ ($NEt_4ClO_4$), 25°C, Ref. 44;

(k) 95% MeOH, I = 0.1 mol $dm^{-3}$ ($NMe_4Cl$), 25°C, Ref. 24;

(l) the accuracy of these values may be in doubt due to precipitation of $LH^+$.

hydrogen bond formation to solvent molecules. The second protonation step is likely to involve the nitrogen furthest from the first protonation site, so that electrostatic repulsions are minimized. Intramolecular hydrogen bonding between distal amines is a feature of cyclic tetraamines such as cyclam.[30] In fact, the dihydroperchlorate of cyclam has been shown by X-ray structure determination to be protonated at distal amine sites.[84] For the cyclam-type ligands 1 to 11 in the key to Table 2.13, although the second protonation constants are lower than the first, they are still generally around a value of 10. For the third protonation step, steric crowding can not be avoided and log $K_{013}$ is much lower, especially for the smaller rings. The fourth protonation step only becomes significant for the larger, more flexible rings. In the ligands 12 and 13, containing a $N_4$ and a $N_2O_2$ donor set, respectively, all the amines are of the anilino type. The low basicity of these is obvious from the data. It is noteworthy that only two protonation constants can be measured even for the $N_4$ donor ligand. The ligands 14 to 17, with a $N_2O_2$ donor set comprising benzyl amines show again only two protonation constants. The first is generally only slightly lower than for ligands 1 to 11, but the second is in the range exhibited for log $K_{013}$ for ligands 6 to 11. The crystal structure of the nitrate salt of ligand 15 shows both amines to be protonated.[85]

By analogy with these compounds, in the case of the present ligands (18 to 21 in Table 2.13), the first two protonation steps (log $K_{011}$ 9-10, log $K_{012}$ 4-8) are associated principally with the two benzylamine bases. The low values of log $K_{012}$ (compared to those of the aliphatic ligands) may be explained by the electrostatic repulsion associated with the protonation of the proximal (rather than a distal) amine. Increasing the length of the alkyl chain between these two

amines increases the basicity, not only because of the small increased inductive effect from additional methylene groups, but also because the increased flexibility of the ring facilitates the inversion of the amine nitrogen, so that protonation and solvation is sterically more favourable. The third protonation step must involve the weak anilino bases and for each ligand log $K_{013}$ is very low (ca. 1-2).

## Chapter Three

### 3. The Nickel(II) Complexes

The nickel(II) complexes of $L^{14}$ and $L^{15}$ have been studied previously as part of a programme of work to investigate the differences in the complexation behaviour of fourteen- or fifteen-membered macrocyclic ligands with $N_4$, $N_2O_2$ and $N_2S_2$ donor sets.[25,52] The $N_4$ series has been extended in the present work to include sixteen-, seventeen- and nineteen-membered ligand complexes. Most of the structural studies in this work have been focussed on the co-ordination of the sixteen- and seventeen-membered ligands, but some complexes of the fourteen- and fifteen-membered ligands were prepared so that trends in the series could be studied. Details of the preparation of the complexes and characterization data are reported in Chapter Six. The torsion angles defining the conformations of the co-ordinated ligand in each complex will be discussed in Chapter Four in comparison with the complexes of zinc(II) and cadmium(II). Discussion of the variation of hole size with ligand structure is deferred to Chapter Five, so that the behaviour of the nickel(II), zinc(II) and cadmium(II) complexes may be compared.

### 3.1 The nickel(II) nitrate complexes

Reaction of $L^{16}$ and $L^{17}$ with hexaaquanickel(II) nitrate in a mixture of refluxing methanol and dichloromethane yielded a blue-green and a grey-green product, respectively and their composition was at first uncertain. The infrared spectra of the complexes with both ligands showed a prominent broad band which is assigned to co-ordinated or strongly hydrogen bonded water at around 3400 $cm^{-1}$ overlapping the N-H absorptions (at 3278, 3232 and 3202 $cm^{-1}$, and at 3321, 3285 and

3209 $cm^{-1}$ in the complexes of $L^{16}$ and $L^{17}$, respectively). After slow evaporation over about eight months, a methanol solution of the very soluble $L^{16}$ complex yielded crystals suitable for X-ray structural study. Vacuum desiccation over phosphorus pentoxide of the above complexes had no effect on the appearance of the infrared spectra, supporting the view that co-ordinated, or at least strongly bound, water molecules were present. Microanalysis (Table 3.1) of the $L^{16}$ complex, before recrystallization from methanol, gave good agreement with the formulation deduced from the X-ray structure analysis; it contains one half molecule of water per nickel atom. No crystals suitable for X-ray crystallographic study were obtained for the $L^{17}$ complex, but from the microanalytical data (Table 3.1), it seems probable that the complex of $L^{17}$ contains one molecule of water per nickel atom, although even if this is so, there remains the possibility that it may consist of one complex, i.e. $[NiL^{17}(NO_3)(H_2O)]NO_3$, or two complexes, i.e. $[NiL^{17}(NO_3)_2]$ and $[NiL^{17}(H_2O)_2](NO_3)_2$ in equal proportion.

TABLE 3.1 Composition of the nitrate complexes of $L^{16}$ and $L^{17}$.

| | $L^{16}$ | | | $L^{17}$ | | |
|---|---|---|---|---|---|---|
| | %C | %H | %N | %C | %H | %N |
| found | 46.5 | 5.5 | 16.1 | 47.1 | 5.7 | 15.2 |
| $NiL(NO_3)_2$ requires | 47.4 | 5.6 | 16.6 | 48.4 | 5.8 | 16.1 |
| " $+\frac{1}{2}$ $H_2O$ " | 46.5 | 5.7 | 16.3 | 47.6 | 5.9 | 15.9 |
| " +1 $H_2O$ " | 45.7 | 5.8 | 16.0 | 46.8 | 6.0 | 15.6 |
| " +2 $H_2O$ " | 44.2 | 5.9 | 15.5 | 45.3 | 6.1 | 15.1 |

The visible spectra of the complexes of the two ligands in

acetonitrile showed more peaks than can be accounted for even with the most pronounced tetragonal distortion, but may be divided broadly into four groups of bands centred around 560, 680, 800 and 1000 nm. The presence of four bands is broadly indicative of weak tetragonal splitting.[86] Such splitting will arise from the differences between the ligand field strengths of the in-plane macrocycle and the axial nitrato or aqua ligands. For the complexes of both ligands, each group of bands consists of two peaks separated by 20-30 nm, indicating the presence of a mixture of complexes. Below 500 nm, the ligand absorption swamps the d-d transitions and all that can be discerned is a shoulder at 463 nm which occurs for the complexes of both ligands.

The blue-green product from $L^{16}$ exhibits a strong NO stretching band in the infrared at 1385 $cm^{-1}$ which is characteristic of the doubly degenerate stretch, $\nu_3$, of the free nitrate ion (Figure 3.1).[87]

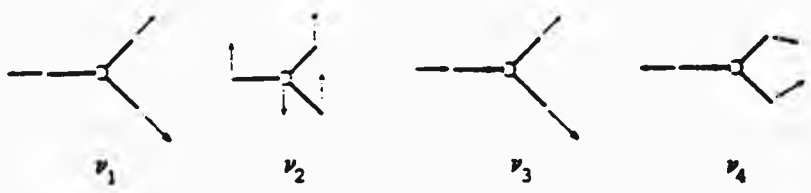


FIGURE 3.1 The normal modes of vibration of the nitrate ion. On complexation and subsequent decrease in symmetry from $D_{3h}$ to $C_{2v}$, the degeneracy of this band is lifted and it splits into two, with the degree of splitting being indicative of the mode of co-ordination. $C_{2v}$ symmetry requires a linear Ni-O-N bond, but X-ray studies (see below) reveal that this bond is bent, reducing the symmetry further to $C_s$. The observed bands at 1296 and 1420-1433 $cm^{-1}$ are characteristic of a monodentate nitrato ligand.[87] In addition, the Raman active

symmetric stretch, $\nu_1$, of the free ion (at ca. 1050 $cm^{-1}$) becomes infrared active on co-ordination and the strong absorption at 982 $cm^{-1}$ can be ascribed to this.[88] The out-of-plane deformation, $\nu_2$, at around 820 $cm^{-1}$ can not be assigned because this region contains several bands arising from the macrocyclic amines. Furthermore, the doubly degenerate in-plane bend, $\nu_4$, expected at around 700 $cm^{-1}$ is either very weak or absent. The grey-green complex of $L^{17}$ exhibits similar characteristic bands for $\nu_3$ at 1384 $cm^{-1}$ due to free nitrate and at 1420 and 1298 $cm^{-1}$ due to monodentate nitrate. The symmetric stretch, $\nu_1$, appears at 991 $cm^{-1}$.

Insufficient sample was obtained for a measurement of the magnetic susceptibility of these complexes, but the infrared and visible spectra provide evidence enough that they are high-spin nickel(II) species. The role of water in the complex of $L^{16}$ was finally resolved by the X-ray structure determination.

3.1.1 The structure of $[NiL^{16}(NO_3)_2][NiL^{16}(NO_3)(H_2O)]NO_3.CH_3OH$
Crystal data and details of the structure solution are given in Chapter Six. Tables of fractional atomic coordinates, thermal parameters, bond lengths, and interbond angles are given in the Appendix (Tables A3.1 to A3.5). The structure contains a 1:1 mixture of two complexes each with the macrocycle affording a near planar donor set: one a neutral trans-dinitrato, and the other a cationic trans-aquanitrato species (Figure 3.2). The complexes both contain the nickel atom in a distorted octahedral environment with the macrocyclic donors occupying four equatorial sites. The co-ordination sphere is completed by two nitrato ligands in the complex containing Ni(2) and by one nitrato ligand and one aqua ligand in that containing Ni(1), the co-ordinated nitrato groups being monodentate. The

**FIGURE 3.2** The structure of $[NiL^{16}(NO_3)(H_2O)]^+$ viewed (a) onto and (b) across the donor plane and comparable views (c) and (d) of the structure of $[NiL^{16}(NO_3)_2]$ at -x,-y,-z. The part of the molecule of $[NiL^{16}(NO_3)_2]$ associated with the minor component of the disordered carbon atom is shown with open bonds.

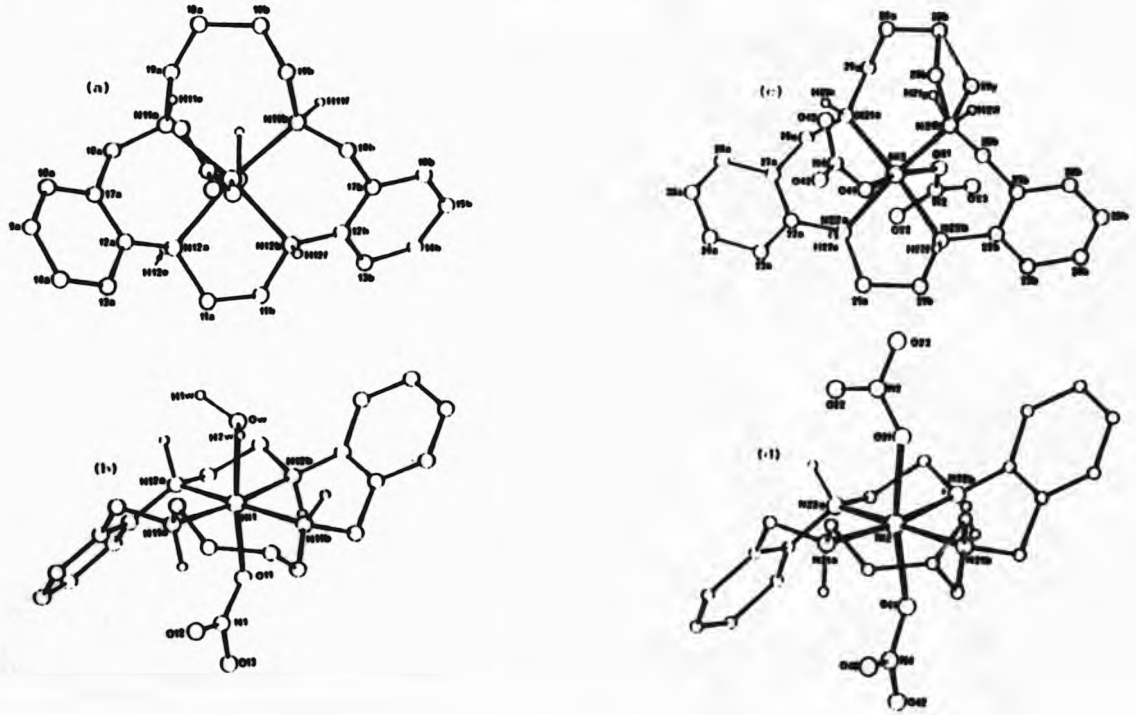

deviations of the metal and donor atoms from the least-squares planes of the donor atoms are given in Figure 3.3. The metal atom is very close to the best plane in each case [Ni(1) 0.012 Å towards the co-ordinated water molecule, Ni(2) 0.011 Å towards O(21)], but the nitrogen atoms show a slight tetrahedral distortion, which is greater in the dinitrato complex (deviations up to 0.091 Å compared to a maximum of 0.059 Å in the aquanitrato complex).

The nickel-donor bond lengths and selected angles at the nickel atom are presented in Table 3.2. For each complex, the Ni-N bond lengths for the anilino donors are generally longer [2.124(9) to 2.157(7) Å] than those for the benzylamino donors [2.096(9) to 2.124(8) Å] although the ranges are not widely separated, reflecting the difference in co-ordinative strengths of the two types of nitrogen atom.[25,52] Anilino nitrogen atoms are the weaker donors due to the effect of delocalization of the lone pair electron density into the aromatic system, giving rise to weaker and consequently longer bonds. The Ni-N bond lengths in both complexes all fall within the range of 2.03-2.16 Å observed previously for the co-ordinate bonds from neutral $sp^3$ hybridized nitrogen atoms in high-spin nickel(II) complexes of macrocyclic ligands.[26,29,34,89,90]

The Ni-O bond length to the co-ordinated water molecule of the cationic complex is 2.109(6) Å, at the upper extreme end of the range previously observed in nickel(II) complexes containing two or three aqua ligands and monodentate nitrato ligands [2.037 to 2.111 Å, mean of seven bonds 2.070 Å].[91,92,93]

FIGURE 3.3 The co-ordination spheres of (a) $[NiL^{16}(NO_3)(H_2O)]^+$ and (b) $[NiL^{16}(NO_3)_2]$ showing the deviations from the least-squares planes of the macrocyclic donor atoms.

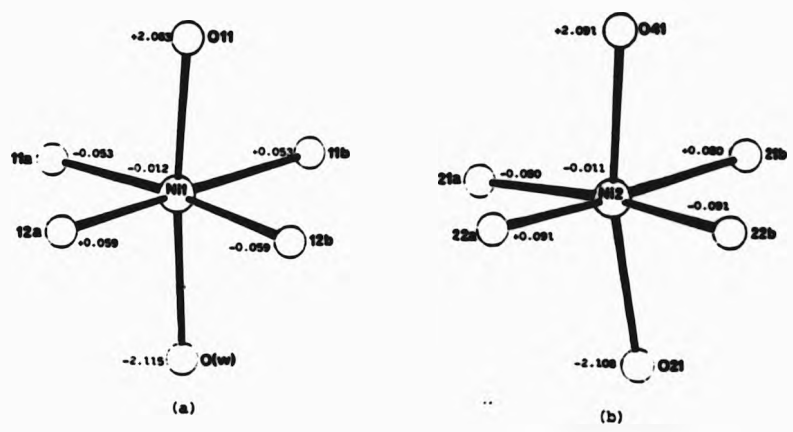


TABLE 3.2 Bond lengths ( Å) in the co-ordination spheres and selected angles (°) at the nickel atoms for $[NiL^{16}(NO_3)_2]$-$[NiL^{16}(NO_3)(H_2O)]NO_3.CH_3OH$.

| | $[NiL^{16}(NO_3)_2]$ | | $[NiL^{16}(NO_3)(H_2O)]^+$ | |
|---|---|---|---|---|
| | (part a) | (part b) | (part a) | (part b) |
| Ni-N1 | 2.104(9) | 2.114(8) | 2.096(9) | 2.124(8) |
| Ni-N2 | 2.125(8) | 2.124(9) | 2.157(7) | 2.156(9) |
| Ni-X | 2.108(8) | 2.135(7) | 2.088(7) | 2.109(6) |
| [ X = | O(21) | O(41) | O(11) | O(w) ] |
| N1-Ni-N1 | 96.7(4) | | 97.7(3) | |
| N2-Ni-N2 | 81.9(3) | | 81.8(3) | |
| N1-Ni-N2 | 90.9(3) | 90.9(4) | 90.8(3) | 89.8(3) |

The Ni-O bond lengths in the three co-ordinated nitrato groups [Ni(1)-O(11) 2.081(7), Ni(2)-O(21) 2.108(8), Ni(2)-O(41) 2.135(7) Å] are well within the range previously observed in ten nickel(II) complexes containing monodentate nitrato groups (2.016 to 2.169 Å, mean of fifteen bonds 2.085 Å).[68,91-99] All three nitrato groups are tilted such that the Ni-O-N angles are identical within experimental error [Ni-O(11)-N 131.0(8)°, Ni-O(21)-N 131.7(7)°, Ni-O(41)-N 131.0(7)°], at the upper end of the range in the complexes referred to above (116 to 132°, mean of fifteen angles 126°).[68,91-99] There may be no simple explanation for the coincidence of these interbond angles in the present complexes, but the co-ordinated nitrato groups share a common feature; all three form intramolecular six-membered hydrogen bonded rings with macrocyclic amine donors (see §3.1.2).

It is convenient at this stage to discuss other aspects of the geometry in the nitrato groups. The O-N-O angles in the nitrate groups range from 117(1) to 122(1)°. The N-O bond lengths can be separated into two types depending on whether or not the oxygen atom is co-ordinated. In the ten complexes to which reference was made above, the N-O bond lengths to the co-ordinated oxygen atoms range from 1.240 to 1.300 Å (mean for fifteen bonds 1.267 Å), whereas the other N-O bonds range from 1.181 to 1.279 Å (mean for thirty bonds 1.223 Å). Even though these ranges overlap, within each co-ordinated nitrato group, the longest bond is invariably that involving the co-ordinated oxygen atom. This situation obtains in the present complexes; the N-O bonds involving non-co-ordinated oxygen atoms range in length from 1.190(12) to 1.252(15) Å with a mean value of 1.227(15) Å. In contrast, the N-O bonds associated with the co-ordinated oxygen atoms are appreciably longer than the others

[N(1)-O(11) 1.267(11), N(2)-O(21) 1.266(14), N(4)-O(41) 1.273(16) Å]. Deviations from the least-squares planes of the four atoms of each nitrate group are all less than 0.005 Å for the oxygen atoms and less than 0.015 Å for the nitrogen atoms, the deviations being smallest for the nitrate counter-ion.

The five-membered chelate rings, containing the anilino donors, have the gauche or half chair conformation, with the carbon atoms between the nitrogens disposed to either side of the $NiN_2$ plane [C(11a) 0.31 Å, C(11b) -0.45 Å, C(21a) 0.30 Å, C(21b) -0.45 Å].

The seven-membered chelate ring in the cationic complex adopts a twist-chair or skew(h) conformation* with a virtual two-fold rotation axis between Ni(1) and the midpoint of the C(10a)-C(10b) bond (Figure 3.4). In the neutral complex one carbon atom of this chelate ring is disordered such that two conformational isomers are present in a 60:40 random arrangement throughout the crystal. The major component has C(29b) in the position required for the skew(h) conformation, but the alternative position of this atom [labelled C(29y)] is inverted giving the chelate ring a chair conformation with a virtual mirror plane replacing the rotation axis of the twist-chair. A necessary corollary of this is that the amine hydrogen atoms of each conformer are in a different configuration with respect to the macrocyclic donor plane.

These combinations of different chelate ring conformations and consequent amine hydrogen atom configurations impart an overall step shape to both complexes. The aromatic a- and b-rings are inclined to the donor plane at 50° and 48°, respectively in the cationic complex

* In this designation h = horizontal as opposed to vertical (v) and refers to the bond between C(10a) and C(10b) which is almost parallel to the $N_4$ plane of the macrocycle.[100]

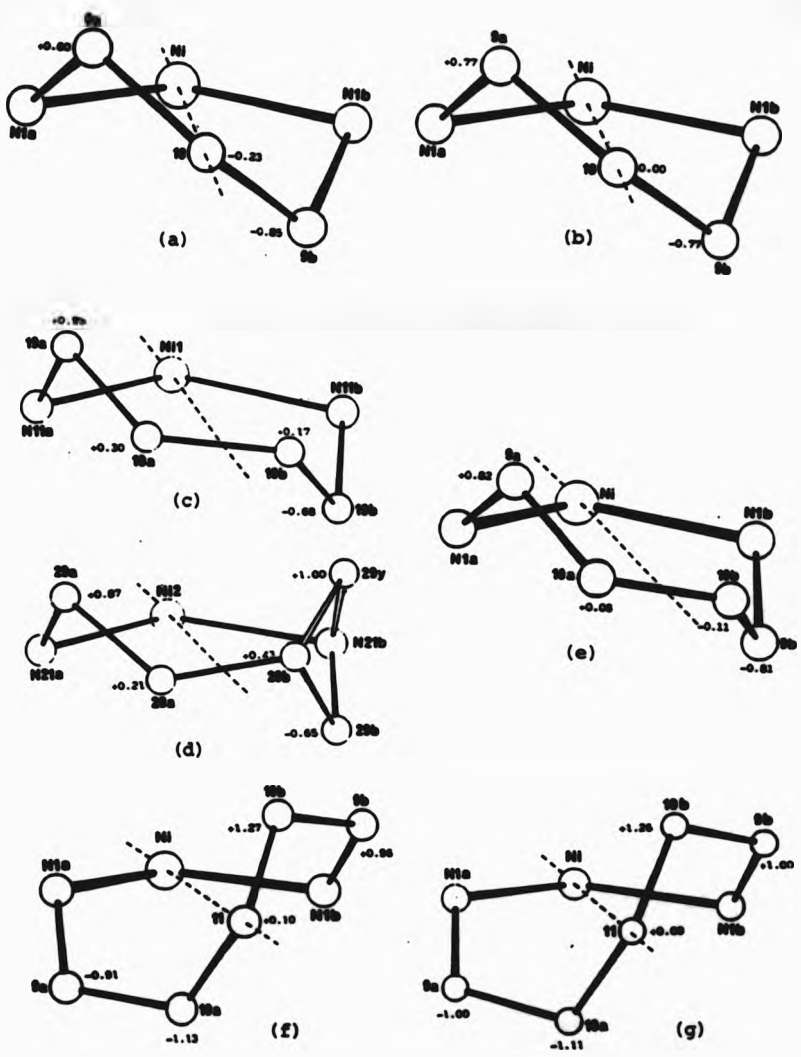


FIGURE 3.4 The conformations of the six- to eight-membered chelate rings bridging the benzylamino donor atoms in the nickel complexes, (a) $[NiL^{15}Cl_2]$, (b) $[NiL^{15}(NCS)_2]$, (c) $[NiL^{16}(NO_3)(H_2O)]^+$, (d) $[NiL^{16}(NO_3)_2]$, (e) $[NiL^{16}(NCS)_2]$, (f) $[NiL^{17}Cl_2]$ and (g) $[NiL^{17}(NCS)_2]$. The deviations of the carbon atoms from the $NiN_2$ plane are indicated. In (d) the minor component of the disordered carbon atom is shown with open bonds to C(20b) and N(21b).

and at 55° and 48° in the neutral complex.

In the cationic complex, the amine hydrogen atoms are disposed alternately above and below the plane of the macrocyclic donors, giving the R,R,R,R absolute configuration of diastereoisomer V (see §1.10). Of course, as the crystal is centrosymmetric, the unit cell also contains the complex of opposite chirality, S,S,S,S. (For ease of comparison with the neutral complex, the cationic complex drawn in Figure 3.2 is that at equivalent position -x,-y,-z and has the reverse hand to that shown in Figure 3.5).

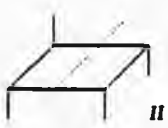

II

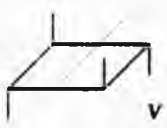

V

Such external compensation of chiralities gives a racemic mixture and each complex may be denoted as a rac-conformer. The rac-conformer is also the major component of the neutral complex. The minor component, with the S,R,S,S configuration, has internal compensation of chiralities of the secondary benzylamine groups and is denoted as a meso-conformer (diastereoisomer II).

### 3.1.2 Hydrogen bonding in the crystal

Figure 3.5 shows the interrelationship between the complexes, counter-ion and solvent molecule. Considerable hydrogen bonding exists in the crystal, both intra- and intermolecular. These hydrogen bonds (labelled A to I in Figure 3.5) are listed in Table 3.3 with contact distances and angles at the hydrogen atoms. In the dinitrato complex both nitrato ligands are oriented such that six-membered hydrogen bonded rings are formed more or less perpendicular to the donor atom plane. These involve (bond A) the hydrogen atom attached

TABLE 3.3 Hydrogen bonding distances ( Å) and angles (°) at the hydrogen atom in $[NiL^{16}(NO_3)_2][NiL^{16}(NO_3)(H_2O)]NO_3.CH_3OH$.

| H-bond | X-H...Y | H...Y | X...Y | angle at H |
|---|---|---|---|---|
| A | N(22a)-H(22e)...O(22) | 2.06 | 2.90 | 134 |
| B | N(21a)-H(21e)...O(43) | 2.13 | 3.04 | 138 |
| C | N(22b)-H(22f)...O(12)i | 1.91 | 2.93 | 153 |
| D | N(11a)-H(11e)...O(12) | 2.03 | 2.86 | 128 |
| E | N(12a)-H(12e)...O(31) | 1.91 | 3.04 | 158 |
| F | N(12b)-H(12f)...O(43) | 1.87 | 2.94 | 164 |
| G | N(11b)-H(11f)...O(m) | 2.33 | 3.24 | 146 |
| H | O(w) -H(w1) ...O(32) | 1.60 | 2.70 | 158 |
| I | O(w) -H(w2) ...O(m) | 1.78 | 2.72 | 165 |

equivalent position i, x,y,1+z

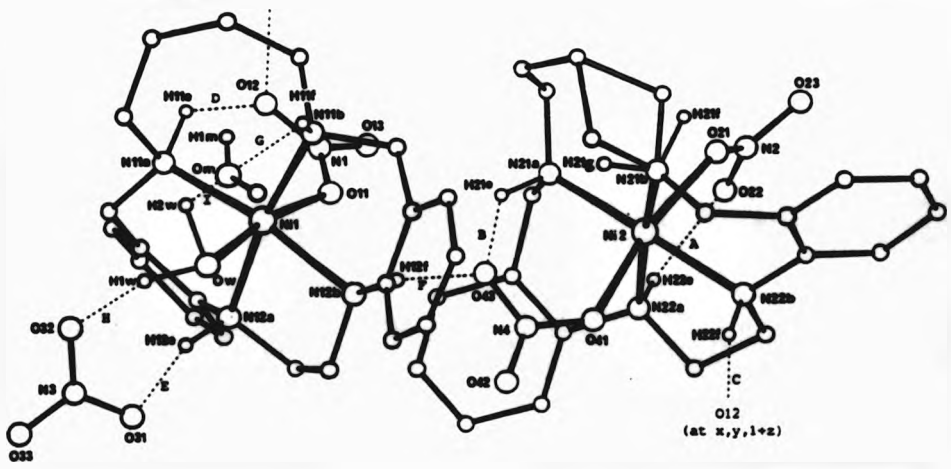


FIGURE 3.5 The asymmetric unit of $[NiL^{16}(NO_3)_2][NiL^{16}(NO_3)(H_2O)] \cdot NO_3.CH_3OH$ showing the spatial relationship between the complexes, the nitrate counter-ion and the methanol of crystallisation. The hydrogen bonds A to I (Table 3.3) are indicated by dashed lines.

to N(22a) and O(22) on one side of the donor plane (N...O 2.90 Å, H...O 2.06 Å, N-H...O 134°) and (bond B) O(43) and the hydrogen atom attached to N(21a) on the other side (N...O 3.04 Å, H...O 2.13 Å, N-H...O 138°). The nitrate oxygen atom O(43) interacts also (bond F) with the hydrogen atom attached to N(12b) in the cationic complex (N...O 2.94 Å, H...O 1.87 Å, N-H...O 164°) and H(22f) interacts with O(12) (bond C) in the cationic complex at x,y,1+z forming a hydrogen bonded chain in the c-direction (N...O 2.93 Å, H...O 2.03 Å, N-H...O 153°). In the cationic complex, O(12) forms hydrogen bonded six-membered ring similar to those observed in the neutral complex, here involving the hydrogen atom attached to N(11a) (N...O 2.86 Å, H...O 2.03 Å, N-H...O 128°). The free nitrate ion is located close to the co-ordinated water molecule in such a way that it forms a three atom bridge between one of the water hydrogen atoms (bond H) (O...O 2.70 Å, H...O 1.60 Å, O-H...O 158°) and the hydrogen atom attached to N(12a) (bond E) (N...O 3.04 Å, H...O 1.91 Å, N-H...O 158°). The oxygen of the methanol molecule bridges the other water hydrogen atom (bond I) (O...O 2.72 Å, H...O 1.78 Å, O-H...O 165°) and the amine hydrogen attached to N(11b) (bond G) (N...O 3.24 Å, H...O 2.33 Å, N-H...O 146°), although the latter is probably the weakest of the hydrogen bonds with the N...O distance of 3.24 Å. Except for this distance, all the others are within the range observed for Y...X distances in hydrogen bonded systems (N...O 2.93±0.11 Å, O...O 2.72±0.04 Å).[63] The hydrogen atom attached to N(21b) (in either rac or meso forms of the neutral complex) is disordered over two sites and is the only amine hydrogen atom not involved in hydrogen bonding interactions. The absence of hydrogen bonding to this particular amine probably explains why the adjacent carbon atom is disordered in the crystal structure.

### 3.2 Complexes with nickel(II) chloride and thiocyanate

The ligands $L^{14}$ to $L^{16}$ form crystalline chloro complexes by reaction with hexaaquanickel(II) chloride in methanol at ambient temperature within twenty-four hours. The corresponding complexes of $L^{17}$ and $L^{19}$ were obtained as powders after heating mixtures of the ligand and the nickel(II) salt in methanol and acetonitrile, respectively. Recrystallization of the complex of $L^{17}$ from methanol/dichloromethane yielded crystals suitable for X-ray structure determination. No such suitable crystals were obtained for the complexes of $L^{14}$, $L^{16}$ and $L^{19}$.

Analogous isothiocyanato complexes of $L^{14}$ to $L^{19}$ (except for the ligand $L^{18}$, which was not synthesized) were obtained by reaction of methanol or methanol/dichloromethane solutions of the ligands and hexaaquanickel(II) perchlorate (in the case of $L^{14}$) or tetrafluoroborate (for the larger ligands), followed by addition of potassium thiocyanate. This procedure yielded the complexes of $L^{14}$ to $L^{17}$ as crystals, which were suitable for X-ray structural study, but that of $L^{19}$ could only be obtained as a powder. Satisfactory microanalytical results (C, H and N) for all the complexes allowed their formulation as NiLX2 (X = Cl or NCS).

The colours of the complexes (purple to blue-green) and their visible spectra (§3.2.5) were consistent with their being pseudo-octahedral high-spin nickel(II) complexes of the tetraaza macrocycles.[101] In addition, the magnetic moments of the nickel(II) chloride derivatives of $L^{14}$ to $L^{17}$ lie in the range 3.15 to 3.30 B.M., as expected for high-spin complexes of nickel(II).[39] Previous X-ray crystallographic studies of $[NiL^{14}(NCS)_2]$,[25] and $[NiL^{15}Cl_2]$,[52] combined with the present structural determinations of $[NiL^{17}Cl_2]$ and $[NiL^{N}(NCS)_2]$ (N = 15 to 17), confirmed the expected trans-diacido

nature of the complexes.

### 3.2.1 The structure of $[NiL^{17}Cl_2]$

Crystal data and details of structure solution and refinement are given in Chapter Six and tables of fractional atomic coordinates etc. are collected in the Appendix (Tables A4.1 to A4.5)

The asymmetric unit contains one molecule of the trans-dichloro complex with the nickel atom in the pseudo-octahedral environment previously observed for $[NiL^{15}Cl_2]$.[52] The macrocycle is co-ordinated around the metal giving a nearly planar arrangement of the nitrogen donors (Figure 3.6). In common with all the other nickel(II) complexes, $[NiL^{17}Cl_2]$ has an overall step shape with the phenylene rings inclined to either side of the macrocycle donor plane (53° for the a-ring, 51° for the b-ring).

The deviations of the metal and amine nitrogen donors from the $N_4$ least-squares plane in $[NiL^{15}Cl_2]$ and $[NiL^{17}Cl_2]$ are given in Figure 3.7. The tetrahedral distortion of the macrocyclic donor set of $[NiL^{17}Cl_2]$ (up to 0.17 Å) is more pronounced than that in $[NiL^{15}Cl_2]$ (up to 0.062 Å). Although the donor atoms become less co-planar as the ring size is increased from fifteen to seventeen, the deviation of the nickel atom from the plane is reduced, from 0.019 Å in $[NiL^{15}Cl_2]$, to 0.008 Å in $[NiL^{17}Cl_2]$.

The bond lengths and angles in the co-ordination spheres are given in Table 3.4. In $[NiL^{17}Cl_2]$, the angle subtended at the nickel atom by the anilino donors is 80.7(3)°, 20° less than that by the benzylamino donors [100.9(3)°], reflecting the strain caused by the inclusion of the $C_5$-chain between the latter. In $[NiL^{15}Cl_2]$, in which only a $C_3$-chain is inserted between the benzylamino donors, this bite

**FIGURE 3.6** The structure of $[NiL^{15}Cl_2]$ viewed (a) onto and (b) across the macrocyclic plane and comparable views (c) and (d) of the structure of $[NiL^{17}Cl_2]$.

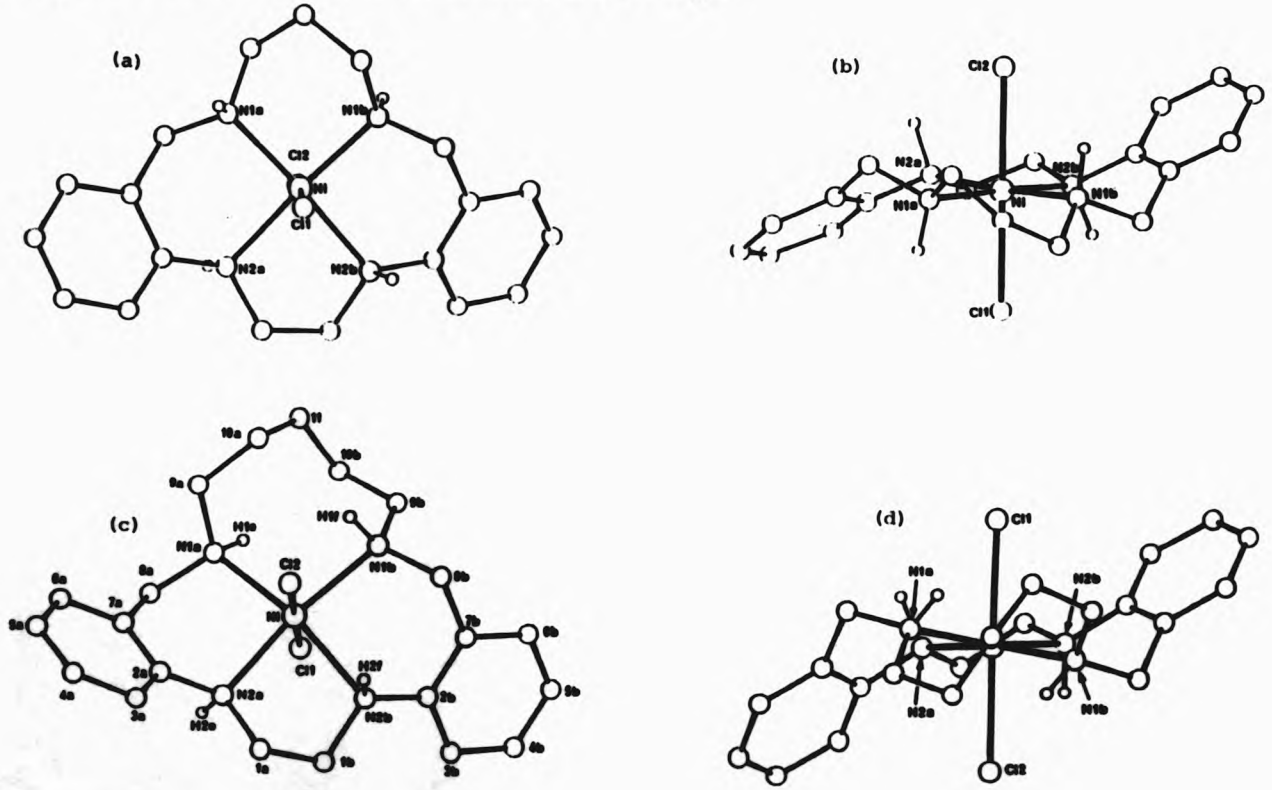

TABLE 3.4 Bond lengths ( Å) and selected angles (°) in the co-ordination spheres for the dichloro complexes of $L^{15}$ and $L^{17}$.

| | $[NiL^{15}Cl_2]$ | | $[NiL^{17}Cl_2]$ | |
|---|---|---|---|---|
| | (part a) | (part b) | (part a) | (part b) |
| Ni-N1 | 2.059(10) | 2.089(10) | 2.140(11) | 2.137(6) |
| Ni-N2 | 2.162(10) | 2.138(9) | 2.156(7) | 2.176(10) |
| Ni-Cl(1) | 2.465(3) | | 2.461(3) | |
| Ni-Cl(2) | 2.471(3) | | 2.437(3) | |
| N1-Ni-N1 | 92.5(4) | | 100.9(3) | |
| N2-Ni-N2 | 83.1(4) | | 80.7(3) | |
| N1-Ni-N2 | 92.4(4) | 92.2(4) | 89.8(3) | 89.9(3) |

FIGURE 3.7 The co-ordination spheres of (a) $[NiL^{15}Cl_2]$ and (b) $[NiL^{17}Cl_2]$ showing the deviations from the least-squares planes of the macrocyclic donor atoms.

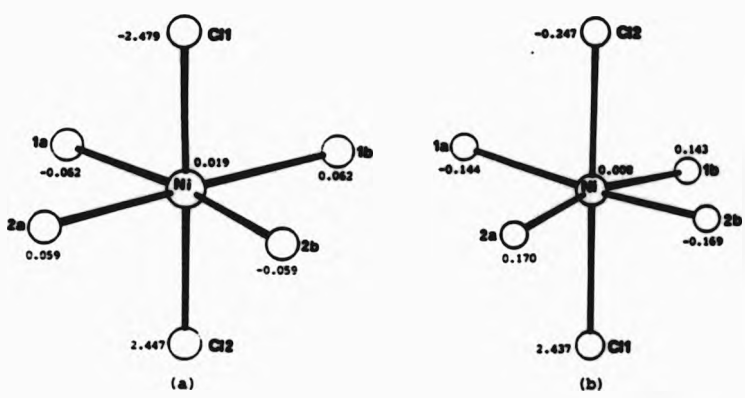

angle is only 92.5(4)°.

As in $[NiL^{15}Cl_2]$ and the nitrato complexes of $L^{16}$, the Ni-N bonds in $[NiL^{17}Cl_2]$ are shorter for the benzylamino [Ni-N(1) 2.140(11) and 2.137(6) Å] than for the anilino nitrogen atoms [Ni-N(2) 2.156(7) and 2.176(10) Å], but the difference is not so great as in $[NiL^{15}Cl_2]$ where the Ni-N(1) bond lengths are only 2.059(19) and 2.089(10) Å.

The Ni-Cl bond lengths in $[NiL^{17}Cl_2]$ are significantly different to each other [Ni-Cl(1) 2.461(3), Ni-Cl(2) 2.437(3) Å], but are comparable with those reported in $[NiL^{15}Cl_2]$ [2.465(3) and 2.471(3) Å],[52] and in the complexes of [14]aneN$_4$, [15]aneN$_4$ and [16]aneN$_4$ (2.428 to 2.510 Å).[89] In the complex $[NiL^{17}Cl_2]$, the difference between Ni-Cl(1) and Ni-Cl(2) may be caused by the formation of a centrosymmetric hydrogen bonded dimeric unit involving Cl(1). The hydrogen atom attached to N(2a) forms a strong hydrogen bond with Cl(1) in the molecule at -x,-y,-z (Cl...N 3.29 Å, Cl...H 2.25 Å, N-H...Cl 162°). The sum of the van der Waals radii gives a calculated contact distance between Cl and N of 3.31 Å.[48] The interaction between N(1b) and Cl(2) at 1-x,1-y,-z, (Cl...N 3.71 Å, Cl...H 3.23 Å, N-H...Cl 113°) is too long for this to be considered as a strong hydrogen bond, especially as the angle at the hydrogen atom is only 113°. A difference in the Ni-Cl bond lengths has been noted previously in the nickel(II) complex of an analogous fourteen-membered $N_2O_2$ ligand (in which the anilino donors are replaced by phenoxy ether donors) [Ni-Cl 2.455(7) and 2.419(7) Å] and a similar scheme of intermolecular hydrogen bonding was thought to cause this difference.[25]

The complex $[NiL^{15}Cl_2]$ has the amine configuration (S,S,S,S) of diastereoisomer V (see §1.10), but $[NiL^{17}Cl_2]$, (although still step-shaped) has the amine hydrogen atoms disposed above the plane in the a-half and below it in the b-half, such that N(2a) and N(2b) retain the S-configuration, but N(1a) and N(1b) are inverted to the R-configuration (diastereoisomer IV).

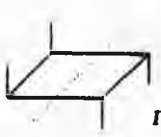

*IV*

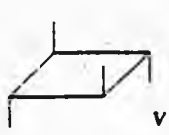

*V*

It may be helpful to compare these two diastereoisomers in terms of the helicities of the chelate rings.[102] The $\delta$ and $\lambda$ helicities are illustrated below (the solid lines are above the plane of the paper).

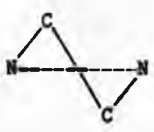


$\delta$

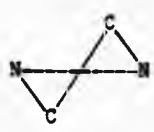


$\lambda$

In the structure of $[NiL^{15}Cl_2]$ drawn in Figure 3.6, the sequence of the helicities of the four chelate rings starting at the five-membered one is $\delta\lambda\delta\lambda$, but in $[NiL^{17}Cl_2]$ it is $\lambda\lambda\delta\lambda$; the helicity of the eight-membered chelate ring is reversed from that of its six-membered counterpart in $[NiL^{15}Cl_2]$.

The five-membered chelate ring in $[NiL^{17}Cl_2]$ adopts the gauche conformation observed for all the other complexes in this series and the eight-membered ring adopts the twist-boat conformation. There is a virtual two-fold rotation axis between Ni and C(11) (Figure 3.4), relating the two halves of the chelate rings. This is considered to

be the least-strained conformation of an eight-membered ring.[103,104,105]

3.2.2 Structures of the thiocyanate complexes of $L^{15}$, $L^{16}$ and $L^{17}$

Crystals obtained in the preparation of the thiocyanate complexes of $L^{15}$, $L^{16}$ and $L^{17}$ were all found suitable for X-ray diffraction analysis without the need for recrystallization and structure determinations were performed by N. Choi.[106] Crystal data and details of refinement are collected in Table 6.1, but it is inappropriate to include here descriptions of the structure solutions. Tables of fractional atomic coordinates, thermal parameters, bond lengths and interbond angles are included in the Appendix (Tables A7.1 to A9.5).

In each of the thiocyanate complexes of $L^{14}$, $L^{15}$, $L^{16}$ and $L^{17}$, the nickel atom is equatorially co-ordinated to all four macrocyclic donor atoms with two trans-axial thiocyanate ligands bonded through the nitrogen atom (Figures 3.8 and 3.9). From the views across the macrocyclic donor plane in Figure 3.9, it can be seen that the macrocyclic ligand in all the complexes adopts the step conformation. Except in the complex of $L^{17}$, the amine hydrogen atoms are disposed alternately above and below the donor plane giving to the chiral nitrogen centres the S,S,S,S configuration of diastereoisomer V (see §1.10) previously observed for $[NiL^{15}Cl_2]$.[52]

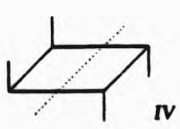

*IV*

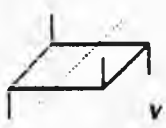

*V*

In contrast, for $[NiL^{17}(NCS)_2]$, the combination of configurations of the nitrogen atoms is the same as those in $[NiL^{17}Cl_2]$ (diastereoisomer

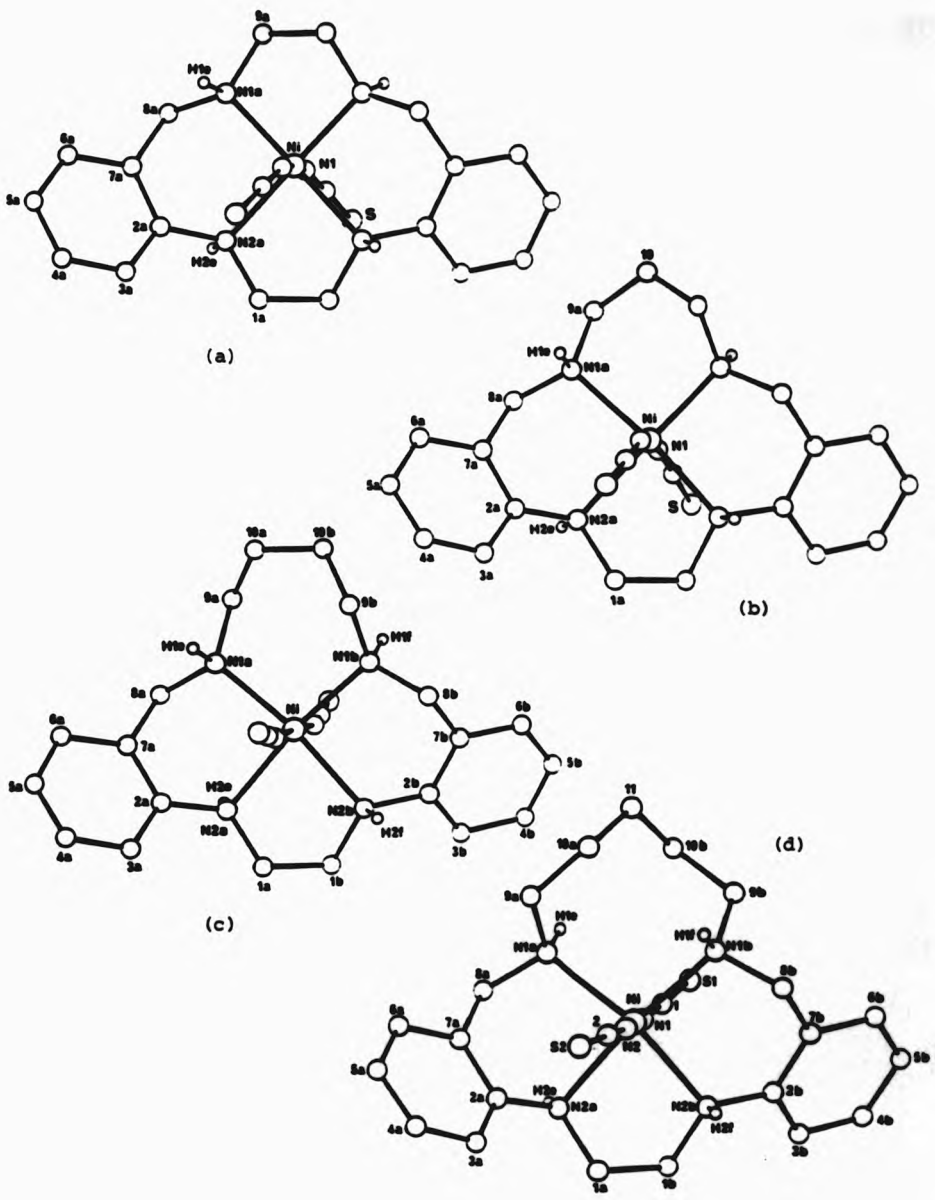


FIGURE 3.8 Views onto the donor plane of the complexes (a) $[NiL^{14}(NCS)_2]$, (b) $[NiL^{15}(NCS)_2]$, (c) $[NiL^{16}(NCS)_2]$ and (d) $[NiL^{17}(NCS)_2]$.

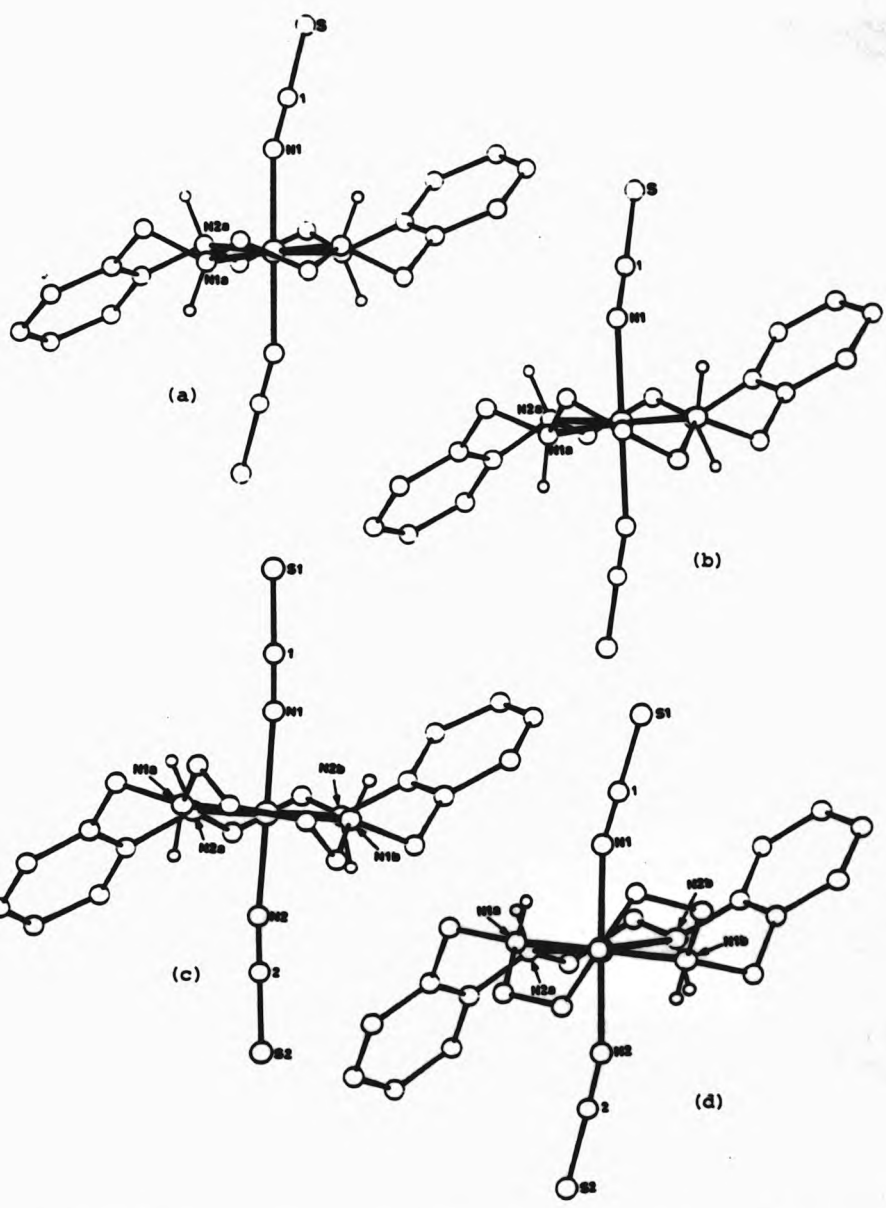


FIGURE 3.9 Views across the donor plane of the complexes (a) $[NiL^{14}(NCS)_2]$, (b) $[NiL^{15}(NCS)_2]$, (c) $[NiL^{16}(NCS)_2]$ and (d) $[NiL^{17}(NCS)_2]$.

IV), with the anilino nitrogen atoms, N(2a) and N(2b), in the S-configuration and the benzylamino nitrogen atoms, N(1a) and N(1b), in the R-configuration.

The dihedral angles between the donor plane and the planes of the phenylene rings increase with increasing ring size: from 35° for both rings of $[NiL^{14}(NCS)_2]$, to 40° for both rings of $[NiL^{15}(NCS)_2]$, 46° for both rings of $[NiL^{16}(NCS)_2]$, up to 55° and 50° for the a- and b-rings of $[NiL^{17}(NCS)_2]$, respectively (Figure 3.10).

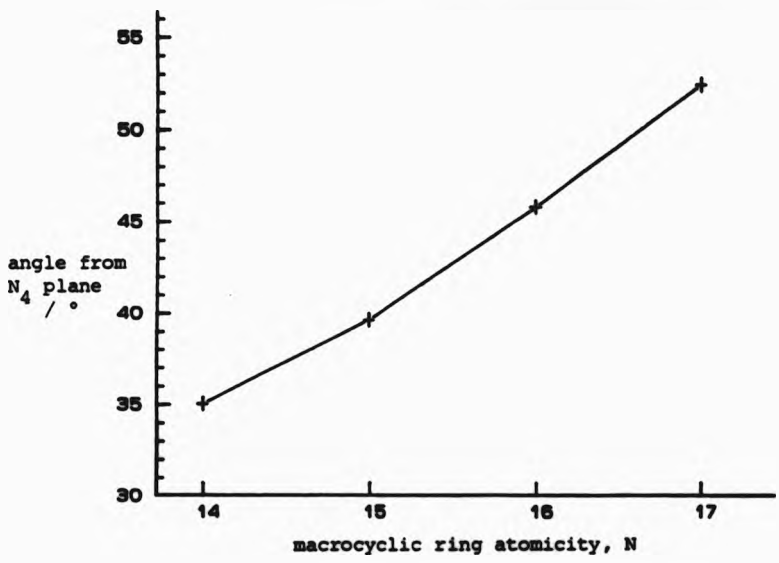


FIGURE 3.10 The variation of the dihedral angle between the least-squares plane of the phenylene rings and the $N_4$ macrocyclic donor set for the complexes $[NiL^{N}(NCS)_2]$ (N = 14 to 17). For $L^{16}$ and $L^{17}$ the angle plotted is the mean of the angles for each phenylene ring (45.7 and 45.9° for the a- and b-rings of $L^{16}$ and 55.4 and 50.0° for those of $L^{17}$).

The increase in this dihedral angle is a consequence of the benzylamino donors having to be brought into closer proximity than they are in the free ligands. The distance N(1a)...N(1b) decreases in the complexes from that in the free ligands ($L^{14}$ 2.90 to 2.79 Å, $L^{15}$ 3.36 to 2.98 Å, $L^{16}$ 3.76 to 3.23 Å, $L^{17}$ 5.38 to 3.29 Å) and the larger the decrease, the greater the dihedral angle.

The bond lengths and selected angles within the co-ordination spheres are listed in Table 3.5.

TABLE 3.5 Bond lengths ( Å) and selected angles (°) at the nickel atom for the nickel(II) thiocyanate complexes of $L^{14}$ to $L^{17}$.

| | $L^{14}$ | $L^{15}$ | $L^{16}$ | | $L^{17}$ | |
|---|---|---|---|---|---|---|
| | | | (part a) | (part b) | (part a) | (part b) |
| Ni-N1 | 2.046(2) | 2.075(10) | 2.137(10) | 2.125(9) | 2.147(6) | 2.138(5) |
| Ni-N2 | 2.091(2) | 2.138(9) | 2.176(8) | 2.181(8) | 2.166(6) | 2.200(6) |
| Ni-NCS(1) | 2.108(2) | 2.093(10) | 2.010(11) | | 2.072(6) | |
| Ni-NCS(2) | " | " | 2.054(11) | | 2.049(5) | |
| N1-Ni-N1 | 86.1(1) | 91.7(5) | 97.4(4) | | 100.4(2) | |
| N2-Ni-N2 | 85.8(1) | 83.7(5) | 81.5(3) | | 81.1(2) | |
| N1-Ni-N2 | 94.5(1) | 92.5(4) | 90.3(3) | 90.4(3) | 89.2(2) | 90.3(2) |

In the complex $[NiL^{14}(NCS)_2]$ the Ni-N bond lengths to each type of macrocyclic nitrogen atom are significantly different [Ni-N(1) 2.046(2), Ni-N(2) 2.091(2) Å] and for $[NiL^{15}(NCS)_2]$, the Ni-N(benzylamino) and Ni-N(anilino) bond lengths are still different [Ni-N(1) 2.114(8), Ni-N(2) 2.124(9) Å], but the higher e.s.d.'s (relative to those for the complex of $L^{14}$) reduce the significance of differences between these two bonds. Although the crystallographic

two-fold symmetry is absent in [NiL$^{16}$(NCS)$_2$], there is little significant difference between pairs of chemically equivalent bonds, but there is a marked difference between bonds to different nitrogen types [Ni-N(1a) 2.137(10), Ni-N(1b) 2.125 Å, Ni-N(2a) 2.176(8), Ni-N(2b) 2.181(8) Å]. In [NiL$^{17}$(NCS)$_2$] the Ni-N(1) bonds are not significantly different [Ni-N(1a) 2.147(6), Ni-N(1b) 2.138(5) Å], but there is a marked difference between the two Ni-N(2) bonds [Ni-N(2a) 2.166(6), Ni-N(2b) 2.200(6) Å].

The Ni-N(thiocyanato) bond lengths change across the series of ligands; in [NiL$^{14}$(NCS)$_2$] they are longer than all the Ni-N(macrocycle) bonds [2.108 Å], in [NiL$^{15}$(NCS)$_2$] they are intermediate between Ni-N(benzylamino and Ni-N(anilino) [2.093(11) Å], and in [NiL$^{16}$(NCS)$_2$] and [NiL$^{17}$(NCS)$_2$] they are shorter than all the Ni-N(macrocycle) bonds [2.010(11) to 2.072(6) Å]. The small but significant difference between the Ni-N(thiocyanate) bonds in [NiL$^{17}$(NCS)$_2$] [Ni-N(1) 2.072(6), Ni-N(2) 2.049(5) Å], may be attributable to an intermolecular hydrogen bond between the sulphur atom, S(1) of the thiocyanate ligand with the longer Ni-N bond and the hydrogen atom attached to N(1b) in the molecule at x,1+y,z (S...N 3.58 Å, S...H 2.70 Å, S...H-N 137°) cf. the calculated N-H...S contact distance 3.35 Å,[48] and the observed contact distance, 3.39±0.12 Å.[47] There is no corresponding interaction between S(2) in [NiL$^{17}$(NCS)$_2$] and an amine hydrogen. It is clear that intermolecular hydrogen bonding in these complexes affects the Ni-N(thiocyanate) bond lengths and the Ni-N-C angle defining the tilt of the thiocyanato ligands. The sulphur atom, S(1), of [NiL$^{15}$(NCS)$_2$] is hydrogen bonded to the hydrogen atom attached to N(1a) of the molecule at $\frac{1}{2}$-x,$\frac{1}{2}$+y,$\frac{1}{2}$-z (S...N 3.57 Å, S...H 2.80 Å, N-H...S 128°) and, by symmetry, S(1)' is likewise

hydrogen bonded to the molecule at x-½,-y-½,z-½. This is the same situation that obtains in [NiL$^{14}$(NCS)$_2$]; the benxylamine amines interact with the thiocyanate sulphur atoms of neighbouring molecules (S...N 3.42 Å, S...H 2.88 Å, N-H...S 127°). No such hydrogen bonded interactions are observed in [NiL$^{16}$(NCS)$_2$].

In all the complexes, the thiocyanato ligands are linear to within 1°, but are tilted to different extents, such that in the complexes of L$^{14}$ and L$^{15}$, (in which the thiocyanato ligands are hydrogen bonded) the angle Ni-N-C is 156.0(2)° and 158.4(9)°, respectively. In the complex of L$^{16}$, where the sulphur atoms are not engaged in hydrogen bonding, this angle is 171(1)° and 172(1)° for the a- and b-halves, respectively. In [NiL$^{17}$(NCS)$_2$], S(1) is hydrogen bonded and the angle of tilt is 159.6(6)°, but S(2) is not hydrogen bonded and the Ni-N-C angle is 166.3(4)°, closer to those seen in [NiL$^{16}$(NCS$_2$]. In the present compounds, this angle and the Ni-N(thiocyanate) bond lengths are strongly influenced by the presence or absence of N-H...S hydrogen bonding; the presence of such a hydrogen bond reduces the Ni-N-C angle from ca. 168° to ca. 158° and increases the Ni-N bond length from ca. 2.05 to ca. 2.10 Å.

In comparison, similar intermolecular hydrogen bonding has been noted in nickel(II) thiocyanate complexes of [14]aneN$_4$ (cyclam) and its homologues, [15]aneN$_4$ and [16]aneN$_4$.[89] The Ni-N-C angles range from 156.2(2)° to 168.2(2)° in the four independent molecules of {Ni[14]aneN$_4$(NCS)$_2$} and the variation in orientation of the thiocyanato groups is attributed to hydrogen bonding, but no details of the hydrogen bonds are given.

The bite angle, N(1a)-Ni-N(1b), of the five- to eight-membered chelate rings increases with ring size from 86.1(1)° in $[NiL^{14}(NCS)_2]$ to 100.4(2)° in $[NiL^{17}(NCS)_2]$ (Figure 3.11). The angle, N(2a)-Ni-N(2b) varies less: from 85.8(1)° in $[NiL^{14}(NCS)_2]$ to 81.5(3)° in $[NiL^{16}(NCS)_2]$.

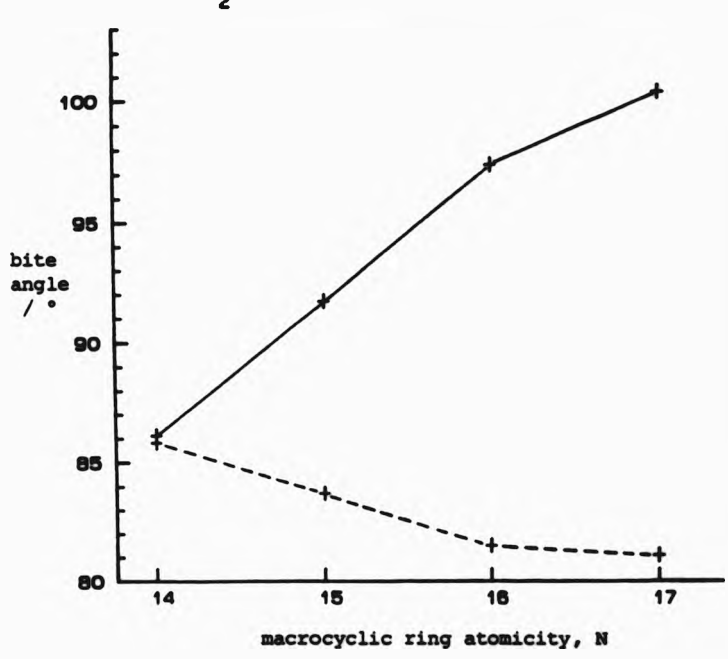


FIGURE 3.11 Variation of chelate ring bite angles for the six- to eight-membered chelate rings containing the benzylamino donor atoms (solid line) and the transoid five-membered rings containing the anilino donor atoms (dashed line) for the complexes $[NiL^{N}(NCS)_2]$ (N = 14 to 17).

Instead of a further decrease in this angle in $[NiL^{17}(NCS)_2]$, it shows a value [81.1(2)°] which is only slightly smaller. The decrease in this bite angle is accompanied by an increase in the puckering of the five-membered chelate ring; the deviations of C(1a) and C(1b) from the

$NiN_2$ plane increase from +0.25 and +0.30 Å in $[NiL^{14}(NCS)_2]$ and $[NiL^{15}(NCS)_2]$, respectively, to C(1a) 0.44, C(1b) -0.40 Å in $[NiL^{16}(NCS)_2]$ and to C(1a) 0.40, C(1b) -0.60 Å in $[NiL^{17}(NCS)_2]$.

Table 3.6 lists the deviations of the metal and the donor atoms from the mean plane of the macrocyclic donor sets. In the complexes of $L^{14}$ and $L^{15}$ the nickel atom is exactly in the mean plane in accordance with the crystallographic two-fold symmetry, virtually in the plane in the complex of $L^{16}$ (deviation 0.005 Å) and 0.025 Å out of the plane in $[NiL^{17}(NCS)_2]$. There is a discontinuity in the way the tetrahedral distortion of the macrocyclic donor set varies as the ligand ring size is increased (Figure 3.12); the distortion is at a minimum for the complex with $L^{16}$ (ca. 0.08 Å). The complexes $[NiL^{14}(NCS)_2]$ and $[NiL^{17}(NCS)_2]$ show relatively large, but mutually similar displacements of the alkylamino nitrogen donors, N(1) (ca. 0.13 Å). Increasing the size of the chelate ring from five- to eight-membered has a greater effect on the transoid five-membered chelate ring, twisting the anilino nitrogens, N(2), further out of the mean plane of the donors {from ca. 0.12 Å in $[NiL^{14}(NCS)_2]$ to ca. 0.15 Å in $[NiL^{17}(NCS)_2]$}. The dihedral angle between the planes defined by Ni, N(1a), N(2a) and by Ni, N(1b), N(2b) show a necessarily similar trend from 9° for the complex of $L^{14}$ through 6° and 3° for those of $L^{15}$ and $L^{16}$, respectively to 11° for the complex of $L^{17}$.

The conformations of the chelate rings incorporating the benzylamino donor atoms, N(1) are illustrated in Figure 3.4, together with those of the other complexes discussed earlier. The six-membered chelate ring in $[NiL^{15}(NCS)_2]$ adopts the same twist conformation as it does in $[NiL^{15}Cl_2]$ with C(9a) displaced above the $NiN_2$ plane by a similar amount as C(9b) is displaced below it (between 0.60 and

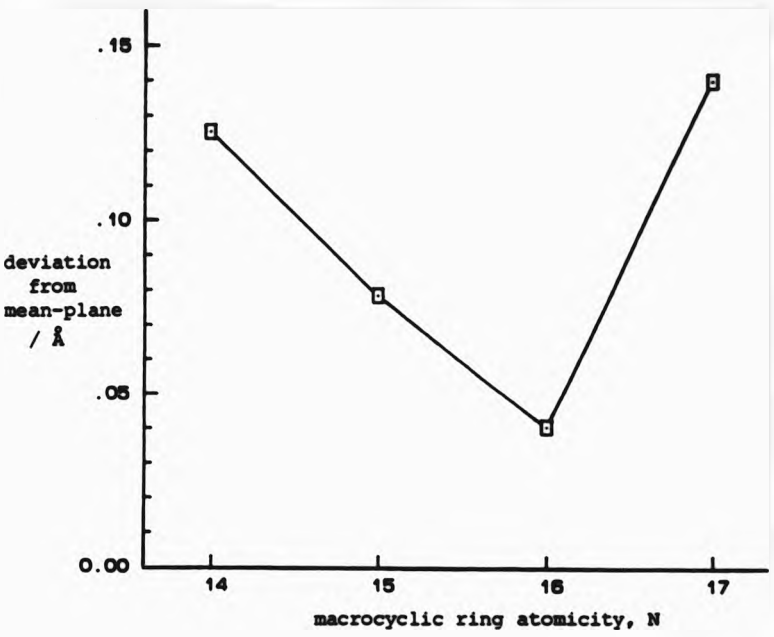


FIGURE 3.12 The mean of the deviations of the macrocyclic donor atoms from their least-squares plane (signs ignored) for the complexes $[NiL^{N}(NCS)_2]$ (N = 14 to 17).

TABLE 3.6 Deviations ( Å) from the least-squares $N_4$ plane in complexes of the type, $[NiL^{N}(NCS)_2]$.

| N | Ni | N(1a) | N(1b) | N(2a) | N(2b) | NCS(1) | NCS(2) |
|---|---|---|---|---|---|---|---|
| 14 | 0.000 | -0.127 | 0.127 | 0.124 | -0.124 | -2.107 | 2.107 |
| 15 | 0.000 | -0.077 | 0.077 | 0.081 | -0.081 | -2.090 | 2.090 |
| 16 | -0.005 | -0.038 | 0.038 | 0.043 | -0.044 | -2.010 | 2.035 |
| 17 | 0.025 | -0.131 | 0.129 | 0.153 | -0.150 | -2.046 | 2.072 |

0.85 Å). The seven-membered chelate ring in $[NiL^{16}(NCS)_2]$ adopts the same skew(h) conformation as it does in $[NiL^{16}(NO_3)(H_2O)]^+$ and in the minor conformer of $[NiL^{16}(NO_3)_2]$. The eight-membered chelate ring of $[NiL^{17}(NCS)_2]$ adopts the same twist-boat conformation as that observed in $[NiL^{17}Cl_2]$ with C(9a) and C(10a) displaced to one side of the $NiN_2$ plane (ca. -0.1 Å) by as much as C(9b) and C(10b) are displaced to the other side (Figure 3.4).

The sequence of chelate ring helicities in the thiocyanate complexes is the same as that seen for the chloride complexes: $\delta\lambda\delta\lambda$ for the $L^{15}$ complex and $\lambda\lambda\delta\lambda$ for the complex of $L^{17}$. The sequences in the complexes of $L^{14}$ and $L^{16}$ match that in $[NiL^{15}Cl_2]$. This change in helicity is discussed further in the following section.

3.2.3 Correlation between axial and in-plane bond lengths

It has been shown by X-ray structural studies of complexes of the type $[NiLX_2]$ {L = [14]aneN$_4$, [15]aneN$_4$ and [16]aneN$_4$; X = Cl or NCS} that the increase in the in-plane Ni-N bond lengths, which occurs with increasing ring size, is accompanied by a decrease in the axial, Ni-X, bond lengths,[89] although the correlation is poor and over a limited range of macrocyclic ligands.

For the present compounds, a similar negative correlation exists for the nickel(II) thiocyanate complexes of $L^{14}$ to $L^{16}$ (Figure 3.13). The anilino and benzylamino donor atoms exhibit Ni-N bond lengths sufficiently distinct to be treated separately, but both types of donor show the same trend. There is an apparent reversal of the correlation for $[NiL^{17}(NCS)_2]$ with the in-plane bond lengths being slightly longer than in $[NiL^{16}(NCS)_2]$ and the axial bond lengths being markedly longer. Interestingly, the minimum in this correlation, at

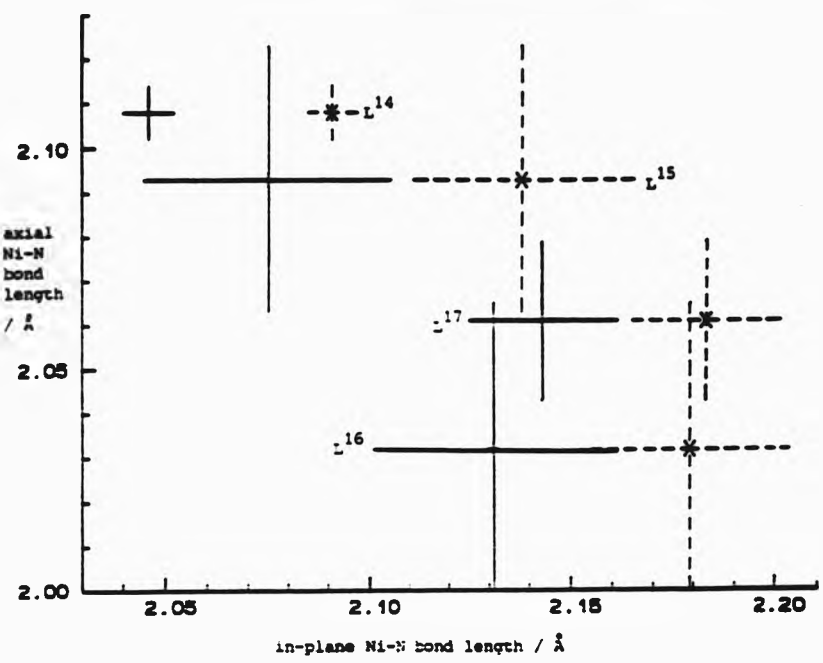


FIGURE 3.13 Correlation between axial and in-plane ligand bond lengths in complexes of the type $[NiL^{N}X_2]$ (N = 14 - 17, X = NCS). The three pairs of chemically equivalent bond lengths, Ni-N(thiocyanate), Ni-N(anilino) and Ni-N(benzylamino) are also crystallographically equivalent in the complexes of $L^{14}$ and $L^{15}$ and the error bars represent three times the e.s.d. on each bond length. For the complexes of $L^{16}$ and $L^{17}$, the mean of each pair of bond lengths is plotted and the error bars represent three times the larger e.s.d.

which point the axial ligands are shortest, occurs at the point in the ligand series where the macrocyclic donors are most co-planar, at $[NiL^{16}(NCS)_2]$. Of course, such a reciprocal relationship can only exist over a limited range; the Ni-N(axial) bond lengths must have a minimum value, no matter how much the Ni-N(in-plane) bond lengths increase. One would expect a levelling off of the bond lengths, but in the present compounds the Ni-N(axial) bond lengths increase sharply with a slight increase in Ni-N(in-plane) at $[NiL^{17}(NCS)_2]$. Changing the conformation of the ligand may relieve some of the strain that would have been associated with Ni-N(in-plane) bond lengths of ca. 2.13 Å (which would be necessary if the negative correlation were to continue to the complex of $L^{17}$). The effect that intermolecular hydrogen bonding has on the axial Ni-N bond lengths has already been discussed. In the light of this, it might be expected that a correlation of the above type would be affected by such hydrogen bonding, in that Ni-N(thiocyanato) would be distorted from their unperturbed value.

It may be that the change of ligand conformation from diastereoisomer V for the complexes of $L^{14}$, $L^{15}$ and $L^{16}$, to that of diastereoisomer IV for the complexes of $L^{17}$ represents a subtle structural dislocation (see §1.4) of the ligand co-ordination mode.

V IV

It will be shown in Chapter Five that the ligand hole size remains virtually constant on increasing the ligand ring size from sixteen- to seventeen-membered.

A further correlation of this type has been observed in the thiocyanate complexes of the series of fourteen-membered $N_4$ ligands (3.i), $L^{14}$ and (3.ii) in which the ligand structure is successively modified to change the nature of the donor atoms to that of weaker anilino donors.[38]

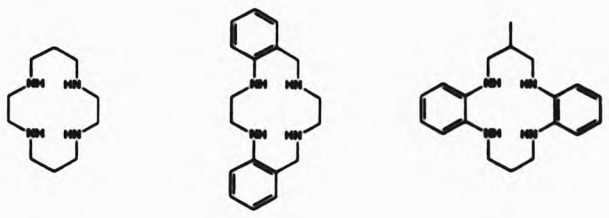

(3.i) $L^{14}$ (3.ii)

Although the structures of only two chloride complexes (of $L^{15}$ and $L^{17}$) have been determined, a correlation of the above type is still apparent for these (see Table 3.4), but it is complicated by the relatively large difference in Ni-Cl bond lengths in $[NiL^{17}Cl_2]$.

### 3.2.4 Infrared spectra of the nickel(II) thiocyanate complexes

The co-ordination mode of the potentially ambidentate thiocyanate ligand may be deduced from its vibrational frequencies; N- and S-bonded thiocyanates are reported to yield C-N stretching frequencies which fall in the range 2040-2080 and 2080-2120 $cm^{-1}$, respectively.[107] The present thiocyanate complexes each exhibit one or two intense bands at the upper end of the range for N-bonded thiocyanates ($L^{14}$ 2074, $L^{15}$ 2073, $L^{16}$ 2080, $L^{17}$ 2085, $L^{19}$ 2073 and 2085 $cm^{-1}$). The thiocyanate complexes of $L^{14}$ and $L^{15}$ each show an intense band at 2073 to 2074 $cm^{-1}$, within the N-bonded range. Although the complexes of $L^{16}$ and $L^{17}$ exhibit this band at 2085 $cm^{-1}$, just outside the expected N-bonded range, the X-ray structure

determinations show that in all these complexes the thiocyanate ligands are N-bonded. Although two bands are observable for $[NiL^{19}(NCS)_2]$, there is no reason to suspect that the thiocyanato ligands in this complex are other than N-bonded. A C-S stretching band should be expected between 780 and 860 $cm^{-1}$,[107] but this could not be assigned because of the presence of macrocyclic ligand absorptions in this region.

In general, the aryl-alkyl amine N-H absorptions are expected at higher energy than those of the dialkyl amines.[76] In the absence of interactions with other parts of the molecule (or with neighbouring molecules), each type of N-H group (ArNHR and RNHR) should exhibit one N-H stretching band. In a wide range of diazidonickel(II) complexes of cyclam and its homologues, all the amine donor atoms are dialkylamines, but exhibit one, two or three N-H bands.[107a] Besides the type of amine present, two other important factors contribute to the number, position and intensity of the N-H bands: the molecular symmetry and the degree and complexity of hydrogen bonding.

The complexes $[NiL^{14}][BF_4]_2$ (see §3.3), $[NiL^{14}(NCS)_2]$ and $[NiL^{15}(NCS)_2]$ have a crystallographic axis of symmetry through the midpoints of the alkyl bridges. In these cases, two N-H stretching bands are observed which are similar in intensity in $[NiL^{14}][BF_4]_2$ (at 3214 and 3174 $cm^{-1}$). Although no crystallographic study has been performed on $[NiL^{14}Cl_2]$, there is no reason to suspect that the structure is much different to that of the corresponding thiocyanate complex and indeed this molecule also exhibits two similarly intense N-H absorptions (at 3247 and 3200 $cm^{-1}$).

The N-H band at lower frequency in both $[NiL^{14}(NCS)_2]$ and $[NiL^{15}(NCS)_2]$ (3241 $cm^{-1}$ in both complexes) is the more intense and this intensity difference may be attributable to the effect of the observed intermolecular hydrogen bonding (N-H...S) involving the benzylamino groups.[46] As mentioned in the last section, no comparable hydrogen bonding is observable in $[NiL^{16}(NCS)_2]$, but the N-H absorptions are not equal in intensity and the molecule shows only a virtual axis of symmetry in the crystal structure. Obviously, the situation is more complicated than the simple considerations above would indicate. Furthermore, many of the complexes show more bands in this region than can be accounted for in this simple way.

### 3.2.5 Electronic spectra of the nickel(II) complexes

The visible spectra of the thiocyanate and chloride complexes were recorded in acetonitrile and dichloromethane, respectively. The range of measurement was extended into the near-infrared (to 1500 nm) so as to locate the lowest energy band. Table 3.7 lists the wavelengths and assignments of the prominent absorption bands in the spectra of the complexes. All spectra contain between three and six weak peaks which are characteristic of pseudo-octahedral nickel(II) with various degrees of distortion.[108] A regular octahedral complex ($O_h$ symmetry), such as $[Ni(H_2O)_6]^{2+}$, shows three peaks due to the spin-allowed transitions indicated in Figure 3.14. Tetragonal distortion (to $D_{4h}$ symmetry) arises from differences in the in-plane and axial ligand field strengths ($Dq^{xy}$ and $Dq^{z}$, respectively). None of the complexes, when viewed in detail, conform to $D_{4h}$ symmetry, and lower point groups such as $C_{2v}$ would be appropriate for particular cases. These reductions in symmetry should provide additional d-orbital splittings and give rise to, for example, band broadening.

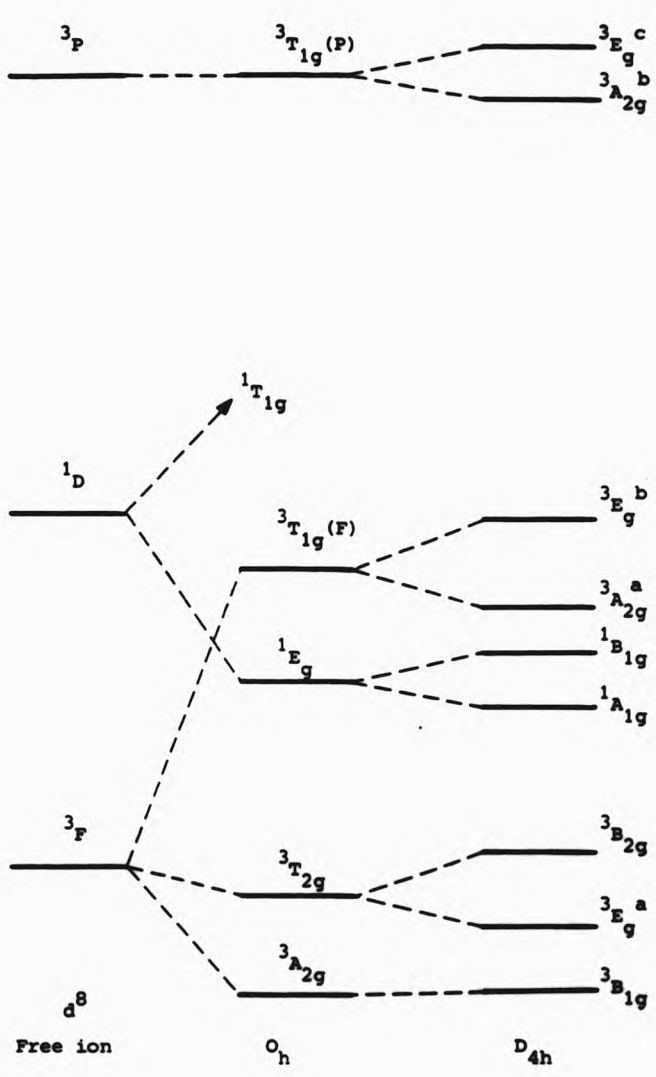


**FIGURE 3.14** Energy level diagram for a $d^8$ ion in octahedral, $O_h$, and tetragonal, $D_{4h}$, symmetry showing expected transitions for each system.

However, if the additional splittings are small compared with the splittings derived from the presence of four nitrogen donors in an approximate equatorial plane and two donors on the axis perpendicular to that plane, then the assumption of $D_{4h}$ symmetry may be adequate for spectral assignment.

TABLE 3.7 The observed electronic spectral transitions (nm) of $[NiL^{N}X_2]$ (N = 14-19, X = Cl or NCS).(a)

| | | transitions | | | | |
|---|---|---|---|---|---|---|
| X | N | $^3B_{1g} \rightarrow$ | $^3E_g{}^a$ | $^3B_{2g}$ | $^3A_{2g}{}^a$ & $^3E_g{}^b$ | $^3A_{2g}{}^b$ & $^3E_g{}^c$ |
| Cl | 14 | | 1090 | 683 | 532 | 336 |
| Cl | 15 | | 1140 | 693 | 580 | 375 |
| Cl | 16 | | 1160 | 910 | 635 | 393 |
| Cl | 17 | | 1130 | 902 | 642 | 393 |
| Cl | 19 | | 1150 | 990 | 661 | 388 |
| NCS | 14 | | 920 | 700 | 510 | 381 |
| NCS | 15 | | 920 | 760 | 545 | 380 |
| | | $^3A_{2g} \rightarrow$ | $^3T_{2g}$ | | $^3T_{1g}(F)$ | $^3T_{1g}(P)$ |
| NCS | 16 | | 910 | | 565 | 350 |
| NCS | 17 | | 975 | | 592 | 370 |
| NCS | 19 | | 950 | | 585 | 418 |

(a) As solutions ($10^{-3}$ mol $dm^{-3}$) in $CH_2Cl_2$ for X = Cl or $CH_3CN$ for X = NCS; (b) shoulder.

For complexes with only weak tetragonal distortion, the splitting is often only detectable in the lowest energy band; the splitting of the other two bands is smaller than the bandwidth.[86] Such a situation seems apparent in the spectra of the chloride complexes and the thiocyanate complexes of $L^{14}$ and $L^{15}$. The thiocyanate complexes of

the larger ligands show no detectable splitting even in the lowest energy band and are essentially octahedral. For each complex, the most prominent band in the visible region is ascribed to the transition to $^3T_{1g}(F)$. As the size of the macrocyclic ring is increased, the energy of this transition decreases in the chloro complexes from 532 nm ($L^{14}$) to 580 nm ($L^{15}$) and from $L^{16}$, it levels off to 635 nm ($L^{16}$), 642 nm ($L^{17}$) and 661 nm ($L^{19}$). For the thiocyanato complexes, this levelling off occurs later in the series (from $L^{17}$); the band maxima here are 510 nm ($L^{14}$), 545 nm ($L^{15}$), 565 nm ($L^{16}$), 592 nm ($L^{17}$) and 585 nm ($L^{19}$).

In most of the complexes, except $[NiL^{15}(NCS)_2]$, there is a shoulder on the lowest energy band at between 800 and 855 $cm^{-1}$. This band is not discernible in $[NiL^{15}(NCS)_2]$, probably because it is between two close bands at 920 and 760 nm. It is not reasonable to assign this band between 800 and 855 nm within the triplet system; although they are weak, they are much less broad than the other bands. These are ascribable to one of the spin-forbidden bands ($^3A_{2g} \longrightarrow {}^1E_g$) often seen in the spectra of octahedral nickel(II) complexes.[109] The high energy bands are equally difficult to assign to particular transitions, these occurring mainly as inflections on a relatively strong ligand band in the region of 300 nm, or as well defined shoulders on the tail of the ligand band. In many cases two or more inflections can be detected, one of which may be the high energy spin-forbidden band ($^3A_{2g} \longrightarrow {}^1T_{1g}$).

Assuming some degree of tetragonal distortion, for $Dq^z < Dq^{xy}$, the low energy band should correspond to the transition $^3B_{1g} \longrightarrow {}^3E_g a$. This band would be expected to shift to higher energies as $Dq^z$ increases, with $Dq^{xy}$ constant.[86] In the spectrochemical series

Cl < NCS and, accordingly, the lowest energy band increases from a range of 8600 to 9200 $cm^{-1}$ in the chloride complexes to a range of 10250 to 10900 $cm^{-1}$ in the thiocyanate species.

When the splitting of the low energy band is observable, ligand field splitting parameters can be calculated using the Wentworth - Piper model for tetragonal distortion.[110] This has been further developed for tetragonal nickel(II) complexes.[111] The use of more sophisticated models requires the entire triplet-triplet spectrum. The splitting of the $^3T_{2g}$ octahedral band is dependent solely on the tetragonal splitting parameter Dt, which is proportional to the difference between the strengths of the in-plane ligand field ($Dq^{xy}$) and the axial ligand field ($Dq^{z}$). The difference between the transition energies is (35/4)Dt. The relationships are;

$$\nu(^3B_{1g} \longrightarrow {}^3B_{2g}) = 10Dq^{xy}$$

$$\nu(^3B_{1g} \longrightarrow {}^3E_g{}^a) = 10Dq^{xy} - (35/4)Dt$$

$$Dt = (4/7)(Dq^{xy} - Dq^{z})$$

$$Dq^{z} = (1/10)[2\,\nu(^3B_{1g} \longrightarrow {}^3E_g{}^a) - \nu(^3B_{1g} \longrightarrow {}^3B_{2g})$$

The ligand field splitting parameters calculated from these equations are listed in Table 3.8. For a particular macrocyclic ligand, $Dq^{xy}$ should be virtually independent of the nature of the axial ligand. The absolute values of $Dq^{xy}$, $Dq^{z}$ and Dt are not very reliable because they depend on visual determination of the maxima of very broad absorption bands, but certain trends can still be discerned. The ligand $L^{14}$ exhibits similar $Dq^{xy}$ in the chloride (1464 $cm^{-1}$) and in the thiocyanate complexes (1443 $cm^{-1}$). The ligand $L^{15}$ has a comparable $Dq^{xy}$ in the chloride complex (1443 $cm^{-1}$), but lower in the thiocyanato complex (1316 $cm^{-1}$). In the chloride complexes of the larger ligands, ($L^{16}$, $L^{17}$ and $L^{19}$), $Dq^{xy}$ changes abruptly and levels off to around 1000 to 1100 $cm^{-1}$ and the tetragonal distortion (Dt) is

TABLE 3.8 The ligand field tetragonal splitting parameters ($cm^{-1}$) for complexes of selected tetraaza macrocycles. $[NiLX_2]$ (X = Cl or NCS).

| X | N | $^3E_g$ [a] | $^3B_{2g}$ | $Dq^{xy}$ | $Dq^z$ | Dt |
|---|---|---|---|---|---|---|
| L = $L^{14}$ to $L^{19}$ (a) | | | | | | |
| Cl | 14 | 9170 | 14640 | 1464 | 370 | 625 |
| Cl | 15 | 8770 | 14430 | 1443 | 311 | 647 |
| Cl | 16 | 8620 | 10990 | 1099 | 625 | 271 |
| Cl | 17 | 8850 | 11090 | 1109 | 661 | 276 |
| Cl | 19 | 8700 | 10100 | 1010 | 730 | 160 |
| NCS | 14 | 10870 | 14290 | 1429 | 745 | 391 |
| NCS | 15 | 10870 | 13160 | 1316 | 858 | 262 |
| NCS | 16 | 10990 | - | - | - | - |
| NCS | 17 | 10260 | - | - | - | - |
| NCS | 19 | 10530 | - | - | - | - |
| L = [14]aneN$_4$ (b) | | | | | | |
| Cl | 14 | 8600 | 15200 | 1520 | 200 | 754 |
| NCS | 14 | 11080 | 17800 | 1780 | 436 | 768 |
| L = [15]aneN$_4$ (b) | | | | | | |
| Cl | 15 | 8664 | 14421 | 1442 | 291 | 658 |
| NCS | 15 | 10326 | 15834 | 1583 | 482 | 629 |
| L = [16]aneN$_4$ (b) | | | | | | |
| Cl | 16 | 8510 | 15758 | 1576 | 126 | 829 |
| NCS | 16 | 9606 | 16500 | 1650 | 271 | 788 |

(a) From the spectral assignments in Table 3.7;

(b) data from Ref. 112.

small, 160 to 270 $cm^{-1}$ compared to 625 to 647 $cm^{-1}$ for the smaller ligands. This abrupt change is also noticeable in the thiocyanate complexes, but the apparent lack of band splitting for those of $L^{16}$, $L^{17}$ and $L^{19}$ indicates that the axial and in-plane ligand field strengths are of comparable magnitude and these complexes are essentially octahedral.

The macrocyclic ligand field strength is expected to decrease with increasing ring size,[101] but it can be seen from the splitting parameters that this decrease is not at all regular, a sudden decrease from $L^{15}$ to $L^{16}$ is apparent. Of course, such a decrease in ligand field strength must level off ($Dq^{xy}$ and $Dq^{z}$ approach each other) and in the present series of complexes this levelling off can be seen to occur with ligands larger than $L^{16}$. In the correlation of axial and in-plane bond lengths discussed earlier, it was after the sixteen-membered ligand that the correlation broke down. Although there may be a relationship between the macrocyclic ligand field strength and the in-plane Ni-N bond lengths, it is difficult to make a definite conclusion by comparing data from the solid state with data from solution studies. Broadly speaking however, as the macrocyclic ligand ring size is increased, the in-plane bond lengths increase and the ligand field strength decreases.

Deeth and Kemp have reassigned the spectra of the tetragonal nickel(II) complexes of the cyclam-type ligands using Cellular Ligand Field (CLF) theory.[112] This study takes into account the spin-forbidden bands ignored in the work of Martin et al.[101] CLF theory provides a consistent set of parameters for the local $\sigma$ and $\pi$ metal-ligand interactions.[112] By relating these local parameters to the global parameters Dq, Dt and Ds, the assignments of Martin et

al. were shown to give either $\pi$-acceptor or $\pi$-donor roles to the axial chloride and thiocyanate ligands across the series of complexes. The reassignment of these spectra leads to chemically reasonable $\sigma$-acceptor behaviour for these ligands throughout the series.[112] A thorough analysis of the spectra of the present complexes has not been attempted because of the difficulty of assigning the high energy bands and no attempt has been made to calculate Ds (calculation of the CLF parameters requires Dq, Dt and Ds). However, the identification (by Deeth and Kemp) of the spin-forbidden bands in the spectra reported by Martin et al. gives support to the assignment of these bands in the spectra of the present complexes, as discussed above.

### 3.2.5 Electrochemical behaviour of the nickel(II) chloride complexes

Nickel(II) complexes of tetraaza macrocyles undergo electrochemical oxidation and reduction in solution.[114] Lovecchio et al. have demonstrated by EPR studies that these redox processes involve the formation of genuine Ni(III),[38] and Ni(I) species.[115]

As an extension of an earlier study of the effect of ligand structure on the oxidation of Ni(II) to Ni(III),[38] the redox behaviour of the nickel(II) chloride complexes of $L^{14}$ to $L^{17}$ in dichloromethane was investigated by cyclic voltammetry at the University of Pavia. Low solubilities in acetonitrile necessitated the use of the less weakly polar solvent, dichloromethane for these studies and it became apparent that the solvent and backing electrolyte can cause significant changes in the redox potentials.[38] The experimental details of the measurements are given in Chapter Six and the oxidation potentials for Ni(II) $\longrightarrow$ Ni(III) are reported in Table 3.9 together with those for complexes of cyclam and its cetylated derivative (3.iii).

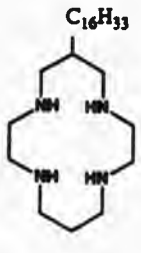

(3.111)

For the complexes of $L^{14}$, $L^{15}$ and $L^{16}$ the oxidation is electrochemically reversible as indicated by the symmetrical shape of the ac voltammograms and by the observation that the half-peak widths are between 90 and 140 mV, which is comparable to the range exhibited by the reversible ferrocenium - ferrocene couple ($Fc^+/Fc$) used as a reference.[116] The seventeen-membered complex, however, shows irreversible oxidation at about 600 mV. None of the complexes undergo reversible reduction. The incorporation of fused benzene rings into $L^{14}$, by limiting the extent to which the ring can contract to accommodate Ni(III), together with the weaker anilino donor atoms, would be expected to make $L^{14}$ less effective than its aliphatic analogue, [14]aneN$_4$ (cyclam) in stabilising the higher oxidation state {Ni(III) octahedral covalent radius,[37] 1.30 Å}. This should result in higher, more positive potentials, but in acetonitrile, the opposite effect is observed, which is interpreted in terms of the effects of both the spin-state equilibria and competition between solvent and anion for the axial co-ordination sites in the low-spin Ni(III) complexes.[38] The use of the polar non-co-ordinating solvent, dichloromethane, and chloro axial ligands in an excess of chloride electrolyte reduces these effects and indeed, under these conditions, the potential obtained for $L^{14}$ is higher than that for the fully

saturated ligand (3.iii) (the complexes of cyclam itself are insoluble in this solvent). The relatively facile oxidation of Ni(II) in $[NiL^{14}Cl_2]$ reflects the observation from the X-ray structural studies that the fit for Ni(II) is better in $L^{15}$ and that $L^{14}$ is slightly too small to accommodate nickel(II) (see Chapter Five). For the larger ligands, it can readily be seen that as the ligand ring size is increased, oxidation to the smaller Ni(III) is progressively disfavoured, the metal fitting best into the smallest cavity.

TABLE 3.9 Half-wave potentials (V) for $Ni^{III}/Ni^{II}$.(a)

| complex | solvent | electrolyte | $E_{\frac{1}{2}}$ |
|---|---|---|---|
| $[NiL^{14}Cl_2]$ | $CH_3CN$ | $[Bu_4N]Cl$ | 0.16(b) |
| $\{Ni[14]aneN_4\}[ClO_4]_2$ | " | $[Bu_4N][ClO_4]$ | 0.59(b) |
| $[NiL^{14}][ClO_4]_2$ | " | $[Bu_4N][ClO_4]$ | 0.47(b) |
| $[NiL^{14}][ClO_4]_2$ | $CH_2Cl_2$ | $[Bu_4N][ClO_4]$ | 0.56(b) |
| $[Ni(3.x)][ClO_4]_2$ | " | $[Bu_4N][ClO_4]$ | 0.92(c) |
| $[Ni(3.x)Cl_2]$ | " | $[Bu_4N]Cl$ | 0.18(c) |
| $[NiL^{14}Cl_2]$ | " | $[Bu_4N]Cl$ | 0.23 |
| $[NiL^{14}Cl_2]$ | " | $[Bu_4N][ClO_4]$ | 0.30 |
| $[NiL^{15}Cl_2]$ | " | $[Bu_4N][ClO_4]$ | 0.50 |
| $[NiL^{16}Cl_2]$ | " | $[Bu_4N][ClO_4]$ | 0.58 |
| $[NiL^{17}Cl_2]$ | " | $[Bu_4N][ClO_4]$ | (d) |

(a) Relative to the ferrocenium/ferrocene couple; (b) data from Ref. 38; (c) data from Ref. 117; (d) irreversible oxidation at ca. 0.6 mV.

### 3.3 The low-spin complex $[NiL^{14}][BF_4]_2$

In order to investigate the effects of changing the spin-state of nickel(II) on the ligand structure, the low-spin complex $[NiL^{14}][BF_4]_2$ was prepared. This complex has already been referred to in connection with the N-H absorption bands in the infrared spectra of the nickel(II) complexes (§3.2.4). The tetrafluoroborate ion is very rarely seen to co-ordinate to nickel(II) and only one X-ray structure is known in which this ion functions as a ligand.[118] Use of the perchlorate ion was considered, but attempts to measure stability constants in perchlorate media (§5.1.2) have indicated possible nickel(II) mediated oxidation reactions. In fact, attempts to obtain the low-spin perchlorate complex by a cognate reaction gave (after twenty four hours) only a methanolic suspension of a brown tar. A mixture of $L^{14}$ in chloroform and hexaaquanickel(II) tetrafluoroborate in methanol yielded orange-red crystals within twenty four hours. Microanalysis (C, H and N) of the crystals gave results consistent with the formulation above. Details of the preparation and characterization data for this complex are given in Chapter Six. The crystals were suitable for X-ray crystallographic study and a structural analysis was undertaken (by B. Shah),[119] and subsequently published.[38]

The visible spectrum in dichloromethane shows one strong band at 457 nm ( $\epsilon$ = 80 $m^2$ $mol^{-1}$) characteristic of low-spin nickel(II).[86] Addition of a small amount of lithium chloride caused a decrease in the intensity of this band and the appearance of another at 575 nm as well as a shoulder at 340 nm. Further addition of (excess) lithium chloride caused the complete disappearance of the spectrum of the low-spin complex; the resulting spectrum is entirely due to the high-spin form.

The N-H stretching region of the infrared spectrum of $[NiL^{14}][BF_4]$ consists of two sharp absorptions at 3214 and 3174 $cm^{-1}$. There are at least four strong peaks between 1000 and 1090 $cm^{-1}$ derived from the $\nu_3$ asymmetric stretch of the tetrafluoroborate ion (Figure 3.15) and conspicuous peaks at 520 and 534 $cm^{-1}$, probably arise from its $\nu_4$ bending mode.[120]

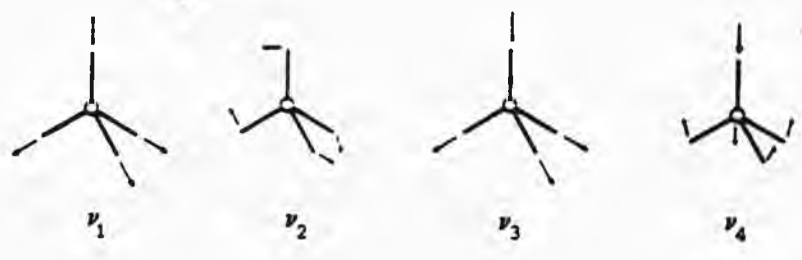


FIGURE 3.15 The normal modes of vibration of the tetrafluoroborate ion.

The apparent splitting of these bands, which would not be expected if the ion were in $T_d$ symmetry, may be caused by a number of factors. Although co-ordination of the tetrahedral ion would reduce its symmetry and cause band splitting, the visible spectrum and the X-ray structure determination indicates co-ordination does not occur (although there may well be some weak covalent interactions, see §3.3.1). Splitting of the $\nu_3$ band of non-co-ordinated perchlorate has been attributed to hydrogen bonding interactions distorting the Td symmetry of this perchlorate ion.[121] Analogous interactions between $BF_4^-$ and the amine hydrogen atoms of the macrocycle would similarly reduce the symmetry of the tetrafluoroborate ion. Some 'splitting' might also be expected from an isotopic effect; two natural isotopes of boron, $^{10}B$ (19.78%) and $^{11}B$ (80.22%),[122] exist and different vibrational frequencies are known for $^{10}BF_4^-$ ($\nu_3$ = 1016,

$\nu_4$ = 529 $cm^{-1}$) and $^{11}BF_4^-$ ($\nu_3$ = 984, $\nu_4$ = 524 $cm^{-1}$).[120] The $\nu_1$ symmetric stretch of the $BF_4^-$ ion at 769 $cm^{-1}$ is normally inactive in the infrared spectrum, but becomes active on distortion of the symmetry.[120] The sharp band at 772 $cm^{-1}$ probably originates from this mode of vibration. This band overlaps to some extent those arising from the aromatic C-H out-of-plane deformations. The spectrum of the free ligand shows three such peaks between 757 and 731 $cm^{-1}$ and the spectrum of $[NiL^{14}][BF_4]_2$ exhibits a weak band at 734 $cm^{-1}$ and a shoulder on the low energy side (ca. 750 $cm^{-1}$) of the $\nu_1(BF_4^-)$ absorption. Of the aromatic skeletal in-plane ring vibrations, that at 1497 $cm^{-1}$ is the most prominent, while those around 1600 $cm^{-1}$ are weak.

3.3.1 The structure of $[NiL^{14}][BF_4]_2$

In the complex cation $[NiL^{14}]^{2+}$, the nickel atom is bonded to all the donors of the macrocycle in a distorted square-planar environment (Figure 3.16). Although the tetrafluoroborate ions are located close to the axial co-ordination sites, the distance between the nickel atom and the nearest fluorine atom of the tetrafluoroborate counter-ions is ca. 2.73 Å. In the structure of $[Ni(en)_2(BF_4)(H_2O)][BF_4]$, the Ni-F bond length is 2.12 Å,[118] so that the tetrafluoroborate ions in the present structure can be considered as at best only 'semi-co-ordinated' in the solid state.[123] The nickel atom lies on a crystallographic two-fold axis passing through the midpoints of the ethylene bridges such that corresponding bond lengths and angles in the a- and b-halves of the macrocycle are crystallographically identical. The phenylene rings are inclined to either side of the co-ordination plane at an angle of 34°, giving the step-shaped conformation observed in $[NiL^{14}(NCS)_2]$. The Ni-N bond lengths in

$[NiL^{14}]^{2+}$ [(Ni-N(1) 1.908(5), Ni-N(2) 1.949(5) Å] are each ca. 0.14 Å less than the corresponding values in the high-spin complex, $[NiL^{14}(NCS)_2]$ [Ni-N(1) 2.046(2), Ni-N(2) 2.091(2) Å] and are comparable with those reported for low-spin complexes of cyclam (1.935 and 1.944 Å),[38] spirocyclam (3.iv) (1.929 to 1.960 Å)[124] and the alkylated cyclams (3.v), (3.vi) and (3.vii) (1.913 to 1.994 Å).[90]

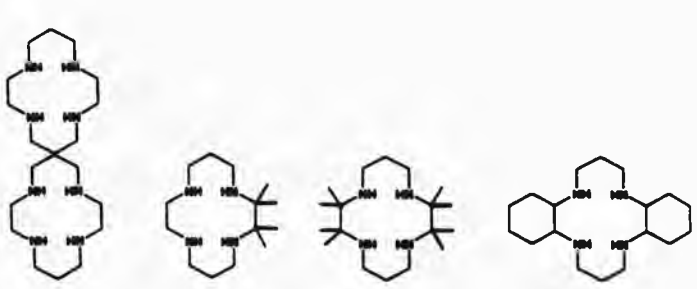

(3.iv) (3.v) (3.vi) (3.vii)

The difference between the bond lengths in the high-spin and low-spin nickel(II) complexes reflects the difference between the covalent radii of low-spin nickel(II) {1.20 Å,[37]} and high-spin nickel(II) {1.39 Å,[37]}. The five-membered chelate rings adopt the normal gauche conformations and, as a consequence of this, the amine hydrogen atoms alternate on either side of the nitrogen donor plane (diastereoisomer V) (see §1.10)

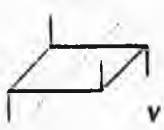

V

All the amine hydrogen atoms of the macrocycle form weak hydrogen bonds to fluorine atoms of the $BF_4^-$ ions: one between the amine nitrogen atom N(2) and F(4) at -x,1-y,-z (N...F 3.06 Å, H...F 2.40 Å, N-H...F 139°) and the other between N(1) and F(1) at

½-x,1½-y,-z (N...F 3.07 Å, H...F 2.38 Å, N-H...F 134°). The calculated N...F van der Waals contact distance is 2.95 Å.[48]

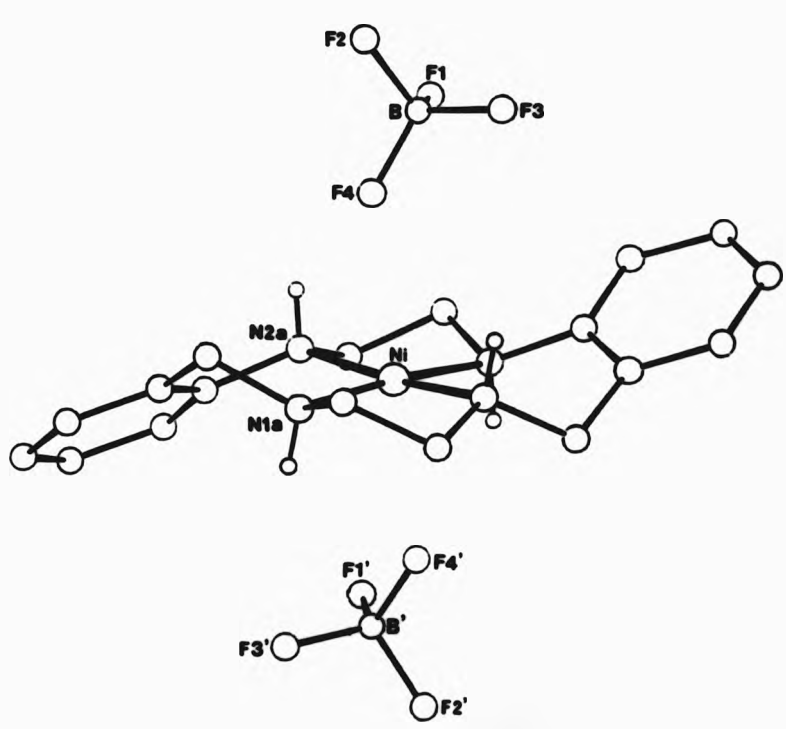


FIGURE 3.16 View of the structure of $[NiL^{14}][BF_4]_2$ showing the location of the tetrafluoroborate counter-ions.

## Chapter Four

### 4 The Zinc(II) and Cadmium(II) Complexes

The zinc(II) and cadmium(II) complexes of $L^{15}$ have been studied previously and the structures of $[ZnL^{15}I]I$,[125] $[ZnL^{15}(NO_3)(H_2O)]NO_3$ and $[CdL^{15}(NO_3)]NO_3$,[44,61] (Figure 4.1) have been reported. Complexes of the series of fifteen-membered ligands in which the benzyl carbons both bear a linear alkyl chain have also been prepared previously and the structure of $[CdL^{15Bu}(NO_3)]NO_3$ (Figure 4.1) has been determined.[44,61] All these complexes have been found to exist in the saddle conformation.

The present work includes the structural analyses of cadmium complexes of $L^{16}$ and $L^{17}$. Attempts to obtain crystals of the analogous zinc(II) complexes suitable for X-ray crystallographic study were unsuccessful. Surprisingly, perhaps, no complexes of $L^{14}$ with zinc(II) or cadmium(II) have been reported and constraints on time have precluded their investigation in the present work.

#### 4.1.1 Synthesis of complexes

Eight complexes of $L^{16}$ and $L^{17}$ with zinc(II) and cadmium(II) have now been prepared by mixing warm solutions of the ligand with the appropriate metal bromide or iodide. Preparative details and characterization data for these complexes are given in Chapter Six. Except for the cadmium(II) bromide complex of $L^{16}$, microanalysis (C, H and N) of the dried white crystalline or microcrystalline products (collected from the cooled reaction mixtures) gave results which were consistent with complexes of the type, $ML_2X_2$ (M = Cd or Zn, X = Br or I). Yields were in the range 61-85%. The cadmium(II) bromide complex of $L^{16}$, prepared either with an excess or with an equimolar quantity

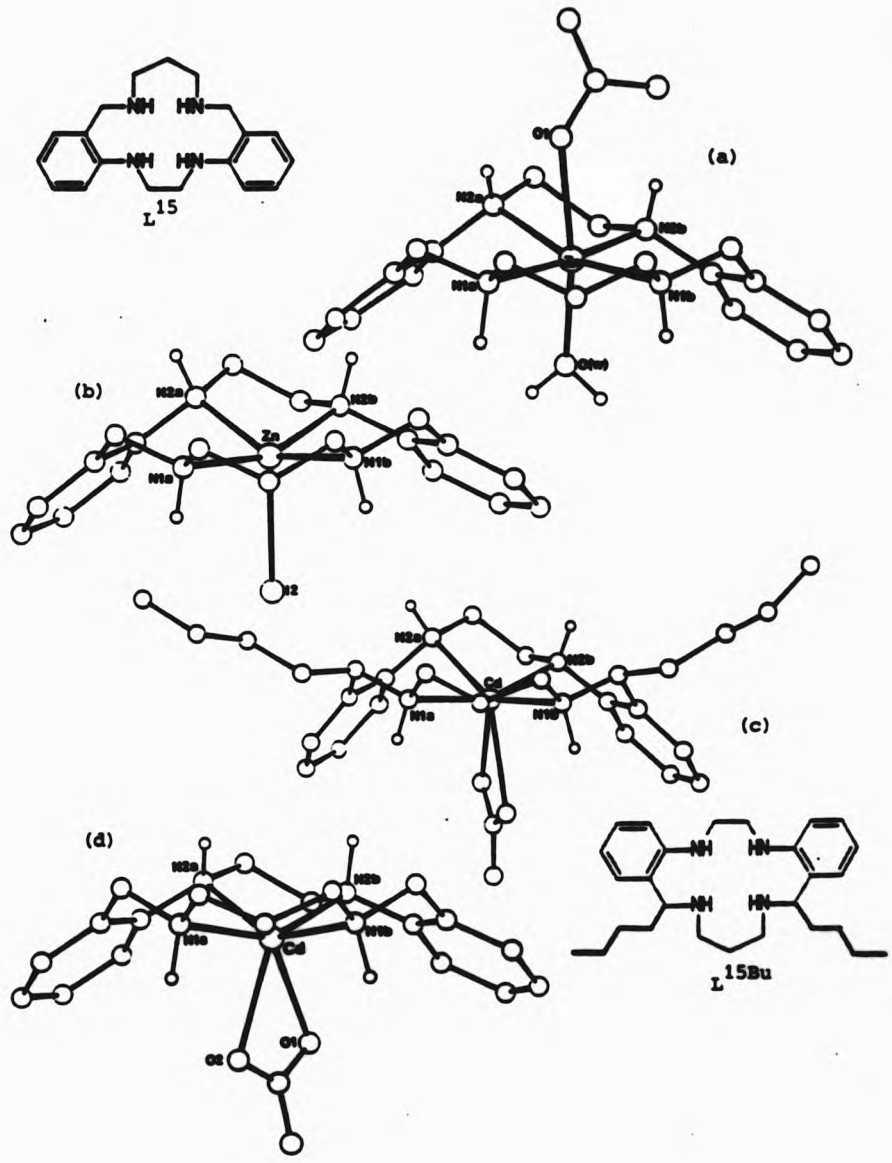


FIGURE 4.1 The structures of (a) $[ZnL^{15}(NO_3)(H_2O)]^+$, (b) $[ZnL^{15}I]^+$, (c) $[CdL^{15Bu}(NO_3)]^+$ and (d) $[CdL^{15}(NO_3)]^+$.[44,125]

of halide, in both cases gave analytical results too low in C, H and N for the complex to be formulated as $[CdL^{16}Br_2]$. Subsequently, an X-ray crystal structure determination (see §4.2.1) showed the complex to be $[CdL^{16}Br]_2[CdBr_4]$ and the microanalytical results agree with this formulation.

4.1.2 Infrared spectra

The infrared spectra of the zinc(II) and cadmium(II) complexes of $L^{16}$ and $L^{17}$ were recorded as microdiscs with potassium bromide and selected peaks, characteristic of each ligand are presented in Table 4.1. When taken together with the results of the structural studies of $[CdL^{16}Br]_2[CdBr_4]$ and $[CdL^{17}Br_2]$, the number and appearance of the N-H stretching bands may provide some clues to the structure/ composition of the other complexes. The two sharp peaks at 3253 and 3158 $cm^{-1}$ in the spectrum of the pseudo-octahedral complex, $[CdL^{17}Br_2]$ may be characteristic of either an octahedral or a square pyramidal complex, but more importantly, probably indicates that only weak intermolecular interactions are present. The pair of complexes in $[CdL^{16}Br]_2[CdBr_4]$ exhibit considerable, albeit weak, hydrogen bonding and, although two complexes are present, the five N-H bands may be a reflection of this hydrogen bonding. Both zinc(II) complexes of $L^{16}$ exhibit only two bands, as does the complex of $L^{16}$ with cadmium(II) iodide. However, the two zinc(II) complexes with $L^{17}$ clearly show four bands and this may indicate that, again, two different complexes are present. The complex of $L^{17}$ with cadmium(II) iodide has only one band in this region which could be attributable to accidental overlap. The acetonitrile of solvation found in the X-ray study of $[CdL^{17}Br_2]$ is indicated quite clearly in the infrared spectrum by the strong band at 2249 $cm^{-1}$.

TABLE 4.1 Selected bands in the infrared spectra of the $Zn^{II}$ and $Cd^{II}$ complexes of $L^{16}$ and $L^{17}$.(a)

| $L^{16}$ | | | | $L^{17}$ | | | | |
|---|---|---|---|---|---|---|---|---|
| $ZnBr_2$ | $ZnI_2$ | $CdBr_2$ | $CdI_2$ | $ZnBr_2$ | $ZnI_2$ | $CdBr_2$ | $CdI_2$ | assignment |
| 3224(s) | 3217(s) | 3298 | 3232 | 3279(w) | 3271 | 3253(s) | 3244 | |
| 3172(s) | 3193(s) | 3268 | 3196 | 3239 | 3228(s) | | | N-H stretch |
| | | 3234 | | 3229 | 3210 | | | |
| | | 3200(s) | | 3172 | 3176 | 3158(s) | | |
| | | 3186(s) | | | | | | |
| | 3045(w) | 3046(w) | 3044(w) | | 3067(w) | 3078(w) | | aromatic C-H |
| | | | | | 3043(w) | 3042(w) | 3053 | stretch |
| 2955 | 2947(w) | 2927 | 2943(w) | | 2961 | | | |
| 2917 | 2909(w) | 2870(s) | 2915(w) | 2921 | 2922 | 2924(s) | 2931 | alkyl C-H stretch |
| 2870(s) | 2867 | | 2866 | 2874 | 2866 | 2868(s) | 2866 | |
| | | | | | | 2249 | | acetonitrile |
| 1609 | 1610 | 1608 | 1606 | 1606 | 1607 | 1605 | 1604 | aromatic skeletal |
| 1590 | 1590 | 1587 | 1585 | 1588 | 1589 | 1586 | 1585 | in-plane ring |
| 1500(s) | 1498(s) | 1498(s) | 1497(s) | 1499(s) | 1498(s) | 1499(s) | 1496(s) | vibrations |
| 1461 | 1460 | 1460 | 1456 | 1458(s) | 1456(s) | 1459(s) | 1458(s) | alkyl C-H |
| 1449 | 1420 | 1427 | 1430 | 1448(sh) | 1440 | 1437 | 1429 | deformations |
| | | | | | 1260 | 1245 | 1243 | |
| 752(s) | 754(s) | 763(s) | 764 | 763(s) | 770 | | | |
| | 745(s) | 733 | 755(s) | 752(s) | 755(s) | 759(s) | 758(s) | aromatic C-H |
| 723(s) | 722 | 710 | 712 | | 749(sh) | 749(s) | | out-of-plane |
| | | | | 733 | 733 | 728 | 722(s) | deformations |

(a) As KBr microdiscs.

4.1.3 NMR spectra

The complexes were not sufficiently soluble in chloroform or acetonitrile for NMR spectra to be obtained in these solvents. However, a $^{1}H$ NMR spectrum of $[CdL^{17}I_2]$ in dimethylsulphoxide-$d_6$ showed broad peaks with chemical shifts comparable to those of the free ligand in the same solvent. Additional peaks are also present at relatively low intensity, probably indicating the existence of at least one ligand exchange process which is slow with respect to the NMR time-scale. Furthermore, two exchangeable proton signals are discernible at $\delta$ = 1.98 and 6.76 ppm (equivalent to those of the free ligand) and one more at $\delta$ = 6.02 ppm. Because of the complexity and the poor resolution of this spectrum, a detailed analysis was not attempted.

4.2 Structures of cadmium(II) complexes of $L^{16}$ and $L^{17}$

Tables of fractional atomic coordinates, thermal parameters, bond lengths and interbond angles are included in the Appendix (Tables A5.1 to A5.5 for $L^{16}$ complex and A6.1 to A6.5 for $L^{17}$ complex). Crystal data and details of the structure solutions and refinement are described in Chapter Six. A brief description of each of these structures will be followed by detailed discussion of key aspects of them and, where appropriate, comparison with those of the fifteen-membered ligands and other reported structures.

4.2.1 Structure of $[CdL^{16}Br]_2[CdBr_4].CH_3OH$

This structure was particularly difficult to solve because of the unexpected presence of three different cadmium(II) complexes (Figure 4.2). Two cationic complexes, I and II, contain cadmium atoms Cd(1) and Cd(2), respectively, each co-ordinated to the macrocyclic ligand

FIGURE 4.2 The asymmetric unit in $[CdL^{16}Br][CdBr_4].CH_3OH$ showing the relationship between the macrocyclic complexes, the $[CdBr_4]^{2-}$ ion and the disordered methanol of solvation. The minor component of the disordered solvent is shown with open bonds. The dashed lines connect the cadmium atoms in each macrocyclic complex with the nearest bromine atom of $[CdBr_4]^{2-}$.

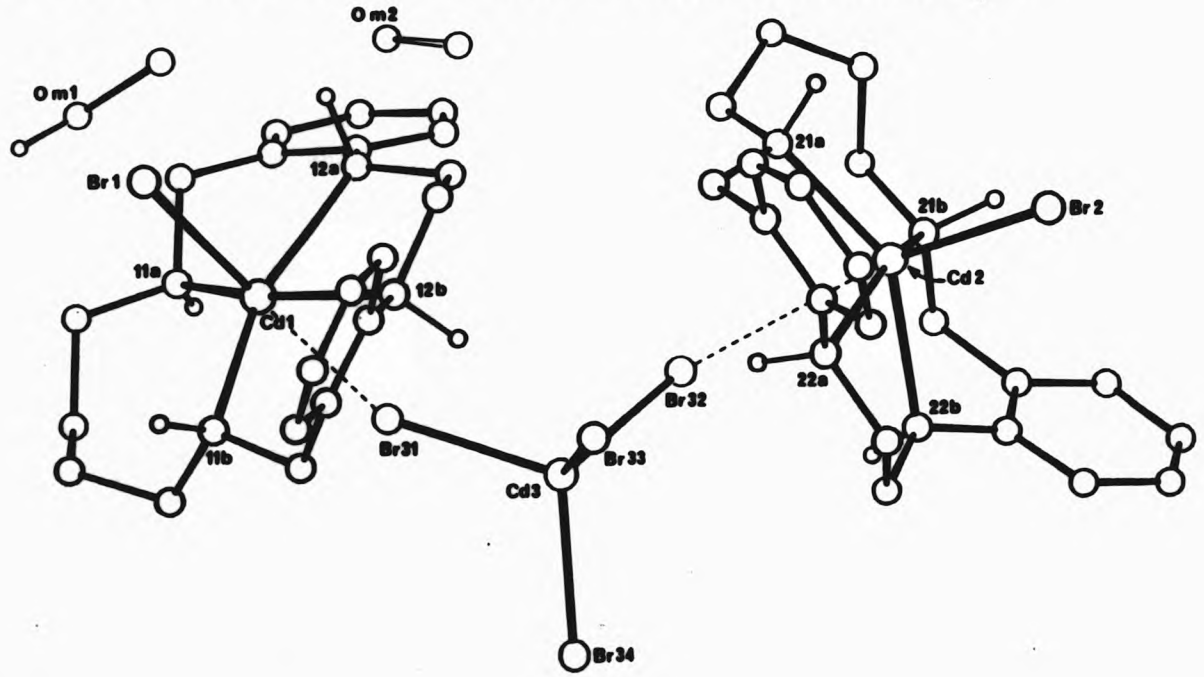

and to a bromo ligand which occupies an apical site giving a distorted square pyramidal geometry. The macrocycle in each complex adopts completely different conformations (Figure 4.3). Sandwiched between these two complexes is a tetrabromocadmate(II) ion, $[CdBr_4]^{2-}$. The two complex cations are tilted such that the angle between the normals to the least-squares plane defined by the nitrogen donor atoms of each complex is 85°. Two of the bromine atoms of the $[CdBr_4]^{2-}$ ion, Br(31) and Br(32) respectively, are directed towards the sixth co-ordination site of the Cd(1) and Cd(2) atoms. The effect of the $[CdBr_4]^{2-}$ counter-ion on the structure of and bonding within the complex cations will be discussed in §4.2.4. A methanol molecule is also present, occupying one of two sites in a 70:30 random distribution throughout the crystal (Figure 4.2). Complex I [Figure 4.3(a) and (b)] has the phenylene rings displaced to either side of the nitrogen donor plane giving the step-shaped arrangement seen in the nickel(II) complexes. In contrast, complex II [Figure 4.3(c) and (d)] has both phenylene rings displaced to the same side of the donor plane as the co-ordinated bromine atom, Br(2), giving it the saddle arrangement seen in the zinc(II) and cadmium(II) complexes of $L^{15}$ and $L^{15Bu}$. The angles between the donor planes and the phenylene rings are 40° and 46° for the a- and b-ring, respectively, of complex I and 45° for each ring of the saddle-shaped complex, II.

### 4.2.2 The structure of $[CdL^{17}Br_2].CH_3CN$

In the complex $[CdL^{17}Br_2]$, the macrocyclic ligand is co-ordinated via all four nitrogen donors to the cadmium atom in a trapezoidally-distorted square-planar arrangement with trans-bromo ligands completing the pseudo-octahedral co-ordination sphere (Figure 4.4). The phenylene rings are inclined to either side of the donor plane,

**FIGURE 4.3** The structures of (a) and (b) the step- and (c) and (d) the saddle-shaped complexes $[CdL^{16}Br]^+$ each viewed onto and across the plane of the macrocycle.

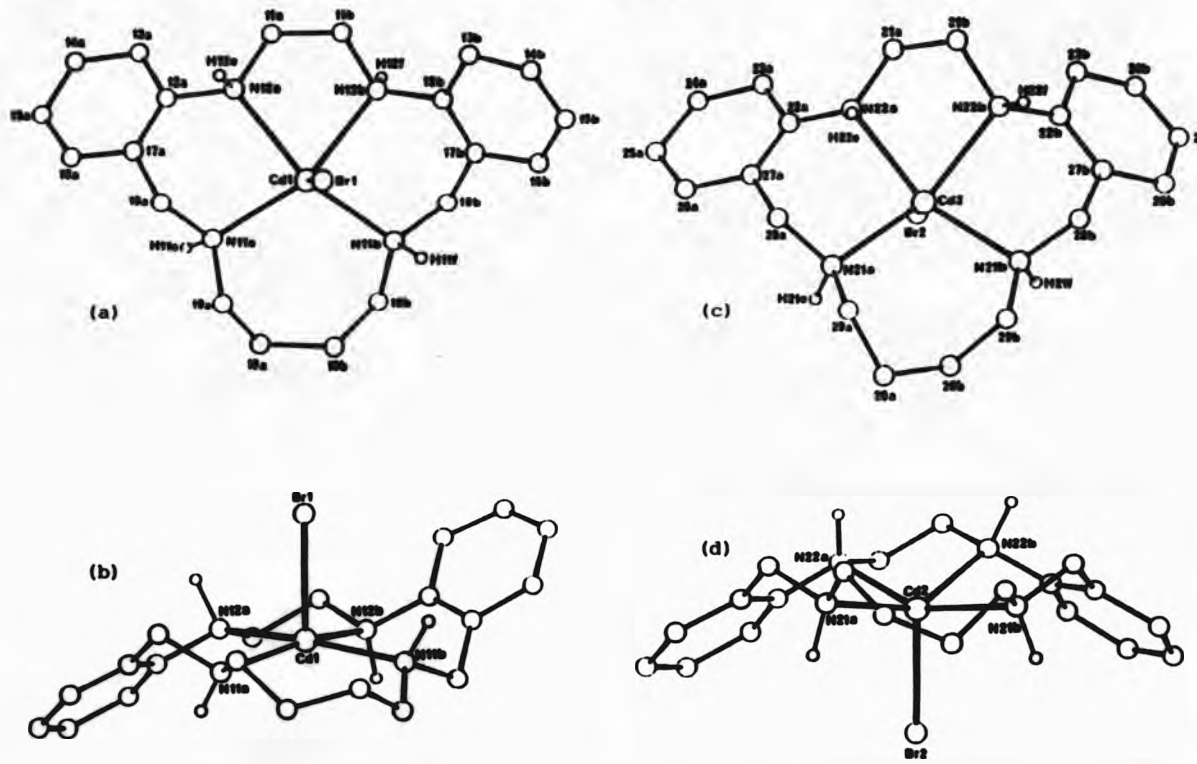

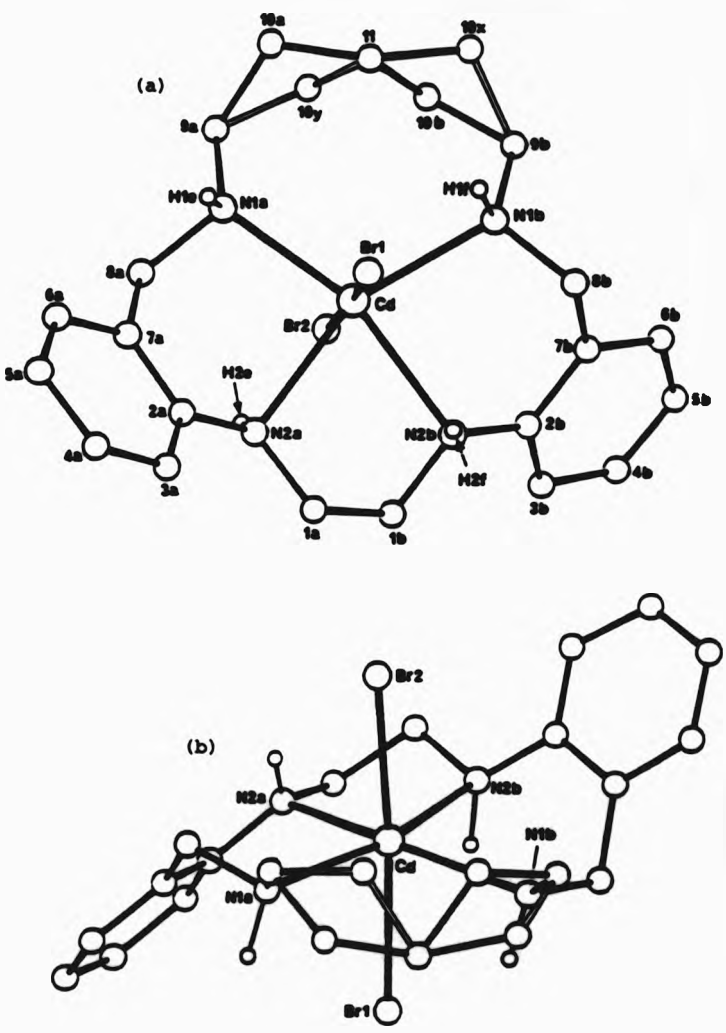


FIGURE 4.4 The structure of $[CdL^{17}Br_2]$ viewed (a) onto and (b) across the plane of the macrocycle. The disorder in the $C_5$ chain is indicated with open bonds connecting the minor component of each C(10) atom to its neighbours.

giving the step-shaped arrangement, but the a- and b-rings are at angles of 55° and 53° to the donor plane, respectively, 10° greater than the angles observed in $[CdL^{16}Br]^+$. Isolated molecules of acetonitrile of crystallisation are present, occupying lattice sites between the cadmium(II) complexes such that the closest contact distance (2.50 Å) is between the acetonitrile nitrogen atom and one of the hydrogen atoms attached to C(8b).

### 4.2.3 The cadmium-nitrogen bonds

For ease of comparison, the Cd-N bond lengths and selected interbond angles in the co-ordination spheres of the cadmium(II) complexes of $L^{16}$ and $L^{17}$ are listed in Table 4.2 together with those for the cadmium(II) and zinc(II) complexes of $L^{15}$ and $L^{15Bu}$. In the cadmium(II) complexes of $L^{15}$, $L^{15Bu}$ and $L^{16}$ the Cd-N(1) bonds range from 2.247(15) to 2.276(15) Å with the exception of one longer bond [2.332(13 Å] in complex II of $L^{16}$. In fact, this complex also possesses the shortest Cd-N(1) bond in the whole series. The high e.s.d.'s in the Cd-N bond lengths in the complexes of $L^{16}$ (caused by the presence of three cadmium and six bromine atoms) make these differences less significant and, by way of illustration, the Cd-N(1) bond lengths in complex I are each virtually identical to corresponding bonds in $[CdL^{15}(NO_3)]^+$. The two Cd-N(1) bonds in $[CdL^{17}Br_2]$ are identical [2.370(7) Å] and are markedly longer than the mean [2.271(10) Å] of those in the other four complexes [the mean of the Cd-N(1) bond lengths across the whole series is 2.291(9) Å]. The variation in lengths of these bonds seems to be, at least partly, related to the extent to which the metal atom lies within the plane of the macrocyclic donors, the cadmium atom in $[CdL^{17}Br_2]$ being closest to the donor plane. The weaker ligating ability of the anilino donors

TABLE 4.2 Bond lengths ( Å) and selected bond angles (°) at the metal atom for the cadmium(II) and zinc(II) complexes.(a)

| complex | Cd-N1 | Cd-N2 | N1-Cd-N1 | N2-Cd-N2 |
|---|---|---|---|---|
| $[CdL^{15}(NO_3)]^+$(b) | 2.275(6) | 2.412(6) | 99.2(2) | 72.2(2) |
| | 2.257(6) | 2.387(6) | | |
| $[CdL^{15Bu}(NO_3)]^+$(b) | 2.274(7) | 2.310(7) | 100.0(5) | 75.0(2) |
| | 2.251(7) | 2.418(7) | | |
| $[Cd(1)L^{16}Br]^+$ | 2.276(15) | 2.427(13) | 110.1(6) | 75.9(5) |
| | 2.257(14) | 2.390(14) | | |
| $[Cd(2)L^{16}Br]^+$ | 2.332(13) | 2.339(13) | 106.0(5) | 73.2(5) |
| | 2.247(15) | 2.431(17) | | |
| $[CdL^{17}Br_2]$ | 2.370(7) | 2.450(6) | 115.5(2) | 74.8(2) |
| | 2.370(6) | 2.440(7) | | |
| $[ZnL^{15}I]^+$(c) | 2.135(5) | 2.214(6) | 99.9(2) | 76.3(2) |
| | 2.089(5) | 2.213(6) | | |
| $[ZnL^{15}(NO_3)(H_2O)]^+$(b) | 2.104(5) | 2.227(5) | 97.8(2) | 80.1(2) |
| | 2.089(5) | 2.168(4) | | |

(a) For each complex, the first and second rows of bond lengths refer to the a- and b-halves of the macrocycle, respectively; (b) from Ref. 44; (c) from Ref. 125.

is reflected in the generally longer Cd-N(2) bonds, which range from 2.310(7) to 2.450(6) Å with a mean of 2.400(10) Å throughout the series. Although bonds to both types of nitrogen donor are longer in $[CdL^{17}Br_2]$, no systematic variation is apparent as the size of the macrocycle is increased from fifteen- to sixteen-membered.

The Cd-N bond lengths may be compared with those reported for three complexes of macrocyclic polyamines in which the nitrogen donors are all aliphatic [equivalent to N(1)]. The bonds in the complexes of (4.i) [16]aneN$_4$ and (4.ii) [16]ane(NMe)$_4$ range from 2.325(6) to 2.47(3) Å,[126,127] In the binuclear complex of (4.iii) the polyazacycloalkane [30]aneN$_{10}$, containing one six-co-ordinate and one four-co-ordinate cadmium atom, the range is smaller, 2.36(1) to 2.43(1) Å.[128]

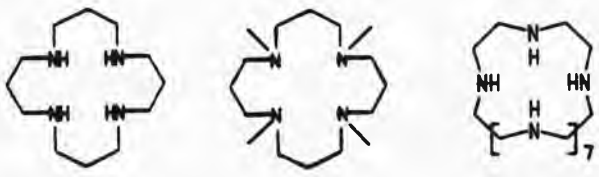

(4.i) (4.ii) (4.iii)

In the complexes of the present series of ligands, the Cd-N(2) bond lengths mostly lie at the high end of the longer range, with the exception of one bond in the complex of $L^{15Bu}$ [2.310(7) Å] and one in complex II of $L^{16}$ [2.339(13) Å]. On the other hand, all but three of the Cd-N(1) bond lengths fall short of this range, the exceptions being those in $[CdL^{17}Br_2]$ and the longer bond in complex II of $L^{16}$. The explanation for this lies in the disparity between the donor ability of the two different types of amine nitrogen atom. This

causes the cadmium atom to be displaced towards the stronger benzylamino donors, N(1), with consequent lengthening of the bonds to the anilino donors, N(2). In fact, the mean of all the Cd-N bond lengths in the present series of ligands [2.346(10) Å] does fall within the expected range.

The angle N(2a)-Cd-N(2b) in the five-membered chelate ring containing the anilino nitrogen atoms varies little throughout the series of complexes, from 72.2(2) to 75.9(5)°. An increase in the size of the chelate ring defined by the aliphatic nitrogen donors from six- to seven-membered is accompanied by an increase in the N(1a)-Cd-N(1b) angle, from around 100° (in the two complexes of the fifteen-membered ligands) to 110.1(6) and 106.0(5)° in complexes I and II of $L^{16}$, respectively. In the complex $[CdL^{17}Br_2]$, there is an even greater difference between these two angles: the N(1a)-Cd-N(1b) angle is only 74.7(2)°, whereas the N(2a)-Cd-N(2b) angle is increased to 115.5(2)°.

4.2.4 The cadmium-bromine bonds

For the purposes of the present discussion, it is convenient to begin with a comparison of the Cd-Br bond lengths in the tetrabromo-cadmate(II) ion with those found in similar structures. A search of the Cambridge Crystallographic Databank, using the CSSR program,[129] revealed only six reported structures incorporating the $[CdBr_4]^{2-}$ ion.[130-134] The Cd-Br bond lengths in these structures are listed in Table 4.3 together with those of the present example. The bond lengths within the six reported structures range from 2.529(6) to 2.685(1) Å with a mean of 2.591 Å and the bond lengths in the present dianion [2.561(3) to 2.613(2) Å] fall within this range and exhibit the same mean (Table 4.3).

TABLE 4.3 Cd-Br bond lengths ( Å) in reported structure determinations of the tetrabromocadmate(II) ion.

| cation | Cd-Br | | mean(a) |
|---|---|---|---|
| $[MeNH_3]^+$(b) | 2.575(4) | 2.580(3) | |
| | 2.582(4) | 2.585(4) | 2.580(3) |
| $Cs^+$(b) | 2.529(6) | 2.564(5) | |
| | 2.554(5) | 2.554(5) | 2.550(13) |
| $[Me_3NH]^+$(c) | 2.556(3) | 2.671(8) | 2.642(50) |
| $[Ph_3BzP]^+$(d) | 2.566(2) | 2.570(2) | |
| | 2.582(2) | 2.635(2) | 2.588(27) |
| $[(Me_2HN(CH_2)_3S)_2]^{2+}$(e) | 2.560(1) | 2.571(1) | |
| | 2.579(1) | 2.685(1) | 2.599(50) |
| [Cd(4.iv)Br]$^+$(f) | 2.583 | 2.597 | 2.590(7) |
| $[CdL^{16}Br]^+$(g) | 2.596(2) | 2.597(3) | |
| | 2.561(3) | 2.613(2) | 2.592(19) |

(a) Population standard deviations in parentheses; (b) Ref. 130; (c) the anion lies on a three-fold axis with the shorter Cd-Br bond unique, Ref. 131; (d) Ref. 132; (e) Ref. 133; (f) bonds are pair-wise equivalent by crystallographic symmetry, no e.s.d.'s are available, Ref. 134; (g) this work.

The association of the $[CdBr_4]^{2-}$ ion with the two complex cations has some interesting effects on the Cd-Br bond lengths, both within the tetrahedron itself and within the five-co-ordinate complexes. In complex II, the Cd(2)-Br(2) bond [at 2.574(3) Å] is markedly shorter than the corresponding bond in complex I [Cd(1)-Br(1), 2.660(3) Å], but both may be considered as having significant covalent character. The relative lengthening of Cd(3)-Br(31) [2.613(2) Å] with respect to the other three bonds in the tetrahedral dianion reflects a weak

covalent interaction of Br(31) with Cd(1) in complex I [Cd(1)...Br(31), 3.09 Å], whereas the interaction of Br(32) with Cd(2), at a distance of 3.53 Å is too great for such a significant interaction to be present. Br(31) may thus be considered to be "semi-co-ordinated" to Cd(1).[123]

In the complex $[CdL^{17}Br_2]$, the Cd-Br bonds are significantly different, with Cd-Br(1) being 2.793(1) Å and Cd-Br(2) being 2.695(1) Å. Both bonds are considerably longer than the Cd-Br bonds in the five co-ordinate complexes of $L^{16}$. The longer Cd-Br(1) bond may be a consequence of interactions with the three amine hydrogen atoms on the same side of the macrocycle, whereas the closer approach of Br(2) to the macrocyclic cavity is impeded by only one amine hydrogen atom.

The Cd-Br bond lengths may be compared with those reported for two complexes of macrocyclic ligands (4.iv) and (4.v).[134,135]

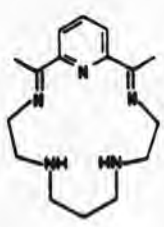

(4.iv)

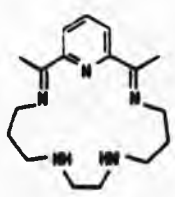

(4.v)

In the structure of $[Cd(4.iv)Br]_n^{n+}$, the cadmium atom is co-ordinated to all five nitrogen donors of the macrocycle in a planar fashion. Bridging bromides occupy the axial donor sites, with Cd-Br bond lengths of 2.775(3) and 3.037(3) Å. The shorter of these distances is of the order of the Cd-Br bond lengths in $[CdL^{17}Br_2]$, whereas the longer is similar to the distance between Cd(1) and Br(31), the

interaction of which is considered here to be semi-co-ordinated. In the structure of [Cd(4.v)Br]Br, the cadmium atom is once again co-ordinated to all five nitrogen donors with a bromide ligand occupying an axial site. The Cd-Br bond length here is 2.582(1) Å, similar to those observed in the complexes of $L^{16}$.

4.2.5 Planarity of the nitrogen donor set and the metal atoms

The cadmium atom in all four complexes of the fifteen- and sixteen-membered ligands is co-ordinated to a fifth ligand, $Br^-$ or bidentate $NO_3^-$, on only one side of the macrocyclic plane. The extent to which the macrocyclic donors are distorted from their mean plane and the position of the cadmium atom with respect to this plane (Table 4.4) does not, at first, seem to be entirely dependent on the size of the macrocycle.

Of the two $[CdL^{16}Br]^+$ complexes, I exhibits the more planar macrocyclic donor set (deviations, 0.051 to 0.065 Å in I, 0.090 to 0.116 Å in II) and Cd(1) is displaced towards the co-ordinated bromine, Br(1) by 0.245 Å, less than half the corresponding distance in II, 0.526 Å. The interaction between Cd(1) and Br(31) of the $[CdBr_4]^-$ counterion is responsible for pulling the cadmium atom nearer to the plane of the macrocycle.

Some allowance may be made for the hydrogen bonding and cation -anion interactions by averaging the distance of the cadmium atom from the $N_4$ best plane in the two complexes of $L^{16}$ and even in the two complexes of $L^{15}$ and $L^{15Bu}$. A gradation in this parameter across the series of ligands is then quite plain; 0.55 Å for the fifteen-membered ligands and 0.39 and 0.19 Å for the sixteen- and seventeen-membered ligands, respectively. This will be discussed

further in Chapter Five.

TABLE 4.4 Deviations ( Å) of metal atoms and donors from least-squares plane of macrocyclic donors for the cadmium(II) and zinc(II) complexes.(a)

| complex | metal | N1 | N2 |
|---|---|---|---|
| $[CdL^{15}(NO_3)]^+$(b) | 0.606 | -0.078 | 0.064 |
| | | 0.077 | -0.063 |
| $[CdL^{15Bu}(NO_3)]^+$(b) | 0.491 | -0.129 | 0.156 |
| | | 0.130 | -0.157 |
| $[Cd(1)L^{16}Br]^+$ | 0.245 | -0.051 | 0.065 |
| | | 0.052 | -0.065 |
| $[Cd(2)L^{16}Br]^+$ | 0.526 | -0.090 | 0.115 |
| | | 0.091 | -0.116 |
| $[CdL^{17}Br_2]$ | 0.191 | 0.111 | -0.151 |
| | | -0.116 | 0.156 |
| $[ZnL^{15}I]^+$(c) | 0.406 | 0.085 | -0.100 |
| | | -0.083 | 0.099 |
| $[ZnL^{15}(NO_3)(H_2O)]^+$(b) | 0.123 | -0.120 | 0.134 |
| | | 0.120 | -0.134 |

(a) For each complex, the first and second rows represent the deviations for the nitrogen atoms in the a- and b-halves of the macrocycle, respectively; (b) from Ref. 44; (c) from Ref. 125.

4.2.6 The configurations of the amines and the conformations of the chelate rings

The amine hydrogens of complex I of $L^{16}$ are disposed alternately above and below the macrocyclic donor plane in the configuration of diastereoisomer V (see §1.10) with the same absolute configurations of all four chiral nitrogens. In contrast, in complex II, the aliphatic amine hydrogen atoms are both on the same side of the macrocyclic plane as the co-ordinated bromine, Br(2), with both anilino hydrogen

atoms directed to the other side of the plane. The absolute configurations of the nitrogen atoms then become S,R,S,R in the order N(1a), N(1b), N(2a) and N(2b). This arrangement (diastereoisomer III) is the same as that seen in the zinc(II) and cadmium(II) complexes of $L^{15}$ and $L^{15Bu}$.

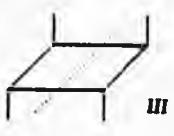

III

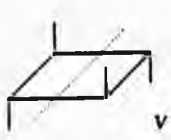

V

The five-membered chelate ring of complex I of $L^{16}$ is distorted from the twist or gauche conformation seen in all the other coplexes, with C(11a) 0.28 Å below the $CdN_2$ plane and C(11b) 0.49 Å above it. In complex (2), greater distortion towards the 'envelope' conformation may be seen, with both C(21a) and C(21b) displaced to one side of the $CdN_2$ plane, by 0.76 and 0.15 Å, respectively. The seven-membered chelate ring of I is in a distorted twist-chair conformation with only C(19b) below the $CdN_2$ plane (Figure 4.5), whereas that in II is forced to adopt a distorted chair conformation {cf. the disordered conformations of the corresponding rings in $[NiL^{16}(NO_3)_2]$}. The five-membered chelate ring in $[CdL^{17}Br_2]$ adopts the half-chair or twist conformation seen in the other complexes [C(1a) 0.30 Å above, C(1b) 0.47 Å below the $CdN_2$ plane]. The pentamethylene bridge between the benzylamino donors is disordered such that C(10a) and C(10b) each occupy two sites in a 80:20 random arrangement throughout the crystal [minor components labelled C(10y) and C(10x), respectively] giving alternative conformations to the eight-membered chelate ring (Figure 4.6). The C-C bond lengths in this chelate ring were constrained in the structure refinement of $[CdL^{17}Br_2]$ to a value of 1.55(2) Å, which value gave the most acceptable thermal parameters

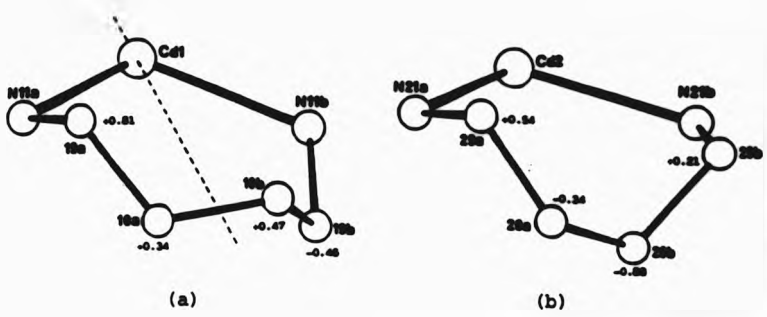


(a) (b)

FIGURE 4.5 The distorted skew and chair conformations of the seven-membered chelate rings in (a) the step-shaped and (b) the saddle-shaped complexes $[CdL^{16}Br]^+$ with the deviations of the carbon atoms from the $CdN_2$ plane. The dashed line represents a pseudo-two-fold rotation axis.

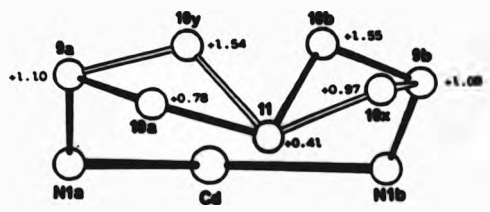


FIGURE 4.6 The alternative twist-boat conformations of the eight-membered chelate ring in $[CdL^{17}Br_2]$ with the deviations of the carbon atoms from the $CdN_2$ plane. The open bonds connect the minor components of the disordered carbon atoms to those of full site occupancy.

for the carbon atoms of this chelate ring. The mean values of the corresponding bond lengths in the eight-membered chelate ring in the ligand $L^{17}$ and in $[NiL^{17}Cl_2]$ are 1.52(1) and 1.52(2) Å, respectively. The configurations of the amine hydrogen atoms are not affected by this disorder and may be written as S,R,S,S, with that attached to N(1b) being R. This results in both benzylamino hydrogen atoms projecting to the same side of the donor plane (diastereoisomer II).


4.2.7 Hydrogen bonding in the complexes of $L^{16}$ and $L^{17}$

Figure 4.7 illustrates the extensive network of intra- and intermolecular hydrogen bonds present in the crystal of the $L^{16}$ complexes, involving the co-ordinated amines and the bromine atoms of the macrocyclic complexes and of the $[CdBr_4]^{2-}$ ion and the geometry of the hydrogen bonds is summarized in Table 4.5. The van der Waals radius of bromine (1.85 Å) and of nitrogen (1.55 Å) result in a calculated contact distance of 3.40 Å.[47] All the observed hydrogen bonds in this structure have N...Br distances greater than this distance. Of these bonds, however, the four most significant interactions (N...Br between 3.40 and 3.50 Å) are: N(12b)...Br(33) (bond A, N...Br 3.49 Å, H...Br 2.38 Å, N-H...Br 147°), N(11a)...Br(31) (bond H, N...Br 3.50 Å, H...Br 3.27 Å, N-H...Br 92°), N(22b)...Br(32) (bond D, N...Br 3.49 Å, H...Br 2.92 Å) and N(21b)...Br(2) (bond J, N...Br 3.46 Å, H...Br 2.47 Å, N-H...Br 152°), the last involving the co-ordinated bromine of complex II at 1-x,-y,1-z. Br(31) also interacts weakly with N(12b) (bond E, N...Br 3.72 Å, H...Br 3.31 Å, N-H...Br 102°) and Br(33) with N(22a) (bond

TABLE 4.5 Hydrogen bonding distances ( Å) and angles (°) at the hydrogen atom in $[CdL^{16}Br]_2[CdBr_4]$.

| H-bond | N-H...Br | N...Br | H...Br | angle at H |
|---|---|---|---|---|
| A | N(12b)-H...Br(33) | 3.49 | 2.38 | 147 |
| B | N(22a)-H...Br(32) | 3.79 | 2.87 | 132 |
| C | N(22a)-H...Br(33) | 3.54 | 2.77 | 121 |
| D | N(22b)-H...Br(32) | 3.49 | 2.92 | 111 |
| E | N(12b)-H...Br(31) | 3.72 | 3.31 | 102 |
| F | N(21b)-H...Br(2) | 3.77 | 3.41 | 101 |
| G | N(12a)-H...Br(1) | 3.74 | 3.46 | 96 |
| H | N(11a)-H...Br(31) | 3.50 | 3.27 | 92 |
| I | N(11b)-H...Br(1) | 3.63 | 3.42 | 92 |
| J | N(21b)-H...Br(2)i | 3.46 | 2.47 | 152 |
| K | N(11b)-H...Br(1)ii | 3.84 | 2.93 | 143 |
| L | N(21a)-H...Br(34)iii | 3.67 | 2.95 | 124 |
| M | N(11a)-H...Br(31)iv | 3.68 | 2.85 | 121 |

equivalent positions; i, 1-x,-y,1-z ii, -1-x,1-y,-z iii, x,y,1+z iv, -x,1-y,-z.

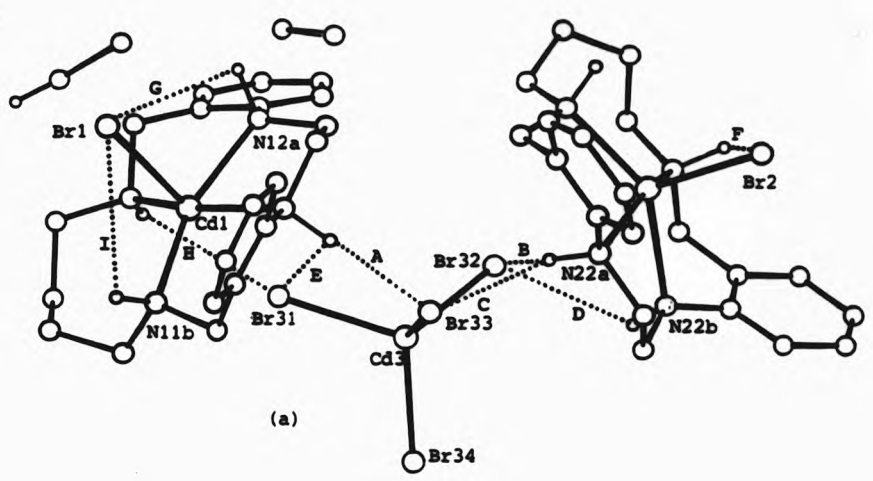


FIGURE 4.7 The hydrogen bonding scheme in (a) the asymmetric unit and (b) between adjacent units at the indicated equivalent positions in $[CdL^{16}Br]_2[CdBr_4].CH_3OH$. The geometry of the hydrogen bonds A to M is summarized in Table 4.5.

C, N...Br 3.54 Å, H...Br 2.77 Å, N-H...Br 121°). Br(1) of complex I exhibits two weak intramolecular hydrogen bonds to N(11b) (bond I, N...Br 3.63 Å, H...Br 3.42 Å, N-H...Br 92°) and N(12a) (bond G, N...Br 3.74 Å, H...Br 3.46 Å, N-H...Br 96°) and an intermolecular bond to N(11b) at -1-x,1-y,-z (bond K, N...Br 3.84 Å, H...Br 2.93 Å, N-H...Br 143°). Br(2) of complex II has also a weak intramolecular bond to N(21b) (bond F, N...Br 3.77 Å, H...Br 3.41 Å, N-H...Br 101°). Table 4.5 lists other putative hydrogen bonds up to a N...Br distance of 3.84 Å. It is noteworthy that the methanol of crystallization takes no part in hydrogen bonding and the site disorder is almost certainly a consequence of this.

The network of inter- and intramolecular hydrogen bonding in $[CdL^{17}Br_2]$, involving the amine hydrogen atoms and the co-ordinated bromine atoms is illustrated in Figure 4.8 and the geometry of these hydrogen bonds is given in Table 4.6. A centrosymmetric hydrogen bonded dimeric unit is formed between N(2b) and Br(1) (bond A, N...Br 3.35 Å, H...Br 2.49 Å, N-H...Br 134°). The only other intermolecular hydrogen bond is that between N(1a) and Br(2) (bond B) which, judging by the N...Br distance is weak (N...Br 3.84 Å, H...Br 3.19 Å, N-H...Br 120°) is weak. Three significant intramolecular hydrogen bonds (C, D and E) may be discerned, two involving Br(1) and the benzylamino hydrogen atoms attached to N(1a) (N...Br 3.51 Å, H...Br 2.97 Å, N-H...Br 112°) and N(1b) (N...Br 3.28 Å, H...Br 2.57 Å, N-H...Br 129°). Of these two, that with the shorter distance (D) also subtends the greater angle at the hydrogen atom, 129°, compared to 112° for the other. The third hydrogen bond (bond E) involves Br(2) and N(2a) with a N...Br distance slightly longer than the other two (N...Br 3.61 Å, H...Br 3.01 Å, N-H...Br 131°).

FIGURE 4.8 The intra- and intermolecular hydrogen bonding scheme in $[CdL^{17}Br_2].CH_3CN$. The geometry of each hydrogen bond A to E is summarized in Table 4.6. The acetonitrile of crystallization associated with each equivalent position is included.

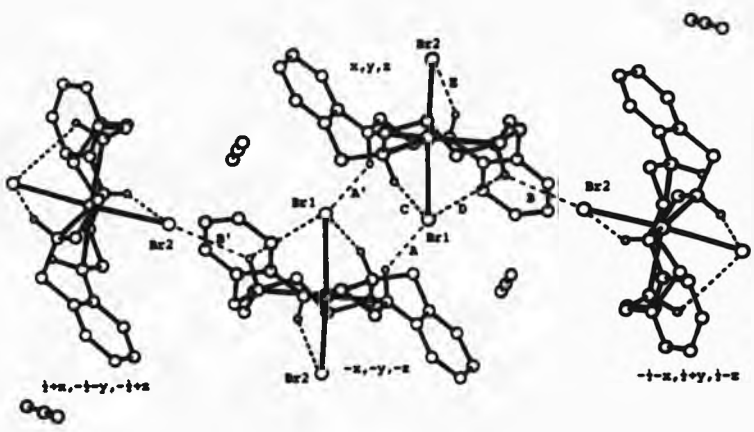


TABLE 4.6 Hydrogen bonding distances ( Å) and angles (°) at the hydrogen atom in $[CdL^{17}Br_2]$.

| H-bond | N-H...Br | N...Br | H...Br | angle at H |
|---|---|---|---|---|
| A | N(2b)-H...Br(1)i | 3.35 | 2.49 | 134 |
| A' | N(2b)i-H...Br(1) | " | " | " |
| B | N(1a)-H...Br(2)ii | 3.84 | 3.19 | 120 |
| B' | N(1a)i-H...Br(2)iii | " | " | " |
| C | N(1a)-H...Br(1) | 3.51 | 2.97 | 112 |
| D | N(1b)-H...Br(1) | 3.28 | 2.57 | 129 |
| E | N(2a)-H...Br(2) | 3.61 | 3.01 | 131 |

equivalent positions; i, -x,-y,-z ii, $-\frac{1}{2}-x,\frac{1}{2}+y,\frac{1}{2}-z$ iii, $\frac{1}{2}+x,-\frac{1}{2}-y,-\frac{1}{2}+z$.

## 4.3 Comparison of ligand conformation in the nickel(II), zinc(II) and cadmium(II) complexes

For each complex, the conformation of the ligand is precisely defined by the sequence of torsion angles in the macrocyclic skeleton. The endocyclic torsion angles in the macrocyclic inner great rings of the present series of ligands and their nickel(II), cadmium(II) and zinc(II) complexes (where the structures have been determined) are collected in Table 4.7: a total of five free ligands and eighteen complexes. The conformations of the free ligands have been discussed earlier (§2.2.3 and Table 2.3), but the torsion angles are included here for completeness. The ligand conformations in the nickel(II) complexes will be described first because they constitute a larger range than the zinc(II) and cadmium(II) complexes and they all exhibit the step conformation.

$L^{14}$ and its nickel(II) complexes all exhibit similar ligand conformations. In each case, the phenylene rings are inclined to opposite sides of the macrocyclic donor plane (the step conformation) and corresponding torsion angles in each half of the ligand are of the same type. The contraction of the ligand hole size in the low-spin complex and its expansion in the high-spin complex has surprisingly little effect on the endocyclic torsion angles; conformation changes are distributed evenly around the ring.

The conformations of the ligands $L^{15Et}$ and $L^{15Bu}$ were discussed in §2.2.3. The introduction of the extra methylene group allows two distinct conformations of the trimethylene bridge equivalent to the chair and twist (skew) conformations in the potential six-membered chelate rings. These are characterised by the sequence of torsion angles from C(8a) through C(8b). In $L^{15Et}$ (chair), the sequence is

TABLE 4.7 Endocyclic torsion angles (°) in the inner great ring of the $N_4$ macrocyclic ligands and complexes.(a,b)

| ligand or complex | Sequence of Torsion Angles | | | | | | | |
|---|---|---|---|---|---|---|---|---|
| | ---1---- | N2 | ----2---- | ----7---- | ----8---- | N1 | ----9---- | |
| $L^{14}$(c) | 62 | 170 | 175 | -2 | -53 | -178 | -162 | 70 |
| | | 174 | 166 | 0 | -55 | 179 | -168 | |
| | g | a | a | -c | -g | -a | -a | g |
| | | a | a | -c | -g | a | -a | |
| $[NiL^{14}(NCS)_2]$ (c) | 59 | -173 | 171 | -5 | -60 | -170 | -168 | 61 |
| | | -173 | 171 | -5 | -60 | -170 | -168 | |
| | g | -a | a | -c | -g | -a | -a | g |
| | | -a | a | -c | -g | -a | -a | |
| $[NiL^{14}](BF_4)_2$ (d) | 56 | -178 | 177 | -7 | -52 | -165 | -173 | 55 |
| | | -178 | 177 | -7 | -52 | -165 | -173 | |
| | g | -a | a | -c | -g | -a | -a | g |
| | | -a | a | -c | -g | -a | -a | |
| | ---1---- | N2 | ----2---- | ----7---- | ----8---- | N1 | ----9---- | 10 (e) |
| $L^{15Et}$(f) | 69 | 174 | 179 | 2 | -50 | -67 | -170 | -65 |
| | | 77 | -174 | 0 | 50 | 67 | 154 | 86 |
| | g | a | a | c | -g | -g | -a | -g |
| | | g | -a | c | g | g | a* | g* |
| $L^{15Bu}$(g) | 63 | 166 | -176 | -3 | -52 | -174 | 166 | 60 |
| | | 82 | 176 | -5 | 50 | 64 | 154 | 54 |
| | g | a | -a | -c | -g | -a | a | g |
| | | g* | a | -c | g | g | a* | g |
| $[NiL^{15}Cl_2]$ (h) | 55 | -176 | 171 | 0 | -62 | -167 | 165 | 44 |
| | | -170 | 174 | 0 | -63 | -174 | 167 | 33 |
| | g | -a | a | c | -g | -a | a | g* |
| | | -a | a | c | -g | -a | a | g* |
| $[NiL^{15}(NCS)_2]$ (i) | 58 | -172 | 174 | -6 | -64 | -170 | 168 | 39 |
| | | -172 | 174 | -6 | -64 | -170 | 168 | 39 |
| | g | -a | a | -c | -g | -a | a | g* |
| | | -a | a | -c | -g | -a | a | g* |
| $[ZnL^{15}(NO_3)(H_2O)]^+$(j) | 57 | 180 | -177 | -4 | -64 | -168 | 178 | 75 |
| | | 94 | 177 | 1 | 67 | 175 | 178 | -74 |
| | g | a | -a | -c | -g | -a | a | g |
| | | ac* | a | c | g | a | -a | -g |
| $[ZnL^{15}I]^+$(k) | 51 | 180 | 180 | -3 | -63 | -169 | 180 | 81 |
| | | 104 | 168 | 2 | 66 | 172 | 180 | -79 |
| | g | a | a | -c | -g | -a | a | g* |
| | | ac | a | c | g | a | a | -g |

TABLE 4.7 (continued)

| | | —1—M2—2—7—8—N1—9—10 (e) | | | | | | | |
|---|---|---|---|---|---|---|---|---|---|
| $[CdL^{15}(NO_3)]^+$(l) | 54 | 179 | 174 | 0 | -73 | -174 | -171 | 88 | |
| | | 109 | 169 | -1 | 75 | 176 | 172 | -87 | |
| | g | a | a | c | -g | -a | -a | g* | |
| | | ac | a | c | g | a | a | -g* | |
| $[CdL^{15Bu}(NO_3)]^+$(g) | 57 | -175 | 178 | 2 | -77 | -174 | -170 | 81 | |
| | | 88 | 180 | -6 | 81 | -174 | 178 | -88 | |
| | g | -a | a | c | -g | -a | -a | g* | |
| | | g* | a | -c | g* | -a | a | -g* | |
| | | —1—M2—2—7—8—N1—9—10— | | | | | | | |
| $L^{16}$ | 69 | 177 | -169 | -2 | -63 | -69 | 162 | -78 | 138 |
| | | -169 | 168 | 5 | -57 | 180 | -166 | -72 | |
| | g | a | -a | -c | -g | -g | a | -g | ac |
| | | -a | a | c | -g | a | -a | -g | |
| $[NiL^{16}(NCS)_2]$ (i) | 64 | -173 | 176 | -3 | -67 | -164 | 145 | 80 | -60 |
| | | -175 | 175 | -1 | -69 | -162 | 147 | 79 | |
| | g | -a | a | -c | -g | -a | ac* | g* | -g |
| | | -a | a | -c | -g | -a | ac* | g | |
| $[NiL^{16}(NO_3)_2]$ (m) | 58 | -170 | -178 | -3 | -65 | -163 | 150 | 89 | -84 |
| | | -179 | -179 | -4 | -64 | -155 | 139 | 93 | |
| | g | -a | -a | -c | -g | -a | ac* | g* | -g* |
| | | -a | -a | -c | -g | -a* | ac | ac* | |
| $[NiL^{16}(NO_3)_2]$ (n) | 58 | -170 | -178 | -3 | -65 | -163 | 150 | 89 | -18 |
| | | -179 | -179 | -4 | -64 | -73 | -125 | -71 | |
| | g | -a | -a | -c | -g | -a | ac* | g* | -c |
| | | -a | -a | -c | -g | -g | -ac | -g | |
| $[NiL^{16}(NO_3)(H_2O)]^+$(p) | 61 | -170 | 175 | 2 | -68 | -167 | 140 | 79 | -62 |
| | | -179 | 180 | -6 | -64 | -158 | 148 | 82 | |
| | g | -a | a | c | -g | -a | ac* | g | -g |
| | | -a | a | -c | -g | -a | ac* | g* | |
| $[CdL^{16}Br]^+$(q) | 66 | -177 | 172 | -2 | -70 | -158 | 167 | 95 | -95 |
| | | -173 | 177 | -2 | -74 | -164 | 171 | 92 | |
| | g | -a | a | -c | -g | -a* | a | ac* | -ac* |
| | | -a | a | -c | -g | -a | a | ac* | |
| $[CdL^{16}Br]^+$(r) | 56 | 180 | 180 | -4 | -71 | -175 | 158 | 57 | 52 |
| | | 106 | 166 | 4 | 72 | 168 | -172 | -119 | |
| | g | a | a | -c | -g | -a | a* | g | g |
| | | ac | a | c | g | a | -a | -ac | |

TABLE 4.7 (continued)

| | | —1— | —N2— | —2— | —7— | —8— | —N1— | —9— | —10— | —11 |
|---|---|---|---|---|---|---|---|---|---|---|
| $L^{17}$(p) | 71 | 175 | 180 | -1 | -56 | -68 | 168 | -66 | -175 |
| | | 163 | -161 | -4 | 51 | 180 | 64 | 54 | -179 |
| | g | a | a | -c | -g | -g | a | -g | -a |
| | | a | -a | -c | g | a | g | g | -a |
| $[NiL^{17}Cl_2]$ | 64 | -176 | -177 | -2 | -66 | -80 | -179 | 61 | -64 |
| | | -176 | 180 | -3 | -66 | -78 | 177 | 64 | -64 |
| | g | -a | -a | -c | -g | -g* | -a | g | -g |
| | | -a | a | -c | -g | -g | a | g | -g |
| $[NiL^{17}(NCS)_2]$ (i) | 63 | -172 | -179 | -1 | -68 | -77 | -173 | 55 | -62 |
| | | -176 | 176 | 1 | -69 | -75 | 180 | 63 | -66 |
| | g | -a | -a | -c | -g | -g | -a | g | -g |
| | | -a | a | c | -g | -g | a | g | -g |
| $[CdL^{17}Br_2]$ (m) | 66 | -174 | 176 | 3 | -78 | -162 | 158 | 53 | 59 |
| | | -175 | 180 | 3 | -75 | -77 | 168 | 57 | -160 |
| | g | -a | a | c | -g | -a | a* | g | g |
| | | -a | a | c | -g | -g | a | g | -a* |
| $[CdL^{17}Br_2]$ (n) | 66 | -174 | 176 | 3 | -78 | -162 | -153 | -52 | 162 |
| | | -175 | 180 | 3 | -75 | -77 | -146 | -37 | -75 |
| | g | -a | a | c | -g | -a | -a* | -g | a* |
| | | -a | a | c | -g | -g | -ac* | -g* | -g |

(a) For each compound, the first and second rows represent the torsion angles in the a- and b-halves of the macrocycle, respectively and the third and fourth rows show the corresponding designations [a = anti, 180±30°; g = gauche, 60±30°; ac = anticlinal, 120±30°; c = cis, 0±30°; * = deformation >20°]. (b) Carbon atoms are denoted by numerals only. For crystals containing two complexes, the numeral extensions to the atom labelling scheme used to distinguish between corresponding atoms in each complex have been omitted. (c) Calculated from Ref. 25. (d) Hand reversed from that given in Ref. 38. (e) This atom is labelled 9(c) in Refs. 38 and 44. (f) Hand reversed from that in Ref. 44. (g) Ref. 44. (h) Ref. 52.(i) Ref. 106. (j) Hand reversed from that in Ref. 44 and the a- and b-halves have been interchanged. (k) Ref. 125. (l) The a- and b-halves have been interchanged from those given in Ref. 44.(m) Major component of disordered structure. (n) Minor component of disordered structure. (p) Hand reversed from that given in Appendix. (q) Step-shaped complex. (r) Saddle-shaped complex.

-g,-a,-g,$g^{e}$,$a^{e}$,g [the abbreviations are explained in Table 4.7, footnote (a)], whereas in $L^{15Bu}$ (twist), it is -a,a,g,g,$a^{e}$,g. In [NiL$^{15}$Cl$_2$] and [NiL$^{15}$(NCS)$_2$], this area of the ligand adopts the twist conformation; the sequence C(8a) to C(8b) is -a,a,$g^{e}$,$g^{e}$,a,-a. Although both $L^{15Et}$ and $L^{15Bu}$ have -C(7)-C(8)- of opposite signs (the saddle conformation), the equality of the signs of -C(7a)-C(8a)- and -C(7b)-C(8b)- in the nickel(II) complexes is indicative of the step conformation. It is also characteristic of this change that the torsion angle -C(1b)-N(2b)- changes from g or $g^{e}$ in the free ligands to -a in the Ni(II) complexes.

The nickel(II) complexes of $L^{16}$ all have the macrocycle co-ordinated in the step conformation as defined above. The torsion angles in the backbone of the ligand through the anilino donor atms from C(8a) to C(8b) are similar in the nickel(II) complexes of $L^{16}$ to those in the free ligand. On co-ordination, the torsion angles in the remainder of the macrocycle exhibit greater changes: -C(8a)-N(1a)- from -g to -a, -N(1a)-C(9a)- and N(1b)-C(9b)- from a to ac or $ac^{e}$, -C(9a)-C(10a)- and -C(9b)-C(10b)- from -g to g with large deviations from 60° (up to 93°). The angle -C(10a)-C(10b)- changes from ac in the free ligand to -g in the thiocyanate and aquanitrato complexes and to $-g^{e}$ (-84°) and -c in the major and minor conformers of the dinitrato complex, respectively.

The free ligand $L^{17}$ has both torsion angles -C(7)-C(8)- of opposite sign, indicating again a saddle conformation, but in contrast to the fifteen-membered ligands, both -C(1a)-N(2a)- and -C(1b)-N(2b)- are anti, rather than one anti and one anticlinal. On complexation with nickel(II) the -C(7)-C(8)- angles are of the same sign indicating the step conformation and the -C(1)-N(2)- angles are similar to those

in the free ligand. As with $L^{16}$, the most obvious changes on co-ordination are in the area of the macrocycle containing the longer alkyl bridge: -N(1b)-C(9a)- from g to a, -C(9a)-C(10a)- from -g to g and both -C(10a)-C(11)- and -C(10b)-C(11)- from -a to -g.

The zinc(II) and cadmium(II) complexes of the fifteen-membered ligands $L^{15}$ and $L^{15Bu}$ are all saddle-shaped with the angles -C(7)-C(8)- in each half of the molecules of opposite sign. The magnitude of these angles is increased from between 63° and 67° in the zinc(II) complexes to between 73° and 81° in the cadmium(II) complexes. The virtual mirror symmetry of the saddle conformation cannot be maintained in the torsion angles on either side of the C(1a)-C(1b) bond without the imposition of a cis torsion angle on this bond and eclipsed hydrogen atoms on these two methylene groups. As a consequence of the gauche -C(1a)-C(1b)- angle, the angle -C(1b)-N(2b)- is deformed to between 88° and 109° in these complexes. The rest of the ligand in each complex does exhibit virtual mirror symmetry with the $-(CH_2)_3-$ bridge in the chair conformation: -C(9a)-C(10)- and -C(9b)-C(10)- of opposite sign.

The two cadmium(II) complexes of $L^{16}$, the step and the saddle, exhibit some notable differences in conformation from the nickel(II) complexes associated with the opening-up of the ligand cavity from a mean of 2.13 Å to a mean of 2.28 Å. In the saddle-shaped complex of $L^{16}$, the torsion angle -C(1b)-N(2b)- is anticlinal as in the zinc(II) and cadmium(II) complexes of $L^{15}$ (and $L^{15Bu}$) and the -C(7)-C(8)- angles in each half are opposite in sign. In the step-shaped complex, these angles are similar to those in the nickel(II) complexes. In the step-shaped complex, the angles $-(C_9)$-C(10)- are both distorted anticlinal (ac*, 95° and 92°) and -C(10a)-C(10b)- is of the same

magnitude but of opposite sign (-95°). In contrast, in the saddle-shaped complex the sequence -C(9a)-C(10a)-C(10b)-C(9b)- is g,g,ac.

In the disordered complex $[CdL^{17}Br_2]$ the sequence of torsion angles from C(8a) through the amilino donor atoms to C(8b) differs little from that in the nickel(II) complexes, except that 7a-8a and 7b-8b are -78° and -75°, respectively. The expansion of the bonding cavity in the cadmium(II) complex and the corresponding increase in the distance between the nitrogen atoms bridged by the disordered $-(CH_2)_5-$ chain is reflected in the differences between the torsion angle sequence in the rest of the ligand [between C(8a) and C(8b)]. The value of -C(8a)-N(1a)- is common to both conformers and, in contrast to that in the nickel(II) complexes, is anti rather than gauche (18° less than the ideal 180°), whereas -C(8b)-N(1b)-, at -77°, is of the same order as that in the nickel(II) complexes. The carbon atoms of the eight-membered chelate ring are all displaced to one side of the $CdN_2$ plane, rather than those in one half of the molecule being above and, in the other half, below, as they are in the nickel(II) complexes. The irregular torsion angles through this $-(CH_2)_5-$ chain, especially -N(1a)-C(9a)- and -N(1b)-C(9b)- show considerable deviations from ideal; in the minor conformer of $[CdL^{17}Br_2]$ -C(9b)-C(10b) is only 37°.

## Chapter Five

### 5. Structural Effects on Complex Stability

An extensive range of structural studies have now been carried out on the ligands and complexes of two intersecting rows of the ligand matrix represented by (5.i).

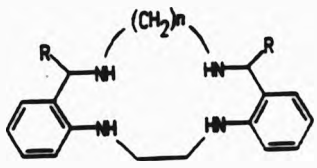


| n | 2 | 3 | 4 | 5 | 6 | 7 |
|---|---|---|---|---|---|---|
| R | | | | | | |
| H | $L^{14}$ | $L^{15}$ | $L^{16}$ | $L^{17}$ | - | $L^{19}$ |
| Me | - | $L^{15Me}$ | - | - | - | - |
| Et | - | $L^{15Et}$ | - | - | - | - |
| Pr | - | $L^{15Pr}$ | - | - | - | - |
| Bu | - | $L^{15Bu}$ | - | - | - | - |

(5.i)

In the present work, these structural studies have been targeted principally at the ligands $L^{16}$ (5.i, n = 4, R = H) and $L^{17}$ (5.i, n = 5, R = H) and their complexes. For the free ligands, when taken together with the structures of $L^{14}$,[25] $L^{15Et}$ (5.i, n = 3, R = Et) and $L^{15Bu}$ (5.i, n = 3, R = Bu),[44,59,61] the structural studies of the ligands $L^{16}$ and $L^{17}$ (Chapter Two) extend the series of available structures to cover fourteen- to seventeen-membered ligands. The lack of suitable crystals of $L^{15}$ has precluded a structural study of this key ligand; its absence is made more frustrating considering the

availability of structural information for a total of five complexes of $L^{15}$ with three different metal-ions (see below). Nevertheless, the hole size of $L^{15}$ may be predicted from the structures of $L^{15Et}$ and $L^{15Bu}$, which have been found to exhibit two different conformations of the macrocyclic skeleton.

The metal complexes studied in this work have been restricted to those of nickel(II), zinc(II) and cadmium(II) and the degree of success of attempts to prepare crystals suitable for X-ray diffraction studies has varied widely from metal to metal. The following summary of the complexes for which structural data is now available illustrates this point.

For the nickel(II) complexes, the structures of $[NiL^{16}(NO_3)_2]$, $[NiL^{16}(NO_3)(H_2O)]^+$ and $[NiL^{17}Cl_2]$ have been determined in the present work and are described in Chapter Three together with those of $[NiL^{15}(NCS)_2]$, $[NiL^{16}(NCS)_2]$ and $[NiL^{17}(NCS)_2]$,[106] and the previously reported structures of $[NiL^{14}(NCS)_2]$,[25] and $[NiL^{15}Cl_2]$.[52] In addition the structure of the low-spin complex $[NiL^{14}][BF_4]_2$ prepared in this work has been determined.[38,119] For the cadmium(II) complexes, the structures of $[CdL^{16}Br]_2[CdBr_4]$ (containing two independent complex cations) and of $[CdL^{17}Br_2]$ described in Chapter Four, augment the previously reported structures of $[CdL^{15}(NO_3)]^+$ and $[CdL^{15Bu}(NO_3)]^+$.[44,61] For the zinc(II) complexes of $L^{16}$ and $L^{17}$, no success was achieved in producing suitable crystals in the present work and the only available structures remain those reported for $[ZnL^{15}I]^+$,[125] and $[ZnL^{15}(NO_3)]^+$.[44,61]

It was intended that these structural studies would complement collaborative studies of the thermodynamic stabilities of the complexes in solution, providing an opportunity to assess the extent to which a structural interpretation can be applied to any observed differences in stability across the ligand series.

The essential differences between the 'frozen' structure observed in the solid state and the changing structures in solution can not be ignored. The forces external to a molecule which affect its structure in the solid state (packing forces) are not the same as those in solution; the environment in solution is constantly changing and the structure of the molecule changes in response to it. Furthermore, exchange processes occur in solution with counter-ion and solvent competing with the ligand for co-ordination to the metal-ion. Despite these obvious limitations, in order to investigate the effects of changes of ligand structure on complex stability in this way, it is necessary to assume that the solid state structure bears some resemblance to the structure of the complex in solution. At this point, the results of attempts to determine the stability constants of the metal complexes must be described.

## 5.1 Complex stability measurements

### 5.1.1 Zinc(II) and cadmium(II) complexes

The formation constants of the zinc(II) and cadmium(II) complexes (corresponding to the formation of $ML^{2+}$) have been determined potentiometrically at James Cook University of North Queensland, along with the protonation constants of the ligands (see §2.6). The results are listed in Table 5.1 and are illustrated graphically in Figure 5.1. Under the conditions and concentrations investigated, the present ligands form only 1:1 complexes with zinc(II) and cadmium(II), in

common with their $N_2O_2$ analogues,[24] and the twelve- to sixteen-membered aliphatic tetraaza macrocycles of the cyclam type.[79,80,136,137,138]

TABLE 5.1 Formation constants (log $K_{110}$) for the Zn(II) and Cd(II) complexes of $L^{14}$ to $L^{17}$ [95% MeOH, I = 0.1 mol $dm^{-3}$ ($NEt_4ClO_4$) at 25°C].(a)

| ligand | Zn(II) | Cd(II) |
|---|---|---|
| $L^{14}$ | 8.6 | 7.75 |
| $L^{15}$ | 8.6 | 5.4 |
| $L^{15Et}$ | 6.3 | 4.0 |
| $L^{15Pr}$ | 6.0 | 3.9 |
| $L^{15Bu}$ | 5.9 | 4.1 |
| $L^{16}$ | 6.4 | 6.2 |
| $L^{17}$ | 4.3(b) | 6.5(b) |

(a) Determined potentiometrically at James Cook University of North Queensland, Ref. 44;

(b) Values for $L^{17}$ were not reported in Ref. 44; errors in the determination of the ligand protonation constants caused by precipitation of $LH^+$ will be reflected in the complex formation constants. However, these errors are not likely to affect the apparent reversal of discrimination to too great an extent.[140]

For each of these cyclams the complex with Zn(II) is more stable than that with Cd(II) with the greatest discrimination seen for cyclam itself (log $K_{110}$ Zn(II) 15.34, Cd(II) 11.23). Simple linear polyamine ligands also exhibit a discrimination for Zn(II) over Cd(II).[139] It might be expected therefore that a similar situation would obtain for the present ligands.

The ligands $L^{14}$ and $L^{15}$ form complexes with zinc(II) which have stability constants (log $K_{110}$) which are identical within experimental error ($L^{14}$ and $L^{15}$ 8.6). For successive ring size increases after $L^{15}$, the stability of the zinc(II) complexes decreases by ca. 2 log K units ($L^{15}$ 8.6, $L^{16}$ 6.4, $L^{17}$ ca. 4.3). For the cadmium(II) complexes, a parallel decrease in stability is observed, but only between $L^{14}$ and $L^{15}$ ($L^{14}$ 7.75, $L^{15}$ 5.4). On passing from $L^{15}$ to $L^{16}$, the stability (log $K_{110}$) of the cadmium(II) complex increases slightly to a value of 6.2, close to that for the zinc(II) complex (6.4). For the Cd(II) complex of $L^{17}$ a further slight increase in log $K_{110}$ is evident (ca. 6.5) While no underlying pattern for the stabilities of the macrocyclic complexes with either metal is apparent, stabilities of the Zn(II) and Cd(II) complexes with the larger sixteen- and seventeen-membered ligands and the Cd(II) complex of $L^{15}$ are substantially lower than the complexes of the smallest ligand, $L^{14}$. However, in complexes of the fifteen-membered ligand, log $K_{110}$ differs by ca. 3 log K units, with $L^{15}$ showing an enhanced discrimination for Zn(II) over Cd(II), $L^{16}$ showing almost no discrimination and $L^{17}$ showing a reversed discrimination, for Cd(II) over Zn(II), although in this case some doubt about the accuracy of the ligand log $K_{011}$ must be reflected in the values of log $K_{110}$. Despite this, the errors in these measurements are not likely to affect the apparent reversal of the discrimination.[140]

The results of the structural and other studies presented in the preceding chapters may give some clues to the origin of the observed Zn(II)/Cd(II) discrimination variation across the series of ligands and will be discussed later.

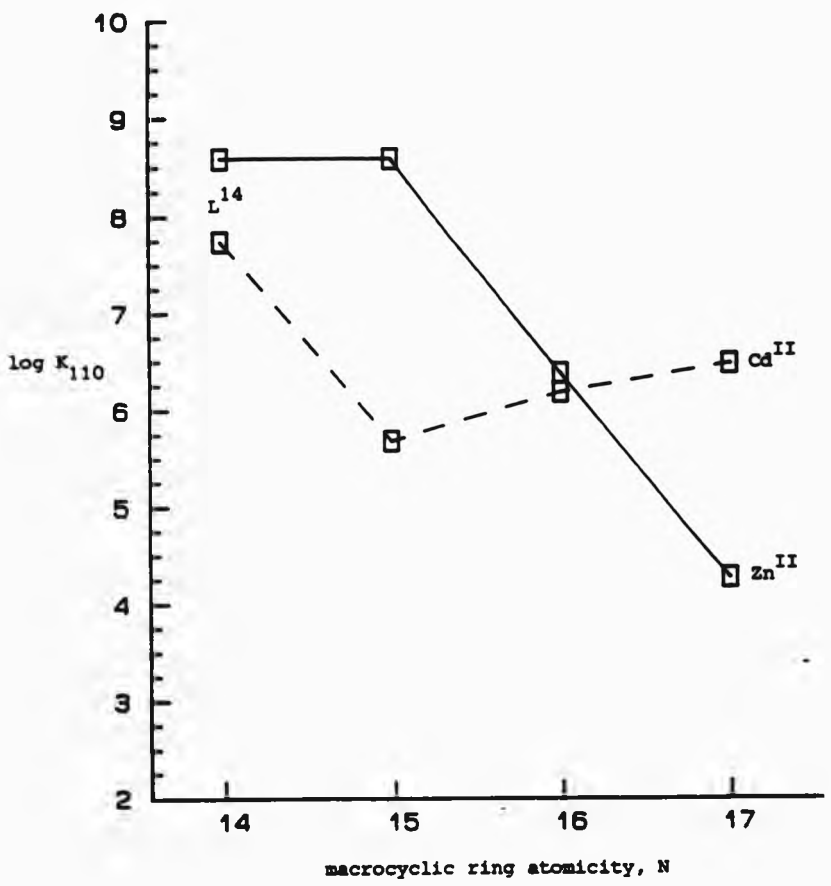


FIGURE 5.1 Formation constants (log $K_{110}$) for the Zn(II) and Cd(II) complexes of $L^{14}$ to $L^{17}$ (plotted from data in Table 5.1).

5.1.2 Nickel(II) complexes

Attempts to determine potentiometrically the thermodynamic formation constants of the nickel(II) complexes were unsuccessful because of precipitation or ligand decomposition as manifested in a darkening of the solution during the course of the titration.[140]

A spectrophotometric study of the kinetics of dissociation of the nickel(II) complexes was envisaged, but a preliminary investigation indicated that the dissociation was generally slow and may be complicated by ligand decomposition over the long times required for spectrophotochemical data collection. Nevertheless, this investigation highlighted the relative kinetic stability of the complex of $L^{15}$. The visible spectra of methanolic solutions of the chloride complexes with added hydrochloric acid showed that the kinetic stability, characterized by the rate of change of the visible spectra, varies in the order $L^{14} < L^{15} > L^{16}$. The spectrum of the complex of $L^{16}$ changes to one similar to that of aquated nickel(II) in one day. A similar transformation occurs with the complex of $L^{14}$ in three days; the spectrum of the complex of $L^{15}$ shows no change after three months.

5.2 Correlation of structural trends and stability across the series of ligands

Structural features that may contribute to the pattern of stability of all the complexes include the following: the fit of the metal into the macrocyclic cavity (§1.5), changes in the co-ordination mode of the metal-ion (dislocation discrimination §1.4) and changes in the conformation of the ligand on complexation. The applicability of these factors to the Zn(II) and Cd(II) complexes will be discussed after consideration of the first of these, the goodness-of-fit

criterion for the Ni(II) complexes, for which the situation is somewhat less complicated.

5.2.1 Hole size considerations

The ligand hole sizes ($R_H$), bonding cavity radii ($R_A$) and goodness-of-fit parameters for the macrocycles have been calculated by the method of Henrick, Tasker and Lindoy.[23] In this convention, the hole size is the mean of the donor-centroid distance (the centroid is at the position defined by the mean of the fractional atomic co-ordinates of the donor atoms). The bonding cavity radius is equal to the hole size less the mean of the appropriate radii for the donor atoms, 0.72 Å for secondary amine donors.[23] The goodness-of-fit parameter is the ratio of the bonding cavity radius to the radius of the metal-ion ($R_A/R_P$) and a value of unity for this parameter indicates an ideal fit for the metal-ion to the macrocyclic cavity ($R_P$ is the Pauling covalent radius for high-spin or low-spin nickel(II), 1.39 and 1.20 Å,[37] respectively).

5.2.1.1 Hole size correlations for the nickel(II) complexes

The three structural parameters of the macrocyclic cavity, hole size, bonding cavity radius and goodness-of-fit, calculated for the available X-ray structure determinations of the present tetraaza macrocycles as nickel(II) complexes are listed in Table 5.2, together with the hole sizes of the free ligands. The structures of the nickel(II) complexes with thiocyanate axial ligands form a continuous series from $L^{14}$ to $L^{17}$. Although no thermodynamic stability data are available for the nickel(II) complexes, the peak in the kinetic stability at $L^{15}$ correlates with the ideal goodness-of-fit for this ligand ($R_A/R_P$ 1.00) with $L^{14}$ being slightly too small (0.97) and $L^{16}$

TABLE 5.2 Ligand hole sizes ($R_H$) and bonding cavity radii ($R_A$) of the ligands, L, and complexes, [MLXY].(a)

| M | L | X | Y | $R_H$/ Å | $R_A$/ Å | goodness-of-fit(b) |
|---|---|---|---|---|---|---|
| - | $L^{14}$ | - | - | 2.02(c) | - | - |
| - | $L^{15Et}$ | - | - | 2.10(d) | - | - |
| - | $L^{15Bu}$ | - | - | 2.14(d) | - | - |
| - | $L^{16}$ | - | - | 2.22 | - | - |
| - | $L^{17}$ | - | - | 2.41 | - | - |
| Ni | $L^{14}$ | - | - | 1.93(e) | 1.21 | 1.01 |
| Ni | $L^{14}$ | NCS | NCS | 2.07(c) | 1.35 | 0.97 |
| Ni | $L^{15}$ | NCS | NCS | 2.11(f) | 1.39 | 1.00 |
| Ni | $L^{16}$ | NCS | NCS | 2.15(f) | 1.43 | 1.03 |
| Ni | $L^{17}$ | NCS | NCS | 2.15(f) | 1.43 | 1.03 |
| Ni | $L^{15}$ | Cl | Cl | 2.11(g) | 1.39 | 1.00 |
| Ni | $L^{17}$ | Cl | Cl | 2.15 | 1.43 | 1.03 |
| Ni | $L^{16}$ | $NO_3$ | $NO_3$ | 2.11 | 1.39 | 1.00 |
| Ni | $L^{16}$ | $NO_3$ | $H_2O$ | 2.13 | 1.41 | 1.01 |
| Zn | $L^{15}$ | $NO_3$ | $H_2O$ | 2.14(d) | 1.42 | 0.99 |
| Zn | $L^{15}$ | I | - | 2.11(h) | 1.39 | 0.97 |
| Cd | $L^{15}$ | $NO_3$ | - | 2.24(d) | 1.52 | 0.93 |
| Cd | $L^{15Bu}$ | $NO_3$ | - | 2.25(d) | 1.53 | 0.94 |
| Cd | $L^{16}$ | Br | - | 2.31(i) | 1.59 | 0.98 |
| Cd | $L^{16}$ | Br | - | 2.26(j) | 1.54 | 0.94 |
| Cd | $L^{17}$ | Br | Br | 2.37 | 1.65 | 1.01 |

(a) Calculated according to Ref. 23; (b) $R_A/R_P$ for Ni(II) ($R_P$ = 1.39 Å), $R_A/R_M$ for Zn(II) ($R_M$ = 1.43 Å) and Cd(II) ($R_M$ = 1.63 Å); (c) Ref. 25; (d) Ref. 44; (e) low-spin complex; (f) Ref. 106; (g) Ref. 52; (h) Ref. 125; (i) step-shaped conformation; (j) saddle-shaped conformation.

and $L^{17}$ being slightly too big (both 1.03). As the ring size of the macrocycle increases from fourteen to fifteen and again to sixteen, the hole size in the complexes increases by 0.04 Å for each additional $CH_2$ group ($L^{14}$ 2.07, $L^{15}$ 2.11, $L^{16}$ 2.15 Å) as expected over this range of ring sizes.[28] Such an increase in hole size is not evident for $L^{17}$ ($R_H$ 2.15 Å); the size of the bonding cavity has contracted substantially from that in the free ligand (2.41 Å) to the same as that in the complex of $L^{16}$ by twisting the pentamethylene chain, bringing the benzylamino donors much closer together than they are in the free ligand (see §3.2.2).

The structures of two nickel(II) chloride complexes (of $L^{15}$ and $L^{17}$) have also been determined and it is apparent for either macrocyclic ligand that changing from the strong thiocyanato to the weaker chloro trans-axial ligands has no significant effect on the bonding cavity radius. The same can not be said for the dinitrato and aquanitrato complexes of $L^{16}$; the goodness-of-fit is 1.00 in the former and 1.01 in the latter. The reasons for this very slight apparent effect of axial ligand on the hole size of $L^{16}$ are not clear, but it may be that it is attributable to packing forces in the extensively hydrogen bonded crystal.

Figure 5.2 illustrates the change in ligand hole sizes on complexation with nickel(II). The hole size of $L^{15}$, when complexed with nickel(II) shows only a slight change from that for the free ligand as estimated from the mean of the hole sizes of the two C-alkylated homologues. The smaller $L^{14}$ shows an increase in the hole size on complexation, $L^{16}$ a comparable decrease and $L^{17}$ a larger decrease to a hole size the same as that in $L^{16}$. The optimum fit of nickel(II) for $L^{15}$ is consistent with the kinetic evidence that

FIGURE 5.2 Plot of hole size ($R_H$) versus macrocyclic ring atomicity of the free ligands (dashed line) $L^{14}$ to $L^{17}$,* and their high-spin nickel(II) complexes,† calculated from X-ray structural data.

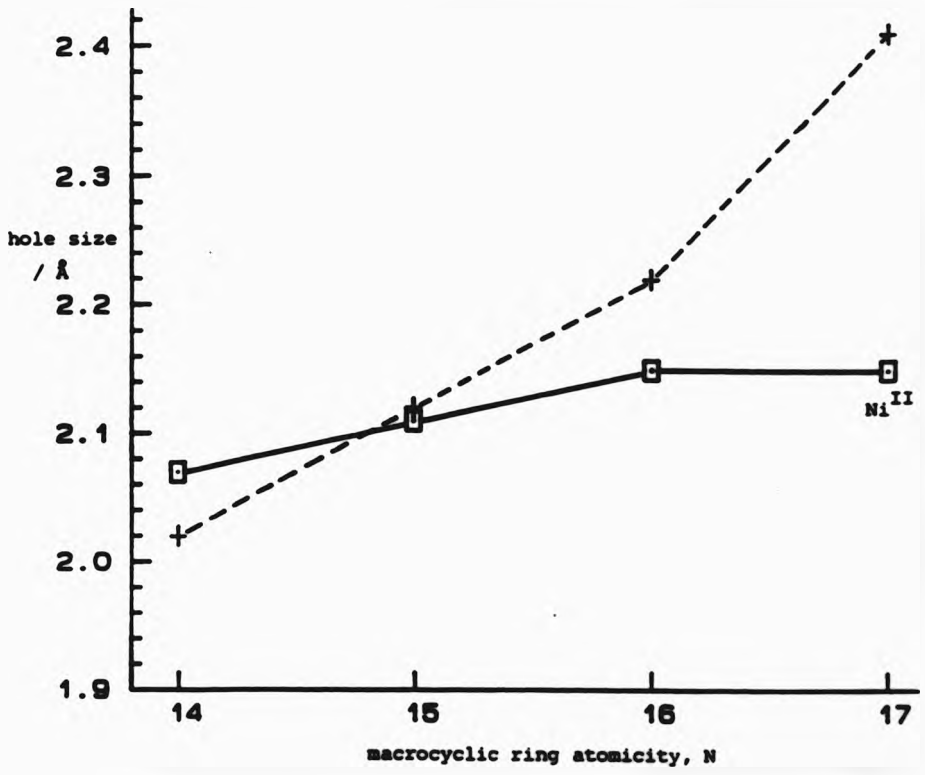


* For $L^{15}$, the hole size plotted is the mean of the values for $L^{15Et}$ and $L^{15Bu}$;

† values obtained from the thiocyanate and chloride complexes.

$[NiL^{15}Cl_2]$ is the least labile of the dichloro complexes.

A comparison of the trend in the hole sizes of the nickel(II) complexes of the present $N_4$ ligands with the hole sizes observed in the related $N_2O_2$ series (5.ii) allows a qualitative prediction of the stabilities of the complexes of the $N_4$ series.

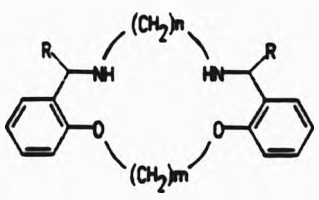


(5.ii)

In the $N_2O_2$ series, the goodness-of-fit is optimized for the complex of the sixteen-membered ligand ($R_A/R_P$ 1.01), which also shows the highest complex formation constant in the series (log $K_{110}$ 5.8).[24] The hole size of the nickel(II) complex of this $N_2O_2$ ligand (2.14 Å) is larger than that of $L^{15}$ (2.11 Å), because the oxygen donors of the $N_2O_2$ ligand, have a covalent radius (0.76 Å) larger than that of the nitrogen donors (0.72 Å).[23] This difference makes the bonding cavity radii in both ligands very similar and they exhibit correspondingly very similar goodness-of-fit parameters. The complex dissociation rates, $k_d$, for the nickel(II) complexes of the $N_2O_2$ ligands have also been reported,[24] and the maximum kinetic stability coincides with the peak in the thermodynamic stability at the sixteen-membered ligand. This gives some justification for presuming that, in the present series of $N_4$ ligands, the thermodynamic stability of the nickel(II) complexes mirrors the kinetic stability and is dependent on the goodness-of-fit of the metal for the macrocycle.

5.2.1.2 Hole size considerations for the Zn(II) and Cd(II) complexes In order to obtain an estimate of the goodness-of-fit parameter for comparative discussion of the zinc(II) and cadmium(II) complexes, it is necessary to find an appropriate radius for the metal atom (see §1.8.2). Pauling gives values for the tetrahedral covalent radii of Zn(II) and Cd(II) of 1.31 and 1.48 Å, respectively, but no values for the octahedral covalent radii.[37] In an attempt to define an appropriate radius within the context of this work, three different approaches were investigated for Cd(II) and the most suitable of these was then applied to Zn(II).

First, subtraction of the tetrahedral covalent radius of iodine (1.28 Å)[37] from the Cd-I bond length in octahedral cadmium(II) iodide (2.99 Å)[141] gives a radius for cadmium(II) of 1.71 Å. Secondly, subtraction of the tetrahedral radius of Cd(II) from the mean of the Cd-Br bond lengths in the seven reported structures (Table 4.4) of $[CdBr_4]^{2-}$ (2.59 Å) gives a value for the radius of bromine in this complex of 1.11 Å, which is equal to Pauling's tetrahedral covalent radius of bromine.[37] Using this radius, from the Cd-Br bond lengths in the two complexes of $[CdL^{16}Br]^{2+}$ (2.574 and 2.660 Å) alternative radii of 1.46 and 1.55 Å are obtained for Cd(II). In the same manner, from the mean of the Cd-Br bond lengths in $[CdL^{17}Br_2]$ (2.74 Å) a value of 1.63 Å is obtained. Thirdly, and probably most appropriately, using the average Cd-N bond length (2.35 Å) in the present series of complexes, and the radius for the nitrogen donors (0.72 Å) used in the evaluation of the bonding cavity radii in the nickel(II) complexes, a value of 1.63 Å is obtained for the octahedral or square pyramidal covalent radius of cadmium(II). Considering that this value agrees with that determined above, based on the Cd-Br bond lengths in $[CdL^{17}Br_2]$, it has been used to calculate

the goodness-of-fit parameter for the cadmium(II) complexes in Table 5.2.

The data for Zn(II) is more limited, but from the average Zn-N bond lengths in the two complexes of $L^{15}$, a value of 1.43 Å is obtained for the equivalent radius of zinc(II). For both these $d^{10}$ metal-ions in the present complexes, the radius calculated as above is larger than the respective tetrahedral radius by a similar amount, 9% for Zn(II) and 10% for Cd(II). These increases correspond to those seen for the ionic radii of the two metals. Both Zn(II) and Cd(II) exhibit similar proportional increases in ionic radius on increasing the co-ordination number (CN) from four to six (ca. 20%) and from six to eight (ca. 16%) {Zn (CN 4) 0.60 Å, (CN 6) 0.72, (CN 8) 0.84 Å; Cd (CN 4) 0.78, (CN 6) 0.95, (CN 8) 1.10 Å,[142]}.

Figure 5.3 illustrates the difference between the hole sizes in the free ligands and in the cadmium(II) complexes. The increase in the thermodynamic stability of the Cd(II) complexes on increasing the ligand ring size from that in $[CdL^{15}(NO_3)]^+$ to that in $[CdL^{16}Br]^+$ and to that in $[CdL^{17}Br_2]$ correlates with the increase in the goodness-of-fit parameter ($R_A/R_M$) for these complexes ($L^{15}$ 0.93, $L^{16}$ 0.96, $L^{17}$ 0.98). Similarly, the decrease in stability of the zinc(II) complexes on increasing the ligand hole size from that in the complex of $L^{15}$ to the presumably larger hole sizes in the complexes of $L^{16}$ and $L^{17}$ may be interpreted in terms of the decreasing goodness-of-fit across the series. Figure 5.4 illustrates the pattern of stabilities expected for the Zn(II) and Cd(II) complexes if the stability were entirely hole size dependent; the peak in stability for Zn(II) is expected lower down the ligand series than the peak for Cd(II). However, it is apparent that this interpretation can not be extended

FIGURE 5.3 Plot of hole size ($R_H$) versus macrocyclic ring atomicity of the free ligands (dashed line) $L^{14}$ to $L^{17}$,* and cadmium(II) complexes,† calculated from X-ray structural data.

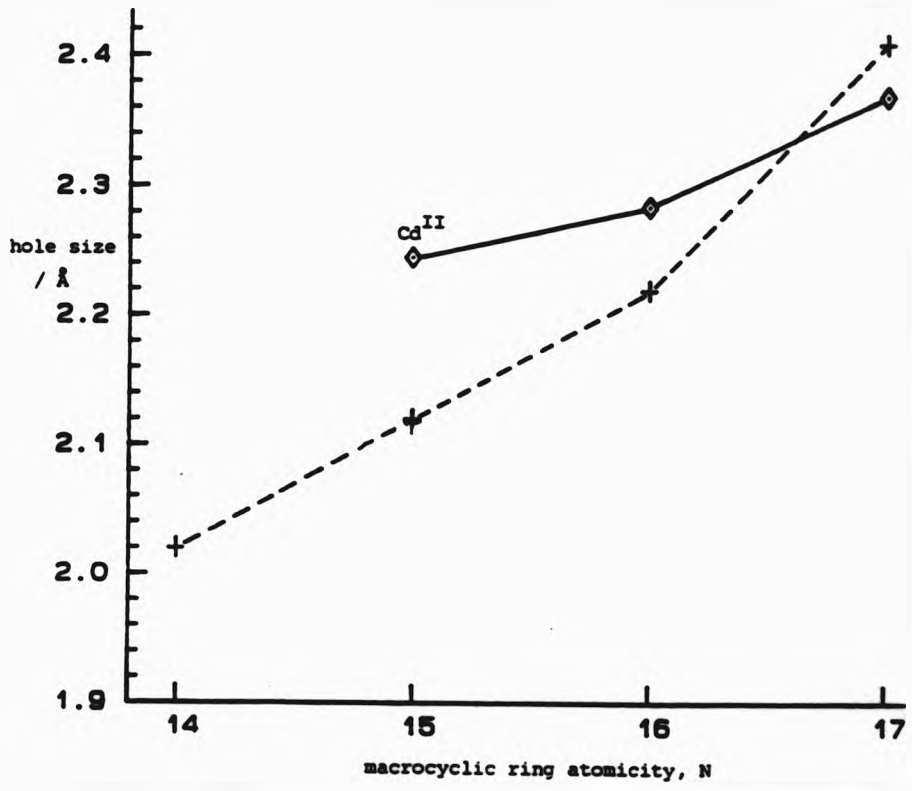


* See footnotes to Figure 5.2;

† the mean of the values for $[CdL^{15}(NO_3)]^+$ and $[CdL^{15Bu}(NO_3)]^+$ and the mean of both conformations of the complex $[CdL^{16}Br]^+$ are plotted.

to account for the similar thermodynamic stabilities of the Zn(II) and Cd(II) complexes of $L^{14}$; the stability of the Zn(II) complex is too low and the Cd(II) complex, too high. Other structural factors may have an effect in determining the apparently anomalous thermodynamic stability of the Zn(II) and Cd(II) complexes of $L^{14}$.

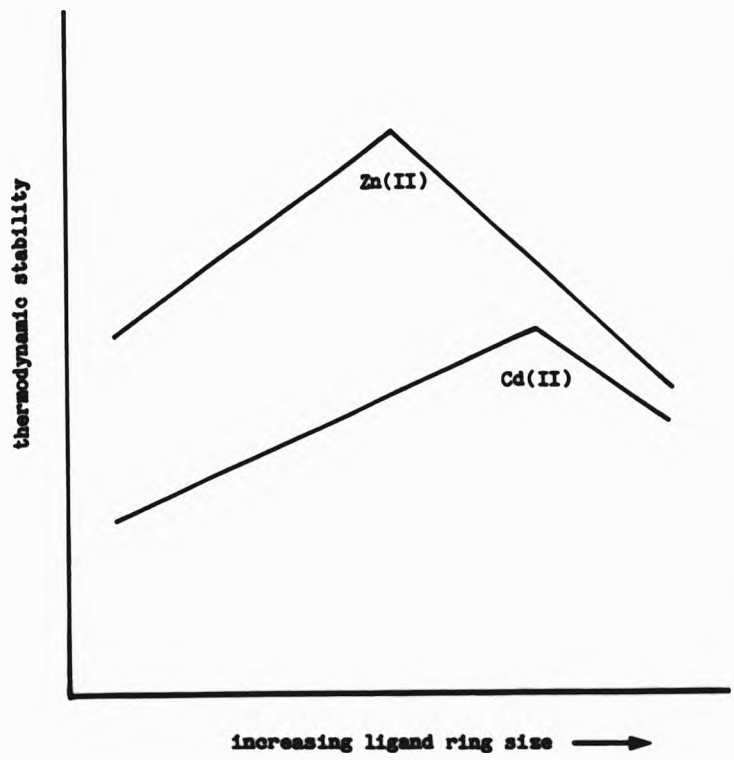


FIGURE 5.4 The pattern of thermodynamic stabilities expected for the zinc(II) and cadmium(II) complexes of the ligands on the basis of a goodness-of-fit only model.

5.2.2 Change of co-ordination geometry

An important structural feature which must affect the pattern of discrimination across the ligand series (see Figure 5.1) is the change from five-co-ordinate square pyramidal to six-co-ordinate pseudo-octahedral geometry. The change can be observed in the Cd(II) complexes of $L^{15}$ (five-co-ordinate) and $L^{17}$ (six-co-ordinate). $L^{16}$ seems to form complexes which are intermediate between these two extremes and will be discussed later. This change has two important effects: a decrease in the extent to which the metal-ion is displaced from the plane of the macrocyclic donor atoms and a change in gross conformation from a saddle-shaped to a step-shaped ligand.

The ligand $L^{15}$ (and its homologue $L^{15Bu}$) gives pseudo-square pyramidal complexes with Cd(II), in which the metal sits out of the donor atom plane. This situation is reminiscent of the 'doming' or 'tenting' seen in some cadmium(II) porphyrin complexes.[143] For example, the metal lies 0.65 Å above the plane in the piperidine adduct of (5,10,15,20-tetraphenylporphyrinato)cadmium(II) (5.ii).[144]

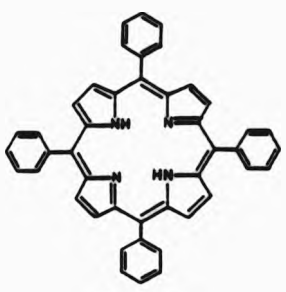


(5.ii)

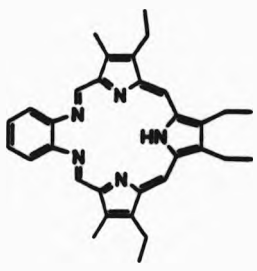


(5.iii)

In the "expanded porphyrin" (5.iii) a displacement of 0.34 Å is observed in the benzimidazole adduct.[145] Such 'doming' of cadmium(II) and zinc(II) complexes reduces the repulsions between the axial donor and the macrocycle donors which would be present if the

cation was in the plane of the macrocyclic donors, closing to some extent the open face of the complex. As the ligand atomicity is increased, doming would result in too long Cd-N bonds, so the metal-ion is drawn closer to the plane of the macrocyclic donors and a further axial ligand is co-ordinated, giving pseudo-octahedral complexes. The addition of the second trans-axial ligand has the effect of pulling the metal into the plane of the macrocyclic donors as is seen in the bis(pyridine) adduct of (5.iii).[145]

In the case of the present complexes, the displacement of the metal-ion from the donor plane may be predicted by treating the metal-ion as a rigid sphere sitting on top of a hole that is slightly too small [based on the bonding cavity radii of the co-ordinated ligands (Table 5.1) and the radii of the metal-ions calculated above (§5.2.1.1)], These estimated displacements ($d_{calc}$) in most cases match very closely those observed ($d_{obs}$) in the structures of the Zn(II) and Cd(II) complexes (Table 5.3). Except for the step-shaped complex of $[CdL^{16}Br]^+$, where $d_{calc} - d_{obs} = 0.11$ Å, the difference between the calculated and observed diplacements in each complex is no more than 0.07 Å. It would not be meaningful to estimate the displacement for $[CdL^{17}Br_2]$ because the hole size is larger than the radius of the metal-ion.

The high stability of the cadmium(II) complex of $L^{14}$ cannot be explained in terms of a goodness-of-fit model. It is unlikely that the ligand can expand its hole size much beyond that observed in the high-spin nickel(II) complex $[NiL^{14}(NCS)_2]$ (2.07 Å). Using the bonding cavity radius for $L^{14}$ in this complex ($R_A$ 1.35 Å), it can be predicted that Zn(II) and Cd(II) would sit out of the plane of the donor atoms by 0.47 Å and 0.91 Å, respectively. It is possible that

the minimization of inter-donor repulsion in this way favours increased thermodynamic stability.

TABLE 5.3 Observed displacement ($d_{obs}$) of the metal-ion from the mean-plane of the macrocyclic donors in the Zn(II) and Cd(II) complexes and the displacement calculated ($d_{calc}$)[a] from the bonding cavity radii ($R_A$) and the metal-ion radii ($R_M$).[b]

| complex | $R_A$ / Å | $d_{obs}$ / Å | $d_{calc}$ / Å |
|---|---|---|---|
| $[CdL^{15}(NO_3)]^+$ | 1.52 | 0.61 | 0.59 |
| $[CdL^{15Bu}(NO_3)]^+$ | 1.53 | 0.49 | 0.56 |
| $[CdL^{16}Br]^+$(c) | 1.59 | 0.25 | 0.36 |
| $[CdL^{16}Br]^+$(d) | 1.54 | 0.53 | 0.53 |
| $[CdL^{17}Br_2]$ | 1.65 | 0.19 | - (e) |
| $[ZnL^{15}I]^+$ | 1.42 | 0.12 | 0.17 |
| $[ZnL^{15}(NO_3)(H_2O)]^+$ | 1.39 | 0.41 | 0.34 |

(a) $d_{calc} = (R_M^2 - R_A^2)^{\frac{1}{2}}$;

(b) $R_M$ Zn(II) 1.43 Å, Cd(II) 1.63 Å;

(c) step-shaped complex; (d) saddle-shaped complex;

(e) the bonding cavity radius is larger than the radius of the metal-ion in this complex.

Figure 5.5 illustrates the differences in the co-ordination modes across the ligand series for Zn(II) and Cd(II) complexes including

possible structures for the complexes whose crystal structures have not yet been determined. The Zn(II) and Cd(II) complexes with $L^{14}$ are expected to be saddle-shaped and five-co-ordinate (square pyramidal) and the Zn(II) complexes of $L^{16}$ and $L^{17}$ are expected to be step-shaped and six-co-ordinate (octahedral). Of particular interest are the complexes which appear to be on the borderline between square pyramidal and octahedral. For the zinc(II) complexes there are two different complexes with $L^{15}$, one square pyramidal, $[ZnL^{15}I]^+$, and the other octahedral, $[ZnL^{15}(NO_3)(H_2O)]^+$ the hole size being larger in the octahedral complex, 2.14 as compared to 2.11 Å. It might be envisaged that for a Zn(II) complex of $L^{15}$, there are two extreme structures, the octahedral complex with the step-shaped ligand and the square pyramidal complex with the saddle-shaped ligand.

Similarly, the two complexes of $[CdL^{16}Br]^+$ exhibit borderline structures, this time in the same crystal. Although both these Cd(II) complexes are five-co-ordinate, the interaction with the counter-ion, $[CdBr_4]^{2-}$, is stronger for the step-shaped complex which may be considered to have a structure intermediate between the two extremes of saddle-shaped five-co-ordinate and step-shaped six-co-ordinate. These complexes differ noticeably in hole size: 2.31 Å for that with the step-shaped ligand conformation and the metal near the donor plane and 2.26 Å for that with the saddle-shaped conformation and the metal further out of the donor plane. The changeover point in the series of ligands from one co-ordination mode to the other would appear to be dependent on the energy difference between the two alternative conformations for each ligand, the lower energy one prevailing in the solid state. The energy difference between the two extremes will be at a minimum for a particular metal at some point in the ligand series. For the smaller Zn(II) ion this minimum would be expected in

FIGURE 5.5 Schematic representation of the change in the metal co-ordination mode from square pyramidal to octahedral across the series of ligands for cadmium(II) (top) and zinc(II) (bottom). The dislocation between the two geometries occurs at $L^{15}$ for zinc(II) and at $L^{16}$ for cadmium(II).

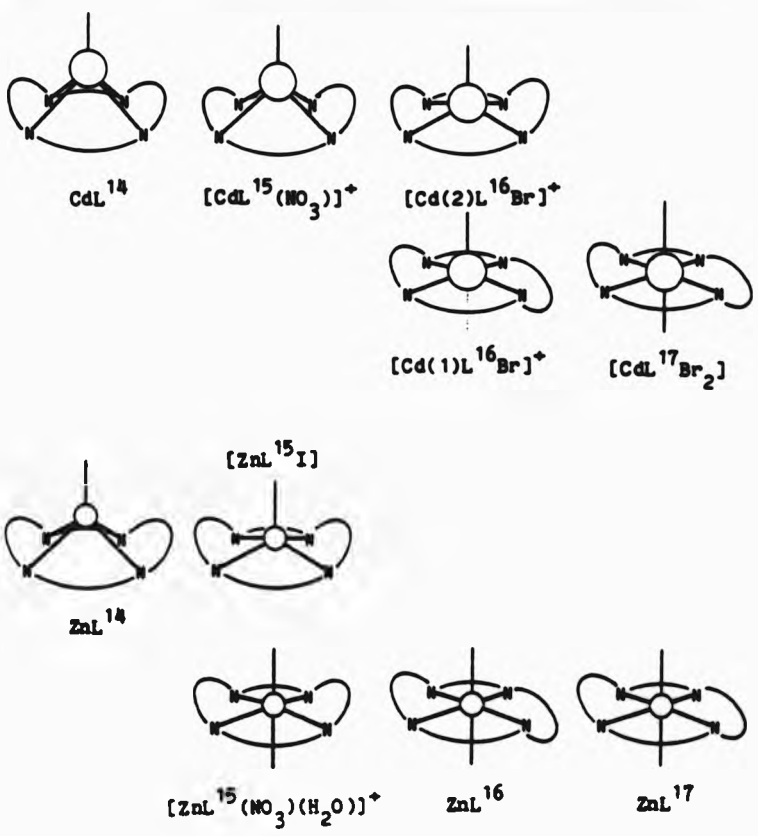

its complexes with a smaller ligand than for the larger Cd(II). It seems that the 'transitional' structures seen for Zn(II) with $L^{15}$ (one octahedral and one square pyramidal) and for Cd(II) with $L^{16}$ (one square pyramidal and the other almost octahedral), represent the minimum in the energy differences between the complexes for each metal. The solid state structures actually observed are not the extremes of structure, but may be considered as transitional structures stabilized by hydrogen bonding and other packing forces.

From the transition seen in the cadmium(II) complexes from five- to six-co-ordinate it may be deduced that zinc(II) would follow a similar pattern. This changeover point along the series of ligands occurs at $L^{15}$ for Zn(II) and at $L^{16}$ for Cd(II) and means that the Zn(II) complex of $L^{16}$ (the structure is unknown) will exhibit an octahedral co-ordination geometry with the metal-ion close to the donor plane and the ligand in the step conformation. This is the situation observed for the Cd(II) complex of $L^{17}$.

Significantly, in all the five- (and six-) co-ordinate Zn(II) and Cd(II) complexes of $L^{15}$ the ligand is saddle-shaped indicating that this is a preferred conformation of this ligand allowing Zn(II) to adopt either co-ordination geometry, but Cd(II) is too large to sit near enough to the donor plane and cannot achieve octahedral co-ordination. There is some evidence from the NMR spectra of $L^{15}$ that there is a significant proportion of the saddle-shaped conformation in solution.

It has been shown that, unlike the metal-ion in the nickel(II) complexes, which adapts the ligand hole size and conformation to retain its near octahedral geometry, the zinc(II) and cadmium(II) complexes adapt to the increasing 'natural' hole sizes across the

ligand series by changing the co-ordination geometry of the metal-ion from five-co-ordinate square pyramidal to six-co-ordinate pseudo-octahedral. This change in co-ordination geometry will be accompanied by changes in the conformation and configurational entropy of the macrocyclic ligand and would be expected to affect the formation constants of the metal complexes, especially if the difference between the configurational entropy change from the free ligand to the complex in the saddle or step conformations is pronounced. For the smaller zinc(II) ion, the relative stability of the square pyramidal and octahedral co-ordination geometries will not be the same as that in complexes of the larger cadmium(II) ion. In the former, the benefits of the more symmetrical donor atom distribution in the octahedral complexes will be outweighed by the reduction in inter-donor repulsion.

In conclusion, it seems that the observed pattern of Zn(II)/Cd(II) discrimination across the ligand series results from a combination of hole size and co-ordination geometry factors with five-co-ordinate geometry being more prevalent in the complexes with the smaller ligands and as the ligand ring size is increased six-co-ordinate geometry becomes more important. This change in co-ordination geometry across the ligand series may be regarded as a subtle example of structural dislocation, but there is a possibility of a more obvious dislocation occurring in the series of zinc(II) complexes: the non-co-ordination of the anilino donor atoms in the complexes of the larger ligands (see §1.8.1.2). But if no further change in co-ordination mode in the zinc(II) complexes is adopted by the metal-ion after that from square pyramidal to octahedral, the decrease in stability from $L^{15}$ to $L^{17}$ can be attributed to a lengthening and weakening of the Zn-N bonds, i.e. as a goodness-of-fit effect.

# Chapter Six

## 6. Experimental

### 6.1 Materials and techniques

#### 6.1.1 Materials

Unless otherwise stated, all materials were used as supplied by the manufacturers without further purification. Solvents were all General Purpose Reagent (GPR) grade. Drying of solvents where necessary was effected in the following ways: toluene and commercial anhydrous diethyl ether were dried with sodium wire; tetrahydrofuran with calcium hydride; methanol, ethanol and dichloromethane with an excess of freshly dried molecular sieve (Union Carbide, 3 Å) at 100 g $dm^{-3}$ followed by storage over fresh sieve at 10 g $dm^{-3}$.

#### 6.1.2 Infrared spectra

[Abbreviations: s = strong, sh = shoulder, vs = very strong w = weak.] Most of the routine spectra were obtained on a Perkin-Elmer 781 infrared spectrophotometer over the range 4000-600 $cm^{-1}$ as mulls with nujol and hexachlorobutadiene. The spectra were calibrated with the 1602 $cm^{-1}$ absorption line of polystyrene.

The spectra of the ligands and their metal complexes, however, were recorded on a Bio-Rad FTS-40 Fourier transform spectrophotometer linked to a 3240-SPC data station with internal He-Ne laser calibration. Spectra recorded on this instrument were prepared as potassium bromide microdiscs (diameter = 3 mm) using potassium bromide as a background. These are indicated in the text thus, (KBr).

6.1.3 Nuclear Magnetic Resonance Spectra (NMR)

[Abbreviations: b = broad, c = complex, d = doublet, q = quartet, s = singlet, t = triplet, vb = very broad.] $^{1}H$ NMR spectra were routinely recorded with a Perkin-Elmer R12B continuous wave spectrometer at 60 MHz, but a Bruker WP-80 Fourier transform spectrometer at 80 MHz was used in some cases and, less frequently a Bruker AM 250 at 250.13 MHz.

The Bruker WP-80 pulsed Fourier transform spectrometer was employed to record the $^{13}C$ NMR spectra at 20.12 MHz. The Bruker AM 250 was used to record $^{13}C$ NMR spectra at 62.896 MHz and $^{15}N$ NMR spectra at 25.35 MHz for some of the ligands. $^{1}H$-$^{1}H$, $^{1}H$-$^{13}C$, and $^{1}H$-$^{15}N$ correlation spectra (COSY) and $^{13}C$ INADEQUATE were also recorded using the same instrument. $^{1}H$ and $^{13}C$ spectra were referenced to tetramethylsilane, but for the $^{15}N$ spectra, external referencing was effected with nitromethane as a 1:1 (v/v) mixture with $CDCl_3$ containing $[Cr(pd)_3]$ (0.033 mol $dm^{-3}$).[73] Shifts are quoted with respect to ammonia at 0 p.p.m.

6.1.4 Electronic spectra

Except for the chloro complexes, a Perkin-Elmer Lambda-5 spectrophotometer with 1 cm quartz cells was used to record the spectra of the nickel complexes over the range 300-900 nm. The range was extended to cover the near infrared, 900-1500 nm, with a Perkin-Elmer Lambda-9 during a visit to ICI at Blackley.

The visible spectra of the dichloro complexes over the range 400-1300 nm were measured as dichloromethane solutions in 4 cm quartz cells on a Varian Cary 17 spectrophotometer at the University of Pavia. The range was extended to 300 nm using the Varian DMS90

uv/visible spectrophotometer.

6.1.5 Mass spectra

The mass spectra were recorded using a AEI MS9 mass spectrometer.

6.1.6 Microanalyses

Microanalytical information (C,H,N) was obtained with a Carlo Erba 1106 elemental analyzer.

6.1.7 Magnetic moments

Where sufficient material was available (60-100 mg) the magnetic moments of the nickel complexes were calculated from measurements of their magnetic susceptibilities using a Johnson Matthey Magnetic Susceptibility Balance.

6.1.8 Electrochemical measurements

(These were undertaken during a visit to the University of Pavia, Italy). Voltammetry was performed with the Electrochemlab System (Amel, Milan), consisting of a potentiostat (Model 552/MHR) and a function generator (Model 556), connected via a 563 multifunction interface. Current/potential curves were recorded on a Hewlett-Packard 7040 X-Y recorder. Electrochemical measurements in dichloromethane made 0.1 mol $dm^{-3}$ in tetrabutylammonium perchlorate $[Bu_4N][ClO_4]$ were carried out in a closed glass vessel at 25.0 ± 0.1°C under a nitrogen atmosphere. A small crystal of ferrocene was dissolved in the solution to act as an internal reference. A platinum microsphere (Metrohm) was used as the working electrode and a platinum foil as the auxiliary electrode. Platinum working electrodes were pretreated by immersion in chromic acid, washed with water and

acetone and anodized at a small positive potential. The tetrabutylammonium perchlorate was already prepared by reaction in aqueous solution of tetrabutylammonium hydroxide (40% solution, Fluka, pract.) and perchloric acid. The product was recrystallised twice from water and twice from acetone/ether and then dried in vacuo over phosphorus pentoxide. Purity of the electrolyte was checked by exploring the electrochemical range of its dichloromethane solution. Dichloromethane was dried over molecular sieve (Union Carbide, 4 Å). In a typical experiment a weighed amount of dichloro complex was added to 25 $cm^3$ of solution to give a millimolar solution.

## 6.2 Preparation of ligands and complexes

**N,N'-Bis(carbomethoxyphenyl)-1,2-diaminoethane (Ia)**

A well-stirred mixture of methyl 2-aminobenzoate (methyl anthranilate) (302 g, 2.00 mol), 1,2-dibromoethane (187 g, 0.99 mol) and anhydrous sodium carbonate (350 g) was heated under nitrogen at 130±5°C for 30 h. The product was extracted with boiling tetrahydrofuran (6 x 350 $cm^3$). The solvent was removed under reduced pressure and the resulting solid was slurried with methanol (100 $cm^3$), filtered at the pump, washed with methanol (2 x 25 $cm^3$) and recrystallised from petroleum spirit (60-80):chloroform (5:1) to give (Ia) (175 g, 0.53 mol, 53%) m.p. 119-120°C (lit.,[55] 118-120°C); (Found: C, 65.7; H, 6.1; N, 8.6. Calc. for $C_{18}H_{20}N_2O_4$: C, 65.8; H, 6.1; N, 8.5%; M 328.3); infrared $\nu_{max}$/ $cm^{-1}$ (nujol mull) 3360, 1677, 1606, 1580, 1518, 1505, 1470, 1440, 1322, 1250, 1224, 1193, 1164, 1118, 1084, 1049, 761 and 707; (HCB mull) 3360, 2985, 2945, 2905, 2865, 1677, 1518, 1505, 1470, 1440, 1321, 1260, 1242, 1224, 1190, 1118, 1080, 1049, 760 and 705; $^1H$ NMR ($CDCl_3$, 60 MHz) $\delta$/ p.p.m. 3.48 (4 H,

c, s with $D_2O$, $NCH_2$), 3.81 (6 H, s, $CH_3$) and 6.5–8.0 (10 H, 8 H with $D_2O$, c, aryl-H and at 7.9 NH); $^{13}C$ NMR ($CDCl_3$, 20.12 MHz) $\delta$/ p.p.m. 42.2, 51.5, 110.6, 111.2, 115.0 and 169.1.

4,7-Diaza-2,3:8,9-dibenzodecane-1,10-diol (Ib)

To a stirred suspension of lithium tetrahydridoaluminate (25 g) in dry tetrahydrofuran (500 $cm^3$) under nitrogen was added dropwise a solution of (Ia) (150 g, 0.46 mol) in dry tetrahydrofuran (1100 $cm^3$). After 5 h the addition was complete and the mixture was stirred at reflux for 1 h. After cooling to room temperature, water (25 $cm^3$) was added, cautiously at first, then sodium hydroxide (15% aq., 25 $cm^3$) and water (75 $cm^3$).[146] Stirring at reflux was resumed for a further 0.5 h, followed by filtration at the pump. The solid was extracted with boiling tetrahydrofuran (5 x 150 $cm^3$) and the combined filtrate was evaporated to dryness under reduced pressure, methanol (300 $cm^3$) was added and the slurry was filtered and washed with cold methanol (2 x 20 $cm^3$). Recrystallization from chloroform, followed by drying at 100°C overnight gave (Ib) (97 g, 0.35 mmol, 77%); m.p. 124.5–126°C (lit.,[55] 124–126°C); (Found: C, 69.5; H, 7.3; N, 10.4. Calc. for $C_{16}H_{20}N_2O_2$: C, 70.6; H, 7.4; N, 10.3%; M 272.3); infrared $\nu_{max}$/ $cm^{-1}$ (nujol mull) 3300, 3200, 1612, 1590, 1516, 1405, 1337, 1297, 1250, 1219, 1193, 1160, 1010, 930, 854, 767, 744 and 615; (HCB mull) 3300, 3200, 3040w, 3020, 2965, 2938, 2912, 2870, 1612, 1590, 1515, 1465, 1405, 1337, 1297, 1250, 1219, 1193, 1058, 1010, 930, 744 and 615; $^{13}C$ NMR ($CDCl_3$, 20.12 MHz) $\delta$/ p.p.m. 42.1, 64.7, 110.9, 116.9, 124.7, 129.4 and 147.4.

4,7-Diaza-2,3:8,9-dibenzodecane-1,10-dione (Ic)

To a solution of (Ib) (14 g, 51.5 mmol) in dry diethyl ether (500 $cm^3$) was added active manganese dioxide (type B, 110 g).* The suspension was stirred vigorously under gentle reflux for 6.5 h. The manganese dioxide was filtered and extracted with boiling dichloromethane (6 x 300 $cm^3$) until the filtrate was colourless. The combined filtrates were concentrated under reduced pressure leaving a yellow solid. This was filtered, washed with small amounts of cold methanol and dried at 120°C overnight to give (Ic) (7.10 g, 26.5 mmol, 51%); m.p. 176-178°C (lit.,[55] 177-179°C); infrared $\nu_{max}$ / $cm^{-1}$ (nujol mull) 3340, 2750, 1660, 1610, 1572, 1523, 1430, 1398, 1341, 1299, 1224, 1190, 1175, 1153, 1124, 1064, 1039, 1105, 871, 814 and 737; (HCB mull) 3340, 2830, 2750, 1660, 1523, 1429, 1397, 1341, 1299, 1223, 1153, 1123, 1064, 1039, 1005, 870, 813 and 737; $^1H$ NMR ($CDCl_3$, 60 MHz) $\delta$/ p.p.m. 3.65 (4 H, b, $CH_2$), 6.5-7.9 (8 H, c, aryl-H), 8.6 (2 H, b, disappears with $D_2O$, NH) and 10.0 (2 H, s, CHO); $^{13}C$ NMR ($CDCl_3$, 20.12 MHz) $\delta$/ p.p.m. 41.6, 110.7, 115.5, 118.9, 135.9, 136.9 and 150.5.

7,8,15,16,17,18-Hexahydrodibenzo[e,m][1,4,8,11] - tetraazacyclotetradecine

$P^{14}$

A solution of 1,2-diaminoethane (0.5 g, 5.9 mmol) in dry methanol (100 $cm^3$) was added to a solution of 4,7-diaza-2,3:8,9-dibenzodecane-1,10-dione (Ic) (2.0 g, 7.45 mmol) in dry methanol (500 $cm^3$) at reflux under nitrogen. The reaction mixture was heated

* Prepared by heating manganese carbonate at 300°C for 48 h, leaving overnight in nitric acid (15% aq.), filtering and washing with water until acid free, then drying at 300°C for 48 h.[147]

under reflux for 6 h, then the hot solution was filtered to remove a small amount of solid material (20 mg) of m.p. 275-278°C. Cooling to 0°C overnight gave crystals which were filtered at the pump and washed with cold methanol (3 x 10 $cm^3$). After drying in air, vacuum drying at 135°C gave $P^{14}$ (1.50 g, 5.1 mmol, 87%); m.p. 176-177°C (lit.,[55] 175-177°C); (Found: C, 74.0; H, 7.0; N, 19.2. Calc. for $C_{18}H_{20}N_4$: C, 73.9; H, 6.9; N, 19.2%; M 292.4); infrared $\nu_{max}$/ $cm^{-1}$ (nujol mull) 1634s, 1606s, 1570w, 1510, 1446(sh), 1335, 1329, 1222w, 1203, 1166, 1155, 1141, 1053, 1044, 1033, 917, 754(sh) and 744s; (HCB mull) 3050w, 3020w, 2945-2850, 1635s, 1609s, 1510, 1446s, 1373, 1336, 1330, 1223w, 1203, 1142, 1053, 1044, 1034, 917, 755(sh) and 745s; $^1H$ NMR ($CDCl_3$, 60 MHz) $\delta$/ p.p.m. 3.57 (4 H, t, collapses to s with $D_2O$, $CH_2NH$), 3.85 (4 H, s, $CH_2N{=}CH$) 6.57-7.42 (8 H, o, aryl-H), 8.52 (2 H, s, CH=N), and 10.26 (2 H, b, disappears with $D_2O$, NH); $^{13}C$ NMR ($CDCl_3$, 20.12 MHz) $\delta$/ p.p.m. 41.9, 61.0, 111.1, 115.0, 118.6, 131.2, 133.7, 149.8 and 163.4.

**5,6,7,8,9,10,15,16,17,18-Decahydrodibenzo[e,m][1,4,8,11] - tetraazacyclotetradecine**

$L^{14}$

To a stirred suspension of lithium tetrahydridoaluminate (2.0 g) in dry diethyl ether (400 $cm^3$) under nitrogen was added $P^{14}$ (1.0 g, 3.4 mmol). After the disappearance of an initial yellow colouration and subsidence of effervescence, the mixture was stirred at reflux for 4 h. After cooling to room temperature, water (2 $cm^3$) was added, cautiously at first, then sodium hydroxide (15% aq., 2 $cm^3$) and water (6 $cm^3$). Stirring at reflux was resumed for a further 0.5 h, followed by filtration at the pump. The solid was washed with boiling dichloromethane (4 x 25 $cm^3$) and the combined filtrate dried with

anhydrous magnesium sulphate overnight. Filtration of the drying agent was followed by removal of the solvent under reduced pressure. Cold methanol (25 $cm^3$) was added and the resulting suspension filtered and washed with cold methanol (10 $cm^3$). Drying at 100°C gave $L^{14}$ (0.55 g, 1.9 mmol, 56%); m.p. 117-118°C (lit.,[60] 118.5-119.5°C); (Found: C, 73.0; H, 8.2; N, 18.8. Calc. for $C_{18}H_{24}N_4$ (M 296.4): C, 72.9; H, 8.2; N, 18.9%; M 296.4); infrared $\nu_{max}$/ $cm^{-1}$ (KBr), 3319s, 3258s, 3186, 3127, 3039, 2887, 2868, 2824s, 1606s, 1584, 1511s, 1449s, 1333, 1322, 1307, 1261, 1221s, 1146s, 1040, 1002, 965, 936, 847, 757s, 746s and 731s; $^1H$ NMR ($CDCl_3$, 250 MHz) $\delta$/ p.p.m. 1.2, (2 H, b, disappears with $D_2O$, $CH_2NHCH_2$), 2.71 (4 H, s, $ArCH_2NHCH_2$), 3.44 (4 H, s, $ArNHCH_2$), 3.81 (4 H, s, $ArCH_2$) and 6.59-7.20 (10 H, 8 H with $D_2O$, c, ArNH and aryl-H); $^{13}C$ NMR ($CDCl_3$, 62.896 MHz) $\delta$/ p.p.m. 42.17, 48.85, 53.64, 110.69, 116.32, 124.16, 128.53, 129.58 and 148.40.

{(5,6,7,8,9,10,15,16,17,18-Decahydrodibenzo[e,m][1,4,8,11] - tetraazacyclotetradecine-$N^6$,$N^9$,$N^{15}$,$N^{18}$)nickel(II)} tetrafluoroborate

$[NiL^{14}](BF_4)_2$

A solution of $L^{14}$ (0.11 g, 0.37 mmol) in chloroform (15 $cm^3$) was added to a solution of hexaaquonickel(II) tetrafluoroborate (0.85 g, 3.17 mmol) in methanol (15 $cm^3$) and left at room temperature. Orange-red crystals appeared within 24 h. The crystals were filtered, washed with cold methanol (6 $cm^3$) and dried under vacuum at room temperature to give $[NiL^{14}](BF_4)_2$ (0.049 g, 0.092 mmol, 25 %); (Found: C, 40.6; H, 4.5; N, 10.2. $C_{18}H_{24}N_4B_2F_4Ni$ requires C, 40.8; H, 4.6; N, 10.6%; M 530.5); electronic spectrum (dichloromethane) $\lambda_{max}$/ nm ($\epsilon$/ $m^2$ $mol^{-1}$) 457(80); infrared $\nu_{max}$/ $cm^{-1}$ (KBr), 3214s, 3174s, 2952w, 2882w, 1610, 1589w, 1497s, 1448, 1313w, 1285, 1224, 1187, 1084vs, 1053vs, 1038vs, 1006vs, 772s and 520.

{(5,6,7,8,9,10,15,16,17,18-Decahydrodibenzo[e,m][1,4,8,11] - tetraazacyclotetradecine-$N^6,N^9,N^{15},N^{18}$)bis(isothiocyanato) - nickel(II)}

$[NiL^{14}(NCS)_2]$

A solution of hexaquonickel(II) perchlorate (0.33 g, 0.90 mmol) in methanol (40 $cm^3$) was added to a solution of $L^{14}$ (0.20 g, 0.70 mmol) in methanol (40 $cm^3$) giving a deep blue solution. To this was added potassium thiocyanate (0.2 g, 2.0 mmol) in methanol (20 $cm^3$) giving a green solution. Nitrogen was bubbled through this solution for 1 h. Filtration at the pump, washing with water (3 x 5 $cm^3$) and drying in a vacuum oven at 110°C gave pink crystals of $[NiL^{14}(NCS)_2]$ (0.13 g, 0.3 mmol, 43%); (Found: C, 48.7; H, 4.9; N, 16.7. Calc. for $C_{20}H_{24}N_6NiS_2$: C, 51.0; H, 5.1; N, 17.8%; M 471.3); electronic spectrum (acetonitrile) $\lambda_{max}$/ nm ($\epsilon$/ $m^2$ $mol^{-1}$) 381, 427(3.0), 510(3.1), 700(1.5), 805(1.7) and 920(1.9); infrared (KBr) $\nu_{max}$/ $cm^{-1}$ 3272, 3241s, 3053w, 2927, 2868s, 2074vs, 1604, 1578w, 1491s, 1467, 1456, 1434, 1215s, 1118, 1089, 1044, 976, 966s, 947s, 926, 887, 816, 779s, 765s and 627; $\mu_{eff.}$ = 2.91 B.M. at 21°C.

{(5,6,7,8,9,10,15,16,17,18-Decahydrodibenzo[e,m][1,4,8,11] - tetraazacyclotetradecine-$N^6,N^9,N^{15},N^{18}$)dichloronickel(II)}

$[NiL^{14}Cl_2]$

The ligand, $L^{14}$ (0.40 g, 1.35 mmol) was warmed to effect solution in methanol (25 $cm^3$) and added to a solution of hexaquonickel(II) chloride (0.50 g, 2.10 mmol) in methanol (25 $cm^3$). The solution became purple and purple crystals precipitated in five minutes. The mixture was left at room temperature overnight, then the crystals were filtered, washed with cold methanol (5 $cm^3$) and dried in a vacuum oven at 110°C giving $[NiL^{14}Cl_2]$ (0.43 g, 0.93 mmol, 69%); (Found: C, 49.6;

H, 5.6; N, 12.6. Calc. for $C_{18}H_{24}N_4Cl_2Ni$: C, 50.7; H, 5.7; N, 13.8%; M 426.0); electronic spectrum (dichloromethane) $\lambda_{max}$/ nm ($\epsilon$/ $m^2$ $mol^{-1}$) 336(13), 532(4.5), 683(2.5) and 1090(1.1); infrared (KBr) $\nu_{max}$/ $cm^{-1}$ 3247s, 3200s, 3058, 3035, 2945, 2926, 2869, 1604, 1580, 1492s, 1454, 1432, 1273, 1220, 1184, 1092, 1052, 987s, 945s, 922s, 886s, 852, 819s, 776s, 753s and 737; electron impact mass spectrum at 350°C m/z 354(13%), 352(48), 350(82), 348(100), 346(46), 344(3), 176(15), 175(19), 118(15) and 91(16); $\mu_{eff.}$ = 3.30 B.M. at 21°C.

8,9,16,17,18,19-Hexahydro-7H-dibenzo[e,n][1,4,8,12] - tetraazacyclopentadecine

$P^{15}$

A mixture of 1,3-diaminopropane (0.6 g, 13.0 mmol) and 4,7-diaza-2,3:8,9-dibenzodecane-1,10-dione (Ic) (1.8 g, 6.7 mmol) in dry methanol (100 $cm^3$) and dry dichloromethane (20 $cm^3$) was heated at reflux under nitrogen for 3 h. The solid product was visible in the solution after 1.5 h. The mixture was cooled in ice to 0-5°C, filtered at the pump and the solid washed with cold methanol (3 x 5 $cm^3$). Drying overnight over desiccant silica-gel, followed by 5 h at 120°C gave white needles of $P^{15}$ (1.7 g, 5.5 mmol, 82%); melting range 187-188°C (lit.,[55] 187-188°C); (Found: C, 72.3; H, 7.2; N, 17.1. Calc. for $C_{19}H_{22}N_4$: C, 74.5; H, 7.2; N, 18.3%; M 306.4); infrared $\nu_{max}$/ $cm^{-1}$, (nujol mull) 3210w, 3080w, 1629, 1596, 1576, 1520, 1352, 1339, 1322, 1206, 1166, 1160, 1137, 1110, 1066, 1045, 933, 922, 875, 833, 751s, 743s, 697 and 636; (HCB mull) 3210w, 3080w, 3020w, 2925, 2905, 2880, 2840, 2820, 1629s, 1596s, 1522, 1459s, 1446, 1379, 1352, 1340, 1322, 1206, 1186, 1137, 1110, 1066, 1044, 922, 875, 833, 809, 751s, 744s, 699 and 637; $^1H$ NMR ($CDCl_3$, 60 MHz) $\delta$/ p.p.m.

2.01 (2 H, o, $CH_2CH_2CH_2$), 3.52 (4 H, t, collapses to s with $D_2O$, $CH_2NH$), 3.76 (4 H, t, $CH_2N{=}CH$), 6.4-7.3 (8 H, o, aryl-H), 8.25 (2 H, s, CH=N) and 9.6 (2 H, b, disappears with $D_2O$, NH); $^{13}C$ NMR ($CDCl_3$, 20.12 MHz) $\delta$/ p.p.m. 33.5, 40.4, 62.9, 110.1, 114.7, 117.9, 131.1, 134.0, 148.9 and 164.0.

**6,7,8,9,10,11,16,17,18,19-Decahydro-5H-dibenzo[e,n][1,4,8,12] - tetraazacyclopentadecine**

$L^{15}$

To a stirred suspension of lithium tetrahydridoaluminate (6.0 g) in dry diethyl ether (400 $cm^3$) under nitrogen was added $P^{15}$ (2.00 g, 6.40 mmol). After the disappearance of an initial yellow colouration and subsidence of effervescence, the mixture was stirred at reflux for 4 h. After cooling to room temperature, water (6 $cm^3$) was added, cautiously at first, then sodium hydroxide (15% aq., 6 $cm^3$) and water (18 $cm^3$). Stirring at reflux was resumed for a further 0.5 h, followed by filtration at the pump. The solid was washed with boiling dichloromethane (4 x 50 $cm^3$) and the combined filtrate dried with anhydrous magnesium sulphate for 3 h. Filtration of the drying agent was followed by removal of the solvent under reduced pressure. Cold methanol (40 $cm^3$) was added and the resulting suspension filtered and washed with cold methanol (20 $cm^3$). Recrystallisation from methanol/water (70:30 v/v, 100 $cm^3$) and vacuum drying over phosphorus pentoxide for 4 h gave fine needles of $L^{15}$ (1.74 g, 5.60 mmol, 87%); m.p. 119-120°C (lit.,[60] 122.5-123.5°C); (Found: C, 73.1; H, 8.4; N, 18.5. Calc. for $C_{19}H_{26}N_4$: C, 73.5; H, 8.4; N, 18.0%; M 310.4); infrared (KBr) $\nu_{max}$/ $cm^{-1}$, 3312, 3292s, 3266, 3197b, 3040, 3017, 2902, 2851, 2819s, 2806s, 2740w, 1607s, 1585s, 1504s, 1485, 1459s, 1321, 1302, 1264, 1222, 1145, 1121, 1040, 743s and 726s; $^1H$ NMR

($CDCl_3$, 250 MHz) $\delta$/ p.p.m. 1.17 (2 H, b, disappears with $D_2O$, $CH_2\underline{NH}CH_2$), 1.71 (2 H, q, $CH_2\underline{CH_2}CH_2$), 2.70 (4 H, t, $C\underline{H_2}CH_2\underline{CH_2}$), 3.45 (4 H, s, $NHC\underline{H_2}CH_2NH$), 3.75 (4 H, s, $ArC\underline{H_2}NH$), 5.97 (2 H, b, disappears with $D_2O$, ArNH) and 6.60-7.21 (8 H, o, aryl-H); $^{13}C$ NMR (DMSO-$d_6$, 20.12 MHz) $\delta$/ p.p.m. 28.6, 40.8, 47.3, 53.4, 109.3, 115.5, 123.6, 128.0, 129.6 and 147.4; $^{13}C$ NMR ($CDCl_3$, 62.896 MHz) 29.93, 41.68, 48.08, 54.25, 109.99, 116.46, 124.20, 128.52, 129.74 and 147.58; $^{15}N$ NMR {$CDCl_3/CH_3NO_2$ 1:1, [Cr(pd)$_3$] (0.033 mol dm$^{-3}$), 25.346 MHz}$\delta$/ p.p.m. 38.03 and 60.42 ($^1J_{NH}$ = 84 Hz); electron impact mass spectrum m/z 311(23%), 310($M^+$, 63), 252(8), 236(23), 204(11), 192(9), 190(38), 180(12), 161(22) 147(61), 133(28), 132(25), 130(27), 120(60), 118(100), 106(53), 91(51), 84(20), 73(9), 65(20) and 58(9).

{(6,7,8,9,10,11,16,17,18,19-Decahydro-5H-dibenzo[e,n] - [1,4,8,12]tetraazacyclopentadecine-$N^6$,$N^{10}$,$N^{16}$,$N^{19}$)dichloro - nickel(II)}

$[NiL^{15}Cl_2]$

The ligand, $L^{15}$ (0.40 g, 1.29 mmol) was warmed to effect solution in methanol (40 cm$^3$) and added to a solution of hexaaquonickel(II) chloride (0.50 g, 2.10 mmol) in methanol (10 cm$^3$) and left at room temperature overnight. The blue crystals were filtered, washed with cold methanol (5 cm$^3$) and dried at 110°C for 8 h giving $[NiL^{15}Cl_2]$ (0.45 g, 0.95 mmol, 74%); (Found: C, 51.5; H, 5.9; N, 12.0. Calc. for $C_{19}H_{26}N_4Cl_2Ni$: C, 51.9; H, 6.0; N, 12.7%; M 440.0); electronic spectrum (dichloromethane) $\lambda_{max}$/ nm ($\epsilon$/ m$^2$ mol$^{-1}$) 375(9), 520(0.6), 585(1.1), 800(0.5), 855(0.4) and 1140(0.4); infrared (KBr) $\nu_{max}$/ cm$^{-1}$ 3314s, 3082w, 3041w, 2968, 2932, 2866s, 1606, 1587, 1496s, 1468, 1458, 1436, 1297w, 1276w, 1240w, 1220s, 1192w, 1119w, 1083s, 1004, 951s, 900, 876s, 848, 822s, 779s, 750s and 730; electron impact

mass spectrum at 350°C m/z 368(2%), 366(6), 364(5), 362(15), 360(22), 358(1), 310(2), 232(1), 147(6), 118(14), 106(10) and 91(13); $\mu_{eff.}$ = 3.19 B.M. at 21°C.

{(6,7,8,9,10,11,16,17,18,19-Decahydro-5H-dibenzo[e,n][1,4,8,12] tetraazacyclopentadecine-$N^6$,$N^{10}$,$N^{16}$,$N^{19}$)bis(isothiocyanato) - nickel(II)}

$[NiL^{15}(NCS)_2]$

A solution of hexaaquonickel(II) tetrafluoroborate (0.074 g, 0.275 mmol) in methanol (2 $cm^3$) was added to a solution of $L^{15}$ (0.053 g, 0.171 mmol) in methanol (15 $cm^3$). After 0.25 h a solution of potassium thiocyanate (0.15 g, 1.54 mmol) in methanol (2 $cm^3$) was added and the mixture was allowed to stand for 48 h. The resultant violet crystals were filtered at the pump, mixed with water (2 $cm^3$), filtered and washed with water (3 x 3 $cm^3$) and diethyl ether (1 $cm^3$) and dried at 110°C for 2 h to give $[NiL^{15}(NCS)_2]$ (0.054 g, 0.111 mol, 65%); (Found: C, 51.7; H, 5.5; N, 17.3. Calc. for $C_{21}H_{26}N_6NiS_2$: C, 52.0; H, 5.4; N, 17.3%; M 485.3); electronic spectrum (acetonitrile) $\lambda_{max}$/ nm ($\epsilon$/ $m^2$ $mol^{-1}$) 380(8.2), 545(1.6), 760(1.2) and 920(1.3); infrared (KBr) $\nu_{max}$/ $cm^{-1}$ 3258sh, 3241s, 3060, 2929, 2866s, 2073vs, 1606, 1586w, 1496s, 1435, 1270w, 1239w, 1219s, 1189, 1134w, 1118, 1083, 1032w, 993, 966s, 945, 938, 882, 824, 780s, 761s and 734.

7,8,9,10,17,18,19,20-Octahydrodibenzo[e,o][1,4,8,13] - tetraazacyclohexadecine

$P^{16}$

A mixture of 1,4-diaminobutane (2.50 g, 28.4 mmol) and 4,7-diaza-2,3:8,9-dibenzodecane-1,10-dione (Ic) (6.50 g, 24.2 mmol) in

dry methanol (250 $cm^3$) and dry dichloromethane (100 $cm^3$) was heated at reflux under nitrogen for 5 h. Solid product was visible in the solution after 3 h. The mixture was cooled in ice to 0-5°C, filtered at the pump and washed with cold methanol (3 x 10 $cm^3$). Drying at 120°C for 5 h gave whitish needles of $P^{16}$ (4.60 g, 14.3 mmol, 59%); m.p. 149-150°C (lit.,[55] 149-151°C); (Found: C, 75.6; H, 7.5; N, 16.2. Calc. for $C_{20}H_{24}N_4$: C, 75.0; H, 7.5; N, 17.5%; M 320.4); infrared $\nu_{max}$/ $cm^{-1}$ (nujol mull) 3210w, 3160w, 3070w, 1632s, 1605, 1590, 1523, 1337, 1282, 1207, 1195, 1159, 1083, 998, 970, 742s, 731 and 637; (HCB mull) 3210w, 3160w, 3080w, 3030w, 2925, 2912, 2850, 2830, 1633s, 1591s, 1523s, 1464, 1457, 1441, 1337, 1282w, 1207, 1195, 1083w, 998, 743s, 731 and 637; $^1H$ NMR ($CDCl_3$, 60 MHz) $\delta$/ p.p.m. 1.75 (4 H, c, $CH_2CH_2CH_2CH_2$), 3.51 (8 H, c, sharpens with $D_2O$, $NHCH_2$), 6.45-7.34 (8 H, c, aryl-H), 8.28 (2 H, s, CH=N) and 9.43 (2 H, b, disappears after 1 h with $D_2O$, NH); $^{13}C$ NMR ($CDCl_3$, 20.12 MHz) $\delta$/ p.p.m. 27.5, 41.2, 60.6, 109.7, 114.5, 117.7, 131.1, 134.0, 148.9 and 164.2.

5,6,7,8,9,10,11,12,17,18,19,20-Dodecahydrodibenzo[e,o] - [1,4,8,13]tetraazacyclohexadecine

$L^{16}$

To a stirred suspension of lithium tetrahydridoaluminate (5.0 g) in dry diethyl ether (200 $cm^3$) under nitrogen was added $P^{16}$ (4.0 g, 12.3 mmol). After the disappearance of an initial yellow colouration and subsidence of effervescence, the mixture was stirred at reflux for 4 h. After cooling to room temperature, water (4 $cm^3$) was added, cautiously at first, then sodium hydroxide (15% aq., 4 $cm^3$) and water (12 $cm^3$). Stirring at reflux was resumed for a further 0.5 h, followed by filtration at the pump. The solid was washed with boiling

dichloromethane (4 x 25 $cm^3$) and the combined filtrate dried with anhydrous magnesium sulphate overnight. Filtration of the drying agent was followed by removal of the solvent under reduced pressure to leave a colourless oil which solidified overnight. Cold methanol (25 $cm^3$) was added and the resulting suspension filtered and washed with cold methanol (10 $cm^3$). Drying at 100°C gave $L^{16}$ (2.7 g, 8.3 mmol, 68%) which was recrystallized from methanol/water (100:10 v/v, 110 $cm^3$) and dried over phosphorus pentoxide in vacuo for 4 h (62% recovery); m.p. 117-118°C; (Found: C, 73.3; H, 8.4; N, 17.6; M 324. $C_{20}H_{28}N_4$ requires C, 74.0; H, 8.7; N, 17.3%; M 324.5); electronic spectrum (acetonitrile) $\lambda_{max}$/ nm ( $\epsilon$ / $m^2$ $mol^{-1}$) 256(3065) and 298(675); infrared (KBr) $\nu_{max}$/ $cm^{-1}$ 3320, 3243b, 3171, 3040, 2940, 2923, 2868, 2818s, 1606s, 1588, 1522s, 1463s, 1441(sh), 1331s, 1311, 1283, 1159, 1147, 1116, 1047w, 931w, 807, 749s and 719; $^1H$ NMR ($CDCl_3$, 250MHz) $\delta$/ p.p.m. 1.2 (2 H, b, disappears with $D_2O$, $CH_2NHCH_2$), 1.56 (4 H, q, $CH_2CH_2CH_2CH_2$), 2.63 (4 H, t, $CH_2CH_2CH_2CH_2$), 3.44 (4 H, s, $NHCH_2CH_2NH$), 3.77 (4 H, s, $ArCH_2NH$) and 6.58-7.19 (10 H, 8 H with $D_2O$, o, ArNH and aryl-H); $^{13}C$ NMR ($CDCl_3$, 62.896 MHz) $\delta$/ p.p.m. 27.40, 42.94, 47.81, 53.52, 110.02, 115.96, 123.86, 128.36, 129.65 and 148.36; electron impact mass spectrum m/z 324($M^+$, 17%), 187(13), 147(11), 133(15), 132(16), 120(69), 118(100), 106(45) and 91(72).

{(5,6,7,8,9,10,11,12,17,18,19,20-Dodecahydrodibenzo[e,o] - [1,4,8,13]tetraazacyclohexadecine-$N^6$,$N^{11}$,$N^{17}$,$N^{20}$)dichloro - nickel(II)}

$[NiL^{16}Cl_2]$

The ligand $L^{16}$ (0.40 g, 1.23 mmol) was warmed to effect solution in methanol (40 $cm^3$) and added to a solution of hexaaquonickel(II)

chloride (0.50 g, 2.10 mmol) in methanol (25 $cm^3$) and allowed to stand at room temperature overnight. Filtration at the pump, washing with cold methanol (5 $cm^3$) and drying at 100°C for 6 h gave turquoise crystals of $[NiL^{16}Cl_2]$ (0.45 g, 0.92 mmol, 75%); (Found: C, 52.6; H 6.2; N 12.1. $C_{20}H_{28}N_4Cl_2Ni$ requires C 52.9; H 6.2; N 12.3%; M 454.1); electronic spectrum (dichloromethane) $\lambda_{max}$/ nm ($\epsilon$ / $m^2$ $mol^{-1}$) 393(4.5), 635(2.3), 695(sh), 820(1.5), 910(1.7) and 1160(0.9); infrared (KBr) $\nu_{max}$/ $cm^{-1}$ 3274, 3245, 3233, 3196, 3042, 2923, 2871, 1608, 1590, 1498s, 1481, 1455, 1441, 1354w, 1299w, 1242, 1219s, 1192, 1119w, 1073, 1056, 1039, 1015, 968s, 935, 926, 901, 884, 854, 816, 808, 774s, 769s, 752 and 738; electron impact mass spectrum at 350°C m/z 382(6%), 380(19), 378(23), 376(56), 374(32), 324(10), 318(2), 120(60), 118(72), 106(63),91(57), 70(35) and 31(100); $\mu_{eff.}$ = 3.15 B.M. at 21°C.

{(5,6,7,8,9,10,11,12,17,18,19,20-Dodecahydrodibenzo[e,o][1,4,8,13] - tetraazacyclohexadecine-$N^6$,$N^{11}$,$N^{17}$,$N^{20}$)bis(isothiocyanato)nickel(II)}

$[NiL^{16}(NCS)_2]$

Addition of a warm solution of $L^{16}$ (0.10 g, 0.31 mmol) in methanol (40 $cm^3$) to a solution of hexaaquonickel(II) tetrafluoroborate (0.15 g, 0.56 mmol) in methanol (10 $cm^3$) produced a turquoise solution which faded to green after a few minutes. After the addition of a solution of potassium thiocyanate (0.30 g, 3.01 mmol) in methanol (10 $cm^3$) the mixture was allowed to stand for four days. The mixture of grey-green crystals and white powder was filtered and the latter removed by dissolution in boiling methanol and decantation (6 x 5 $cm^3$). The insoluble grey-green crystals were filtered and dried in air to give $[NiL^{16}(NCS)_2]$ (0.082 g, 0.16 mmol, 52%); (Found: C, 53.1; H, 5.7; N 16.9. $C_{22}H_{28}N_6NiS_2$ requires C, 52.9; H, 5.7;

N, 16.8%; M 499.3); electronic spectrum (acetonitrile) $\lambda_{max}$/ nm ($\epsilon$/ $m^2$ $mol^{-1}$) 350(22.8), 565(5.8), 800(4.5) and 910(1.0); infrared $\nu_{max}$/ $cm^{-1}$ (KBr) 3281w, 3247, 3059w, 3026w, 2926, 2876, 2080vs, 1605, 1590, 1497s, 1457, 1441, 1426, 1244, 1219s, 1194, 1119, 1075, 1036s, 969, 945, 915, 892, 862, 802, 778s, 760s and 735; $\mu_{eff.}$ = 3.25 B.M. at 21°C.

**The reaction of $L^{16}$ with hexaaquonickel(II) nitrate.**

**{Aqua(5,6,7,8,9,10,11,12,17,18,19,20-dodecahydrodibenzo[e,o] - [1,4,8,13]tetraazacyclohexadecine-$N^6$,$N^{11}$,$N^{17}$,$N^{20}$)nitratonickel(II)} - nitrate and {(5,6,7,8,9,10,11,12,17,18,19,20-Dodecahydrodibenzo[e,o] - [1,4,8,13]tetraazacyclohexadecine-$N^6$,$N^{11}$,$N^{17}$,$N^{20}$)dinitratonickel(II)}**

**$[NiL^{16}(NO_3)(H_2O)]NO_3$ and $[NiL^{16}(NO_3)_2]$**

A mixture of hexaaquonickel(II) nitrate (0.083 g, 0.28 mmol) and $L^{16}$ (0.083 g, 0.26 mmol) in methanol (50 $cm^3$) and chloroform (20 $cm^3$) was heated at reflux under nitrogen for 1 h. Evaporation of the deep green solution under reduced pressure followed by addition of acetone (5 $cm^3$) to the residue gave a dark green powder which was filtered, washed with a few drops of cold acetone and dried in air to give the dark-green complex (0.070 g); (Found: C, 46.54; H, 5.48; N, 16.07. $C_{20}H_{28}N_6O_6Ni$ requires C, 47.36; H, 5.56; N, 16.57%; M 507.2. $C_{40}H_{56}N_{12}O_{12}Ni.H_2O$ requires C, 46.53; H, 5.66; N, 16.28%; M 1032.3; electronic spectrum (acetonitrile) $\lambda_{max}$/ nm 466, 548, 573, 664, 696, 790 and 813; infrared $\nu_{max}$/ $cm^{-1}$ (KBr) 3340b, 3278, 3232s, 3050, 2937, 2873, 1703w, 1608, 1592, 1500s, 1433s, 1420s, 1385vs, 1296s, 1223s, 1038s, 982, 947, 908, 825, 791 and 758s.

Bis{(5,6,7,8,9,10,11,12,17,18,19,20-dodecahydrodibenzo[e,o] - [1,4,8,13]tetraazacyclohexadecine-$N^6$,$N^{11}$,$N^{17}$,$N^{20}$)bromocadmium(II)} - tetrabromocadmate(II)

$[CdL^{16}Br]_2[CdBr_4]$

(1) To a warm solution of $L^{16}$ (0.056 g, 0.17 mmol) in acetonitrile (7 $cm^3$) was added a solution of cadmium(II) bromide tetrahydrate (0.110 g, 0.32 mmol) in methanol (5 $cm^3$). The turbid solution was filtered and, after two days at room temperature, the white crystalline product was filtered and washed with a small amount of cold methanol. After removal of a few crystals for X-ray diffraction study, the remainder was dried over phosphorus pentoxide in vacuo to give $[CdL^{16}Br]_2[CdBr_4]$ (0.042 g, 0.028 mmol, 34%); (Found: C, 33.3; H, 3.9; N, 8.2. $C_{40}H_{56}N_8Br_6Cd_3$ requires C, 32.8; H, 3.9; N, 7.7%; M 1465.6); infrared (KBr) $\nu_{max}$/ $cm^{-1}$ 3513b, 3470b, 3298, 3268, 3234, 3200, 3186, 3046, 2927, 2870, 1608s, 1587s, 1498s, 1460s, 1427, 1301, 1242s, 1219s, 1188, 1127, 1087, 1045s, 995, 943s, 927s, 896, 862, 763s, 733 and 710.

(2) The experiment was repeated using an equimolar mixture of $CdBr_2.4H_2O$ (0.053 g, 0.154 mmol) in acetonitrile (7 $cm^3$) and $L^{16}$ (0.050 g, 0.154 mmol) in methanol (5 $cm^3$) to give a white crystalline product (0.032 g, 0.022 mmol, 22%); (Found: C, 34.2; H, 4.06; N, 8.5%); infrared spectrum as in (1) above.

(5,6,7,8,9,10,11,12,17,18,19,20-Dodecahydrodibenzo[e,o][1,4,8,13] - tetraazacyclohexadecine)cadmium(II) iodide complex

$CdL^{16}I_2$

To a refluxing solution of cadmium(II) iodide (0.37 g, 1.0 mmol) in dichloromethane (40 $cm^3$) and methanol (20 $cm^3$) under nitrogen was

added $L^{16}$ (0.32 g, 1.0 mmol) in dichloromethane (5 $cm^3$). The turbid solution was heated at reflux for 0.5 h and, after cooling, evaporated to 5 $cm^3$ under reduced pressure. The white powder was filtered at the pump, washed with methanol (3 x 5 $cm^3$) and recrystallized from acetonitrile to give white microcrystals of $CdL^{16}I_2$ (0.56 g, 0.81 mmol, 81%); (Found: C, 34.8; H, 4.1; N, 8.1. $C_{20}H_{28}N_4CdI_2$ requires C, 34.8; H, 4.1; N, 8.1%; M 690.7); infrared $\nu_{max}$/ $cm^{-1}$ (KBr) 3232, 3196, 3044w, 2943w, 2915w, 2866, 1606, 1585, 1497s, 1481, 1456, 1430, 1242, 1226w, 1141w, 1129w, 1080, 1047, 1020, 995w, 962w, 938, 881, 835w, 802, 764s, 755s and 712.

(5,6,7,8,9,10,11,12,17,18,19,20-Dodecahydrodibenzo[e,o] - [1,4,8,13]tetraazacyclohexadecine)zinc(II) bromide complex

$ZnL^{16}Br_2$

A mixture of zinc(II) bromide (0.15 g, 0.67 mmol) and $L^{16}$ (0.11 g, 0.34 mmol) in acetonitrile (40 $cm^3$) was heated at reflux under nitrogen for 0.5 h and the resulting white powder was filtered at the pump, washed with acetonitrile (2 x 0.5 $cm^3$) and dried over silica-gel for 18 h to give $ZnL^{16}Br_2$ (0.13 g, 0.24 mmol, 70%); (Found: C, 43.1; H, 5.1; N, 9.9. $C_{20}H_{28}N_4Br_2Zn$ requires C, 43.7; H, 5.1; N, 10.2%; M 549.6); infrared $\nu_{max}$/ $cm^{-1}$ (KBr) 3225s, 3172s, 2955, 2917, 2870s, 1609, 1590, 1500s, 1462s, 1449s, 1421w, 1297w, 1265w, 1243, 1139, 1079, 1031s, 973, 954, 936, 926, 897, 885, 844, 818, 752s and 723s.

(5,6,7,8,9,10,11,12,17,18,19,20-Dodecahydrodibenzo[e,o][1,4,8,13] - tetraazacyclohexadecine)zinc(II) iodide complex

$ZnL^{16}I_2$

To a solution of zinc(II) iodide (0.319 g, 1.00 mmol) at reflux in dichloromethane (40 $cm^3$) and methanol (20 $cm^3$) under nitrogen was

added a solution of $L^{16}$ (0.324 g, 1.00 mmol) in dichloromethane (5 $cm^3$). Heating at reflux was continued for 1 h. The cold solution was evaporated to 5 $cm^3$ and the white solid was filtered, washed with methanol (3 x 5 $cm^3$) and recrystallized from acetonitrile to give white needles of $ZnL^{16}I_2$ (0.55 g, 0.85 mmol, 85%); (Found: C, 37.4; H, 4.4; N, 8.7. $C_{20}H_{28}N_4I_2Zn$ requires C, 37.3; H, 4.4; N, 8.7%; M 643.7); infrared $\nu_{max}$/ $cm^{-1}$ (KBr) ; 3217s, 3193s, 3045w, 2947w, 2909w, 2867, 1610w, 1590, 1498s, 1486, 1460, 1420, 1297w, 1263w, 1241w, 1138, 1078, 1028s, 949s, 926, 818, 754s, 745s and 722.

8,9,10,11,18,19,20,21-Octahydro-7H-dibenzo[e,p][1,4,8,14] - tetraazacycloheptadecine

$P^{17}$

To a suspension of 4,7-diaza-2,3:8,9-dibenzodecane- 1,10-dione (Ic) (4.01 g, 12.0 mmol) in dry ethanol (250 $cm^3$) at reflux under nitrogen was added 1,5-diaminopentane (1.33 g, 13.0 mmol) Heating at reflux was continued for 4 h. The clear solution was cooled in ice and the cream coloured matted needles were filtered at the pump, washed with cold methanol (10 $cm^3$) and allowed to dry in air overnight giving $P^{17}$ (3.50 g, 10.5 mmol, 87%); m.p. 188-190°C (lit.,[60] 182.5-184.0°C); infrared $\nu_{max}$/ $cm^{-1}$ (nujol mull) 3240w, 1638, 1606, 1586, 1580(sh), 1519, 1465(sh), 1450, 1384, 1368(sh), 1337, 1325, 1234, 1210(sh), 1200, 1160, 1150, 1138, 1100, 1058, 1040, 972, 960, 933, 914, 744 and 732(sh); (HCB mull) 3240w, 2955, 2930, 2920, 2880, 2850, 2825, 1638, 1607, 1585, 1579, 1560(sh), 1526, 1520, 1470(sh), 1458, 1450(sh), 1435, 1386, 1370(sh), 1338, 1327, 1235, 1210, 1200, 1187, 1152, 1140, 1102, 1060, 1042, 812(sh) and 745; $^1H$ NMR ($CDCl_3$, 60 MHz) $\delta$/ p.p.m. 1.73 (6 H, o, $CH_2CH_2CH_2CH_2CH_2$), 3.54 (8 H, o, sharpens with $D_2O$, $NHCH_2$), 6.48-7.32 (8 H, o, aryl-H), 8.32 (2 H, s, CH=N) and 9.35 (2 H,

b, disappears slowly with $D_2O$, NH); $^{13}C$ NMR ($CDCl_3$, 20.12 MHz) $\delta$/ p.p.m. 24.2, 30.9, 42.1, 60.5, 109.7, 114.5, 117.7, 131.1, 133.9, 149.1 and 164.0.

**6,7,8,9,10,11,12,13,18,19,20,21-Dodecahydro-5H-dibenzo[e,p] - [1,4,8,12]tetraazacycloheptadecine**

$L^{17}$

The diimine $P^{17}$ (3 g, 8.97 mmol) was added over 1 h to a suspension of lithium tetrahydridoaluminate (6 g) in dry diethyl ether (500 $cm^3$) under nitrogen. After 0.5 h, the mixture was heated to reflux for 6 h, then water (6 $cm^3$) was added cautiously, followed by sodium hydroxide (15% aq., 6 $cm^3$) and water (18 $cm^3$). The mixture was again heated to reflux for 0.5 h until the solids were white. The mixture was filtered at the pump and the solids extracted with dichloromethane, using a soxhlet extractor for 3 h. The combined extracts were evaporated under reduced pressure to leave a colourless oil. Addition of methanol (15 $cm^3$) caused the oil to solidify. Filtration at the pump, followed by washing with ice cold methanol (2 x 5 $cm^3$) and drying at 70°C gave white crystals of $L^{17}$ (2.83 g, 8.36 mmol, 93%). Recrystallization from acetonitrile and drying over phosphorus pentoxide under vacuum gave $L^{17}$ (70% recovery); m.p. 93.5-94.5°C; (Found: C, 74.5; H, 9.0; N, 16.6; $M^+$ 338. $C_{21}H_{30}N_4$ requires C, 74.5; H, 8.9; N, 16.6%; M 338.5); electronic spectrum (acetonitrile) $\lambda_{max}$/ nm ( $\epsilon$ / $m^2$ $mol^{-1}$) 256(3275) and 298(790); infrared $\nu_{max}$/ $cm^{-1}$ (KBr) 3327, 3269s, 3228, 3040, 3018, 2954, 2934, 2903, 2840s, 2830(sh), 1606s, 1585s, 1512vs, 1476, 1462s, 1448s, 1326, 1316, 1304s, 1265, 1224, 1140s, 1103, 1050, 798, 748vs, 722s and 607; $^1H$ NMR (DMSO-$d_6$, 250 MHz) $\delta$/ p.p.m. 1.39 (4 H, b,$CH_2CH_2CH_2CH_2CH_2$), 1.51 (2 H, b, $CH_2CH_2CH_2CH_2CH_2$), 1.95 (2 H, b, $CH_2NHCH_2$), 2.56 (4 H, b,

$CH_2CH_2CH_2CH_2CH_2$), 3.32 (4 H, s, $NHCH_2CH_2NH$), 3.62 (4 H, s, $ArCH_2NH$), 6.53-7.09 (8 H, c, aryl-H) and 6.78 (2 H, b, $CNHCH_2$); $^1$H NMR ($CDCl_3$, 250 MHz) $\delta$/ p.p.m. 1.05 (2 H, b, disappears with $D_2O$, $CH_2NHCH_2$), 1.46 (4 H, c, $CH_2CH_2CH_2CH_2CH_2$), 1.60 (2 H, c, $CH_2CH_2CH_2CH_2CH_2$), 2.70 (4 H, t, $CH_2CH_2CH_2CH_2CH_2$), 3.46 (4 H, s, $NHCH_2CH_2NH$), 3.75 (4 H, s, $ArCH_2NH$) and 6.58-7.20 (10 H, 8 H with $D_2O$, c, ArNH and aryl-H); $^{13}$C NMR ($CDCl_3$, 62.896 MHz) $\delta$/ p.p.m. 24.15, 29.05, 43.47, 48.42, 53.59, 109.99, 116.06, 124.32, 128.0, 129.62 and 148.60; $^{15}$N NMR {$CDCl_3/CH_3NO_2$ 1:1, $[Cr(pd)_3]$ (0.033 mol $dm^{-3}$), 25.346 MHz}$\delta$/ p.p.m. 35.77 and 63.67 ($^1J_{NH}$ = 85 Hz); electron impact mass spectrum m/z 338($M^+$, 23%), 232(10), 218(29), 203(18), 189(22), 147(25), 132(31), 120(96), 118(100), 106(94) and 91(96).

{(6,7,8,9,10,11,12,13,18,19,20,21-Dodecahydro-5H-dibenzo[e,p] - [1,4,8,12]tetraazacycloheptadecine-$N^6$,$N^{12}$,$N^{18}$,$N^{21}$) - bis(isothiocyanato)nickel(II)}

$[NiL^{17}(NCS)_2]$

A solution of $L^{17}$ (0.031 g, 0.09 mmol) in dichloromethane (15 $cm^3$) was added to a solution of hexaaquonickel(II) tetrafluoroborate (0.035 g, 0.13 mmol) in methanol (15 $cm^3$), followed by potassium thiocyanate (0.10 g, 1.03 mmol) in methanol (20 $cm^3$). After twelve days at room temperature the mixture of large blue crystals and white powder was filtered at the pump and boiled with water (2 x 10 $cm^3$) to dissolve the white powder. The insoluble blue crystals were refiltered, washed with water (2 x 5 $cm^3$) and ether (5 $cm^3$) and dried in air to give $[NiL^{17}(NCS)_2]$ (0.045 g, 0.088 mmol, 92%); (Found: C, 53.3; H, 5.8; N, 16.2. $C_{23}H_{30}N_6NiS_2$ requires C, 53.8; H, 5.9; N, 16.4%; M 513.3); electronic spectrum (acetonitrile) $\lambda_{max}$/ nm ( $\epsilon$/ $m^2$ $mol^{-1}$) 370(sh), 592(1.4), 816(0.7) and 975(2.0); infrared (KBr) $\nu_{max}$/ $cm^{-1}$ 3327w,

3279, 3250, 3163b, 3044w, 2962, 2929, 2879, 2851, 2085vs, 1610w, 1591w, 1496, 1457s, 1258, 1221s, 1142, 993, 975, 857, 812, 757s and 737.

$L^{17}$ nickel(II) nitrate complex

A mixture of hexaaquonickel(II) nitrate (0.079 g, 0.27 mmol) and $L^{17}$ (0.084 g, 0.25 mmol) in methanol (60 $cm^3$) and chloroform (20 $cm^3$) was heated at reflux for 1 h. Evaporation of the deep green solution under reduced pressure followed by addition of acetone (5 $cm^3$) to the sticky residue gave a powder which was filtered, washed with a few drops of cold acetone and dried in air to give the grey-green complex (0.061 g); (Found: C, 47.11; H, 5.71; N, 15.15. $C_{21}H_{30}N_6O_6Ni$ requires C, 48.39; H, 5.80; N, 16.13%; M 521.2. $C_{21}H_{30}N_6O_6Ni.H_2O$ requires C, 46.77; H, 5.98; N, 15.59%; M 539.2); electronic spectrum (acetonitrile) $\lambda_{max}$/ nm 463, 543, 570, 694, 797, 817, 945; infrared $\nu_{max}$/ $cm^{-1}$ (KBr) 3406b, 3321, 3285, 3209, 3046, 2936-2882, 1707, 1609, 1592, 1501, 1470, 1420s, 1384s, 1298s, 1222, 1035, 991, 861, 821 and 760.

{(6,7,8,9,10,11,12,13,18,19,20,21-Dodecahydro-5H-dibenzo - [e,p][1,4,8,12]tetraazacycloheptadecine-$N^6$,$N^{12}$,$N^{18}$,$N^{21}$) - dichloronickel(II)}

$[NiL^{17}Cl_2]$

A mixture of hexaaquonickel(II) chloride (0.20 g, 0.80 mmol) and $L^{17}$ (0.20 g, 0.60 mmol) in dry methanol (20 $cm^3$) was heated at reflux for 0.5 h. The blue green flocculent precipitate was filtered, washed with cold methanol (3 x 5 $cm^3$) and dried at 100°C for 6 h to give $[NiL^{17}Cl_2]$ (0.13 g, 0.30 mmol, 50%); electronic spectrum (dichloromethane) $\lambda_{max}$/ nm ( $\epsilon$/ $m^2$ $mol^{-1}$) 393(sh), 642(5.1),

830(1.5), 902(3.0) and 1130(1.7); infrared (KBr) $\nu_{max}$/ $cm^{-1}$ 3298, 3283, 3246, 3140, 2940, 2858, 1608, 1591, 1499s, 1486, 1460, 1450, 1352, 1300, 1259, 1219s, 1195, 1145, 1092, 1068, 1034, 993s, 956, 940, 915, 885, 860s, 821, 812s, 776, 753s and 734; $\mu_{eff.}$ = 3.17 B.M. at 21°C.

{(6,7,8,9,10,11,12,13,18,19,20,21-Dodecahydro-5H-dibenzo[e,p] - [1,4,8,12]tetraazacycloheptadecine-$N^6$,$N^{12}$,$N^{18}$,$N^{21}$)dibromocadmium(II)}

$[CdL^{17}Br_2]$

To a warm solution of $L^{17}$ (0.020 g, 0.059 mmol) in acetonitrile (3 $cm^3$) was added a solution of cadmium(II) bromide tetrahydrate (0.020 g, 0.058 mmol) in methanol (1 $cm^3$). The mixture was allowed to stand at room temperature. After one day the colourless crystals were filtered, washed with methanol (2 x 1 $cm^3$) and acetone (0.5 $cm^3$). After removal of a few crystals for X-ray diffraction study,* the remainder was dried in a vacuum oven at 115°C to give $[CdL^{17}Br_2]$ (0.022 g, 0.036 mmol, 62%); (Found: C, 41.5; H, 4.9; N, 9.1. $C_{21}H_{30}N_4CdBr_2$ requires C, 41.3; H, 4.9; N, 9.2%; M 610.7); infrared (KBr) $\nu_{max}$/ $cm^{-1}$ 3253s, 3158s, 3078, 3042, 2924s, 2868s, 1605s, 1586s, 1499s, 1459s, 1437, 1357, 1302, 1245s, 1219s, 1080s, 1021, 1001, 962s, 939, 929, 897, 873, 852, 808s, 759s, 749s and 728.

* The infrared spectrum of the crystals removed for X-ray diffraction study was identical except for the appearance of a band at 2249 $cm^{-1}$.

(6,7,8,9,10,11,12,13,18,19,20,21-Dodecahydro-5H-dibenzo[e,p] - [1,4,8,12]tetraazacycloheptadecine)cadmium(II) iodide complex

$CdL^{17}I_2$

A mixture of cadmium(II) iodide (0.734 g, 2.00 mmol) and $L^{17}$ (0.677 g, 2.00 mmol) in dichloromethane (10 $cm^3$) and methanol (40 $cm^3$) was heated at reflux under nitrogen for 2 h. The white powder was filtered at the pump, washed with dichloromethane (5 $cm^3$) and methanol (5 $cm^3$) and dried over silica-gel for 14 h to give $CdL^{17}I_2$ (1.21 g, 1.71 mmol, 85%); (Found: C, 36.8; H, 4.4; N, 8.1. $C_{21}H_{30}N_4I_2Cd$ requires C, 35.8; H, 4.3; N, 8.0%; M 704.7); infrared $\nu_{max}$/ $cm^{-1}$ (KBr) 3274(sh), 3244, 3053w, 2931, 2866, 1604, 1585, 1496s, 1458s, 1429, 1299w, 1243, 1218, 1184w, 1078, 1021, 958, 938, 893, 803, 758 and 722.

(6,7,8,9,10,11,12,13,18,19,20,21-Dodecahydro-5H-dibenzo - [e,p][1,4,8,12]tetraazacycloheptadecine)zinc(II) bromide complex

$ZnL^{17}Br_2$

A mixture of zinc(II) bromide (0.036 g, 0.16 mmol) and $L^{17}$ (0.054 g, 0.16 mmol) was heated at reflux under nitrogen in acetonitrile (40 $cm^3$) for 1 h. The clear solution was evaporated under reduced pressure to 6 $cm^3$ and cooled to 0°C overnight. The resulting white crystalline solid was filtered at the pump, washed with cold acetonitrile (2 x 0.5 $cm^3$) and allowed to dry in air to give $ZnL^{17}Br_2$ (0.060 g, 0.11 mmol, 69%); (Found: C, 44.9; H, 5.4; N, 9.9. $C_{21}H_{30}N_4Br_2Zn$ requires C, 44.8; H, 5.4; N, 9.9%; M 563.7); infrared $\nu_{max}$/ $cm^{-1}$ (KBr) 3280, 3239, 3229, 3172, 1606, 1588, 1500s, 1458, 1448(sh), 1356w, 1304w, 1260w, 1219s, 1192w, 1153w, 1077, 1042, 1005w, 995, 967, 939, 859, 807, 763s, 753s and 733.

(6,7,8,9,10,11,12,13,18,19,20,21-Dodecahydro-5H-dibenzo -
[e,p][1,4,8,12]tetraazacycloheptadecine)zinc(II) iodide complex

$ZnL^{17}I_2$

To a solution of zinc(II) iodide (0.378 g, 1.18 mmol) in methanol (20 $cm^3$) and dichloromethane (40 $cm^3$) at reflux under nitrogen was added a solution of $L^{17}$ (0.338 g, 1.00 mmol) in dichloromethane (20 $cm^3$). Heating was continued for 1 h and after cooling to room temperature the volume was reduced to 40 $cm^3$ by evaporation under reduced pressure. The white microcrystalline solid which precipitated on cooling to 0°C was filtered at the pump, washed with cold methanol (5 $cm^3$) and diethyl ether (5 $cm^3$), recrystallised slowly from acetonitrile and vacuum dried for 2 h to give $ZnL^{17}I_2$ (0.40 g, 0.61 mmol, 61%); (Found: C, 38.3; H, 4.7; N, 8.5. $C_{21}H_{30}N_4I_2Zn$ requires C, 38.4; H, 4.6; N, 8.5%; M 657.6); infrared $\nu_{max}$/ $cm^{-1}$ (KBr) 3271, 3228s, 3210, 3176, 3067w, 3043w, 2959, 2929, 2863, 1607, 1589, 1498s, 1456s, 1440, 1414w, 1303w, 1260, 1251, 1218s, 1189w, 1149w, 1122w, 1074, 1051, 992, 977, 954, 859, 822, 811, 770, 755s, 749(sh) and 733.

8,9,10,11,12,13,20,21,22,23-Decahydro-7H-dibenzo[e,r]
[1,4,8,16]tetraazacyclononadecine

$P^{19}$

To a suspension of 4,7-diaza-2,3:8,9-dibenzodecane-1,10-dione (Ic) (5.36 g, 20.0 mmol) in dry ethanol (600 $cm^3$) at reflux under nitrogen was added 1,7-diaminoheptane (2.64 g, 20.1 mmol) in ethanol (100 $cm^3$). Heating was continued for 4 h and the mixture was allowed to cool overnight. The resulting cream-coloured precipitate was filtered at the pump, washed with cold methanol (3 x 10 $cm^3$) and dried in air to give microcrystals of $P^{19}$ (4.64 g, 12.8 mmol, 64%); infrared (KBr)

$\nu_{max}$/ $cm^{-1}$ 3209, 3153, 3091, 3013, 2934, 2923, 2832, 2742, 1633, 1604, 1584, 1519, 1458, 1335, 1321, 1294, 1216, 1201, 1158, 1093, 1051, 1043, 1017, 970, 942, 745, 724, 641; $^1$H NMR ($CDCl_3$, 60 MHz) $\delta$/ p.p.m. 1.1-1.7 (10 H, c, $CH_2(CH_2)_5CH_2$), 3.3-3.6 (8 H, c, $ArNHCH_2$ and $CH_2(CH_2)_5CH_2$), 6.5-7.3 (8 H, c, aryl-H), 8.26 (2 H, s, N=CH) and 9.35 (2 H, b, disappears with $D_2O$, NH).

6,7,8,9,10,11,12,13,14,15,20,21,22,23-Tetradecahydro-5H-dibenzo - [e,r][1,4,8,16]tetraazacyclononadecine

$L^{19}$

To a stirred suspension of lithium tetrahydridoaluminate (8.0 g) in dry diethyl ether (750 $cm^3$) under nitrogen was added $P^{19}$ (4.0 g, 11.0 mmol). After the disappearance of an initial yellow colouration and subsidence of effervescence, the mixture was stirred at reflux for 8 h. After cooling to room temperature, water (8 $cm^3$) was added, cautiously at first, then sodium hydroxide (15% aq., 8 $cm^3$) and water (24 $cm^3$). Stirring at reflux was resumed for a further 0.5 H, followed by filtration at the pump. The solid was washed with boiling dichloromethane (4 x 50 $cm^3$) and the combined filtrate dried with anhydrous sodium sulphate overnight. Filtration of the drying agent was followed by removal of the solvent under reduced pressure to give $L^{19}$ as a colourless oil (3.1 g, 8.5 mmol, 77%); infrared (KBr) $\nu_{max}$/ $cm^{-1}$, 3275b, 3043w, 2927s, 2852s, 2826s, 1606s, 1588s, 1517s, 1460s, 1363w, 1326, 1307, 1264, 1225w, 1142w, 1113, 1047 and 747vs; $^{13}$C NMR ($CDCl_3$, 20.12 MHz) $\delta$/ p.p.m. 26.1, 27.5, 28.8, 44.3, 48.2, 53.8, 110.5, 116.3, 124.3, 128.5, 129.6 and 148.8; electron impact mass spectrum at 350°C m/z 366($M^+$, 14%), 260(20), 248(10), 246(45), 234(10), 161(7), 147(24), 132(21), 120(76), 118(100), 106(87) and 91(66).

(6,7,8,9,10,11,12,13,14,15,20,21,22,23-Tetradecahydro-5*H*-dibenzo - [*e*,*r*][1,4,8,16]tetraazacyclononadecine)nickel(II) thiocyanate complex

$NiL^{19}(NCS)_2$

To a solution of hexaaquonickel(II) perchlorate (0.15 g, 0.41 mmol) in methanol (15 $cm^3$) was added a solution of $L^{19}$ (0.14 g, 0.38 mmol) in chloroform/acetonitrile (1:1, 6 $cm^3$) After 0.5 h a solution of potassium thiocyanate (0.08 g, 0.82 mmol) in methanol (10 $cm^3$) was added to this mixture and the solution allowed to evaporate to half volume under nitrogen. The pale blue powder was filtered at the pump, washed with hot water (2 x 5 $cm^3$) and acetone (0.5 $cm^3$) and dried in a vacuum oven at 115°C to give $NiL^{19}(NCS)_2$ (0.032 g, 0.059 mmol, 42%); (Found: C, 55.6; H, 6.1; N, 15.3. $C_{25}H_{34}N_6NiS_2$ requires C, 55.5; H, 6.3; N, 15.5%; M 541.4); electronic spectrum (acetonitrile) $\lambda_{max}$/ nm ( $\epsilon$ / $m^2$ $mol^{-1}$) 452, 585, 810 and 950; infrared $\nu_{max}$/ $cm^{-1}$ (KBr) 3320, 3249, 3230, 3160, 2962, 2924s, 2859, 2086vs, 2073vs, 1608, 1591, 1498s, 1460, 1446, 1354w, 1243w, 1221s, 1119, 1075, 1056, 1024, 970, 859, 813s, 777 and 755s.

(6,7,8,9,10,11,12,13,14,15,20,21,22,23-Tetradecahydro-5*H*-dibenzo - [*e*,*r*][1,4,8,16]tetraazacyclononadecine)nickel(II) chloride complex

$NiL^{19}Cl_2$

A mixture of $L^{19}$ (0.20 g, 0.55 mmol) and hexaaquonickel(II) chloride (0.24 g, 1.01 mmol) in acetonitrile (50 $cm^3$) was heated at reflux under nitrogen for 15 h. After filtration of a small amount of insoluble material, the solution was evaporated to dryness under reduced pressure. Methanol (2 $cm^3$) was added and the powder filtered at the pump, washed with cold acetonitrile (5 $cm^3$) then cold methanol (3 $cm^3$) and dried at 100°C for 2 h to give $NiL^{19}Cl_2$ as a pale blue powder (0.12 g, 0.24 mmol, 44%); (Found: C, 53.9; H, 6.8; N, 10.4.

$C_{23}H_{34}N_4Cl_2Ni$ requires C, 55.7; H, 6.9; N, 11.3%; M 496.1); electronic spectrum (chloroform) $\lambda_{max}$ / nm ( $\epsilon$ / $m^2$ $mol^{-1}$) 388, 661, 831, 990 and 1150; infrared $\nu_{max}$ / $cm^{-1}$ (KBr) 3321, 3228, 3181, 3043w, 3024w, 2962, 2919s, 2870, 1608, 1591, 1498s, 1476, 1458, 1446, 1244, 1221s, 1074, 1054, 1024, 992, 963, 878, 855, 814 and 775s.

## 6.3 X-ray structural studies

This section contains the experimental descriptions of the X-ray structure determinations undertaken in this work. Brief notes on the concepts necessary to understand the experimental procedures are presented in §6.4.[148] Details of the data collection and refinement parameters are given in Table 6.1. Major computations were performed on the University of North London VAX 4000-500 cluster using the SHELX suite of programs.[149,150,151] The molecular structures throughout the work were drawn using the ORTEP package.[152]

### 6.3.1 Data collection and reduction

A standard method of X-ray data collection was used for all the compounds studied. Intensity measurements, $(I_{hkl})raw$, were made on a Philips PW1100 four-circle diffractometer using a $\omega$-$2\theta$ scan technique and graphite monochromatized Mo-K$\alpha$ radiation of wavelength 0.71069 Å.

A crystal of less than 0.5 mm maximum dimensions was selected and fixed to a quartz fibre with quick-setting epoxy resin and mounted in the goniometer head of the diffractometer. After the crystal had been centred in the X-ray beam, the four circles were incrementally driven by the computer until twenty five reflections (hkl) were detected. For each reflection the optimum values of the angles $\varphi$, $X$, $\omega$ and $2\theta$ were determined. From these the parameters, a, b, c, $\alpha$, $\beta$ and $\gamma$ were calculated for a primitive unit cell together with an orientation matrix relating the crystal geometry to that of the diffractometer. This allowed calculation of the four-circle angles required to orient the crystal in the positions necessary to measure reflections from each of the sets of planes (hkl) in the crystal. For each hkl the $\omega$ and $2\theta$ circles synchronously scanned the diffracted beam with a suitable scan width and the total counts, $I_t$, for the scan were

recorded together with background counts at the beginning and end of the scan. For those compounds containing metal atoms weak reflections which gave $I_t - 2(I_t)^{\frac{1}{2}} < I_b$ on the first scan were omitted, but for the free ligands all reflections were measured. $I_t$ is the intensity at the maximum of the reflection peak and $I_b$ is the mean of the two preliminary 5 s background measurements at the extremities of the scan. The background measuring time for each recorded reflection was proportional to $I_b/I_i$, where $I_i$ is the total count recorded in the first scan. Reflections for which $I_i$ was less than a pre-selected value were scanned a second time. Three reference reflections were measured at intervals of five hours during data collection and showed no significant changes in intensity unless the crystal moved in the X-ray beam. In these cases, the crystal was recentred and data collection was continued. Loss of solvent or chemical decomposition can also cause a change in the reference reflections, but such misfortunes were not encountered with the present compounds.
I and $\sigma(I)$ were calculated and corrected for Lorentz and polarization factors using a program written for the PW1100 diffractometer.[153] Reflections which were equivalent by Laue symmetry were averaged giving a total of n data with $I/\sigma(I) > 3.0$ (see Table 6.1).

6.3.2 Identification of the crystal system and space group

Only two space groups were encountered in the present series, $P\bar{1}$ (No. 2) and $P2_1/n$, an alternative setting of $P2_1/c$,(No. 14).[154] For $L^{17}$, $[NiL^{16}(NO_3)_2][NiL^{16}(NO_3)(H_2O)]NO_3.CH_3OH$, $[NiL^{17}Cl_2]$ and $[CdL^{16}Br]_2CdBr_4.CH_3OH$ the unit cell geometry indicated a triclinic crystal system. A triclinic system requires a primitive lattice type

and the structures were successfully refined using the centrosymmetric space group, $P\bar{1}$. For $L^{16}$ and $[CdL^{17}Br_2].CH_3CN$ a monoclinic crystal system was indicated by the cell geometry and confirmed by the existence of the intensity relationships. No general systematic absences were observed, but reflections of the type h0l where h+l = 2n+1 and 0k0 where k = 2n+1 were absent indicating an n-glide plane and a two-fold screw axis, respectively. The structures were successfully refined using the space group $P2_1/n$.

6.3.3 Structure solutions and refinement of $[NiL^{16}(NO_3)_2]$ - $[NiL^{16}(NO_3)(H_2O)]NO_3.CH_3OH$

A calculation of the density of the crystal ($D_c$), based on the molecular mass ($M_r$) of the supposed structure, $[NiL^{16}(NO_3)_2]$, and the volume of the unit cell (U) using;

$$D_c = M_r.Z \;/\; R.U$$

where Z is the number of equivalent positions in the unit cell (Z = 2 for a triclinic cell) gave $D_c$ = 0.690 g $cm^{-3}$. The expected density range for mononuclear first row transition metal complexes is about 1.4 to 2.0 g $cm^{-3}$. That the density was only half of this indicated that there were two crystallographically independent molecules per equivalent position. The metal atoms were located from a Patterson synthesis in the following way. For two independent metal atoms in a triclinic cell, the four positions (in fractional cell coordinates) may be expressed algebraically as; $x_1,y_1,z_1$ and $-x_1,-y_1,-z_1$ for Ni(1) and $x_2,y_2,z_2$ and $-x_2,-y_2,-z_2$ for Ni(2).

From these, the positions of the Patterson maxima are calculated as;

(i) $(x_1-x_2),(y_1-y_2),(z_1-z_2)$ (ii) $(x_1+x_2),(y_1+y_2),(z_1+z_2)$

(iii) $2x_1,2y_1,2z_1$ (iv) $2x_2,2y_2,2z_2$

The vectors chosen to locate the nickel atoms were;

| height/ arbitrary units | u | v | w | distance/ Å |
|---|---|---|---|---|
| 345 | 0.191 | 0.288 | -0.283 | 7.336 |
| 300 | 0.483 | 0.444 | 0.403 | 11.614 |
| 179 | 0.291 | 0.155 | 0.689 | 8.373 |
| 163 | 0.329 | 0.264 | 0.868 | 8.730 |

In order to locate the two molecules as close together as possible, the shortest high vector was chosen as (i) and the next highest as (ii). From these two vectors,

$$2x_1, 2y_1, 2z_1 = 0.674, 0.732, 0.120$$

which is present in the map as its symmetry related vector at height = 163, and

$$2x_2, 2y_2, 2z_2 = 0.292, 0.156, 0.686$$

which is in the map at height = 179.

The two nickel atoms were inserted at positions indicated by these found vectors and an observed-Fourier map revealed peaks of electron-density in positions identifiable as those of the non-hydrogen atoms of the macrocyclic ligands of both complexes. This process required the careful consideration of distances between peaks to check whether or not they were compatible with expected bond lengths. The carbon atoms of the aromatic rings were readily identified. Insertion of all these atoms with one cycle of refinement reduced R to 0.2872 and facilitated the identification of two nitrate groups, each with an oxygen atom within bonding distance of one of the nickel atoms. Other peaks ca. 2.1 Å from either nickel atom were ascribed to oxygen. A further group of peaks not within bonding

distance of any other atoms was identified as a free nitrate ion. The R factor was reduced to 0.2113 on inclusion of these atoms in the refinement. Inspection of the isotropic thermal parameters computed for all the atoms supported the assignments; all were between 0.02 and 0.09 $Å^2$ with the exception of one carbon atom which proved to be disordered (see below). Further difference-Fourier maps allowed the identification of a second nitrate group co-ordinated to Ni(2) and a molecule of methanol. No other peaks being found near it, the sixth co-ordination site of Ni(1) was considered to be occupied by a water molecule. At this and subsequent stages, each molecule was refined in separate cycles using blocked full-matrix least-squares procedures. The free nitrate ion was included with molecule (1) in the first block and the methanol molecule was included with molecule (2) in the second block. Hereafter, the number of cycles of refinement refers to that for the parameters of each group of molecules/ions. At this stage, two cycles of refinement reduced R to 0.1035.

The apparent disorder of C(29b), manifested in the relatively high thermal parameter (U = 0.12 $Å^2$) was resolved in the following way. Allotting zero site occupancy to C(29b) revealed another peak between the atoms bonded to C(29b) which was regarded as an alternative position of this atom (C(29y) in the tables). Refinement of the occupancy ratio with thermal parameters fixed at 0.05 $Å^2$ gave 0.6:0.4 when rounded to one significant figure. Thereafter, the thermal parameters were allowed to refine with the occupancies fixed at these values, and two cycles of refinement at this stage gave R = 0.1010. Assignment of anisotropic thermal parameters to the nickel atoms and the atoms of the nitrate groups further reduced R to 0.0779 in three cycles of refinement. A difference-Fourier synthesis in which the structure factors were calculated only for those

reflections with sin $\theta/\lambda < 0.35$ revealed peaks possibly attributable to hydrogen atoms. By inserting hydrogen atoms at possible locations and rejecting those that gave unacceptable local geometry, thirty-one hydrogen atoms were found including all those attached to the amine-nitrogen atoms of molecule (1). The hydrogen atoms attached to the oxygen atoms of the co-ordinated water molecule and the methanol solvent were found only after several attempts. One amine-hydrogen atom of molecule (2) was found, but no acceptable locations for the other three were apparent. This is not surprising for that attached to the nitrogen atom adjacent to the disordered carbon atom because each component of the disorder of C(29b)/C(29y) requires different positions for the hydrogen atoms attached to its neighbours. Of the remaining hydrogen atoms, those not associated with the disorder were included in calculated positions with idealized geometry and were constrained to 'ride' on the appropriate atoms at a fixed distance of 1.08 Å. The disordered hydrogen atoms attached to C(29b)/C(29y) were included in alternative calculated positions and were assigned zero occupancy. The two alternative positions for the hydrogen atom attached to N(21b) were likewise calculated and each assigned half occupancy. The parameters of these hydrogen atoms were not refined. All hydrogen atoms were assigned a fixed isotropic thermal parameter ($U = 0.08$ Å$^2$). After two cycles of refinement for each molecule the refinement converged to the final value of $R = 0.0642$, $R_w = 0.0590$. Final tables of fractional atomic coordinates, thermal parameters, bond lengths and interbond angles are given in the Appendix (Tables A3.1 to A3.5).

### 6.3.4 Structure solution and refinement of $[NiL^{17}Cl_2]$

The positions of the nickel and chlorine atoms were deduced from a

Patterson synthesis in the following way. Let the coordinates of the nickel and chlorine atoms be $x_1,y_1,z_1$, $x_2,y_2,z_2$ and $x_3,y_3,z_3$. For three heavy atoms in a triclinic cell, nine Patterson vectors would be expected. Due to the linear nature of the trans-dihalo complex, several of these vectors are coincident.

The vectors are;

(i) $2x_1,2y_1,2z_1$

(ii) $2x_2,2y_2,2z_2$

(iii) $2x_3,2y_3,2z_3$

(iv) $(x_1+x_2),(y_1+y_2),(z_1+z_2)$

(v) $(x_1-x_2),(y_1-y_2),(z_1-z_2)$

(vi) $(x_1+x_3),(y_1+y_3),(z_1+z_3)$

(vii) $(x_1-x_3),(y_1-y_3),(z_1-z_3)$ coincident with (v)

(viii) $(x_2+x_3),(y_2+y_3),(z_2+z_3)$ coincident with (i)

(ix) $(x_2-x_3),(y_2-y_3),(z_2-z_3)$.

The vectors used to locate the nickel and chlorine atoms were;

| height/ arbitrary units | u | v | w | distance / Å | assignment |
|---|---|---|---|---|---|
| 450 | 0.457 | 0.500 | 0.973 | 6.493 | (i) and (viii) |
| 450 | 0.152 | 0.087 | 0.804 | 2.471 | (v) and (vii) |
| 222 | 0.302 | 0.407 | 0.159 | 4.756 | (iv) |
| 222 | 0.393 | 0.417 | 0.221 | 5.469 | (vi) |
| 153 | 0.306 | 0.177 | 0.622 | 4.879 | (ix) |
| 94 | 0.155 | 0.321 | 0.358 | 4.016 | (ii) |
| 67 | 0.232 | 0.325 | 0.402 | 4.590 | (iii) |

Of the two highest vectors, the shortest was assumed to be that between the nickel atom and each of the chlorine atoms at approximately twice the expected height betwen nickel and chlorine because they are coincident vectors. The other high vector was assumed to be that between the two nickel atoms in the unit cell, combined with the Cl(1)-Cl(2) vector. From this vector the nickel atom can be located at,

$$x_1, y_1, z_1 = 0.228, 0.250, -0.013$$

Subtraction of the short vector from this gives a location of one of the chlorine atoms at,

$$x_2, y_2, z_2 = 0.076, 0.163, 0.183$$

and $2x_2, 2y_2, 2z_2$ is found at height = 94 as,

$$0.155, 0.321, 0.358$$

giving,

$$x_2, y_2, z_2 = 0.077, 0.160, 0.179$$

which matches closely the vector calculated above.

Subtracting the found $x_2, y_2, z_2$ from the long vector gives the position of the second chlorine atom,

$$x_3, y_3, z_3 = 0.380, 0.340, -0.206$$

The expected vector,

$$2x_3, 2y_3, 2z_3 = 0.760, 0.680, -0.412$$

can be found as its symmetry related vector at height = 67. The two vectors at height = 222 were assumed to be,

$$x_1, y_1, z_1 + x_2, y_2, z_2 \text{ and}$$

$$x_1, y_1, z_1 + x_3, y_3, z_3.$$

Subtracting the found $x_1, y_1, z_1$ from each of these gives,

$$x_2, y_2, z_2 = 0.074, 0.157, 0.172$$

which agrees closely with that deduced earlier and,

$$x_3, y_3, z_3 = 0.165, 0.167, 0.234$$

which cannot be found on the map. Taking the inverse of the second vector of height = 222 ( i.e. 0.607, 0.583, 0.779) and then subtracting $x_1, y_1, z_1$ from it we get

$$x_3, y_3, z_3 = 0.379, 0.333, 0.779$$

which can be rewritten as,

$$0.379, 0.333, -0.208.$$

This vector matches that calculated above for $x_3, y_3, z_3$.

Insertion of the nickel and chlorine atoms at positions deduced from the above gave R = 0.3603. The remaining non-hydrogen atoms were found from a series of difference-Fourier maps; inclusion of the nitrogen atoms in three cycles of refinement reduced R to 0.2746; addition of the carbon atoms of the benzyl groups in two further refinement cycles gave R = 0.1921; two more refinement cycles after inclusion of the alkyl bridges reduced R to 0.0967. Assignment of anisotropic thermal parameters to the nickel and chlorine atoms and the carbon atoms of the five-membered alkyl bridge gave R = 0.0751. All the amine-hydrogen atoms and most of the hydrogen atoms attached to carbon atoms were inserted in positions found from a difference-Fourier map calculated using the structure factors for reflections with $\sin\theta/\lambda < 0.35$. The seven remaining hydrogen atoms were included in geometrically idealized positions and were constrained to 'ride' on the appropriate carbon atoms. Each hydrogen atom was assigned a fixed thermal parameter of 0.08 Å and in four cycles, the least-squares refinement converged to the final value of R = 0.0591, $R_w$ = 0.0570. Final tables of fractional atomic coordinates, thermal parameters, bond lengths and interbond angles are given in the Appendix (Tables A4.1 to A4.5).

### 6.3.5 Structure solution and refinement of $[CdL^{16}Br]_2[CdBr_4].CH_3OH$

The initial assumption that the cadmium complex of $L^{16}$ was a single trans-dibromo complex proved incorrect when the volume of the unit cell (2664.88 $\AA^3$) was calculated. For $C_{20}H_{28}N_4Br_2Cd$ ($M_r$ = 596.68) in a triclinic unit cell of this volume, the calculated density of 0.744 g $cm^3$ was too low and implied that there were two crystallographically independent molecules in the crystal.

The Patterson map showed forty-two peaks with heights between 90 and 177 (arbitrary units) and a solution on the basis of two trans-dibromo complexes was attempted. A short vector (2.864 $\AA$) at height = 154 was assumed to be that between Cd(1) and Br(1),

$$\text{i.e. } x_1-x_2,\ y_1-y_2,\ z_1-z_2$$

No clues to the identification of

$$x_1-(-x_2),\ y_1-(-y_2),\ z_1-(-z_2)$$

were present in the map, so a systematic examination of the peaks was begun, starting at the top in the following way. If the peak at height 177 is this vector then,

$$2x_1, 2y_1, 2z_1 = 0.661,\ 0.301,\ -0.323$$

which is not present in the map so the assignment was rejected. This process was continued and when a possible vector was located for $2x_1, 2y_1, 2z_1$ (although never a close match), an observed-Fourier map was calculated, but no recognisable structure was found. With the best fit, there were still too many high vectors that could not be assigned.

At this stage it was decided to enlist the help of the automatic direct methods solution which, although all reflections are required for a sensible structure to emerge and weak reflections had been

omitted in the data collection, it was hoped that positions of 'heavy atoms' might be revealed. The solution that emerged contained thirty molecules, the first nine of which contained a peak of relatively high electron-density. Using the coordinates of the six highest peaks (it was still assumed that two trans-dibromo complexes formed the asymmetric unit) the six vectors of the type 2x,2y,2z and a further thirty interatomic vectors were calculated from these coordinates and all were found on the Patterson map. An observed-Fourier map calculated with these six positions occupied by two cadmium atoms in those of highest electron-density and four bromine atoms occupying the other positions, revealed three other high peaks. Overcoming the initial prejudice, these positions were included as one extra cadmium and two extra bromine atoms. On the basis of calculated thermal parameters, the 'bromine' atom with the highest electron-density was changed to cadmium and the extra 'cadmium' to bromine.

Refinement of the scale factor followed by one cycle of refinement on the positional and thermal parameters of the three cadmium and six bromine atoms gave R = 0.2428. An observed-Fourier map calculated at this stage revealed electron-density peaks in positions recognizable as those of the majority of the atoms of both macrocycles. Difficulty was experienced in identifying the atoms of complex (1), because the projection of the electron-density peaks computed for this complex was that across the plane of the macrocyclic donors, a 'side on' projection. However, inclusion of the a-half of complex (1) and all the atoms of complex (2), with one cycle of refinement on each complex reduced R to 0.1666. Unacceptable thermal parameters for several of the macrocycle atoms indicated that they were incorrectly located or wrongly assigned. Relocation from subsequent difference-Fourier maps and inclusion of the b-half of

complex (1) reduced R to 0.1382 and most of the atoms had acceptable thermal parameters.

At this stage, two groups of three and five peaks were tentatively identified as solvent molecules, although their exact nature was not immediately apparent. Initial attempts to identify the solvents as methanol or acetonitrile proved unsuccessful in terms of bond lengths, linearity of the acetonitrile and thermal parameters. It was hoped that subsequent improvement of the structure would simplify the identification of these peaks and they were omitted from further analysis until later.

The relatively high thermal parameter of C(21b) (U = 0.1020 $Å^2$) was thought to imply some disorder in this region, but a search for an alternative location proved fruitless. After several attempts, it was finally decided to refine the solvents as one molecule of methanol disordered over two sites in the ratio 0.7:0.3, identifying the two major peaks in each set as oxygen or carbon depending upon which combination gave the more acceptable thermal parameters.

A difference-Fourier synthesis in which the structure factors were calculated only for those reflections with $\sin\theta/\lambda < 0.35$ revealed only fifteen hydrogen atoms of the macrocycles in acceptable positions. All the amine hydrogen atoms and four others of complex (1), the anilino-hydrogen atoms and five others of complex (2), and the hydroxy-hydrogen atom of the major component of the methanol solvent were included in observed positions. The remaining hydrogen atoms of the macrocyclic ligands were included in geometrically idealized positions and were constrained to 'ride' on the appropriate carbon or nitrogen atoms at a distance of 1.08 Å. The hydroxy-hydrogen atom of the minor component of the disordered solvent

and the methyl hydrogen atoms of both components were not included in the refinement. At this stage (R = 0.1279) an empirical absorption correction was applied using the program DIFABS.[155] Anisotropic thermal parameters were assigned to the cadmium and bromine atoms, all the nitrogen and some of the carbon atoms of the macrocycles (see Table A5.3) and to the oxygen and carbon atoms of the major component of the disordered methanol molecule. Two cycles of refinement using the corrected data gave a final R factor of 0.0600, $R_w$ = 0.0593. Final tables of fractional atomic coordinates, thermal parameters, bond lengths and interbond angles are given in the Appendix (Tables A5.1 to A5.5).

### 6.3.6 Structure solution and refinement of $[CdL^{17}Br_2].CH_3CN$

Based on the assumption that the asymmetric unit contained only a molecule of the trans-dibromo complex $[CdL^{17}Br_2]$ ($M_r$ = 610.70), the density of the unit cell was calculated to be 1.530 g $cm^{-3}$, which is in the expected range of densities for this type of compound. The positions of the cadmium and bromine atoms were located from a Patterson synthesis in the following way.

The equivalent positions in the space group $P2_1/n$ are,

$x,y,z$ $\quad\quad$ $-x,-y,-z$

$\frac{1}{2}+x,\frac{1}{2}-y,\frac{1}{2}+z$ $\quad$ $\frac{1}{2}-x,\frac{1}{2}+y,\frac{1}{2}-z$

The relative heights of expected vectors are;

Cd-Cd.....2304 $\quad$ Br-Br.....1225 $\quad$ Cd-Br.....1680

For a trans-dibromo cadmium complex, the relative height of the Cd-Br vectors is twice as high as that above, i.e. 3360.

Let the positions of Cd, Br(1) and Br(2) be $x_1,y_1,z_1$, $x_2,y_2,z_2$, and $x_3,y_3,z_3$, respectively.

The vectors used to locate the cadmium and one of the bromine atoms were,

| height/ arbitrary units | u | v | w | distance/ Å |
|---|---|---|---|---|
| 306 | 0.443 | 0.500 | -0.401 | 10.67 |
| 299 | 0.057 | 0.148 | -0.103 | 2.55 |
| 286 | 0.257 | 0.000 | -0.155 | 4.21 |
| 235 | 0.315 | 0.137 | -0.264 | 5.81 |
| 161 | 0.243 | 0.345 | -0.346 | 7.15 |
| 102 | 0.105 | 0.297 | -0.211 | 5.10 |

The short vector at height = 299 of length 2.55 Å (the expected Cd-Br bond length) was assumed to be,

$$x_1-x_2,\ y_1-y_2,\ z_1-z_2$$

The four equivalent positions in the space group $P2_1/n$ give rise also to vectors of the type;

$$\tfrac{1}{2}+(x_1-x_2),\ \tfrac{1}{2}+(y_1+y_2),\ \tfrac{1}{2}+(z_1-z_2)$$

As we know $x_1-x_2$ and $z_1-z_2$ from the vector at height = 299, we can look for a vector with $\tfrac{1}{2}+(x_1-x_2)$ and $\tfrac{1}{2}+(z_1-z_2)$. This vector cannot be found directly, but that at height = 306, (with v = $\tfrac{1}{2}$) can be rewritten as

$$0.557,\ 0.500,\ 0.401$$

by changing the signs on u and w and adding 1 to u. This then closely matches the expected vector. In order to find the vector

$$\tfrac{1}{2}+(x_1+x_2),\tfrac{1}{2}+(y_1-y_2),\tfrac{1}{2}+(z_1+z_2)$$

we know $y_1-y_2$ = 0.148 and need to find a vector with v = 0.648 (or 1 - 0.648 = 0.352). The vector at height = 161 has avalue of v close

to this i.e. 0.345. This vector can be rewritten as,

-0.243 0.655 0.346

so $x_1+x_2, y_1-y_2, z_1+z_2$ is -0.743 0.155 -0.154 and the vector at height = 286

i.e. 0.257 0.000 -0.155

is $x_1+x_2, y_1+y_2, z_1+z_2$. By addition of the vector at height = 299 and this last one, we can now obtain $2x_1, 2y_1, 2z_1$ = 0.314 0.148 -0.258. Therefore,

$x_1, y_1, z_1$ = 0.157 0.074 -0.129

and $2x_2, 2y_2, 2z_2$ = 0.200 -0.148 -0.052

giving $x_2, y_2, z_2$ = 0.100 -0.074 -0.026.

Insertion of a cadmium atom and a bromine atom at the positions deduced above was sufficient to solve the structure. An observed-Fourier map revealed electron-density peaks in positions recognizable as those of the atoms of the macrocycle. All these atoms, except C(1b) whose position could not unambiguously be determined were included in a difference-Fourier synthesis. Their parameters were not refined, but refinement of the scale factor gave R = 0.2287. Inclusion of C(1b) in a position indicated in this difference map and one cycle of refinement for each of the a- and b-halves of the macrocycle reduced R to 0.1121. Two further cycles of refinement of the parameters of all the atoms of the complex gave R = 0.0964.

The relatively high thermal parameter of C(10a) (0.0869 $\text{Å}^2$) was thought to be indicative of disorder in this region and indeed an alternative position for this atom was found in the difference-Fourier map and included as C(10y). The site occupancy and thermal parameters of both components of this atom were refined as before. The site occupancy was fixed at 0.8:0.2 and thermal parameters were refined to

0.0536 and 0.0576 for C(10a) and C(10y), respectively.

A group of four peaks, three of which were collinear and the other of low electron-density, were interpreted as arising from the molecule of acetonitrile indicated in the infrared spectrum. Including the two carbon atoms and the nitrogen atom of the acetonitrile and the disorder of C(10a)/C(10y) in the refinement reduced R to 0.0716 after one least-squares cycle.

The bond lengths C(10y)-C(11) and C(10y)-C(9a) were unusually disparate for this type of bond, being 1.78 and 1.43 Å, respectively indicating that the least-squares refinement had moved C(10y) to an inappropriate position, probably because of its low electron-density (only one-fifth of that of a carbon atom). Bond length constraints were applied to these two bonds such that they were equal to 1.54(2) Å after which treatment, the thermal parameters of C(10a) and C(10y) refined to 0.0568 and 0.0479 $Å^2$, respectively

At this stage it was noticed that, although the thermal parameter of C(10b) was quite reasonable (0.0890 $Å^2$), a residual electron-density peak near this atom was in a position relative to C(11), C(10b) and C(9b) which indicated possible further disorder. This peak was included in the refinement, as C(10x), with the same occupancy as C(10y) and the occupancy of C(10b) was equated with that of C(10a). The bond length constraints mentioned above were extended to include the whole of the five-carbon chain so that all the bonds between C(9a), C(10a)/C(10y), C(11), C(10b)/C(10x) and C(9b) were equal to 1.54(2) Å and the R factor after one cycle of refinement changed to 0.0711.

The amine-hydrogen atoms were located from a difference-Fourier map in which the structure factors used were only for those reflections for which $\sin\theta/\lambda < 0.35$ and were inserted in observed positions. Most of the remaining hydrogen atoms were included in geometrically idealised positions and were constrained to 'ride' on the appropriate carbon atoms at a distance of 1.08 Å and were assigned a fixed thermal parameter of 0.08 Å$^2$. The hydrogen atoms associated with the atoms of the five-carbon chain were not included in the refinement.

An empirical absorption correction was computed as in §6.3.5 using all the atoms and R was reduced to 0.0621. In the final cycles of full-matrix least-squares refinement, anisotropic thermal parameters were assigned to the cadmium and bromine atoms and to the nitrogen atoms and some of the carbon atoms of the macrocycle (see Table A6.3) and to the carbon and nitrogen atoms of the acetonitrile solvent molecule. Refinement converged to the final values of $R = 0.0416$, $R_w = 0.0393$. Final tables of fractional atomic coordinates, thermal parameters, bond lengths and interbond angles are given in the Appendix (Tables A6.1 to A6.5).

### 6.3.7 Structure solution and refinement of $L^{16}$

The structure of the free ligand $L^{16}$ was solved by direct methods using the automatic centrosymmetric structure-solving routine in SHELX86,[150] enabling the location of all the non-hydrogen atoms. Refinement of the overall scale factor followed by two cycles of least-squares refinement of the atomic parameters gave $R = 0.1313$. The amine hydrogen atoms were inserted in positions found from a difference Fourier synthesis in which the structure factors used were calculated for reflections with $\sin\theta/\lambda < 0.35$. The remaining

hydrogen atoms were included in geometrically idealised positions and were constrained to 'ride' on the appropriate carbon atoms. Common group isotropic thermal parameters were refined for the methylene hydrogen atoms (U = 0.08726), while those of the aromatic hydrogen atoms were refined in two groups, one for each phenylene ring, U = 0.11293 and 0.08626 for the a- and b-rings, respectively. Anisotropic thermal parameters were assigned to the nitrogen atoms and the unsubstituted carbon atoms of the phenylene rings in the final cycles of least-squares refinement which converged at R = 0.0657, $R_w$ = 0.0663. Final tables of fractional atomic coordinates, thermal parameters, bond lengths and interbond angles are given in the Appendix (Tables A1.1 to A1.5).

6.3.8 Structure solution and refinement of $L^{17}$

The structure of the free ligand $L^{17}$ was solved by direct methods using the automatic centrosymmetric structure solving routine in SHELX86,[150] enabling the location of all the non-hydrogen atoms. A difference-Fourier synthesis with three cycles of least-squares refinement of the parameters of the nitrogen atoms and the carbon atoms of the benzyl groups gave R = 0.3758. Inclusion of the carbon atoms of the two- and five-carbon bridges and two further refinement cycles reduced R to 0.1263. The amine hydrogen atoms and those attached to the alkyl carbon atoms and C(3a) and C(3b) were inserted in positions found from a difference-Fourier map using the structure factors calculated for reflections with $\sin\theta/\lambda < 0.35$. The remaining six phenyl hydrogen atoms were included in geometrically idealised positions and were constrained to 'ride' on the appropriate carbon atoms. All the hydrogen atoms were included in the structure factor calculations with thermal parameters of 0.08 $Å^2$, but their parameters

were not refined. The nitrogen atoms and the carbon atoms of the five-membered bridge were assigned anisotropic thermal parameters in the final cycles of full-matrix refinement which converged at $R = 0.0797$, $R_w = 0.0761$. Final tables of fractional atomic coordinates, thermal parameters, bond lengths and interbond angles are given in the Appendix (Tables A2.1 to A2.5).

TABLE 6.1 Details of data collection and refinement for X-ray crystallographic structure analyses of ligands $L^{16}$ and $L^{17}$ and the nickel(II) and cadmium(II) complexes.(a)

| compound | $L^{16}$ | $L^{17}$ (b) | $L^{17}$ (c) |
|---|---|---|---|
| formula | $C_{20}H_{28}N_4$ | $C_{21}H_{30}N_4$ | |
| $M_r$ | 324.5 | 338.5 | |
| crystal size/mm | 0.38x0.26x0.20 | 0.30x0.30x0.35 | 0.48x0.24x0.16 |
| Z | 4 | 2 | |
| space group | $P2_1/n$ | $P\bar{1}$ | |
| a/Å | 19.374(4) | 11.440(3) | 11.437(3) |
| b/Å | 8.403(2) | 9.603(3) | 9.592(3) |
| c/Å | 11.225(3) | 9.032(3) | 9.024(3) |
| α/° | 90 | 96.70(2) | 96.72(2) |
| β/° | 94.18(2) | 102.60(2) | 102.60(2) |
| γ/° | 90 | 88.64(2) | 88.64(2) |
| U/ Å$^3$ | 1822.57 | 959.50 | |
| F(000) | 704 | 368 | |
| $D_c$/g cm$^{-3}$ | 1.182 | 1.171 | |
| μ(Mo-Kα)/cm$^{-1}$ | 0.39 | 0.38 | |
| no. of reflections measured | 2745 | 2680 | 2676 |
| no. of unique data used in refinement(d) | 1160 | 1506 | |
| no. of parameters refined | 160 | 127 | |
| R | 0.0657 | 0.0797 | |
| $R_w$ | 0.0663 | 0.0761 | |
| scan width/° | 0.80 | 0.70 | 0.90 |
| θ range/° | 3–23 | 3–23 | |
| reference reflections | 4 0 0<br>3 1 1<br>6 0 2 | 2 1 0<br>0 1 1<br>-1 0 2 | -2 -1 0<br>1 0 -2<br>0 2 0 |

TABLE 6.1 (continued)

| compound | $[NiL^{16}(NO_3)(H_2O)]NO_3$ $[NiL^{16}(NO_3)_2].CH_3OH$ | $[NiL^{17}Cl_2]$ |
|---|---|---|
| formula | $C_{41}H_{60}N_{12}Ni_2O_{14}$ | $C_{21}H_{30}N_4Cl_2Ni$ |
| $M_r$ | 1062.4 | 468.1 |
| crystal size/mm | 0.25x0.28x0.18 | 0.19x0.34x0.29 |
| Z | 2 | 2 |
| space group | $P\bar{1}$ | $P\bar{1}$ |
| a/Å | 21.660(4) | 11.757(3) |
| b/Å | 11.965(3) | 11.661(3) |
| c/Å | 10.305(3) | 8.803(2) |
| $\alpha$/° | 109.68(2) | 111.44(2) |
| $\beta$/° | 103.56(2) | 79.32(2) |
| $\gamma$/° | 82.14(2) | 109.88(2) |
| U/ Å$^3$ | 2439.69 | 1053.85 |
| F(000) | 1120 | 492 |
| $D_c$/g cm$^{-3}$ | 1.446 | 1.475 |
| $\mu$(Mo-K$\alpha$)/cm$^{-1}$ | 7.90 | 11.20 |
| no. of reflections measured | 3884 | 1746 |
| no. of unique data used in refinement(d) | 3093 | 1622 |
| no. of parameters refined | 183 + 191(e) | 173 |
| R | 0.0642 | 0.0591 |
| $R_w$ | 0.0590 | 0.0570 |
| scan width/° | 0.90 | 0.80 |
| $\theta$ range/° | 3–25 | 3–25 |
| reference reflections | 0 1 1<br>3 1 0<br>-3 0 1 | -1 -1 1<br>0 -2 1<br>1 1 0 |

TABLE 6.1 (continued)

| compound | $[CdL^{16}Br]_2[CdBr_4].CH_3OH$ | $[CdL^{17}Br_2].CH_3CN$ |
|---|---|---|
| formula | $C_{41}H_{60}N_8OBr_6Cd_3$ | $C_{23}H_{33}N_5Br_2Cd$ |
| $M_r$ | 1497.6 | 651.7 |
| crystal size/mm | 0.25x0.27x0.19 | 0.27x0.35x0.41 |
| Z | 2 | 4 |
| space group | $P\bar{1}$ | $P2_1/n$ |
| a/ Å | 13.135(3) | 16.035(4) |
| b/ Å | 19.633(4) | 14.537(3) |
| c/ Å | 10.993(3) | 11.532(3) |
| $\alpha$/° | 100.25(2) | 90 |
| $\beta$/° | 103.53(2) | 107.48(2) |
| $\gamma$/° | 77.31(2) | 90 |
| U/ Å$^3$ | 2664.88 | 2564.04 |
| F(000) | 1448 | 1296 |
| $D_c$/g cm$^{-3}$ | 1.866 | 1.688 |
| $\mu$(Mo-K$\alpha$)/cm$^{-1}$ | 55.34 | 38.47 |
| no. of reflections measured | 4627 | 2397 |
| no. of unique data used in refinement(d) | 3865 | 2387 |
| no. of parameters refined | 345 | 291 |
| R | 0.0600 | 0.0416 |
| $R_w$ | 0.0593 | 0.0393 |
| scan width/° | 0.80 | 0.80 |
| $\theta$ range/° | 3-25 | 3-25 |
| reference reflections | 3 1 -1<br>1 0 2<br>1 3 -1 | 4 0 0<br>-2 1 1<br>1 2 2 |

TABLE 6.1 (continued)

| compound | $[NiL^{15}(NCS)_2](f)$ | $[NiL^{16}(NCS)_2](f)$ | $[NiL^{17}(NCS)_2](f)$ |
|---|---|---|---|
| formula | $C_{21}H_{26}N_6NiS_2$ | $C_{22}H_{28}N_6NiS_2$ | $C_{23}H_{30}N_6NiS_2$ |
| $M_r$ | 485.3 | 499.3 | 513.3 |
| crystal size/mm | 0.10x0.25x0.45 | 0.15x0.15x0.50 | 0.35x0.30x0.15 |
| Z | 4 | 2 | 4 |
| space group | C2/c | $P\bar{1}$ | $P2_1/c$ |
| a/Å | 15.225(3) | 13.632(3) | 18.707(3) |
| b/Å | 10.110(3) | 9.378(2) | 8.342(2) |
| c/Å | 15.544(3) | 9.350(2) | 17.968(3) |
| $\alpha$/° | 90 | 94.73(2) | 90 |
| $\beta$/° | 108.92(2) | 90.55(2) | 109.02(2) |
| $\gamma$/° | 90 | 89.40(2) | 90 |
| U/ Å$^3$ | 2263.34 | 1191.13 | 2448.96 |
| F(000) | 988 | 536 | 1080 |
| $D_c$/g cm$^{-3}$ | 1.424 | 1.392 | 1.392 |
| $\mu$(Mo-K$\alpha$)/cm$^{-1}$ | 9.88 | 9.42 | 9.50 |
| no. of reflections measured | 703 | 2028 | 2226 |
| no. of unique data used in refinement(d) | 703 | 1951 | 2100 |
| no. of parameters refined | 92 | 162 | 291 |
| R | 0.0633 | 0.0842 | 0.0485 |
| $R_w$ | 0.0659 | 0.0857 | 0.0488 |
| scan width/° | 0.90 | 0.90 | 0.70 |
| $\theta$ range/° | 3-25 | 3-25 | 3-25 |
| reference reflections | 2 0 2<br>0 2 -1<br>1 1 -3 | 3 1 0<br>1 2 0<br>1 0 -2 | 4 0 0<br>-1 1 3<br>0 2 0 |

(a) Data collected on Philips PW1100 four-circle diffractometer using a $\omega$-$2\theta$ scan technique and graphite monochromatised Mo-K$\alpha$ radiation of wavelength 0.71069 Å at a constant scan speed of 0.05°/min$^{-1}$;
(b) crystal from nitromethane; (c) crystal from chloroform;
(d) with $I > 3\sigma(I)$; (e) refined in alternate cycles; (f) Ref. 106.

## 6.4 Notes on molecular structure determination by X-ray diffraction

### 6.4.1 The diffraction of X-rays

X-rays are scattered by the electrons of atoms. The combination of scattering from a regular three dimensional array of electrons gives rise to a corresponding diffraction pattern. Electrons in a lattice will result in a diffracted beam whenever the condition of the Bragg equation obtains,

$$2d_{hkl} \sin \theta_{hkl} = \lambda$$

where $\theta_{hkl}$ is the angle between the Bragg planes (hkl) and the incident beam, $\lambda$ is the wavelength of the X-rays and $d_{hkl}$ is the inter-plane distance. The planes were defined by Bragg using three integers, h, k and l, where a set of planes (hkl) intercepts the a, b and c axes at a/h, b/k and c/l and a, b and c are the dimensions of the unit cell. Extending this idea to a regular array of electron density that occurs in a real crystal, the diffraction pattern obtained is a combination of the patterns produced by a multitude of interpenetrating lattices and the interference produced by these (they will not all be in phase) causes variations in the intensity of the diffracted beams. By measurement of the angle of the Bragg reflections, the size and shape of the repeat unit in the crystal (the unit cell) can be determined. Measurements of the intensities of the reflections yield information about the distribution of the electron density and hence the atomic arrangement within the unit cell.

### 6.4.2 Lattice types

The unit cell, or the repeat pattern of a crystal can usually be chosen in one of several ways, starting at different points in the pattern. If the pattern is represented by an array of points reproducing the size and shape of the unit cell, the array formed is a

lattice and the points, lattice points. Only primitive lattice types (not face- or body-centred) were encountered in the present study.

### 6.4.3 Crystal systems

If a unit cell has no symmetry or a centre of symmetry only, there are no restrictions on its shape; all three angles, $\alpha$, $\beta$ and $\gamma$ have to be specified and the crystal system is triclinic. If a unit cell has an axis of symmetry of order 2 the b-axis is taken parallel to it and the other two axes are taken perpendicular to it. The choice of unit cell is restricted to a parallelipiped having two right angles and only one angle has to be specified, so the crystal system is monoclinic. Higher symmetry imposes further restrictions on the unit cell, giving the other crystal systems, but only triclinic and monoclinic crystal systems were encountered in this work.

Crystal systems may be identified by inspection of the relative intensities of diffraction maxima $I_{hkl}$ In general,

$$I_{hkl} = I_{\bar{h}\bar{k}\bar{l}} .$$

This is known as Friedel's Law and in a triclinic system no other intensity relationships are observed. In a monoclinic system, not only does Friedel's Law hold, but also

$$I_{hkl} = I_{\bar{h}\bar{k}\bar{l}} = I_{h\bar{k}l} = I_{\bar{h}kl} .$$

Noticing these intensity relationships is crucial to the identification of the crystal system and, because it is unnecessary to measure the equivalent reflections, a great deal of time may be saved by taking these into account during the data collection.

### 6.4.4 Point group symmetry

A finite object has symmetry if it can be divided into parts, or asymmetric units, that correspond to each other by reflection across a

plane, rotation around an axis or inversion through a point. Performing the symmetry operations on the part generates the whole. The collection of symmetry elements needed to describe completely the object's symmetry is called its point symmetry, or point group, because there is always at least one point which is not changed by the symmetry operation. A symmetry operator generates from a point x,y,z, an equivalent position of the point, e.g. the inversion centre generates a point, -x,-y,-z.

### 6.4.5 Space group symmetry

In crystallographic notation, a rotation axis is specified by its order. The Hermann-Mauguin notation is used in crystallography rather than the Schoenflies notation of spectroscopy. A one-fold axis, which is equivalent to no symmetry at all is given the symbol 1 and a two-fold axis, the symbol 2. The centre of symmetry, or inversion centre is a special case of the n-fold inversion axis, and is given the symbol, $\bar{1}$. A mirror plane, m is equivalent to a two-fold rotatory inversion axis $\bar{2}$, oriented perpendicular to the plane. In an extended array, such as a crystal, there may exist symmetry elements which involve translation combined with the point symmetry elements. Two types of translational symmetry elements exist; the screw axis and the glide plane. The first involves rotation around the axis followed by a translation parallel to it and the second involves a reflection across the plane followed by a translation parallel to the plane. A glide plane is usually parallel to one face of the unit cell and perpendicular to another, but it can also be across a cell diagonal. The translation is in the direction specified by the glide type and, in the monoclinic system, is by half a unit cell.

The combination of lattice types with point and translational symmetry elements in ways compatible with crystal structures gives the 230 different arrays of symmetry elements or space groups. In the present study, only two space groups were encountered, $P\bar{1}$, a primitive lattice with an inversion centre only, and $P2_1/n$, again primitive with a two-fold screw axis parallel to b and an n-glide plane perpendicular to b. The n-glide plane arises in a non-standard setting of the standard cell (in which the glide is parallel to c) and the resetting of the cell needs further explanation.

### 6.4.6 The n-glide plane

The n-glide in $P2_1/n$ is related to the c-glide in $P2_1/c$ in the following way. If the c-axis is redefined across the B-face diagonal of the standard unit cell, the glide plane remains unchanged, but the direction of the translation is now parallel to the diagonal of the non-standard cell. It is sometimes necessary to reverse the direction of the a-axis so that $\beta$ remains obtuse. One of the criteria in the choice of unit cell is that $\beta$ should be as close to 90° as possible so that correlations in refinement are minimized.

The equivalent positions of a point x,y,z generated by the symmetry operators in the space group $P2_1/c$ are;

(1) x,y,z

(2) -x,-y,-z

(3) $x,\frac{1}{2}-y,\frac{1}{2}+z$ and

(4) $-x,\frac{1}{2}+y,\frac{1}{2}-z$

(2) is related to (1) by the inversion centre at the origin. (3) is generated by the reflection of (1) through the glide plane followed by a translation of c/2 and (4) by rotation of (1) about the screw axis followed by a translation of b/2. So that the positions generated by

the screw axis and the glide plane are related by the centre of symmetry at the origin, the cell is chosen such that the c-glide plane is at $y = \frac{1}{4}$ and the $2_1$ screw axis is at $x = 0$, $z = \frac{1}{4}$.

If the cell is redefined as described above the equivalent positions now include a translational component in x and become;

(1) x,y,z

(2) -x,-y,-z

(3) $\frac{1}{2}+x, \frac{1}{2}-y, \frac{1}{2}+z$ and

(4) $\frac{1}{2}-x, \frac{1}{2}+y, \frac{1}{2}-z$

6.4.7 Conditions limiting diffraction

Inspection of a set of diffraction data may reveal that certain reflections have zero intensity: that there are 'systematic absences' in the data. These absences arise because of the cancellation of diffracted beams which are directly out of phase and they reveal the presence of lattice centring and translational symmetry elements. For example, if all reflections of the type hkl are absent when $h+k = 2n+1$ a C-centred lattice is indicated and if they are absent when $h+k+l = 2n+1$, a body-centred lattice is indicated (general systematic absences). If absences are noticed in h0l when $h+l = 2n+1$ an n-glide plane perpendicular to b is indicated and if in 0k0 when $k = 2n+1$ a two-fold axis parallel to b (special systematic absences).

6.4.8 The structure factor, $F_{hkl}$

The intensity of a particular reflection (hkl) will depend upon how the positions of the atoms are related to the planes of that particular set. The coordinates (x,y,z) of the atoms making up the contents of the asymmetric unit can be deduced from a comparison of the relative electron concentrations on a large number of different

sets of planes. The atom scattering factor, f, depends on the number of electrons in the atom and on how the electron density diminishes with the distance from the nucleus. At the nucleus it equals the atomic number of the atom. In this work, the scattering factors are taken from Reference 156.

Combination of the scattering factor, position and one or more parameters to account for thermal motion for all the atoms leads to the structure factor, $F_{hkl}$, for each measured reflection. $F_{hkl}$ is in general a complex quantity, but the observed amplitude $|F_{hkl}|$ is obtainable from the corresponding intensity. Explicitly,

$$I_{hkl} = F_{hkl}^2$$

If the structure is known, the structure factor may be calculated, but x, y and z cannot be calculated directly from the measured structure factors.

A periodic function, such as the electron density distribution in a crystal may be reproduced by summation of a Fourier series, which should be infinite but in practice is limited by the range of hkl available. To carry out the Fourier synthesis, both the coefficients of the various harmonics $|F_{o(hkl)}|$ and their phases $\alpha_{hkl}$ must be known. The phase, however, cannot be directly observed. This is the celebrated phase problem of X-ray crystallography. For centrosymmetric structures the problem reduces to one of determining correct signs for each $|F_o|$ and

$$F_{hkl} = \sum_{r=1}^{N} f_r \cos 2\pi(hx_r + ky_r + lz_r)$$

where $f_r$ is the scattering factor for the rth atom. Several methods of circumventing it are available, each depending upon finding a

solution in which the positions of some of the atoms are known approximately, a 'trial structure'. These methods will be discussed later. Calculation of the structure factors for the known atoms will give calculated signs that are right. A Fourier synthesis using observed $|F_o|$ but calculated signs will show positions for many other atoms. Repetition of the process, adding the new atoms to the trial structure is continued until all the atomic parameters are known.

When approximate positions have been found for all the atoms in the asymmetric unit it is necessary to refine the solution to obtain the best possible structure. Least-squares refinement calculates and applies small shifts in the atomic parameters and the overall scale factor K to improve the agreement between $|F_o|$ and $|F_c|$. The quantity minimized is $\sum w(F_o - F_c)^2$, the summation being over all reflections, and w is a weighting factor for each term. Least-squares refinement requires that the data be in great excess over the number of parameters to be refined. In crystallographic analysis the ratio of data to parameters is usually between 7 and 12. The R factor is one measure of the correctness of a structure determination. However, it is only a measure of the precision of the fit of the model used to the experimental data, not a measure of accuracy of the structure. R is defined as,

$$R = \frac{\sum|(K|F_o| - |F_c|)|}{\sum(K|F_o|)}$$

A measurement of precision is afforded by the estimated standard deviation, e.s.d. or $\sigma$, of the final parameters and an example will illustrate its usefulness. Consider two C-C bonds having lengths of 1.377 and 1.388 Å, each with an e.s.d. of 0.009 Å, generally written as 1.377(9) and 1.388(9) Å. The difference is 0.011 Å which, being less than $3\sigma$, is usually described as 'not significant'. If the

e.s.d.'s were 0.002 Å, i.e. 1.377(2) and 1.388(2) Å, the difference now being greater than $3\sigma$ would be considered to be 'significant'.

6.4.9 The Patterson function

Although it is not possible to compute the electron-density map directly because of the uncertainty about the phases of $|F_o|$, there is no such uncertainty about $|F_o|^2$ values. From these the Patterson function $P_{uvw}$, which is always centrosymmetric, can be computed directly. The resulting 'Patterson map' is a three-dimensional vector map in which each peak (maximum) arises from two atoms in the real unit cell. Each peak is situated at a distance and in a direction from the origin corresponding to the vector between the two atoms in the real unit cell which gives rise to it. A peak in the Patterson map at u,v,w implies that there are two atoms in the structure at $x_1,y_1,z_1$ and $x_2,y_2,z_2$ such that $x_2 - x_1 = u$, $y_2 - y_1 = v$ and $z_2 - z_1 = w$ The height of the peak is proportional to the product of the atomic numbers of the two atoms concerned. The peaks due to metal atoms are very much higher than any others in the map and are therefore readily identified. If a compound contains one or more atoms of relatively high atomic number, e.g. Ni in a structure containing otherwise only C, H, N and O the contribution due to the 'heavy atom' will be dominant. Because of this dominance it is usually possible to find its coordinates by Patterson methods and produce a partial structure.

6.4.10 Direct methods

For crystals in which the molecules contain only C, H, N and O it would be possible to produce a Fourier synthesis by systematically trying combination of the large number of sign combinations for each

$|F_o|$. A great proportion of these maps would be readiy recognisable as incorrect either because they contain extensive regions of negative electron-density or because they fail to meet the requirement that the asymmetric unit must contain positive regions of the right number, size, and shape to correspond to the known number of atoms in the molecule. A statistical treatment is used to produce the most probable sets of signs. Only the strongest terms are used and the method produces a small number of probable sets of signs and usually one of these sets leads to a promising Fourier synthesis with maxima in chemically reasonable positions.

6.4.11 Thermal parameters

The vibration of an atom can be allowed for by adding a term, U to the atomic parameters in the structure factor calculation. This gives a simple model of the atom vibrating isotropically. If sufficient data are available a more sophisticated treatment is possible representing the vibration by an ellipsoid (anisotropic vibration). Six parameters are necessary to describe such an ellipsoid, three giving the radii along its principal axes and three giving its orientation in space. The vibration is defined by a symmetric tensor characterized by three diagonal elements, $U_{11}$, $U_{22}$, and $U_{33}$ and three off-diagonal elements, $U_{12}$, $U_{13}$, and $U_{23}$.

6.4.12 Hydrogen atoms

Hydrogen atoms are difficult to locate because hydrogen only has one electron and, furthermore the electron density drawn from the nucleus into the covalent bond. However, they can often be located by calculation of a difference-Fourier map using only those reflections for which $\sin\theta/\lambda < 0.35$; i.e. the low angle reflections

($\theta <$ ca. 14°). Below this angle the relative contribution of the hydrogen atoms to the total scattering power is at its highest.

6.4.13 Absorption effects

An X-ray beam travelling through matter is attenuated by interaction with the electrons of the atoms in addition to any scattering effect. The reduction in intensity is given by;

$$I = I_o e^{-\mu t}$$

where $I_o$ is the initial intensity of the beam, I is the reduced intensity after travelling a distance t through the substance and $\mu$ is the linear absorption coefficient, which is dependent on the X-ray wavelength. The absorption coefficient is calculated from tables using the formula and density of the crystal. As the distance t varies with $\theta$, irregular crystals can present a different pathlength at different $\theta$. Applying a correction to the intensity measurements is not a straightforward matter. The shape and dimensions of the crystal must be known and a correction must be calculated for each reflection. Depending upon the magnitude of $\mu$, it is possible to deal with absorption effects in a number of different ways. For crystals containing only 'light' atoms, the absorption correction is minimal and it is acceptable to ignore it. Even for structures containing a few atoms of intermediate mass, with a short wavelength radiation such as Mo-K$\alpha$, errors arising from absorption effects are still quite small. In the present study, an empirical absorption correction program has been applied only in the cases of the complexes of cadmium (which also contain bromine atoms).[155]

## References


1. L. F. Lindoy, The Chemistry of Macrocyclic Ligand Complexes, Cambridge University Press, Cambridge, 1989.

2. G. A. Melson, in Coordination Chemistry of Macrocyclic Compounds, ed. G. A. Melson, Plenum, New York, 1979, 2.

3. The U. K. Macrocycles Group was affiliated to the Royal Society of Chemistry at Manchester in 1991.

4. R. W. Hay, Bio-inorganic Chemistry, Ellis Horwood, Chichester, 1987.

5. A. M. Sargeson, presented at the 16th International Symposium on Macrocyclic Chemistry, Sheffield, 1991.

6. P. A. Tasker, presented at the 14th International Symposium on Macrocyclic Chemistry, Townsville, 1989.

7. S. K. Cabbiness and D. W. Margerum, J. Am. Chem. Soc., 1969, 91, 6540.

8. S. K. Cabbiness and D. W. Margerum, J. Am. Chem. Soc., 1970, 92, 2151.

9. G. B. Reibnegger and B. M. Rode, Inorg. Chim. Acta, 1983, 72, 47.

10. G. Schwarzenbach, Helv. Chim. Acta, 1952, 35, 2344.

11. R. D. Hancock and A. E. Martell, Comments Inorg. Chem., 1988, 6, 237.

12. R. D. Hancock, Pure Appl. Chem., 1986, 58, 1445.

13. D. J. Cram, T. Kaneda, R. C. Helgeson, S. B. Brown, C. B. Knobler, E. Maverick, and K. N. Trueblood, J. Am. Chem. Soc., 1985, 107, 3645.

14. G. J. McDougall, R. D. Hancock and J. C. A. Boeyens, J. Chem. Soc., Dalton Trans., 1978, 1438.

15. A. Anichini, L. Fabbrizzi, P. Paoletti and R. M. Clay, J. Chem. Soc., Dalton Trans., 1978, 577.

16. D. H. Busch, K. Farmery, V. Goedken, V. Katovic, A. C. Melnyk, C. R. Sperati, and N. Tokel, Adv. Chem. Ser., 1971, 100, 52.

17. J-M. Lehn, Angew. Chem., Int. Ed. Engl., 1988, 27, 89.

18. D. H. Busch, Proceedings of the 14th International Symposium on Macrocyclic Chemistry, Townsville, 1989.

19. S. Imajo, K. Nakanishi, M. Roberts, S. J. Lippard and T. Nozoe, J. Am. Chem. Soc., 1983, 105, 2071.

20. K. R. Adam, K. P. Dancey, B. A. Harrison, A. J. Leong, L. F. Lindoy, M. McPartlin and P. A. Tasker, J. Chem. Soc., Chem. Commun., 1983, 1351.

21. K. R. Adam, A. J. Leong, L. F. Lindoy, H. C. Lip, B. W. Skelton and A. H. White, J. Am. Chem. Soc., 1983, 105, 4645.

22. D. H. Busch, Acc. Chem. Res., 1978, 11, 392.

23. K. Henrick, P. A. Tasker and L. F. Lindoy, Prog. in Inorg. Chem., 1985, 33, 1.

24. G. Anderegg, A. Ekstrom, L. F. Lindoy and R. J. Smith, J. Am. Chem. Soc., 1980, 102, 2670.

25. K. Henrick, L. F. Lindoy, M. McPartlin, P. A. Tasker and M. P. Wood, J. Am. Chem. Soc., 1984, 106, 1641.

26. A. Ekstrom, L. F. Lindoy, H. C. Lip, R. J. Smith, H. J. Goodwin, M. McPartlin and P. A. Tasker, J. Chem. Soc., Dalton Trans., 1979, 1027.

27. L. P. Battaglia, A. B. Corradi and A. Mangia, Inorg. Chim. Acta, 1980, 39, 211.

28. K. R. Adam, L. F. Lindoy, R. J. Smith, G. Anderegg, K. Henrick, M. McPartlin and P. A. Tasker, J. Chem. Soc., Chem. Commun., 1979, 812.

29. H. J. Goodwin, K. Henrick, L. F. Lindoy, M. McPartlin and P. A. Tasker, Inorg. Chem., 1982, 21, 3261.

30. M. Micheloni, P. Paoletti and A. Vacca, J. Chem. Soc., Perkin Trans. 2, 1978, 945.

31. A. E. Martell and R. J. Motekaitis, The Determination and Use of Stability Constants, VCH Publishing, New York, 1988.

32. F. L. Urbach, in Coordination Chemistry of Macrocyclic Compounds, ed. G. A. Melson, Plenum, New York, 1979, 345.

33. L. Sabatini and L. Fabbrizzi, Inorg. Chem., 1979, 18, 438.

34. M. Sugimoto, J. Fujita, H. Ito, K. Toriumi and T. Ito, Inorg. Chem., 1983, 22, 955.

35. M. Sugimoto, H. Ito, K. Toriumi and T. Ito, Acta Crystallogr., Sect. B, 1982, B38, 2453.

36. R. I. Haines and A. McAuley, Coord. Chem. Rev., 1981, 39, 77.

37. L. Pauling, The Nature of the Chemical Bond, 3rd edn., Cornell University Press, Ithaca, 1960, 249.

38. K. R. Adam, M. Antolovich, L. G. Brigden, A. J. Leong, L. F. Lindoy, P. J. Baillie, D. K. Uppal, M. McPartlin, B. Shah, D. Proserpio, L. Fabbrizzi and P. A. Tasker, J. Chem. Soc., Dalton Trans., 1991, 2493.

39. F. A. Cotton and G. Wilkinson, Advanced Inorganic Chemistry, 3rd edn., Wiley, New York, 1972.

40. D. C. Liles, M. McPartlin and P. A. Tasker, J. Chem. Soc., Dalton Trans., 1987, 1631.

41. M. G. B. Drew and S. Hollis, J. Chem. Soc., Dalton Trans., 1978, 511.

42. L. F. Lindoy, in Progress in Macrocyclic Chemistry, eds. R. M. Izatt and J. J. Christensen, Wiley, New York, 1987, p. 53.

43. L. F. Lindoy, H. C. Lip, J. H. Rea, R. J. Smith, K. Henrick, M. McPartlin and P. A. Tasker, Inorg. Chem., 1980, 19, 3360.

44. K. R. Adam, B. J. McCool. A. J. Leong, L. F. Lindoy, C. W. G. Ansell, P. J. Baillie, K. P. Dancey, L. A. Drummond, K. Henrick, M. McPartlin, D. K. Uppal and P. A. Tasker, J. Chem. Soc., Dalton Trans., 1990, 3435.

45. C. W. G. Ansell, M. McPartlin, P. A. Tasker and A. Thambythurai, Polyhedron, 1983, 2, 83.

46. S. N. Vinogradov and R. H. Linnell, Hydrogen Bonding, Van Nostrand Reinhold, New York, 1971.

47. G. C. Pimentel and A. L. McClellan, Ann. Revs. Phys. Chem., 1971, 22, 347.

48. M. D. Joesten and L. J. Schaad, Hydrogen Bonding, Dekker, New York, 1974.

49. R. Taylor and O. Kennard, Acc. Chem. Res., 1984, 17, 320.

50. B. Bosnich, C. K. Poon and M. L. Tobe, Inorg. Chem., 1965, 4, 1102.

51. R. W. Hay and M. T. H. Tarafder, J. Chem. Soc., Dalton Trans., 1991, 823.

52. L. A. Drummond, K. Henrick, M. J. L. Kanagasundaram, L. F. Lindoy, M. McPartlin and P. A. Tasker, Inorg. Chem., 1982, 21, 3923.

53. K. R. Adam, C. W. G. Ansell, K. P. Dancey, L. A. Drummond, A. J. Leong, L. F. Lindoy and P. A. Tasker, J. Chem. Soc., Chem. Commun., 1986, 1011.

54. L. F. Lindoy, in Current Topics in Macrocyclic Chemistry in Japan, ed. E. Kimura, 1987, p. 78.

55. M. Green, J. Smith and P. A. Tasker, Inorg. Chim. Acta, 1971, 5, 17.

56. P. G. Owston, R. Peters, E. Ramsammy, P. A. Tasker and J. Trotter, J. Chem. Soc., Chem. Commun., 1980, 1218.

57. P. A. Tasker, personal communication.

58. K. P. Dancey, Ph. D. Thesis, The Polytechnic of North London, 1982.

59. K. Henrick, P. M. Judd, P. G. Owston, R. Peters, P. A. Tasker and R. W. Turner, J. Chem. Soc., Chem. Commun., 1983, 1253.

60. R. Peters, Ph. D. Thesis, The Polytechnic of North London, 1981.

61. L. A. Drummond, Ph. D. Thesis, The Polytechnic of North London, 1990.

62. G. M. Sheldrick and J. Trotter, Acta Crystallog., Sect. B, 1978, B34, 3122.

63. S. C. Wallwork, Acta Crystallogr., 1962, 15, 758.

64. A. Novak, Struct. Bonding, 1974, 18, 177.

65. K. Mislow and M. Raban, Top. Stereochem., 1967, 1, 1.

66. D. H. Williams and I. Fleming, Spectroscopic Methods in Organic Chemistry, 3rd edn., McGraw Hill, London, 1980.

67. S. Waikar, Ph. D. Thesis, University of North London, 1992.

68. D. E. Fenton, B. P. Murphy, A. J. Leong, L. F. Lindoy, A. Bashall and M. McPartlin, J. Chem. Soc., Dalton Trans., 1987, 2543.

69. T. H. Siddall and W. E. Stewart, Prog. Nucl. Magn. Reson. Spectrosc., 1969, 5, 33.

70. E. Breitmaier and W. Voelter, $^{13}C$ NMR Spectroscopy, Verlag Chemie, Weinheim, 1978, p. 213.

71. J. K. M. Sanders and B. K. Hunter, Modern NMR Spectroscopy, Oxford University Press, Oxford, 1987.

72. D. Live and S. I. Chan, J. Am. Chem. Soc., 1976, 98, 3769.

73. P. R. Srinivasan and R. L. Lichter, J. Mag. Reson., 1977, 28, 227.

74. R. L. Lichter, in The Multinuclear Approach to NMR Spectroscopy, eds. J. B. Lambert and F. G. Riddell, Reidel, Dordrecht, 1983, p. 222; G. C. Levy and R. L. Lichter, Nitrogen-15 Nuclear Magnetic Resonance Spectroscopy, Wiley-Interscience, New York, 1979.

75. G. Binsch, J. B. Lambert, B. W. Roberts and J. D. Roberts, J. Am. Chem. Soc., 1964, 86, 5564; A. J. R. Bourn and E. W. Randall, Mol. Phys., 1964, 8, 567.

76. K. Kiss-Eröss, in Wilson and Wilson's Comprehensive Analytical Chemistry, ed. G. Svehla, Elsevier, Amsterdam, 1976, vol. 6, 288.

77. F. W. McLafferty, Interpretation of Mass Spectra, 2nd edn., W. A. Benjamin, Reading, Mass., 1973.

78. M. Kodama and E. Kimura, J. Chem. Soc., Dalton Trans., 1980, 327.

79. R. D. Hancock and M. P. Ngwenya, J. Chem. Soc., Dalton Trans., 1987, 2911.

80. R. C. Luckay and R. D. Hancock, J. Chem. Soc., Dalton Trans., 1991, 1491.

81. M. Bartolini, A. Bianchi, M. Micheloni and P. Paoletti, J. Chem. Soc., Perkin Trans. 2, 1982, 1345.

82. A. P. Leugger, L. Hertli and T. A. Kaden, Helv. Chim. Acta, 1978, 61, 2296.

83. M. Micheloni, A. Sabatini and P. Paoletti, J. Chem. Soc., Perkin Trans. 2, 1978, 828.

84. C. Mave and M. R. Truter, J. Chem. Soc., Dalton Trans., 1974, 2351.

85. A. Mangia and A. Tiripicchio, Cryst. Struct. Commun., 1979, 8, 699.

86. C. J. Ballhausen, Introduction to Ligand Field Theory, McGraw-Hill, New York, 1962.

87. N. F. Curtis and Y. M. Curtis, Inorg. Chem., 1965, 4, 804.

88. C. C. Addison and B. M. Gatehouse, J. Chem. Soc., 1960, 613.

89. T. Ito, M. Kato and H. Ito, Bull. Chem. Soc. Jpn., 1984, 57, 2641.

90. K. Kobiro, A. Nakayama, T. Hiro, M. Suwa and Y. Tobe, Inorg. Chem., 1992, 31, 676.

91. E. B. Fleischer and E. Klem, Inorg. Chem., 1965, 4, 637.

92. A. F. Cameron, D. W. Taylor and R. H. Nuttall, J. Chem. Soc., Dalton Trans., 1972, 422.

93. F. Walmsley, A. A. Pinkerton and J. A. Walmsley, Polyhedron, 1989, 8, 689.

94. P. Gallezot, D. Weigel and M. Prettre, Acta Crystallogr., 1967, 22, 699.

95. E. C. Alyea, G. Ferguson and R. J. Restivo, Inorg. Chem., 1975, 14, 2491.

96. V. J. Thom, C. C. Fox, J. C. A. Boeyens and R. D. Hancock, J. Am. Chem. Soc., 1984, 106, 5947.

97. J. W. F. M. Schoonhoven, W. L. Driessen, J. Reedijk and G. C. Verschoor, J. Chem. Soc., Dalton Trans., 1984, 1053.

98. G. A. Pearse, P. R. Raithby, C. M. Hay and J. Lewis, Polyhedron, 1989, 8, 305.

99. J. L. Atwood, S. G. Bott and R. L. Vincent, J. Cryst. Spectrosc., 1990, 20, 631.

100. K. Kashiwabara, K. Hanaki and J. Fujita, Bull. Chem. Soc. Jpn., 1980, 53, 2275; S. Sato and Y. Saito, Acta Crystallogr., Sect. B, 1975, B31, 1378.

101. L. Y. Martin, C. R. Sperati and D. H. Busch, J. Am. Chem. Soc., 1977, 99, 2968.

102. IUPAC Commission on the Nomenclature of Inorganic Chemistry, K. A. Jensen (Chairman), Inorg. Chem., 1970, 9, 1.

103. F. A. L. Anet in Conformational Analysis, Scope and Present Limitations, ed. G. Chiurdoglu, Academic Press, New York, 1971.

104. E. L. Eliel, N. L. Allinger. S. J. Angyal and G. A. Morrison, Conformational Analysis, Wiley Interscience, New York, 1967.

105. E. L. Eliel, Stereochemistry of Carbon Compounds, McGraw-Hill, New York, 1962.

106. N. Y. C. Choi, personal communication.

107. A. H. Norbury and A. I. P. Sinha, Quart. Rev., 1970, 24, 69.

107a. M. Sugimoto, M. Monoyama, T. Ito and J. Fujita, Inorg. Chem., 1983, 22, 950.

108. C. K. Jörgensen, Absorption Spectra and Chemical Bonding in Complexes, Pergamon, Oxford, 1962.

109. A. B. P. Lever, Inorganic Electronic Spectroscopy, Elsevier, Amsterdam, 1968.

110. R. A. D. Wentworth and T. S. Piper, Inorg. Chem., 1965, 4, 709; R. A. D. Wentworth and T. S. Piper, Inorg. Chem., 1965, 4, 1524.

111. G. R. Brubaker and D. H. Busch, Inorg. Chem., 1966, 5, 2114.

112. R. J. Deeth and C. M. Kemp, J. Chem. Soc., Dalton Trans., 1992, 2013.

113. M. Gerloch, J. H. Harding and R. G. Woolley, Struct. Bonding, 1981, 46, 1.

114. D. P. Rillema, J. F. Endicott and E. Papaconstantinou, Inorg. Chem., 1971, 10, 1739.

115. F. V. Lovecchio, E. S. Gore and D. H. Busch, J. Am. Chem. Soc., 1974, 96, 3109.

116. L. I. Denisovich, N. V. Zakurin, A. A. Bezrukova and S. P. Gubin, J. Organomet. Chem., 1974, 81, 207.

117. G. De Santis, M. Di Casa, M. Mariani, B. Seghi and L. Fabbrizzi, J. Am. Chem. Soc., 1989, 111, 2422.

118. A. A. G. Tomlinson, M. Bonamico, G. Dessy, V. Fares and L. Scaramuzza, J. Chem. Soc., Dalton Trans., 1972, 1671.

119. B. Shah, undergraduate project, The Polytechnic of North London, 1985.

120. K. Nakamoto, Infrared Spectra of Inorganic and Co-ordination Compounds, 2nd edn., Wiley, New York, 1970.

121. S. S. Tandon and V. McKee, J. Chem. Soc., Dalton Trans., 1989, 19.

122. CRC Handbook of Chemistry and Physics, ed. R. C. Weast, 66th edn., CRC Press, Boca Raton, 1985.

123. D. S. Brown, J. D. Lee, B. G. A. Melsom, B. J. Hathaway, I. M. Proctor and A. A. G. Tomlinson, J. Chem. Soc., Chem. Commun., 1967, 369.

124. A. McAuley, S. Subramanian and T. W. Whitcombe, J. Chem. Soc., Chem. Commun., 1987, 539.

125. C. W. G. Ansell, K. P. Dancey, M. McPartlin, P. A. Tasker and L. F. Lindoy, J. Chem. Soc., Dalton Trans., 1983, 1789.

126. N. W. Alcock, E. H. Curzon and P. Moore, J. Chem. Soc., Dalton Trans., 1984, 2813.

127. N. W. Alcock, E. H. Curzon, P. Moore and C. Pierpoint, J. Chem. Soc., Dalton Trans., 1984, 605.

128. A. Bencini, A. Bianchi, M. Castello, M. Di Vaira, J. Faus, E. Garcia-Espana, M. Micheloni and P. Paoletti, Inorg. Chem., 1989, 28, 347.

129. M. Elder, S. E. Hull, P. A. Machin and O. S. Mills, Crystal Structure Search Retrieval (CSSR) System, 3rd edn., SERC Daresbury Laboratory, Warrington, WA4 4AD, UK, 1985.

130. D. Altermatt, H. Arend, A. Niggli and W. Petter, Mater. Res. Bull., 1979, 14, 1391.

131. A. Daoud, R. Perret and Y. Dusausoy, Acta Crystallogr. Sect. B, 1979, 35, 2718.

132. J. C. J. Bart, I. W. Bassi, M. Calcaterra, Phosphorus and Sulfur, 1981, 9, 347.

133. I. Casals, P. Gonzalez-Duarte, J. Sola, M. Font-Bardia, J. Solans and X. Solans, J. Chem. Soc., Dalton Trans., 1987. 2391.

134. S. M. Nelson, S. G. McFall, M. G. B. Drew, A. H. bin Othman and N. B. Mason, J. Chem. Soc., Chem. Commun., 1977, 167.

135. M. G. B. Drew, S. G. McFall and S. M. Nelson, J. Chem. Soc., Dalton Trans., 1979, 575.

136. M. Micheloni and P. Paoletti, Inorg. Chim. Acta, 1980, 43, 109.

137. V. J. Thom, G. D. Hosken and R. D. Hancock, Inorg. Chem., 1985, 24, 3378.

138. M. Kodama and E. Kimura, J. Chem. Soc., Dalton Trans., 1977. 2269.

139. A. E. Martell and R. M. Smith, Critical Stability Constants, Plenum Press, New York, 1974.

140. L. F. Lindoy, personal communication, 1991.

141. R. W. G. Wyckoff, Crystal Structures, Vol. 1, 2nd edn., Interscience, New York, 1963, p. 267.

142. R. D. Shannon, Acta Crystallogr. Sect. A, 1976, A32, 751.

143. J. L. Hoard, in Porphyrins and Metalloporphyrins, ed. K. M. Smith, Elsevier, Amsterdam, 1975.

144. P. F. Rodesiler, E. A. H. Griffith, W. G. Charles, L. Lebioda and E. L. Amma, Inorg. Chem., 1985, 24, 4595.

145. J. L. Sessler, T. Murai and V. Lynch, Inorg. Chem., 1989, 28, 1333; J. L. Sessler, T. Murai, V. Lynch and M. Cyr, J. Am. Chem. Soc., 1988, 110, 5586.

146. V. M. Micovic and M. L. Mihailovic, J. Org. Chem., 1953, 18, 1190.

147. M. Harfenist, A. Bavley and W. A. Lazier, J. Org. Chem., 1954, 19, 1608.

148. see for example L. S. Dent Glasser, Crystallography and its Applications, Van Nostrand-Reinhold, New York, 1977; J. P. Glusker and K. N. Trueblood, Crystal Structure Analysis, a Primer, 2nd edn., Oxford University Press, New York, 1985.

149. G. M. Sheldrick, SHELX76 Program for Crystal Structure Solution, University of Cambridge, 1976.

150. G. M. Sheldrick, SHELX86 Program for Crystal Structure Solution, University of Göttingen, 1986.

151. G. M. Sheldrick, SHELX90 Program for Crystal Structure Refinement, University of Göttingen, 1990.

152. C. K. Johnson, ORTEP II, Report ORNL-5138, Oak Ridge National Laboratory, Oak Ridge, Tennessee, 1976.

153. J. Hornstra and B. Stubbe, PW1100 Data Processing Program, Philips Research Laboratories, Eindhoven, The Netherlands, 1972.

154. International Tables for X-Ray Crystallography, Vol. I, 2nd edn., ed. N. F. M. Henry and K. Lonsdale, The Kynoch Press, Birmingham, 1965.

155. D. Stuart and N. Walker, Acta Crystallogr., Sect. A, 1983, A39, 158.

156. D. Cromer and J. Mann, Acta Crystallogr., Sect. A, 1968, A24, 321.

# APPENDIX

Tables of Fractional Atomic Coordinates, Thermal Parameters, Bond Lengths and Bond Angles for,

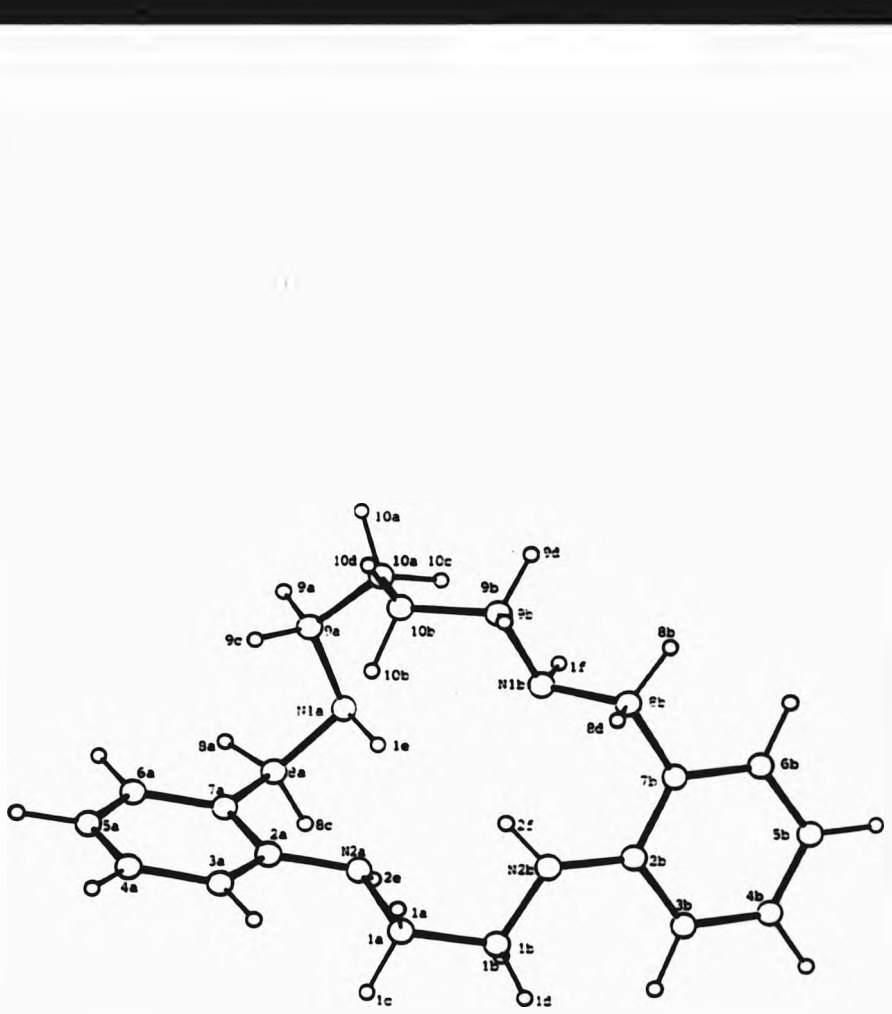


FIGURE A1 Labelled diagram of the ligand $L^{16}$.

Table A1.1 Fractional atomic coordinates and thermal parameters ( $Å^2$) for $L^{16}$

| Atom | x | y | z | $U_{iso}$ or $U_{eq}$ |
|---|---|---|---|---|
| N(2a) | 0.3620(2) | -0.0793(6) | -0.0686(4) | 0.045(3) |
| N(1a) | 0.4929(2) | 0.0981(7) | -0.1377(4) | 0.057(4) |
| N(2b) | 0.3167(2) | 0.1174(6) | 0.1318(4) | 0.049(3) |
| N(1b) | 0.3833(2) | 0.3815(6) | 0.0256(4) | 0.046(3) |
| C(3a) | 0.3029(4) | -0.1736(8) | -0.2538(7) | 0.065(5) |
| C(4a) | 0.3047(6) | -0.2217(9) | -0.3717(8) | 0.090(7) |
| C(5a) | 0.3667(7) | -0.2248(10) | -0.4256(8) | 0.102(8) |
| C(6a) | 0.4258(5) | -0.1731(9) | -0.3596(6) | 0.078(6) |
| C(3b) | 0.3422(3) | 0.1115(8) | 0.3484(6) | 0.055(4) |
| C(4b) | 0.3640(4) | 0.1868(11) | 0.4524(6) | 0.070(6) |
| C(5b) | 0.3826(4) | 0.3462(10) | 0.4511(6) | 0.070(6) |
| C(6b) | 0.3786(3) | 0.4257(9) | 0.3426(6) | 0.060(5) |
| C(1a) | 0.2999(3) | -0.1067(7) | -0.0039(5) | 0.049(2) |
| C(2a) | 0.3627(3) | -0.1256(7) | -0.1882(5) | 0.048(2) |
| C(7a) | 0.4256(3) | -0.1243(8) | -0.2423(6) | 0.055(2) |
| C(8a) | 0.4915(3) | -0.0687(8) | -0.1757(6) | 0.063(2) |
| C(9a) | 0.4942(3) | 0.2113(7) | -0.2384(5) | 0.058(2) |
| C(10a) | 0.4728(3) | 0.3752(8) | -0.1977(6) | 0.062(2) |
| C(1b) | 0.3106(3) | -0.0561(7) | 0.1240(5) | 0.053(2) |
| C(2b) | 0.3385(3) | 0.1897(7) | 0.2379(5) | 0.043(2) |
| C(7b) | 0.3563(3) | 0.3530(7) | 0.2372(5) | 0.044(2) |
| C(8b) | 0.3465(3) | 0.4480(7) | 0.1239(5) | 0.052(2) |
| C(9b) | 0.3723(3) | 0.4782(8) | -0.0829(5) | 0.054(2) |
| C(10b) | 0.3944(3) | 0.3916(8) | -0.1917(5) | 0.059(2) |

Table A1.2 Fractional atomic coordinates for the found hydrogen atoms for $L^{16}$

| Atom | x | y | z |
|---|---|---|---|
| H(2e) | 0.4088 | -0.1164 | -0.0193 |
| H(1e) | 0.4397 | 0.1016 | -0.0962 |
| H(2f) | 0.3352 | 0.1454 | 0.0594 |
| H(1f) | 0.4351 | 0.3974 | 0.0569 |

Table A1.3 Anisotropic thermal parameters ( $Å^2$ ) for $L^{16}$

| Atom | $U_{11}$ | $U_{22}$ | $U_{33}$ | $U_{23}$ | $U_{13}$ | $U_{12}$ |
|---|---|---|---|---|---|---|
| N(2a) | 0.035(3) | 0.049(3) | 0.053(3) | 0.000(3) | 0.006(2) | 0.001(2) |
| N(1a) | 0.043(3) | 0.077(4) | 0.051(3) | 0.011(3) | 0.010(3) | -0.005(3) |
| N(2b) | 0.048(3) | 0.036(3) | 0.063(4) | -0.006(3) | 0.010(3) | 0.000(3) |
| N(1b) | 0.055(3) | 0.046(3) | 0.038(3) | 0.009(3) | 0.015(2) | 0.004(3) |
| C(3a) | 0.072(5) | 0.045(4) | 0.077(5) | -0.011(4) | -0.014(4) | 0.003(4) |
| C(4a) | 0.152(10) | 0.051(5) | 0.068(6) | -0.013(5) | -0.042(6) | 0.005(6) |
| C(5a) | 0.200(12) | 0.055(6) | 0.051(6) | -0.011(5) | -0.012(7) | 0.036(7) |
| C(6a) | 0.131(7) | 0.059(5) | 0.042(4) | 0.002(4) | 0.011(5) | 0.019(5) |
| C(3b) | 0.045(4) | 0.069(5) | 0.052(4) | 0.014(4) | 0.019(3) | 0.009(4) |
| C(4b) | 0.073(5) | 0.096(7) | 0.039(5) | 0.009(5) | 0.009(4) | 0.014(5) |
| C(5b) | 0.079(6) | 0.086(6) | 0.043(5) | -0.013(5) | 0.013(4) | 0.005(5) |
| C(6b) | 0.057(5) | 0.064(5) | 0.058(5) | -0.010(4) | 0.020(4) | 0.001(4) |

Table A1.4 Bond lengths ( Å) for $L^{16}$

| | | | |
|---|---|---|---|
| N(2a) -C(1a) | 1.467(8) | N(2a) -C(2a) | 1.399(8) |
| N(2a) -H(2e) | 1.074(4) | N(1a) -C(8a) | 1.464(9) |
| N(1a) -C(9a) | 1.478(8) | N(1a) -H(1e) | 1.162(5) |
| N(2b) -C(1b) | 1.465(8) | N(2b) -C(2b) | 1.375(8) |
| N(2b) -H(2f) | 0.941(5) | N(1b) -C(8b) | 1.468(8) |
| N(1b) -C(9b) | 1.466(8) | N(1b) -H(1f) | 1.047(5) |
| C(1a) -C(1b) | 1.497(8) | C(2a) -C(3a) | 1.387(9) |
| C(2a) -C(7a) | 1.401(9) | C(3a) -C(4a) | 1.386(12) |
| C(4a) -C(5a) | 1.385(17) | C(5a) -C(6a) | 1.388(14) |
| C(6a) -C(7a) | 1.379(10) | C(7a) -C(8a) | 1.506(9) |
| C(9a) -C(10a) | 1.518(9) | C(10a)-C(10b) | 1.531(9) |
| C(2b) -C(3b) | 1.401(9) | C(2b) -C(7b) | 1.415(9) |
| C(3b) -C(4b) | 1.367(10) | C(4b) -C(5b) | 1.388(12) |
| C(5b) -C(6b) | 1.387(10) | C(6b) -C(7b) | 1.373(9) |
| C(7b) -C(8b) | 1.502(8) | C(9b) -C(10b) | 1.511(9) |

Table A1.5 Bond angles (°) for $L^{16}$

| | | | |
|---|---|---|---|
| C(2a) -N(2a) -C(1a) | 119.8(4) | H(2e) -N(2a) -C(1a) | 113.0(4) |
| H(2e) -N(2a) -C(2a) | 110.3(4) | C(9a) -N(1a) -C(8a) | 113.2(5) |
| H(1e) -N(1a) -C(8a) | 98.2(4) | H(1e) -N(1a) -C(9a) | 110.8(4) |
| C(2b) -N(2b) -C(1b) | 120.7(5) | H(2f) -N(2b) -C(1b) | 103.4(5) |
| H(2f) -N(2b) -C(2b) | 121.7(5) | C(9b) -N(1b) -C(8b) | 111.4(5) |
| H(1f) -N(1b) -C(8b) | 101.9(4) | H(1f) -N(1b) -C(9b) | 106.6(4) |
| C(1b) -C(1a) -N(2a) | 111.6(5) | C(3a) -C(2a) -N(2a) | 121.6(6) |
| C(7a) -C(2a) -N(2a) | 118.9(5) | C(7a) -C(2a) -C(3a) | 119.5(6) |
| C(4a) -C(3a) -C(2a) | 120.9(8) | C(5a) -C(4a) -C(3a) | 120.4(9) |
| C(6a) -C(5a) -C(4a) | 118.0(8) | C(7a) -C(6a) -C(5a) | 122.9(9) |
| C(6a) -C(7a) -C(2a) | 118.3(6) | C(8a) -C(7a) -C(2a) | 121.3(6) |
| C(8a) -C(7a) -C(6a) | 120.3(7) | C(7a) -C(8a) -N(1a) | 116.0(5) |
| C(10a)-C(9a) -N(1a) | 109.5(5) | C(10b)-C(10a)-C(9a) | 112.8(5) |
| C(1a) -C(1b) -N(2b) | 110.2(5) | C(3b) -C(2b) -N(2b) | 123.5(6) |
| C(7b) -C(2b) -N(2b) | 118.9(5) | C(7b) -C(2b) -C(3b) | 117.5(6) |
| C(4b) -C(3b) -C(2b) | 122.1(7) | C(5b) -C(4b) -C(3b) | 120.1(7) |
| C(6b) -C(5b) -C(4b) | 118.4(7) | C(7b) -C(6b) -C(5b) | 122.5(7) |
| C(6b) -C(7b) -C(2b) | 119.2(6) | C(8b) -C(7b) -C(2b) | 120.3(5) |
| C(8b) -C(7b) -C(6b) | 120.4(6) | C(7b) -C(8b) -N(1b) | 113.3(5) |
| C(10b)-C(9b) -N(1b) | 111.8(5) | C(9b) -C(10b)-C(10a) | 114.8(5) |

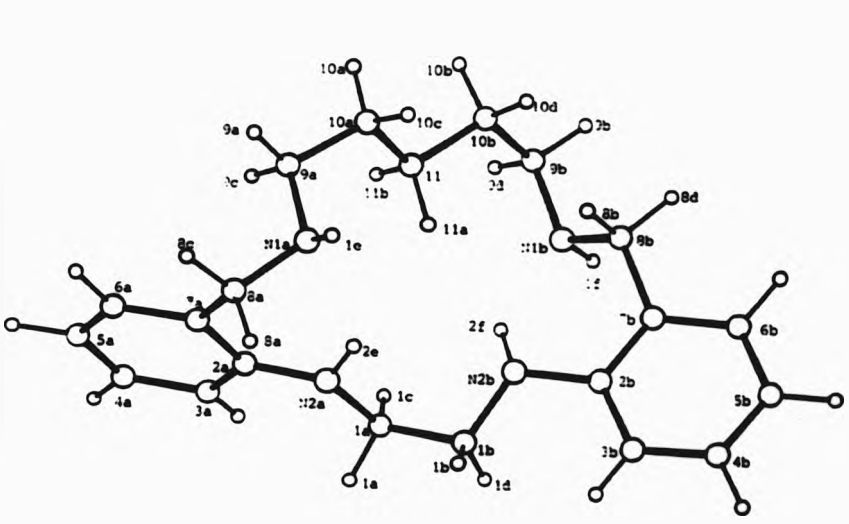


FIGURE A2 Labelled diagram of the ligand $L^{17}$.

Table A2.1 Fractional atomic coordinates and thermal parameters ( $Å^2$) for $L^{17}$

| Atom | x | y | z | $U_{iso}$ or $U_{eq}$ |
|---|---|---|---|---|
| N(2a) | 0.5023(3) | -0.1498(4) | 0.1510(5) | 0.052(3) |
| N(2b) | 0.2540(3) | -0.0446(4) | 0.1672(5) | 0.053(3) |
| N(1a) | 0.5886(4) | -0.1466(5) | 0.4768(5) | 0.064(3) |
| N(1b) | 0.1202(3) | -0.2567(5) | 0.2571(5) | 0.059(3) |
| C(9a) | 0.5843(5) | -0.2766(7) | 0.5468(7) | 0.067(4) |
| C(10a) | 0.4643(6) | -0.2972(6) | 0.5861(7) | 0.073(4) |
| C(11) | 0.3620(5) | -0.3208(6) | 0.4466(6) | 0.063(4) |
| C(9b) | 0.1388(5) | -0.3754(6) | 0.3497(8) | 0.080(5) |
| C(10b) | 0.2443(5) | -0.3545(6) | 0.4850(7) | 0.075(4) |
| C(1a) | 0.3989(5) | -0.1492(5) | 0.0230(6) | 0.056(1) |
| C(2a) | 0.5932(4) | -0.2481(5) | 0.1459(6) | 0.046(1) |
| C(3a) | 0.5949(5) | -0.3450(6) | 0.0194(7) | 0.062(2) |
| C(4a) | 0.6920(5) | -0.4353(6) | 0.0192(7) | 0.073(2) |
| C(5a) | 0.7847(5) | -0.4301(6) | 0.1408(7) | 0.071(2) |
| C(6a) | 0.7851(5) | -0.3375(6) | 0.2679(7) | 0.068(2) |
| C(7a) | 0.6902(4) | -0.2436(5) | 0.2736(6) | 0.053(1) |
| C(8a) | 0.6942(5) | -0.1392(6) | 0.4104(7) | 0.067(2) |
| C(1b) | 0.3180(4) | -0.0261(5) | 0.0481(6) | 0.056(1) |
| C(2b) | 0.1534(4) | 0.0393(5) | 0.1752(6) | 0.047(1) |
| C(3b) | 0.1371(4) | 0.1672(5) | 0.1129(6) | 0.053(1) |
| C(4b) | 0.0391(5) | 0.2502(6) | 0.1294(6) | 0.062(2) |
| C(5b) | -0.0439(5) | 0.2085(6) | 0.2029(6) | 0.067(2) |
| C(6b) | -0.0292(5) | 0.0828(6) | 0.2652(6) | 0.061(2) |
| C(7b) | 0.0700(4) | -0.0018(5) | 0.2560(6) | 0.048(1) |
| C(8b) | 0.0902(5) | -0.1276(6) | 0.3427(6) | 0.059(2) |

Table A2.2 Fractional atomic coordinates for the found hydrogen atoms for $L^{17}$

| Atom | x | y | z |
|---|---|---|---|
| H(2e) | 0.4847 | -0.1250 | 0.2358 |
| H(2f) | 0.2413 | -0.1453 | 0.1823 |
| H(1e) | 0.5871 | -0.0741 | 0.5381 |
| H(1f) | 0.0522 | -0.2761 | 0.1776 |
| H(1a) | 0.4342 | -0.1350 | -0.0733 |
| H(1c) | 0.3581 | -0.2411 | 0.0103 |
| H(3a) | 0.5334 | -0.3491 | -0.0561 |
| H(8a) | 0.6964 | -0.0433 | 0.3696 |
| H(8c) | 0.7799 | -0.1490 | 0.5022 |
| H(9a) | 0.6525 | -0.2790 | 0.6359 |
| H(9c) | 0.5958 | -0.3639 | 0.4653 |
| H(10a) | 0.4653 | -0.3803 | 0.6426 |
| H(10c) | 0.4409 | -0.2147 | 0.6517 |
| H(11a) | 0.3565 | -0.2297 | 0.3806 |
| H(11b) | 0.3747 | -0.4020 | 0.3743 |
| H(1b) | 0.3628 | 0.0610 | 0.0787 |
| H(1d) | 0.2667 | -0.0320 | -0.0510 |
| H(3b) | 0.1937 | 0.1941 | 0.0537 |
| H(8b) | 0.1612 | -0.1178 | 0.4282 |
| H(8d) | 0.0166 | -0.1400 | 0.3973 |
| H(9b) | 0.0621 | -0.3878 | 0.3909 |
| H(9d) | 0.1571 | -0.4572 | 0.2830 |
| H(10b) | 0.2571 | -0.4536 | 0.5316 |
| H(10d) | 0.2234 | -0.2744 | 0.5701 |

Table A2.3 Anisotropic thermal parameters ( $Å^2$) for $L^{17}$

| Atom | $U_{11}$ | $U_{22}$ | $U_{33}$ | $U_{23}$ | $U_{13}$ | $U_{12}$ |
|---|---|---|---|---|---|---|
| N(2a) | 0.038(2) | 0.063(3) | 0.054(3) | 0.009(2) | 0.010(2) | 0.008(2) |
| N(2b) | 0.038(2) | 0.061(3) | 0.061(3) | 0.024(2) | 0.016(2) | 0.006(2) |
| N(1a) | 0.086(4) | 0.052(3) | 0.053(3) | -0.006(3) | 0.003(3) | 0.008(3) |
| N(1b) | 0.052(3) | 0.055(3) | 0.069(3) | 0.007(3) | 0.007(3) | -0.005(2) |
| C(9a) | 0.067(4) | 0.077(5) | 0.056(4) | 0.011(4) | -0.009(4) | 0.009(3) |
| C(10a) | 0.089(5) | 0.077(4) | 0.055(4) | 0.016(4) | 0.017(4) | 0.018(4) |
| C(11) | 0.058(4) | 0.076(4) | 0.053(4) | 0.016(3) | 0.008(3) | 0.007(3) |
| C(9b) | 0.062(4) | 0.061(4) | 0.116(6) | 0.034(4) | 0.028(4) | 0.005(3) |
| C(10b) | 0.066(4) | 0.079(4) | 0.079(5) | 0.038(4) | 0.026(4) | 0.016(3) |

Table A2.4 Bond lengths ( Å) for $L^{17}$

| | | | |
|---|---|---|---|
| N(2a) -C(1a) | 1.461(6) | N(2a) -C(2a) | 1.392(6) |
| N(2a) -H(2e) | 0.839(4) | N(2b) -C(1b) | 1.453(8) |
| N(2b) -C(2b) | 1.399(6) | N(2b) -H(2f) | 1.010(4) |
| N(1a) -C(8a) | 1.467(8) | N(1a) -C(9a) | 1.469(8) |
| N(1a) -H(1e) | 0.839(4) | N(1b) -C(8b) | 1.455(7) |
| N(1b) -C(9b) | 1.474(8) | N(1b) -H(1f) | 0.942(4) |
| C(1a) -C(1b) | 1.510(7) | C(2a) -C(3a) | 1.388(7) |
| C(2a) -C(7a) | 1.412(7) | C(3a) -C(4a) | 1.393(8) |
| C(4a) -C(5a) | 1.346(8) | C(5a) -C(6a) | 1.366(8) |
| C(6a) -C(7a) | 1.399(8) | C(7a) -C(8a) | 1.489(8) |
| C(9a) -C(10a) | 1.514(10) | C(10a)-C(11) | 1.519(8) |
| C(11) -C(10b) | 1.513(9) | C(2b) -C(3b) | 1.400(8) |
| C(2b) -C(7b) | 1.409(8) | C(3b) -C(4b) | 1.384(8) |
| C(4b) -C(5b) | 1.362(9) | C(5b) -C(6b) | 1.381(8) |
| C(6b) -C(7b) | 1.391(7) | C(7b) -C(8b) | 1.500(8) |
| C(9b) -C(10b) | 1.516(8) | | |

Table A2.5 Bond angles (°) for $L^{17}$

| | | | |
|---|---|---|---|
| C(2a) -N(2a) -C(1a) | 120.5(4) | H(2e) -N(2a) -C(1a) | 112.7(4) |
| H(2e) -N(2a) -C(2a) | 118.0(4) | C(2b) -N(2b) -C(1b) | 117.8(4) |
| H(2f) -N(2b) -C(1b) | 115.1(4) | H(2f) -N(2b) -C(2b) | 112.7(4) |
| C(9a) -N(1a) -C(8a) | 112.6(5) | H(1e) -N(1a) -C(8a) | 108.3(5) |
| H(1e) -N(1a) -C(9a) | 112.9(5) | C(9b) -N(1b) -C(8b) | 112.3(5) |
| H(1f) -N(1b) -C(8b) | 104.4(4) | H(1f) -N(1b) -C(9b) | 108.3(4) |
| C(1b) -C(1a) -N(2a) | 111.0(4) | C(3a) -C(2a) -N(2a) | 123.0(4) |
| C(7a) -C(2a) -N(2a) | 117.7(4) | C(7a) -C(2a) -C(3a) | 119.2(5) |
| C(4a) -C(3a) -C(2a) | 120.0(5) | C(5a) -C(4a) -C(3a) | 120.7(6) |
| C(6a) -C(5a) -C(4a) | 120.9(6) | C(7a) -C(6a) -C(5a) | 120.7(5) |
| C(6a) -C(7a) -C(2a) | 118.6(5) | C(8a) -C(7a) -C(2a) | 121.3(5) |
| C(8a) -C(7a) -C(6a) | 120.1(5) | C(7a) -C(8a) -N(1a) | 112.7(4) |
| C(10a)-C(9a) -N(1a) | 112.2(5) | C(11) -C(10a)-C(9a) | 113.3(5) |
| C(10b)-C(11) -C(10a) | 113.3(5) | C(1a) -C(1b) -N(2b) | 111.5(5) |
| C(3b) -C(2b) -N(2b) | 121.7(5) | C(7b) -C(2b) -N(2b) | 119.1(5) |
| C(7b) -C(2b) -C(3b) | 119.1(5) | C(4b) -C(3b) -C(2b) | 119.9(5) |
| C(5b) -C(4b) -C(3b) | 121.2(5) | C(6b) -C(5b) -C(4b) | 119.7(5) |
| C(7b) -C(6b) -C(5b) | 121.1(6) | C(6b) -C(7b) -C(2b) | 118.9(5) |
| C(8b) -C(7b) -C(2b) | 121.9(4) | C(8b) -C(7b) -C(6b) | 119.0(5) |
| C(7b) -C(8b) -N(1b) | 115.4(5) | C(10b)-C(9b) -N(1b) | 113.3(5) |
| C(9b) -C(10b)-C(11) | 115.2(6) | | |

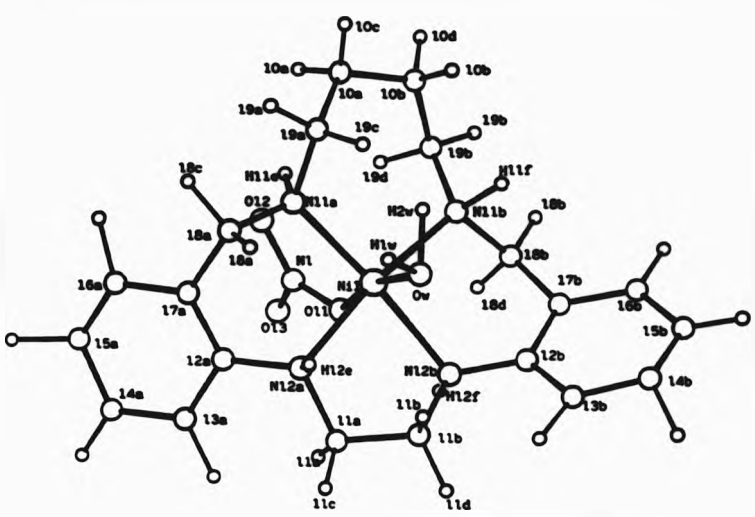


FIGURE A3(a) Labelled diagram of $[NiL^{16}(NO_3)(H_2O)]^+$.

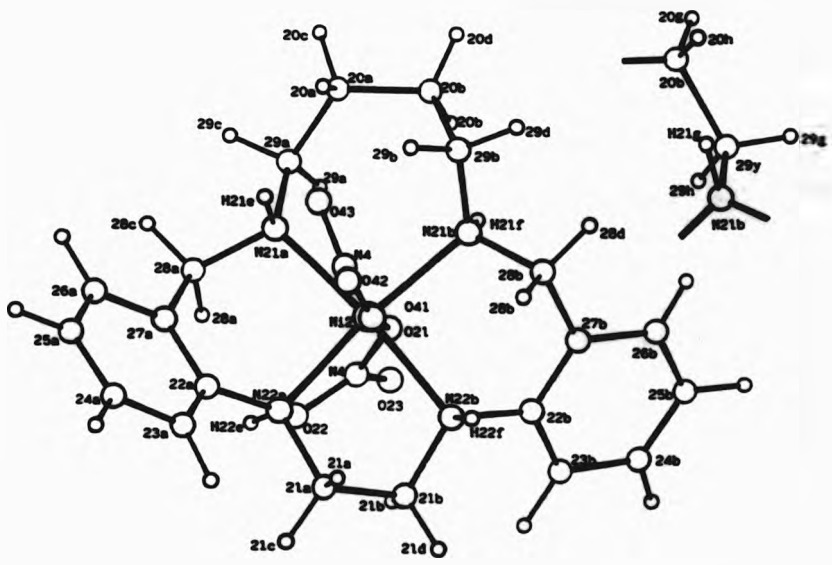


FIGURE A3(b) Labelled diagram of the major component of $[NiL^{16}(NO_3)_2]$ [differences in the minor component are indicated in the inset].

Table A3.1 Fractional atomic coordinates and thermal parameters ( $Å^2$) for $[NiL^{16}(NO_3)_2][NiL^{16}(NO_3)(H_2O)]NO_3 . CH_3OH$

| Atom | x | y | z | $U_{iso}$ or $U_{eq}$ |
|---|---|---|---|---|
| Ni(1) | 0.33647(6) | 0.36561(12) | 0.06291(15) | 0.0368(8) |
| N(1) | 0.2104(4) | 0.2470(8) | -0.0847(11) | 0.044(6) |
| O(11) | 0.2511(3) | 0.2873(6) | 0.0275(8) | 0.049(5) |
| O(12) | 0.2210(4) | 0.2367(7) | -0.2027(8) | 0.065(6) |
| O(13) | 0.1609(4) | 0.2131(8) | -0.0768(9) | 0.094(7) |
| N(3) | 0.4109(5) | 0.7464(11) | 0.1813(14) | 0.068(9) |
| O(31) | 0.3745(4) | 0.7326(8) | 0.2512(10) | 0.080(7) |
| O(32) | 0.4345(4) | 0.6581(8) | 0.0963(10) | 0.079(7) |
| O(33) | 0.4242(4) | 0.8475(8) | 0.1948(12) | 0.109(8) |
| Ni(2) | 0.14867(6) | 0.07801(13) | 0.34458(15) | 0.0403(9) |
| N(2) | 0.0423(5) | -0.0990(11) | 0.2435(11) | 0.061(8) |
| O(21) | 0.1005(4) | -0.0804(7) | 0.2639(8) | 0.064(6) |
| O(22) | 0.0012(4) | -0.0146(8) | 0.2529(9) | 0.071(7) |
| O(23) | 0.0280(4) | -0.2025(8) | 0.2180(10) | 0.094(7) |
| N(4) | 0.2357(4) | 0.2890(9) | 0.4284(11) | 0.049(7) |
| O(41) | 0.2043(3) | 0.2266(7) | 0.4656(8) | 0.061(6) |
| O(42) | 0.2606(4) | 0.3744(8) | 0.5116(9) | 0.084(7) |
| O(43) | 0.2405(5) | 0.2553(9) | 0.3066(10) | 0.110(8) |
| N(12a) | 0.2835(3) | 0.5339(6) | 0.1304(8) | 0.035(2) |
| N(11a) | 0.3261(4) | 0.3808(7) | -0.1380(8) | 0.037(2) |
| C(11a) | 0.2708(4) | 0.5437(9) | 0.2718(11) | 0.044(3) |
| C(12a) | 0.2281(5) | 0.5514(9) | 0.0277(12) | 0.044(3) |
| C(13a) | 0.1688(6) | 0.5901(10) | 0.0638(13) | 0.064(4) |
| C(14a) | 0.1164(6) | 0.6019(10) | -0.0394(13) | 0.069(4) |
| C(15a) | 0.1228(5) | 0.5770(10) | -0.1792(13) | 0.060(3) |

table A3.1 continued

| | | | | |
|---|---|---|---|---|
| C(16a) | 0.1830(5) | 0.5464(10) | -0.2104(13) | 0.061(3) |
| C(17a) | 0.2361(5) | 0.5338(9) | -0.1072(12) | 0.044(3) |
| C(18a) | 0.3022(5) | 0.5012(9) | -0.1433(12) | 0.050(3) |
| C(19a) | 0.3834(5) | 0.3444(9) | -0.2062(12) | 0.058(3) |
| C(10a) | 0.3846(5) | 0.2142(10) | -0.2954(12) | 0.064(4) |
| N(12b) | 0.3441(3) | 0.3760(7) | 0.2791(8) | 0.035(2) |
| N(11b) | 0.3844(4) | 0.1940(7) | 0.0234(9) | 0.042(2) |
| C(11b) | 0.3297(4) | 0.5019(9) | 0.3572(11) | 0.043(3) |
| C(12b) | 0.3993(4) | 0.3210(9) | 0.3421(11) | 0.038(3) |
| C(13b) | 0.4407(5) | 0.3797(9) | 0.4667(11) | 0.047(3) |
| C(14b) | 0.4945(5) | 0.3178(10) | 0.5223(12) | 0.058(3) |
| C(15b) | 0.5053(6) | 0.1992(10) | 0.4586(13) | 0.065(4) |
| C(16b) | 0.4662(5) | 0.1400(10) | 0.3322(13) | 0.062(3) |
| C(17b) | 0.4146(4) | 0.2013(9) | 0.2731(11) | 0.038(3) |
| C(18b) | 0.3771(5) | 0.1391(9) | 0.1300(12) | 0.051(3) |
| C(19b) | 0.3695(5) | 0.1086(10) | -0.1191(12) | 0.058(3) |
| C(10b) | 0.4069(5) | 0.1203(10) | -0.2223(12) | 0.056(3) |
| O(w) | 0.4223(3) | 0.4526(5) | 0.1397(7) | 0.042(2) |
| N(22a) | 0.0697(4) | 0.2004(7) | 0.3899(9) | 0.040(2) |
| N(21a) | 0.1333(3) | 0.0921(7) | 0.1412(8) | 0.037(2) |
| C(21a) | 0.0697(5) | 0.2286(9) | 0.5439(11) | 0.048(3) |
| C(22a) | 0.0652(4) | 0.3015(9) | 0.3418(11) | 0.038(3) |
| C(23a) | 0.0659(5) | 0.4171(10) | 0.4286(13) | 0.060(3) |
| C(24a) | 0.0650(5) | 0.5117(11) | 0.3755(14) | 0.068(4) |
| C(25a) | 0.0605(5) | 0.4837(11) | 0.2348(14) | 0.068(4) |
| C(26a) | 0.0614(5) | 0.3709(11) | 0.1473(13) | 0.062(4) |
| C(27a) | 0.0631(5) | 0.2747(9) | 0.1992(11) | 0.042(3) |

table A3.1 continued

| | | | | |
|---|---|---|---|---|
| C(28a) | 0.0688(5) | 0.1508(9) | 0.1039(12) | 0.052(3) |
| C(29a) | 0.1440(5) | -0.0158(9) | 0.0209(13) | 0.060(3) |
| C(20a) | 0.2155(5) | -0.0395(11) | 0.0161(14) | 0.075(4) |
| N(22b) | 0.1495(3) | 0.0685(6) | 0.5471(8) | 0.032(2) |
| N(21b) | 0.2337(4) | -0.0319(8) | 0.3333(10) | 0.053(3) |
| C(21b) | 0.0860(4) | 0.1156(8) | 0.5819(11) | 0.045(3) |
| C(22b) | 0.1735(5) | -0.0419(9) | 0.5727(11) | 0.046(3) |
| C(23b) | 0.1383(5) | -0.1036(10) | 0.6194(12) | 0.060(3) |
| C(24b) | 0.1654(6) | -0.2120(11) | 0.6412(14) | 0.075(4) |
| C(25b) | 0.2247(6) | -0.2539(12) | 0.6175(15) | 0.088(5) |
| C(26b) | 0.2593(6) | -0.1939(11) | 0.5678(13) | 0.071(4) |
| C(27b) | 0.2338(5) | -0.0881(10) | 0.5428(12) | 0.050(3) |
| C(28b) | 0.2684(5) | -0.0286(10) | 0.4777(12) | 0.058(3) |
| C(29b) | 0.2780(8) | -0.0245(16) | 0.2494(21) | 0.055(6) |
| C(29y) | 0.2324(13) | -0.1373(25) | 0.2212(31) | 0.059(8) |
| C(20b) | 0.2583(6) | -0.1147(12) | 0.0927(15) | 0.081(4) |
| O(m) | 0.5246(4) | 0.2944(7) | 0.1070(10) | 0.086(3) |
| C(m) | 0.5774(6) | 0.2804(12) | 0.2071(14) | 0.096(5) |

Table A3.2

Fractional atomic coordinates for selected hydrogen atoms† for $[NiL^{16}(NO_3)_2][NiL^{16}(NO_3)(H_2O)]NO_3 . CH_3OH$

| Atom | x | y | z |
|---|---|---|---|
| H(22e) | 0.0261 | 0.1595 | 0.3289 |
| †H(22f) | 0.1850 | 0.1261 | 0.6214 |
| H1(m) | 0.5141 | 0.2486 | 0.0391 |
| H(12e) | 0.3233 | 0.5996 | 0.1592 |
| H(11e) | 0.3022 | 0.2987 | -0.2109 |
| H(12f) | 0.3027 | 0.3291 | 0.2709 |
| H(11f) | 0.4373 | 0.1786 | 0.0406 |
| †H(21g) | 0.2676 | -0.0007 | 0.2926 |
| †H(21f) | 0.2154 | -0.1221 | 0.2665 |
| H1(w) | 0.4376 | 0.5273 | 0.1072 |
| H2(w) | 0.4578 | 0.3957 | 0.1439 |
| †H(21e) | 0.1674 | 0.1561 | 0.1493 |
| H(11a) | 0.2310 | 0.5196 | 0.2591 |
| H(13a) | 0.1585 | 0.5995 | 0.1766 |
| H(15a) | 0.0733 | 0.6016 | -0.2554 |
| H(16a) | 0.2008 | 0.5195 | -0.3220 |
| H(18a) | 0.3351 | 0.5583 | -0.0759 |
| H(18c) | 0.2964 | 0.4942 | -0.2604 |
| H(19c) | 0.4227 | 0.3626 | -0.1244 |
| H(10a) | 0.3380 | 0.1873 | -0.3631 |
| H(11b) | 0.3645 | 0.5433 | 0.3536 |
| H(11d) | 0.3224 | 0.5177 | 0.4681 |
| H(13b) | 0.4255 | 0.4793 | 0.5092 |

† Atoms marked thus were included in calculated positions.

table A3.2 continued

| | | | |
|---|---|---|---|
| H(14b) | 0.5056 | 0.3767 | 0.6482 |
| H(16b) | 0.4745 | 0.0394 | 0.2833 |
| H(18b) | 0.3830 | 0.0422 | 0.0805 |
| H(18d) | 0.3342 | 0.1592 | 0.1325 |
| H(10b) | 0.4566 | 0.1410 | -0.1781 |
| H(10d) | 0.4022 | 0.0317 | -0.2980 |
| H(23a) | 0.0640 | 0.4424 | 0.5380 |
| H(26a) | 0.0618 | 0.3524 | 0.0393 |
| H(28a) | 0.0311 | 0.1001 | 0.1173 |
| H(29a) | 0.1279 | -0.0851 | 0.0356 |
| H(24b) | 0.1297 | -0.2710 | 0.6525 |
| H(26b) | 0.2982 | -0.2306 | 0.5399 |

Table A3.3

Anisotropic thermal parameters ( $Å^2$ ) for $[NiL^{16}(NO_3)_2][NiL^{16}(NO_3)(H_2O)]NO_3 \cdot CH_3OH$

| Atom | $U_{11}$ | $U_{22}$ | $U_{33}$ | $U_{23}$ | $U_{13}$ | $U_{12}$ |
|---|---|---|---|---|---|---|
| Ni(1) | 0.037(1) | 0.037(1) | 0.036(1) | 0.010(1) | 0.009(1) | -0.011(1) |
| N(1) | 0.043(6) | 0.050(6) | 0.040(7) | 0.014(6) | 0.002(6) | -0.014(5) |
| O(11) | 0.043(4) | 0.062(5) | 0.041(5) | 0.020(4) | -0.002(4) | -0.026(4) |
| O(12) | 0.072(6) | 0.091(7) | 0.031(5) | 0.007(5) | 0.005(5) | -0.048(5) |
| O(13) | 0.062(6) | 0.145(9) | 0.075(7) | 0.047(6) | -0.001(5) | -0.061(6) |
| N(3) | 0.042(7) | 0.057(8) | 0.104(11) | 0.042(8) | -0.003(7) | -0.007(7) |
| O(31) | 0.045(5) | 0.086(7) | 0.108(8) | 0.047(6) | 0.012(5) | -0.017(5) |
| O(32) | 0.103(7) | 0.053(6) | 0.080(8) | 0.021(6) | 0.028(6) | -0.013(5) |
| O(33) | 0.088(7) | 0.060(6) | 0.179(12) | 0.047(7) | 0.029(7) | -0.019(6) |
| Ni(2) | 0.037(1) | 0.050(1) | 0.034(1) | 0.013(1) | 0.006(1) | -0.015(1) |
| N(2) | 0.060(8) | 0.080(10) | 0.042(7) | 0.009(7) | 0.012(7) | -0.017(7) |
| O(21) | 0.050(5) | 0.080(6) | 0.064(6) | 0.014(5) | 0.012(5) | -0.028(5) |
| O(22) | 0.055(6) | 0.084(7) | 0.075(7) | 0.022(6) | 0.014(5) | -0.023(5) |

table A3.3 continued

| | | | | | | |
|---|---|---|---|---|---|---|
| O(23) | 0.094(7) | 0.076(7) | 0.113(9) | 0.013(6) | 0.030(6) | -0.049(6) |
| N(4) | 0.052(6) | 0.055(7) | 0.040(7) | 0.010(6) | 0.014(6) | -0.015(5) |
| O(41) | 0.063(5) | 0.065(6) | 0.056(6) | 0.011(5) | 0.015(5) | -0.040(4) |
| O(42) | 0.111(7) | 0.077(6) | 0.064(7) | -0.016(6) | 0.029(6) | -0.064(6) |
| O(43) | 0.149(9) | 0.133(9) | 0.049(6) | -0.019(6) | 0.043(6) | -0.109(7) |

Table A3.4

Bond lengths (Å) for $[NiL^{16}(NO_3)_2][NiL^{16}(NO_3)(H_2O)]NO_3 \cdot CH_3OH$

| | | | |
|---|---|---|---|
| Ni(1) -N(12a) | 2.157(7) | Ni(1) -N(11a) | 2.096(9) |
| Ni(1) -N(12b) | 2.156(9) | Ni(1) -N(11b) | 2.124(8) |
| Ni(1) -O(11) | 2.088(7) | Ni(1) -O(w) | 2.109(6) |
| N(12a)-C(11a) | 1.508(15) | N(12a)-C(12a) | 1.446(13) |
| N(12a)-H(12e) | 1.165(8) | N(11a)-C(18a) | 1.477(14) |
| N(11a)-C(19a) | 1.510(15) | N(11a)-H(11e) | 1.122(7) |
| C(11a)-C(11b) | 1.499(14) | C(12a)-C(13a) | 1.397(17) |
| C(12a)-C(17a) | 1.382(18) | C(13a)-C(14a) | 1.390(17) |
| C(14a)-C(15a) | 1.406(20) | C(15a)-C(16a) | 1.387(17) |
| C(16a)-C(17a) | 1.402(15) | C(17a)-C(18a) | 1.529(16) |
| C(19a)-C(10a) | 1.519(14) | C(10a)-C(10b) | 1.522(19) |
| N(12b)-C(11b) | 1.479(11) | N(12b)-C(12b) | 1.411(12) |
| N(12b)-H(12f) | 1.094(8) | N(11b)-C(18b) | 1.504(18) |
| N(11b)-C(19b) | 1.471(12) | N(11b)-H(11f) | 1.116(8) |
| C(12b)-C(13b) | 1.404(13) | C(12b)-C(17b) | 1.401(13) |
| C(13b)-C(14b) | 1.404(15) | C(14b)-C(15b) | 1.361(15) |
| C(15b)-C(16b) | 1.392(15) | C(16b)-C(17b) | 1.384(15) |
| C(17b)-C(18b) | 1.501(13) | C(19b)-C(10b) | 1.531(20) |
| N(1) -O(11) | 1.267(11) | N(1) -O(12) | 1.252(15) |
| N(1) -O(13) | 1.227(15) | O(w) -H1(w) | 1.164(8) |
| O(w) -H2(w) | 0.958(6) | N(3) -O(31) | 1.246(18) |
| N(3) -O(32) | 1.258(14) | N(3) -O(33) | 1.235(17) |
| Ni(2) -N(22a) | 2.125(8) | Ni(2) -N(21a) | 2.104(9) |
| Ni(2) -N(22b) | 2.124(9) | Ni(2) -N(21b) | 2.114(8) |
| Ni(2) -O(21) | 2.108(8) | Ni(2) -O(41) | 2.135(7) |

table A3.4 continued

| | | | |
|---|---|---|---|
| N(22a)-H(22e) | 1.080(10) | N(22a)-C(21a) | 1.506(14) |
| N(22a)-C(22a) | 1.438(16) | N(21a)-C(28a) | 1.502(12) |
| N(21a)-C(29a) | 1.494(12) | N(21a)-H(21e) | 1.106(9) |
| C(21a)-C(21b) | 1.505(16) | C(22a)-C(23a) | 1.371(14) |
| C(22a)-C(27a) | 1.385(16) | C(23a)-C(24a) | 1.409(21) |
| C(24a)-C(25a) | 1.356(20) | C(25a)-C(26a) | 1.347(16) |
| C(26a)-C(27a) | 1.417(19) | C(27a)-C(28a) | 1.483(13) |
| C(29a)-C(20a) | 1.545(16) | C(20a)-C(20b) | 1.483(19) |
| N(22b)-H(22f) | 1.080(9) | N(22b)-C(21b) | 1.490(12) |
| N(22b)-C(22b) | 1.438(14) | N(21b)-C(28b) | 1.491(15) |
| N(21b)-C(29b) | 1.464(25) | N(21b)-C(29y) | 1.39(3) |
| N(21b)-H(21g) | 1.087(11) | N(21b)-H(21f) | 1.133(8) |
| C(22b)-C(23b) | 1.387(20) | C(22b)-C(27b) | 1.408(15) |
| C(23b)-C(24b) | 1.416(18) | C(24b)-C(25b) | 1.362(19) |
| C(25b)-C(26b) | 1.383(24) | C(26b)-C(27b) | 1.392(18) |
| C(27b)-C(28b) | 1.491(20) | C(29b)-C(20b) | 1.607(21) |
| C(29y)-C(20b) | 1.66(4) | N(2) -O(21) | 1.266(14) |
| N(2) -O(22) | 1.245(14) | N(2) -O(23) | 1.244(17) |
| N(4) -O(41) | 1.273(16) | N(4) -O(42) | 1.190(12) |
| N(4) -O(43) | 1.207(15) | O(m) -C(m) | 1.381(15) |
| O(m) -H1(m) | 0.737(8) | | |

Table A3.5

Bond angles (°) for $[NiL^{16}(NO_3)_2][NiL^{16}(NO_3)(H_2O)]NO_3 . CH_3OH$

| | | | |
|---|---|---|---|
| N(11a)-Ni(1) -N(12a) | 90.8(3) | N(12b)-Ni(1) -N(12a) | 81.8(3) |
| N(12b)-Ni(1) -N(11a) | 172.1(3) | N(11b)-Ni(1) -N(12a) | 170.8(4) |
| N(11b)-Ni(1) -N(11a) | 97.7(3) | N(11b)-Ni(1) -N(12b) | 89.8(3) |
| O(11) -Ni(1) -N(12a) | 86.3(3) | O(11) -Ni(1) -N(11a) | 97.4(3) |
| O(11) -Ni(1) -N(12b) | 84.8(3) | O(11) -Ni(1) -N(11b) | 89.1(3) |
| O(w) -Ni(1) -N(12a) | 90.1(3) | O(w) -Ni(1) -N(11a) | 93.0(3) |
| O(w) -Ni(1) -N(12b) | 84.5(3) | O(w) -Ni(1) -N(11b) | 92.9(3) |
| O(w) -Ni(1) -O(11) | 169.0(3) | C(11a)-N(12a)-Ni(1) | 105.9(6) |
| C(12a)-N(12a)-Ni(1) | 114.2(5) | C(12a)-N(12a)-C(11a) | 115.4(8) |
| H(12e)-N(12a)-Ni(1) | 100.7(4) | H(12e)-N(12a)-C(11a) | 103.1(6) |
| H(12e)-N(12a)-C(12a) | 115.7(9) | C(18a)-N(11a)-Ni(1) | 112.6(6) |
| C(19a)-N(11a)-Ni(1) | 117.2(6) | C(19a)-N(11a)-C(18a) | 108.1(9) |
| H(11e)-N(11a)-Ni(1) | 104.3(6) | H(11e)-N(11a)-C(18a) | 122.5(7) |
| H(11e)-N(11a)-C(19a) | 91.1(6) | C(11b)-C(11a)-N(12a) | 109.2(8) |
| C(13a)-C(12a)-N(12a) | 122(1) | C(17a)-C(12a)-N(12a) | 117.8(9) |
| C(17a)-C(12a)-C(13a) | 120(1) | C(14a)-C(13a)-C(12a) | 120(1) |
| C(15a)-C(14a)-C(13a) | 121(1) | C(16a)-C(15a)-C(14a) | 119(1) |
| C(17a)-C(16a)-C(15a) | 121(1) | C(16a)-C(17a)-C(12a) | 119(1) |
| C(18a)-C(17a)-C(12a) | 120.4(9) | C(18a)-C(17a)-C(16a) | 120(1) |
| C(17a)-C(18a)-N(11a) | 111(1) | C(10a)-C(19a)-N(11a) | 112(1) |
| C(10b)-C(10a)-C(19a) | 119(1) | C(11b)-N(12b)-Ni(1) | 106.9(7) |
| C(12b)-N(12b)-Ni(1) | 117.1(7) | C(12b)-N(12b)-C(11b) | 115.4(7) |
| H(12f)-N(12b)-Ni(1) | 101.3(4) | H(12f)-N(12b)-C(11b) | 105.6(7) |
| H(12f)-N(12b)-C(12b) | 109.1(8) | C(18b)-N(11b)-Ni(1) | 109.7(6) |
| C(19b)-N(11b)-Ni(1) | 118.2(7) | C(19b)-N(11b)-C(18b) | 110.0(9) |

table A3.5 continued

| | | | |
|---|---|---|---|
| H(11f)-N(11b)-Ni(1) | 123.6(6) | H(11f)-N(11b)-C(18b) | 95.0(7) |
| H(11f)-N(11b)-C(19b) | 97.6(7) | N(12b)-C(11b)-C(11a) | 107.0(7) |
| C(13b)-C(12b)-N(12b) | 124.2(8) | C(17b)-C(12b)-N(12b) | 117.6(8) |
| C(17b)-C(12b)-C(13b) | 118.2(9) | C(14b)-C(13b)-C(12b) | 120.3(9) |
| C(15b)-C(14b)-C(13b) | 120.0(9) | C(16b)-C(15b)-C(14b) | 121(1) |
| C(17b)-C(16b)-C(15b) | 120(1) | C(16b)-C(17b)-C(12b) | 120.8(8) |
| C(18b)-C(17b)-C(12b) | 120.3(9) | C(18b)-C(17b)-C(16b) | 118.8(8) |
| C(17b)-C(18b)-N(11b) | 111.0(9) | C(10b)-C(19b)-N(11b) | 114.6(9) |
| C(19b)-C(10b)-C(10a) | 119.4(9) | O(12) -N(1) -O(11) | 121(1) |
| O(13) -N(1) -O(11) | 119(1) | O(13) -N(1) -O(12) | 119.7(9) |
| N(1) -O(11) -Ni(1) | 131.0(8) | H1(w) -O(w) -Ni(1) | 128.2(4) |
| H2(w) -O(w) -Ni(1) | 110.1(5) | H2(w) -O(w) -H1(w) | 107.6(6) |
| O(32) -N(3) -O(31) | 120(1) | O(33) -N(3) -O(31) | 120(1) |
| O(33) -N(3) -O(32) | 119(1) | N(21a)-Ni(2) -N(22a) | 90.9(3) |
| N(22b)-Ni(2) -N(22a) | 81.9(3) | N(22b)-Ni(2) -N(21a) | 171.6(3) |
| N(21b)-Ni(2) -N(22a) | 171.0(3) | N(21b)-Ni(2) -N(21a) | 96.7(4) |
| N(21b)-Ni(2) -N(22b) | 90.9(4) | O(21) -Ni(2) -N(22a) | 98.4(3) |
| O(21) -Ni(2) -N(21a) | 90.5(3) | O(21) -Ni(2) -N(22b) | 86.3(3) |
| O(21) -Ni(2) -N(21b) | 86.6(3) | O(41) -Ni(2) -N(22a) | 84.6(3) |
| O(41) -Ni(2) -N(21a) | 101.5(3) | O(41) -Ni(2) -N(22b) | 82.3(3) |
| O(41) -Ni(2) -N(21b) | 88.9(3) | O(41) -Ni(2) -O(21) | 167.6(3) |
| H(22e)-N(22a)-Ni(2) | 109.6(6) | C(21a)-N(22a)-Ni(2) | 107.4(6) |
| C(21a)-N(22a)-H(22e) | 109(1) | C(22a)-N(22a)-Ni(2) | 114.5(7) |
| C(22a)-N(22a)-H(22e) | 100.7(9) | C(22a)-N(22a)-C(21a) | 115.6(7) |
| C(28a)-N(21a)-Ni(2) | 110.9(7) | C(29a)-N(21a)-Ni(2) | 119.5(7) |
| C(29a)-N(21a)-C(28a) | 109.4(7) | H(21e)-N(21a)-Ni(2) | 104.8(5) |
| H(21e)-N(21a)-C(28a) | 104.9(8) | H(21e)-N(21a)-C(29a) | 106.2(8) |
| C(21b)-C(21a)-N(22a) | 108.7(8) | C(23a)-C(22a)-N(22a) | 124(1) |

table A3.5 continued

| | | | |
|---|---|---|---|
| C(27a)-C(22a)-N(22a) | 115.2(8) | C(27a)-C(22a)-C(23a) | 121(1) |
| C(24a)-C(23a)-C(22a) | 121(1) | C(25a)-C(24a)-C(23a) | 117(1) |
| C(26a)-C(25a)-C(24a) | 123(1) | C(27a)-C(26a)-C(25a) | 120(1) |
| C(26a)-C(27a)-C(22a) | 117.5(9) | C(28a)-C(27a)-C(22a) | 123(1) |
| C(28a)-C(27a)-C(26a) | 120(1) | C(27a)-C(28a)-N(21a) | 111.4(7) |
| C(20a)-C(29a)-N(21a) | 110.7(8) | C(20b)-C(20a)-C(29a) | 122(1) |
| H(22f)-N(22b)-Ni(2) | 107.4(8) | C(21b)-N(22b)-Ni(2) | 107.9(6) |
| C(21b)-N(22b)-H(22f) | 108.6(7) | C(22b)-N(22b)-Ni(2) | 116.9(6) |
| C(22b)-N(22b)-H(22f) | 99.6(8) | C(22b)-N(22b)-C(21b) | 115.6(9) |
| C(28b)-N(21b)-Ni(2) | 109.9(6) | C(29b)-N(21b)-Ni(2) | 122(1) |
| C(29b)-N(21b)-C(28b) | 110(1) | C(29y)-N(21b)-Ni(2) | 118(1) |
| C(29y)-N(21b)-C(28b) | 121(1) | H(21g)-N(21b)-Ni(2) | 113.1(7) |
| H(21g)-N(21b)-C(28b) | 103.5(8) | H(21g)-N(21b)-C(29y) | 89(2) |
| H(21f)-N(21b)-Ni(2) | 102.3(5) | H(21f)-N(21b)-C(28b) | 113.3(9) |
| H(21f)-N(21b)-C(29b) | 98.5(9) | N(22b)-C(21b)-C(21a) | 107(1) |
| C(23b)-C(22b)-N(22b) | 122.1(9) | C(27b)-C(22b)-N(22b) | 117(1) |
| C(27b)-C(22b)-C(23b) | 121(1) | C(24b)-C(23b)-C(22b) | 118(1) |
| C(25b)-C(24b)-C(23b) | 120(1) | C(26b)-C(25b)-C(24b) | 121(1) |
| C(27b)-C(26b)-C(25b) | 120(1) | C(26b)-C(27b)-C(22b) | 119(1) |
| C(28b)-C(27b)-C(22b) | 121(1) | C(28b)-C(27b)-C(26b) | 120(1) |
| C(27b)-C(28b)-N(21b) | 111.7(9) | C(20b)-C(29b)-N(21b) | 109(1) |
| C(20b)-C(29y)-N(21b) | 109(2) | C(29b)-C(20b)-C(20a) | 103(1) |
| C(29y)-C(20b)-C(20a) | 116(1) | O(22) -N(2) -O(21) | 120(1) |
| O(23) -N(2) -O(21) | 118(1) | O(23) -N(2) -O(22) | 122(1) |
| N(2) -O(21) -Ni(2) | 131.7(7) | O(42) -N(4) -O(41) | 121(1) |
| O(43) -N(4) -O(41) | 117(1) | O(43) -N(4) -O(42) | 122(1) |
| N(4) -O(41) -Ni(2) | 131.0(7) | H1(m) -O(m) -C(m) | 124(1) |

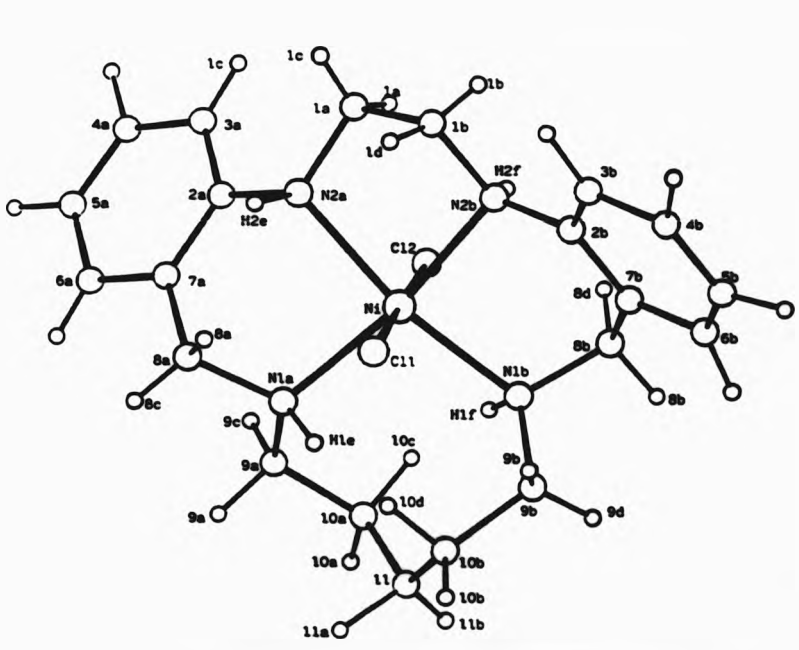


FIGURE A4 Labelled diagram of $[NiL^{17}Cl_2]$.

Table A4.1

Fractional atomic coordinates and thermal parameters ( $Å^2$) for [NiL$^{17}$Cl$_2$]

| Atom | x | y | z | $U_{iso}$ or $U_{eq}$ |
|---|---|---|---|---|
| Ni | 0.2278(1) | 0.2479(1) | -0.0153(2) | 0.030(1) |
| Cl(1) | 0.0745(2) | 0.1598(2) | 0.1772(3) | 0.041(2) |
| Cl(2) | 0.3796(2) | 0.3377(2) | -0.2038(3) | 0.041(2) |
| N(1b) | 0.3129(7) | 0.4265(7) | 0.1624(9) | 0.034(5) |
| N(2b) | 0.1002(7) | 0.3338(7) | -0.0482(10) | 0.036(5) |
| N(2a) | 0.1418(6) | 0.0953(7) | -0.2243(9) | 0.031(5) |
| N(1a) | 0.3171(7) | 0.1240(7) | 0.0093(10) | 0.038(5) |
| C(9a) | 0.4485(9) | 0.1533(10) | 0.0094(14) | 0.055(8) |
| C(10a) | 0.5166(9) | 0.2878(11) | 0.1117(16) | 0.060(8) |
| C(11) | 0.4822(11) | 0.3273(11) | 0.2956(16) | 0.066(9) |
| C(9b) | 0.3226(9) | 0.4425(10) | 0.3353(12) | 0.041(7) |
| C(10b) | 0.3566(10) | 0.3382(10) | 0.3651(12) | 0.049(7) |
| C(1a) | 0.0764(9) | 0.1490(9) | -0.2952(13) | 0.043(3) |
| C(2a) | 0.2208(9) | 0.0245(9) | -0.3371(13) | 0.041(3) |
| C(3a) | 0.2383(10) | 0.0106(11) | -0.5037(15) | 0.059(3) |
| C(4a) | 0.3155(10) | -0.0606(11) | -0.6040(15) | 0.061(3) |
| C(5a) | 0.3708(10) | -0.1143(11) | -0.5438(15) | 0.063(3) |
| C(6a) | 0.3564(11) | -0.1013(12) | -0.3792(16) | 0.064(3) |
| C(7a) | 0.2785(9) | -0.0307(9) | -0.2724(12) | 0.038(2) |
| C(8a) | 0.2633(9) | -0.0131(10) | -0.0948(13) | 0.043(3) |
| C(1b) | 0.0079(9) | 0.2252(10) | -0.1545(13) | 0.046(3) |
| C(2b) | 0.0541(9) | 0.4142(9) | 0.1009(12) | 0.036(2) |
| C(3b) | -0.0703(9) | 0.3965(10) | 0.1438(13) | 0.047(3) |
| C(4b) | -0.1077(10) | 0.4831(10) | 0.2902(14) | 0.054(3) |
| C(5b) | -0.0246(9) | 0.5806(10) | 0.3877(13) | 0.049(3) |
| C(6b) | 0.0977(10) | 0.5985(10) | 0.3476(13) | 0.048(3) |
| C(7b) | 0.1387(9) | 0.5152(9) | 0.2020(12) | 0.038(2) |
| C(8b) | 0.2736(9) | 0.5340(9) | 0.1579(12) | 0.043(3) |

Table A4.2 Fractional atomic coordinates for the found hydrogen atoms for [NiL$^{17}Cl_2$]

| Atom | x | y | z |
|---|---|---|---|
| H(2e) | 0.0790 | 0.0182 | -0.1821 |
| H(1e) | 0.2970 | 0.1543 | 0.1251 |
| H(2f) | 0.1663 | 0.3718 | -0.1117 |
| H(1f) | 0.3857 | 0.4125 | 0.1076 |
| H(1a) | 0.1355 | 0.2133 | -0.3269 |
| H(1c) | 0.0194 | 0.0886 | -0.3635 |
| H(3a) | 0.1955 | 0.0449 | -0.5505 |
| H(6a) | 0.3866 | -0.1364 | -0.3226 |
| H(8a) | 0.1783 | -0.0198 | -0.0445 |
| H(8c) | 0.3022 | -0.0712 | -0.0809 |
| H(10a) | 0.6160 | 0.3030 | 0.1052 |
| H(11a) | 0.4849 | 0.2404 | 0.3329 |
| H(11b) | 0.5438 | 0.3984 | 0.3394 |
| H(1b) | -0.0057 | 0.2823 | -0.1845 |
| H(1d) | -0.0348 | 0.1545 | -0.1133 |
| H(3b) | -0.1415 | 0.3210 | 0.0658 |
| H(4b) | -0.1994 | 0.4640 | 0.2845 |
| H(5b) | -0.0592 | 0.6487 | 0.4904 |
| H(6b) | 0.1675 | 0.6535 | 0.4196 |
| H(8b) | 0.3356 | 0.6126 | 0.2376 |
| H(8d) | 0.2734 | 0.5287 | 0.0534 |
| H(9b) | 0.2275 | 0.4064 | 0.3811 |
| H(10b) | 0.3218 | 0.3244 | 0.4808 |

Table A4.3 Anisotropic thermal parameters ( $Å^2$) for [$NiL^{17}Cl_2$]

| Atom | $U_{11}$ | $U_{22}$ | $U_{33}$ | $U_{23}$ | $U_{13}$ | $U_{12}$ |
|---|---|---|---|---|---|---|
| Ni | 0.032(1) | 0.030(1) | 0.030(1) | 0.013(1) | 0.001(1) | 0.003(1) |
| Cl(1) | 0.039(2) | 0.039(2) | 0.044(2) | 0.018(1) | 0.004(1) | -0.001(1) |
| Cl(2) | 0.044(2) | 0.044(2) | 0.036(2) | 0.017(1) | 0.003(1) | -0.001(1) |
| N(1b) | 0.041(5) | 0.034(5) | 0.029(5) | 0.015(4) | -0.006(4) | 0.003(4) |
| N(2b) | 0.035(5) | 0.041(5) | 0.032(5) | 0.013(4) | 0.004(4) | 0.005(4) |
| N(2a) | 0.025(4) | 0.038(5) | 0.031(5) | 0.011(4) | 0.006(4) | -0.002(4) |
| N(1a) | 0.034(5) | 0.037(5) | 0.042(5) | 0.007(4) | -0.008(4) | 0.007(4) |
| C(9a) | 0.040(7) | 0.061(8) | 0.064(9) | 0.010(7) | 0.000(7) | 0.020(6) |
| C(10a) | 0.037(7) | 0.063(8) | 0.081(10) | 0.028(7) | -0.008(7) | 0.013(6) |
| C(11) | 0.072(9) | 0.065(8) | 0.060(9) | 0.009(7) | -0.026(8) | 0.029(7) |
| C(9b) | 0.038(6) | 0.052(7) | 0.033(6) | 0.018(6) | 0.003(5) | 0.003(5) |
| C(10b) | 0.075(9) | 0.037(6) | 0.035(6) | 0.011(5) | -0.004(6) | 0.017(6) |

Table A4.4 Bond lengths ( Å) for [NiL$^{17}$Cl$_2$]

| | | | | | |
|---|---|---|---|---|---|
| Ni | -Cl(1) | 2.461(3) | Ni | -Cl(2) | 2.437(3) |
| Ni | -N(1b) | 2.137(6) | Ni | -N(2b) | 2.176(10) |
| Ni | -N(2a) | 2.156(7) | Ni | -N(1a) | 2.140(11) |
| N(1b) | -C(8b) | 1.492(16) | N(1b) | -C(9b) | 1.485(14) |
| N(1b) | -H(1f) | 0.936(8) | N(2b) | -C(1b) | 1.494(11) |
| N(2b) | -C(2b) | 1.442(12) | N(2b) | -H(2f) | 0.948(8) |
| N(2a) | -C(1a) | 1.471(17) | N(2a) | -C(2a) | 1.453(13) |
| N(2a) | -H(2e) | 1.087(8) | N(1a) | -C(8a) | 1.501(11) |
| N(1a) | -C(9a) | 1.464(13) | N(1a) | -H(1e) | 0.961(8) |
| C(1a) | -C(1b) | 1.512(14) | C(2a) | -C(3a) | 1.399(17) |
| C(2a) | -C(7a) | 1.381(19) | C(3a) | -C(4a) | 1.405(17) |
| C(4a) | -C(5a) | 1.320(23) | C(5a) | -C(6a) | 1.385(19) |
| C(6a) | -C(7a) | 1.424(16) | C(7a) | -C(8a) | 1.484(16) |
| C(9a) | -C(10a) | 1.514(13) | C(10a) | -C(11) | 1.529(18) |
| C(11) | -C(10b) | 1.519(18) | C(2b) | -C(3b) | 1.404(14) |
| C(2b) | -C(7b) | 1.391(12) | C(3b) | -C(4b) | 1.420(14) |
| C(4b) | -C(5b) | 1.352(13) | C(5b) | -C(6b) | 1.377(15) |
| C(6b) | -C(7b) | 1.413(14) | C(7b) | -C(8b) | 1.520(14) |
| C(9b) | -C(10b) | 1.519(20) | | | |

Table A4.5 Bond angles (°) for $[NiL^{17}Cl_2]$

| | | | | | |
|---|---|---|---|---|---|
| Cl(2) -Ni | -Cl(1) | 179.3(1) | N(1b) -Ni | -Cl(1) | 96.3(2) |
| N(1b) -Ni | -Cl(2) | 83.1(2) | N(2b) -Ni | -Cl(1) | 88.2(2) |
| N(2b) -Ni | -Cl(2) | 91.5(2) | N(2b) -Ni | -N(1b) | 89.9(3) |
| N(2a) -Ni | -Cl(1) | 92.2(2) | N(2a) -Ni | -Cl(2) | 88.3(2) |
| N(2a) -Ni | -N(1b) | 167.1(4) | N(2a) -Ni | -N(2b) | 80.7(3) |
| N(1a) -Ni | -Cl(1) | 82.7(2) | N(1a) -Ni | -Cl(2) | 97.8(2) |
| N(1a) -Ni | -N(1b) | 100.9(3) | N(1a) -Ni | -N(2b) | 166.5(3) |
| N(1a) -Ni | -N(2a) | 89.8(3) | C(8b) -N(1b) | -Ni | 111.3(6) |
| C(9b) -N(1b) | -Ni | 124.3(6) | C(9b) -N(1b) | -C(8b) | 109.1(7) |
| H(1f) -N(1b) | -Ni | 85.1(4) | H(1f) -N(1b) | -C(8b) | 120.9(8) |
| H(1f) -N(1b) | -C(9b) | 105.0(9) | C(1b) -N(2b) | -Ni | 105.7(7) |
| C(2b) -N(2b) | -Ni | 114.9(7) | C(2b) -N(2b) | -C(1b) | 116.4(7) |
| H(2f) -N(2b) | -Ni | 83.5(6) | H(2f) -N(2b) | -C(1b) | 111.3(8) |
| H(2f) -N(2b) | -C(2b) | 119.9(8) | C(1a) -N(2a) | -Ni | 107.5(5) |
| C(2a) -N(2a) | -Ni | 114.6(6) | C(2a) -N(2a) | -C(1a) | 116.4(8) |
| H(2e) -N(2a) | -Ni | 108.0(5) | H(2e) -N(2a) | -C(1a) | 110.6(7) |
| H(2e) -N(2a) | -C(2a) | 99.1(7) | C(8a) -N(1a) | -Ni | 110.9(7) |
| C(9a) -N(1a) | -Ni | 125.1(7) | C(9a) -N(1a) | -C(8a) | 110.2(8) |
| H(1e) -N(1a) | -Ni | 87.8(6) | H(1e) -N(1a) | -C(8a) | 122.1(8) |
| H(1e) -N(1a) | -C(9a) | 99.7(8) | C(1b) -C(1a) | -N(2a) | 106.8(9) |
| C(3a) -C(2a) | -N(2a) | 123(1) | C(7a) -C(2a) | -N(2a) | 116.7(9) |
| C(7a) -C(2a) | -C(3a) | 121(1) | C(4a) -C(3a) | -C(2a) | 119(1) |
| C(5a) -C(4a) | -C(3a) | 121(1) | C(6a) -C(5a) | -C(4a) | 121(1) |
| C(7a) -C(6a) | -C(5a) | 120(1) | C(6a) -C(7a) | -C(2a) | 118(1) |
| C(8a) -C(7a) | -C(2a) | 120.9(9) | C(8a) -C(7a) | -C(6a) | 121(1) |

table A4.5 continued

| | | | |
|---|---|---|---|
| C(7a) -C(8a) -N(1a) | 113.0(9) | C(10a)-C(9a) -N(1a) | 116.8(9) |
| C(11) -C(10a)-C(9a) | 117(1) | C(10b)-C(11) -C(10a) | 122(1) |
| C(1a) -C(1b) -N(2b) | 107.0(8) | C(3b) -C(2b) -N(2b) | 122.9(8) |
| C(7b) -C(2b) -N(2b) | 117.2(8) | C(7b) -C(2b) -C(3b) | 119.9(8) |
| C(4b) -C(3b) -C(2b) | 119.2(8) | C(5b) -C(4b) -C(3b) | 120(1) |
| C(6b) -C(5b) -C(4b) | 121.0(9) | C(7b) -C(6b) -C(5b) | 120.4(9) |
| C(6b) -C(7b) -C(2b) | 119.2(9) | C(8b) -C(7b) -C(2b) | 120.3(8) |
| C(8b) -C(7b) -C(6b) | 120.5(8) | C(7b) -C(8b) -N(1b) | 112.8(8) |
| C(10b)-C(9b) -N(1b) | 116.8(8) | C(9b) -C(10b)-C(11) | 115(1) |

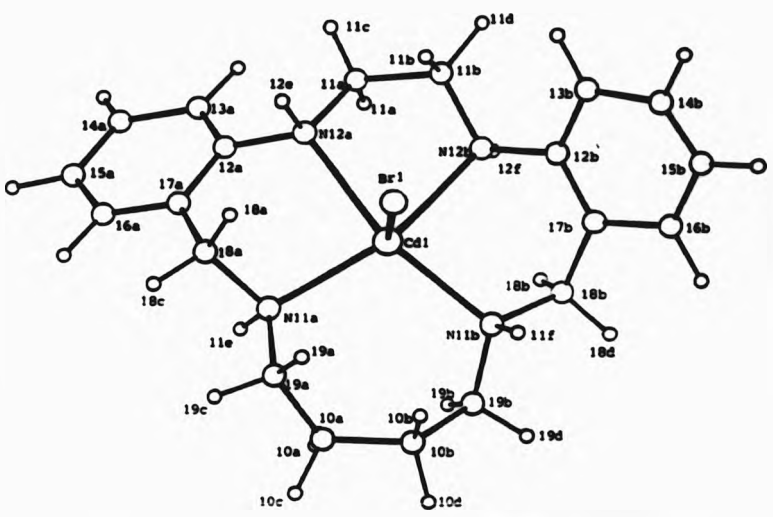


FIGURE A5(a) Labelled diagram of $[Cd(1)L^{16}Br]^+$.

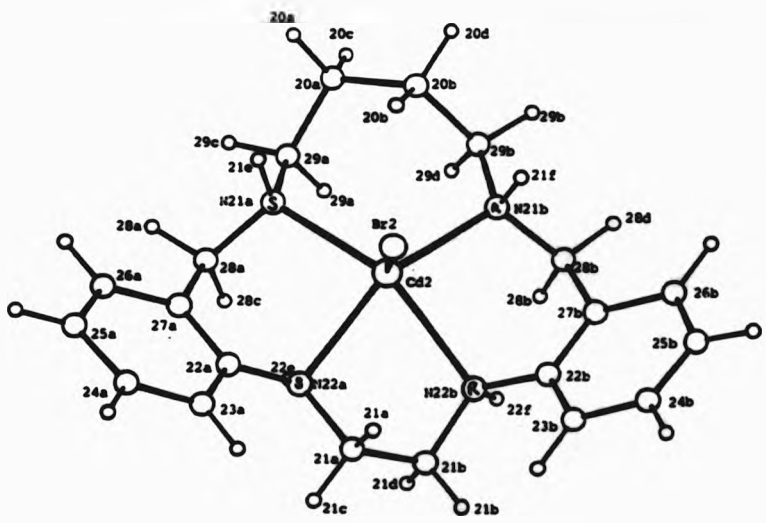


FIGURE A5(b) Labelled diagram of $[Cd(2)L^{16}Br]^+$.

Table A5.1 Fractional atomic coordinates and thermal parameters ( $Å^2$) for $[CdL^{16}Br]_2CdBr_4$

| Atom | x | y | z | $U_{iso}$ or $U_{eq}$ |
|---|---|---|---|---|
| Cd(1) | -0.22445(11) | 0.45250(7) | 0.12649(14) | 0.0409(9) |
| Br(1) | -0.3798(2) | 0.5192(1) | 0.2460(2) | 0.070(2) |
| Cd(2) | 0.29009(10) | 0.08151(7) | 0.32676(14) | 0.0380(9) |
| Br(2) | 0.3279(2) | -0.0323(1) | 0.4282(2) | 0.060(1) |
| Cd(3) | 0.05366(11) | 0.24972(7) | -0.03205(14) | 0.0421(9) |
| Br(31) | -0.0333(1) | 0.3830(1) | -0.0001(2) | 0.051(1) |
| Br(32) | 0.2288(2) | 0.2233(1) | 0.1341(2) | 0.059(1) |
| Br(33) | -0.0772(2) | 0.1830(1) | 0.0211(2) | 0.051(1) |
| Br(34) | 0.0830(2) | 0.2168(1) | -0.2590(2) | 0.067(2) |
| N(12a) | -0.0914(11) | 0.4355(7) | 0.3185(14) | 0.042(10) |
| N(11a) | -0.1547(10) | 0.5490(7) | 0.1272(14) | 0.039(10) |
| N(12b) | -0.2233(11) | 0.3353(6) | 0.1601(16) | 0.045(10) |
| N(11b) | -0.3344(11) | 0.4290(7) | -0.0606(15) | 0.044(10) |
| C(11a) | -0.0674(14) | 0.3587(9) | 0.3298(19) | 0.044(13) |
| C(18a) | -0.1180(13) | 0.5780(8) | 0.2630(18) | 0.038(12) |
| C(19a) | -0.2334(14) | 0.6021(9) | 0.0563(18) | 0.039(12) |
| C(10a) | -0.2497(16) | 0.5799(10) | -0.0830(20) | 0.062(15) |
| C(11b) | -0.1733(17) | 0.3314(9) | 0.2956(21) | 0.057(15) |
| C(18b) | -0.3302(14) | 0.3490(9) | -0.0928(20) | 0.052(14) |
| C(19b) | -0.3168(15) | 0.4591(10) | -0.1633(20) | 0.059(14) |
| C(10b) | -0.3410(15) | 0.5422(10) | -0.1438(21) | 0.058(15) |
| N(22a) | 0.1301(11) | 0.0655(7) | 0.1876(14) | 0.039(9) |
| N(21a) | 0.1854(10) | 0.1645(7) | 0.4485(13) | 0.033(9) |

table A5.1 continued

| | | | | |
|---|---|---|---|---|
| N(22b) | 0.3316(12) | 0.0427(9) | 0.1182(16) | 0.064(12) |
| N(21b) | 0.4509(11) | 0.1128(7) | 0.3731(14) | 0.035(9) |
| C(21a) | 0.1632(16) | 0.0079(11) | 0.0861(22) | 0.067(16) |
| C(28a) | 0.0730(13) | 0.1755(9) | 0.3759(19) | 0.043(12) |
| C(29a) | 0.2190(15) | 0.2322(10) | 0.4838(18) | 0.050(14) |
| C(20a) | 0.3152(17) | 0.2345(10) | 0.5916(22) | 0.066(16) |
| C(21b) | 0.2396(19) | 0.0213(16) | 0.0261(25) | 0.117(24) |
| C(28b) | 0.5009(14) | 0.1062(9) | 0.2613(19) | 0.045(12) |
| C(29b) | 0.4540(14) | 0.1816(10) | 0.4483(20) | 0.053(14) |
| C(20b) | 0.4132(16) | 0.1820(11) | 0.5722(21) | 0.061(15) |
| C(13a) | 0.1011(15) | 0.4315(10) | 0.3863(19) | 0.056(6) |
| C(14a) | 0.1890(15) | 0.4649(10) | 0.4132(20) | 0.056(6) |
| C(15a) | 0.1737(15) | 0.5320(9) | 0.3920(19) | 0.050(5) |
| C(16a) | 0.0721(15) | 0.5670(10) | 0.3474(19) | 0.057(6) |
| C(17a) | -0.0137(13) | 0.5366(9) | 0.3182(17) | 0.037(5) |
| C(12b) | -0.3284(14) | 0.3171(9) | 0.1166(20) | 0.045(5) |
| C(13b) | -0.3797(16) | 0.2982(10) | 0.1998(22) | 0.061(6) |
| C(14b) | -0.4810(18) | 0.2846(11) | 0.1473(24) | 0.075(7) |
| C(15b) | -0.5310(17) | 0.2873(10) | 0.0343(22) | 0.065(6) |
| C(16b) | -0.4818(16) | 0.3072(10) | -0.0456(23) | 0.065(6) |
| C(17b) | -0.3765(17) | 0.3235(11) | -0.0049(24) | 0.064(6) |
| C(22a) | 0.0584(13) | 0.0550(9) | 0.2573(18) | 0.040(5) |
| C(23a) | 0.0145(15) | -0.0064(10) | 0.2344(19) | 0.051(5) |
| C(24a) | -0.0584(16) | -0.0130(11) | 0.3036(21) | 0.068(6) |
| C(25a) | -0.0944(17) | 0.0421(11) | 0.3917(22) | 0.072(7) |
| C(26a) | -0.0473(16) | 0.1036(11) | 0.4133(21) | 0.066(6) |
| C(27a) | 0.0273(13) | 0.1094(9) | 0.3460(18) | 0.039(5) |

table A5.1 continued

| | | | | |
|---|---|---|---|---|
| C(22b) | 0.4331(15) | -0.0009(10) | 0.1349(19) | 0.049(5) |
| C(23b) | 0.4470(20) | -0.0717(13) | 0.0856(25) | 0.091(8) |
| C(24b) | 0.5513(19) | -0.1120(14) | 0.1099(25) | 0.092(8) |
| C(25b) | 0.6359(19) | -0.0838(12) | 0.1701(22) | 0.079(7) |
| C(26b) | 0.6265(16) | -0.0116(10) | 0.2215(21) | 0.063(6) |
| C(27b) | 0.5204(14) | 0.0296(9) | 0.2010(19) | 0.046(5) |
| C(12a) | 0.0013(14) | 0.4691(9) | 0.3429(18) | 0.042(5) |
| C(m1) | 0.2395(23) | 0.7313(21) | 0.4250(31) | 0.082(26) |
| O(m1) | 0.2287(19) | 0.7912(16) | 0.3386(28) | 0.130(24) |
| C(m2) | 0.4875 | 0.5664 | 0.5114 | 0.0728 |
| O(m2) | 0.5132 | 0.6388 | 0.5051 | 0.0651 |

Table A5.2 Fractional atomic coordinates for the found hydrogen atoms for $[CdL^{16}Br]_2CdBr_4$

| Atom | x | y | z |
|---|---|---|---|
| H(11e) | -0.0951 | 0.5509 | 0.1020 |
| H(12e) | -0.1212 | 0.4653 | 0.4023 |
| H(12f) | -0.1631 | 0.2921 | 0.1169 |
| H(11f) | -0.4181 | 0.4489 | -0.0659 |
| H(21e) | 0.1946 | 0.1443 | 0.5364 |
| H(21f) | 0.5011 | 0.0745 | 0.4315 |
| H(22e) | 0.1141 | 0.1197 | 0.1597 |
| H(22f) | 0.3484 | 0.0821 | 0.0717 |
| H(11c) | -0.0329 | 0.3521 | 0.4209 |
| H(14a) | 0.2578 | 0.4379 | 0.4363 |
| H(11b) | -0.2192 | 0.3662 | 0.3570 |
| H(11d) | -0.1757 | 0.2771 | 0.3247 |
| H(21a) | 0.2020 | -0.0317 | 0.1307 |
| H(23a) | 0.0361 | -0.0508 | 0.1666 |
| H(20a) | 0.2949 | 0.2225 | 0.6861 |
| H(20c) | 0.3362 | 0.2810 | 0.5990 |
| H(20b) | 0.3870 | 0.1318 | 0.5735 |
| H(m1) | 0.1639 | 0.8197 | 0.2735 |

Table A5.3 Anisotropic thermal parameters ( $Å^2$ ) for $[CdL^{16}Br]_2CdBr_4$

| Atom | $U_{11}$ | $U_{22}$ | $U_{33}$ | $U_{23}$ | $U_{13}$ | $U_{12}$ |
|---|---|---|---|---|---|---|
| Cd(3) | 0.048(1) | 0.039(1) | 0.039(1) | 0.005(1) | 0.012(1) | -0.001(1) |
| Br(31) | 0.055(1) | 0.040(1) | 0.059(2) | 0.004(1) | 0.028(1) | 0.001(1) |
| Br(32) | 0.049(1) | 0.063(1) | 0.066(2) | 0.023(1) | -0.002(1) | -0.007(1) |
| Br(33) | 0.056(1) | 0.044(1) | 0.053(2) | 0.008(1) | 0.013(1) | -0.009(1) |
| Br(34) | 0.088(2) | 0.064(1) | 0.048(2) | -0.005(1) | 0.033(1) | -0.013(1) |
| Cd(1) | 0.046(1) | 0.038(1) | 0.039(1) | 0.007(1) | 0.004(1) | -0.011(1) |
| Br(1) | 0.053(1) | 0.088(2) | 0.069(2) | -0.003(1) | 0.027(1) | -0.009(1) |
| N(12a) | 0.053(10) | 0.039(9) | 0.034(11) | -0.006(8) | 0.024(9) | 0.001(7) |
| N(11a) | 0.038(9) | 0.047(9) | 0.030(11) | 0.009(8) | 0.006(8) | -0.012(7) |
| C(11a) | 0.054(13) | 0.034(10) | 0.046(15) | -0.006(10) | 0.003(11) | -0.009(9) |
| C(18a) | 0.048(11) | 0.031(10) | 0.036(14) | -0.010(9) | 0.012(10) | -0.009(8) |
| C(19a) | 0.051(12) | 0.042(11) | 0.024(13) | 0.006(10) | -0.005(10) | -0.015(9) |
| C(10a) | 0.073(15) | 0.060(13) | 0.052(17) | 0.028(13) | 0.006(13) | -0.017(11) |

table A5.3 continued

| | | | | | | |
|---|---|---|---|---|---|---|
| N(12b) | 0.046(9) | 0.027(8) | 0.061(14) | 0.012(8) | 0.002(9) | -0.003(7) |
| N(11b) | 0.048(9) | 0.045(9) | 0.041(12) | 0.007(8) | 0.010(9) | -0.016(7) |
| C(11b) | 0.081(16) | 0.039(11) | 0.051(16) | 0.025(11) | 0.016(14) | 0.010(11) |
| C(18b) | 0.041(12) | 0.054(12) | 0.061(17) | 0.000(12) | -0.001(11) | -0.020(10) |
| C(19b) | 0.063(13) | 0.070(14) | 0.045(16) | -0.005(12) | 0.027(12) | -0.040(11) |
| C(10b) | 0.045(13) | 0.059(14) | 0.068(18) | 0.005(12) | -0.026(12) | -0.006(10) |
| Cd(2) | 0.038(1) | 0.040(1) | 0.036(1) | 0.001(1) | 0.006(1) | -0.006(1) |
| Br(2) | 0.056(1) | 0.058(1) | 0.066(2) | 0.028(1) | -0.005(1) | -0.010(1) |
| N(22a) | 0.047(9) | 0.047(9) | 0.023(10) | 0.004(8) | 0.005(8) | 0.003(7) |
| N(21a) | 0.044(9) | 0.039(8) | 0.015(9) | -0.004(7) | -0.002(8) | -0.011(7) |
| C(21a) | 0.046(13) | 0.100(18) | 0.056(18) | -0.020(15) | -0.003(13) | -0.010(12) |
| C(28a) | 0.035(11) | 0.046(11) | 0.048(15) | 0.007(10) | 0.012(10) | -0.001(9) |
| C(29a) | 0.052(13) | 0.071(14) | 0.027(14) | 0.009(11) | 0.014(11) | -0.008(11) |
| C(20a) | 0.068(15) | 0.052(13) | 0.077(20) | -0.009(13) | 0.032(15) | -0.026(11) |
| N(22b) | 0.041(10) | 0.106(14) | 0.044(13) | 0.021(11) | 0.004(9) | -0.027(10) |
| N(21b) | 0.055(10) | 0.036(8) | 0.015(10) | -0.005(8) | 0.005(8) | -0.004(7) |

table A5.3 continued

| | | | | | | |
|---|---|---|---|---|---|---|
| C(21b) | 0.086(20) | 0.180(29) | 0.086(24) | -0.013(21) | 0.048(19) | -0.070(20) |
| C(28b) | 0.043(11) | 0.052(12) | 0.039(14) | 0.012(11) | -0.001(10) | -0.018(9) |
| C(29b) | 0.037(11) | 0.070(14) | 0.051(17) | 0.008(13) | -0.002(11) | -0.018(10) |
| C(20b) | 0.057(14) | 0.087(16) | 0.040(16) | 0.019(13) | 0.002(12) | -0.013(12) |
| O(m1) | 0.074(18) | 0.194(28) | 0.122(26) | -0.095(23) | 0.025(18) | -0.048(18) |
| C(m1) | 0.053(20) | 0.145(33) | 0.049(24) | 0.032(24) | 0.015(18) | 0.025(20) |

Table A5.4 Bond lengths ( Å) for $[CdL^{16}Br]_2CdBr_4$

| | | | |
|---|---|---|---|
| Cd(3) -Br(31) | 2.613(2) | Cd(3) -Br(32) | 2.596(2) |
| Cd(3) -Br(33) | 2.597(3) | Cd(3) -Br(34) | 2.561(3) |
| Cd(1) -Br(1) | 2.660(3) | Cd(1) -N(12a) | 2.427(13) |
| Cd(1) -N(11a) | 2.276(15) | Cd(1) -N(12b) | 2.390(14) |
| Cd(1) -N(11b) | 2.257(14) | N(12a)-C(11a) | 1.492(22) |
| N(12a)-C(12a) | 1.459(25) | N(12a)-H(12e) | 1.105(15) |
| N(11a)-C(18a) | 1.505(22) | N(11a)-C(19a) | 1.484(21) |
| N(11a)-H(11e) | 0.899(16) | C(11a)-C(11b) | 1.54(3) |
| C(12a)-C(13a) | 1.378(24) | C(12a)-C(17a) | 1.36(3) |
| C(13a)-C(14a) | 1.40(3) | C(14a)-C(15a) | 1.34(3) |
| C(15a)-C(16a) | 1.380(24) | C(16a)-C(17a) | 1.34(3) |
| C(17a)-C(18a) | 1.484(21) | C(19a)-C(10a) | 1.49(3) |
| C(10a)-C(10b) | 1.51(3) | N(12b)-C(11b) | 1.49(3) |
| N(12b)-C(12b) | 1.453(24) | N(12b)-H(12f) | 1.144(14) |
| N(11b)-C(18b) | 1.538(23) | N(11b)-C(19b) | 1.45(3) |
| N(11b)-H(11f) | 1.075(14) | C(12b)-C(13b) | 1.40(3) |
| C(12b)-C(17b) | 1.35(3) | C(13b)-C(14b) | 1.38(3) |
| C(14b)-C(15b) | 1.27(3) | C(15b)-C(16b) | 1.36(4) |
| C(16b)-C(17b) | 1.44(3) | C(17b)-C(18b) | 1.46(4) |
| C(19b)-C(10b) | 1.58(3) | Cd(2) -Br(2) | 2.574(3) |
| Cd(2) -N(22a) | 2.339(13) | Cd(2) -N(21a) | 2.332(13) |
| Cd(2) -N(22b) | 2.431(17) | Cd(2) -N(21b) | 2.247(15) |
| N(22a)-C(21a) | 1.508(25) | N(22a)-C(22a) | 1.41(3) |
| N(22a)-H(22e) | 1.122(15) | N(21a)-H(21e) | 1.080(21) |

table A5.4 continued

| | | | |
|---|---|---|---|
| N(21a)-C(28a) | 1.494(20) | N(21a)-C(29a) | 1.451(25) |
| C(21a)-C(21b) | 1.41(4) | C(22a)-C(23a) | 1.41(3) |
| C(22a)-C(27a) | 1.371(24) | C(23a)-C(24a) | 1.39(3) |
| C(24a)-C(25a) | 1.40(3) | C(25a)-C(26a) | 1.43(3) |
| C(26a)-C(27a) | 1.39(3) | C(27a)-C(28a) | 1.502(25) |
| C(29a)-C(20a) | 1.52(3) | C(20a)-C(20b) | 1.50(3) |
| N(22b)-C(21b) | 1.47(3) | N(22b)-C(22b) | 1.409(23) |
| N(22b)-H(22f) | 1.085(20) | N(21b)-H(21f) | 1.080(19) |
| N(21b)-C(28b) | 1.50(3) | N(21b)-C(29b) | 1.457(23) |
| C(22b)-C(23b) | 1.39(3) | C(22b)-C(27b) | 1.40(3) |
| C(23b)-C(24b) | 1.42(3) | C(24b)-C(25b) | 1.33(3) |
| C(25b)-C(26b) | 1.42(3) | C(26b)-C(27b) | 1.438(25) |
| C(27b)-C(28b) | 1.524(24) | C(29b)-C(20b) | 1.57(3) |
| O(m1) -C(m1) | 1.60(5) | O(m2) -C(m2) | 1.548(1) |

Table A5.5 Bond angles (°) for $[CdL^{16}Br]_2CdBr_4$

| | | | |
|---|---|---|---|
| Br(32)-Cd(3) -Br(31) | 110.8(1) | Br(33)-Cd(3) -Br(31) | 105.5(1) |
| Br(33)-Cd(3) -Br(32) | 105.2(1) | Br(34)-Cd(3) -Br(31) | 108.5(1) |
| Br(34)-Cd(3) -Br(32) | 112.5(1) | Br(34)-Cd(3) -Br(33) | 114.1(1) |
| N(12a)-Cd(1) -Br(1) | 94.6(4) | N(11a)-Cd(1) -Br(1) | 96.5(4) |
| N(11a)-Cd(1) -N(12a) | 85.0(5) | N(12b)-Cd(1) -Br(1) | 98.2(4) |
| N(12b)-Cd(1) -N(12a) | 75.9(5) | N(12b)-Cd(1) -N(11a) | 156.7(5) |
| N(11b)-Cd(1) -Br(1) | 95.0(4) | N(11b)-Cd(1) -N(12a) | 160.9(5) |
| N(11b)-Cd(1) -N(11a) | 110.1(6) | N(11b)-Cd(1) -N(12b) | 86.5(5) |
| C(11a)-N(12a)-Cd(1) | 107(1) | C(12a)-N(12a)-Cd(1) | 119(1) |
| C(12a)-N(12a)-C(11a) | 115(1) | H(12e)-N(12a)-Cd(1) | 111.2(8) |
| H(12e)-N(12a)-C(11a) | 109(1) | H(12e)-N(12a)-C(12a) | 94(1) |
| C(18a)-N(11a)-Cd(1) | 107(1) | C(19a)-N(11a)-Cd(1) | 111(1) |
| C(19a)-N(11a)-C(18a) | 112(1) | H(11e)-N(11a)-Cd(1) | 128(1) |
| H(11e)-N(11a)-C(18a) | 96(1) | H(11e)-N(11a)-C(19a) | 101(1) |
| C(11b)-C(11a)-N(12a) | 108(1) | C(13a)-C(12a)-N(12a) | 119(2) |
| C(17a)-C(12a)-N(12a) | 118(1) | C(17a)-C(12a)-C(13a) | 122(2) |
| C(14a)-C(13a)-C(12a) | 119(2) | C(15a)-C(14a)-C(13a) | 119(2) |
| C(16a)-C(15a)-C(14a) | 120(2) | C(17a)-C(16a)-C(15a) | 123(2) |
| C(16a)-C(17a)-C(12a) | 117(1) | C(18a)-C(17a)-C(12a) | 124(2) |
| C(18a)-C(17a)-C(16a) | 119(2) | C(17a)-C(18a)-N(11a) | 111(1) |
| C(10a)-C(19a)-N(11a) | 112(1) | C(10b)-C(10a)-C(19a) | 117(2) |
| C(11b)-N(12b)-Cd(1) | 106(1) | C(12b)-N(12b)-Cd(1) | 111(1) |
| C(12b)-N(12b)-C(11b) | 117(2) | H(12f)-N(12b)-Cd(1) | 116(1) |
| H(12f)-N(12b)-C(11b) | 98(1) | H(12f)-N(12b)-C(12b) | 109(1) |
| C(18b)-N(11b)-Cd(1) | 110(1) | C(19b)-N(11b)-Cd(1) | 115(1) |

table A5.5 continued

| | | | |
|---|---|---|---|
| C(19b)-N(11b)-C(18b) | 112(1) | H(11f)-N(11b)-Cd(1) | 117(1) |
| H(11f)-N(11b)-C(18b) | 102(1) | H(11f)-N(11b)-C(19b) | 100(1) |
| N(12b)-C(11b)-C(11a) | 111(2) | C(13b)-C(12b)-N(12b) | 121(2) |
| C(17b)-C(12b)-N(12b) | 117(2) | C(17b)-C(12b)-C(13b) | 122(2) |
| C(14b)-C(13b)-C(12b) | 115(2) | C(15b)-C(14b)-C(13b) | 128(3) |
| C(16b)-C(15b)-C(14b) | 117(2) | C(17b)-C(16b)-C(15b) | 122(2) |
| C(16b)-C(17b)-C(12b) | 117(2) | C(18b)-C(17b)-C(12b) | 124(2) |
| C(18b)-C(17b)-C(16b) | 119(2) | C(17b)-C(18b)-N(11b) | 111(2) |
| C(10b)-C(19b)-N(11b) | 113(2) | C(19b)-C(10b)-C(10a) | 118(1) |
| N(22a)-Cd(2) -Br(2) | 98.3(4) | N(21a)-Cd(2) -Br(2) | 105.1(4) |
| N(21a)-Cd(2) -N(22a) | 86.2(5) | N(22b)-Cd(2) -Br(2) | 104.5(4) |
| N(22b)-Cd(2) -N(22a) | 73.2(5) | N(22b)-Cd(2) -N(21a) | 145.9(5) |
| N(21b)-Cd(2) -Br(2) | 102.5(4) | N(21b)-Cd(2) -N(22a) | 151.9(6) |
| N(21b)-Cd(2) -N(21a) | 106.0(5) | N(21b)-Cd(2) -N(22b) | 83.5(5) |
| C(21a)-N(22a)-Cd(2) | 104(1) | C(22a)-N(22a)-Cd(2) | 109(1) |
| C(22a)-N(22a)-C(21a) | 119(2) | H(22e)-N(22a)-Cd(2) | 93.2(8) |
| H(22e)-N(22a)-C(21a) | 113(2) | H(22e)-N(22a)-C(22a) | 114(1) |
| H(21e)-N(21a)-Cd(2) | 107(1) | C(28a)-N(21a)-Cd(2) | 108(1) |
| C(28a)-N(21a)-H(21e) | 113(2) | C(29a)-N(21a)-Cd(2) | 114(1) |
| C(29a)-N(21a)-H(21e) | 105(1) | C(29a)-N(21a)-C(28a) | 109(1) |
| C(21b)-C(21a)-N(22a) | 115(2) | C(23a)-C(22a)-N(22a) | 123(2) |
| C(27a)-C(22a)-N(22a) | 117(2) | C(27a)-C(22a)-C(23a) | 120(2) |
| C(24a)-C(23a)-C(22a) | 120(2) | C(25a)-C(24a)-C(23a) | 121(2) |
| C(26a)-C(25a)-C(24a) | 117(2) | C(27a)-C(26a)-C(25a) | 122(2) |
| C(26a)-C(27a)-C(22a) | 120(2) | C(28a)-C(27a)-C(22a) | 122(2) |
| C(28a)-C(27a)-C(26a) | 118(2) | C(27a)-C(28a)-N(21a) | 113(1) |
| C(20a)-C(29a)-N(21a) | 115(1) | C(20b)-C(20a)-C(29a) | 115(2) |
| C(21b)-N(22b)-Cd(2) | 111(1) | C(22b)-N(22b)-Cd(2) | 107(1) |

table A5.5 continued

| | | | |
|---|---|---|---|
| C(22b)-N(22b)-C(21b) | 122(2) | H(22f)-N(22b)-Cd(2) | 117(1) |
| H(22f)-N(22b)-C(21b) | 100(2) | H(22f)-N(22b)-C(22b) | 99(2) |
| H(21f)-N(21b)-Cd(2) | 104(1) | C(28b)-N(21b)-Cd(2) | 114(1) |
| C(28b)-N(21b)-H(21f) | 106(1) | C(29b)-N(21b)-Cd(2) | 114(1) |
| C(29b)-N(21b)-H(21f) | 106(1) | C(29b)-N(21b)-C(28b) | 111(2) |
| N(22b)-C(21b)-C(21a) | 112(2) | C(23b)-C(22b)-N(22b) | 121(2) |
| C(27b)-C(22b)-N(22b) | 118(2) | C(27b)-C(22b)-C(23b) | 121(2) |
| C(24b)-C(23b)-C(22b) | 118(2) | C(25b)-C(24b)-C(23b) | 123(2) |
| C(26b)-C(25b)-C(24b) | 122(2) | C(27b)-C(26b)-C(25b) | 116(2) |
| C(26b)-C(27b)-C(22b) | 121(2) | C(28b)-C(27b)-C(22b) | 119(1) |
| C(28b)-C(27b)-C(26b) | 120(2) | C(27b)-C(28b)-N(21b) | 110(2) |
| C(20b)-C(29b)-N(21b) | 108(2) | C(29b)-C(20b)-C(20a) | 117(2) |

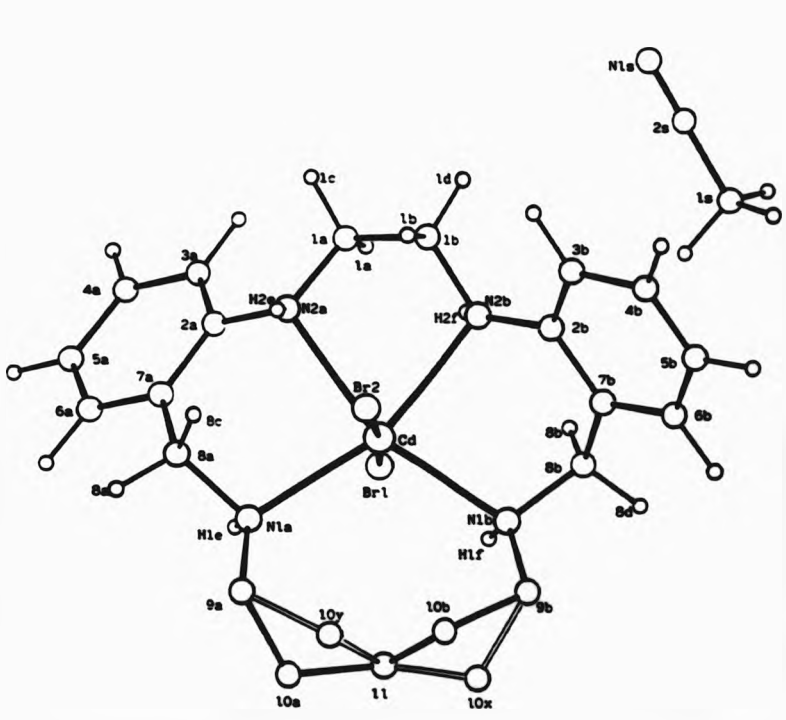


FIGURE A6 Labelled diagram of $[CdL^{17}Br_2].CH_3CN$.

Table A6.1 Fractional atomic coordinates and thermal parameters ( $Å^2$) for $[CdL^{17}Br_2].CH_3CN$

| Atom | x | y | z | $U_{iso}$ or $U_{eq}$ |
|---|---|---|---|---|
| Cd | -0.15787(4) | -0.07139(4) | 0.12825(6) | 0.0342(4) |
| Br(1) | -0.10215(6) | 0.08286(7) | 0.02746(9) | 0.0537(7) |
| Br(2) | -0.20887(6) | -0.21351(7) | 0.24092(9) | 0.0494(6) |
| N(2a) | -0.0290(4) | -0.0529(5) | 0.3060(6) | 0.036(4) |
| N(1a) | -0.2273(4) | 0.0362(4) | 0.2232(6) | 0.035(4) |
| C(1a) | 0.0444(5) | -0.0960(6) | 0.2750(8) | 0.046(6) |
| C(2a) | -0.0169(6) | 0.0380(6) | 0.3556(7) | 0.036(5) |
| C(3a) | 0.0617(6) | 0.0841(6) | 0.3753(7) | 0.040(6) |
| C(4a) | 0.0721(7) | 0.1732(7) | 0.4208(8) | 0.048(6) |
| C(5a) | 0.0022(7) | 0.2158(7) | 0.4447(8) | 0.052(7) |
| C(6a) | -0.0751(6) | 0.1704(6) | 0.4231(7) | 0.044(6) |
| C(7a) | -0.0877(6) | 0.0826(6) | 0.3782(7) | 0.038(5) |
| C(8a) | -0.1759(5) | 0.0371(6) | 0.3571(7) | 0.041(6) |
| C(9a) | -0.3211(5) | 0.0192(7) | 0.2124(8) | 0.049(6) |
| C(10a) | -0.3815(7) | 0.0545(9) | 0.0879(9) | 0.053(8) |
| C(11) | -0.3617(6) | 0.0207(7) | -0.0277(9) | 0.055(7) |
| N(2b) | -0.0470(4) | -0.1723(5) | 0.0911(6) | 0.036(4) |
| N(1b) | -0.2264(4) | -0.0949(5) | -0.0823(6) | 0.043(5) |
| C(1b) | 0.0182(6) | -0.1871(6) | 0.2112(8) | 0.043(6) |
| C(2b) | -0.0839(6) | -0.2522(6) | 0.0235(8) | 0.043(6) |
| C(3b) | -0.0638(7) | -0.3409(7) | 0.0684(9) | 0.064(7) |
| C(4b) | -0.1045(9) | -0.4162(7) | -0.0023(12) | 0.083(9) |
| C(5b) | -0.1624(8) | -0.4052(8) | -0.1122(12) | 0.082(9) |
| C(6b) | -0.1829(7) | -0.3164(8) | -0.1558(10) | 0.067(8) |
| C(7b) | -0.1454(6) | -0.2385(7) | -0.0912(8) | 0.050(6) |

table A6.1 continued

| | | | | |
|---|---|---|---|---|
| C(8b) | -0.1679(6) | -0.1443(6) | -0.1428(8) | 0.048(6) |
| C(9b) | -0.3178(6) | -0.1256(7) | -0.1251(8) | 0.056(7) |
| C(10b) | -0.3660(7) | -0.0872(7) | -0.0394(11) | 0.051(8) |
| C(10y) | -0.3699(26) | -0.0270(24) | 0.0904(16) | 0.042(12) |
| C(10x) | -0.3881(20) | -0.0504(22) | -0.1311(31) | 0.067(14) |
| C(1s) | 0.0784(7) | -0.3134(7) | -0.1486(9) | 0.066(8) |
| C(2s) | 0.1420(9) | -0.3371(8) | -0.0342(11) | 0.073(9) |
| N(1s) | 0.1900(8) | -0.3544(9) | 0.0541(9) | 0.113(10) |

Table A6.2 Fractional atomic coordinates for the found hydrogen atoms for $[CdL^{17}Br_2].CH_3CN$

| Atom | x | y | z |
|---|---|---|---|
| H(1e) | -0.2040 | 0.1016 | 0.2025 |
| H(2e) | -0.0540 | -0.0890 | 0.3410 |
| H(1f) | -0.2158 | -0.0309 | -0.0999 |
| H(2f) | -0.0118 | -0.1107 | 0.0752 |

Table A6.3 Anisotropic thermal parameters ( Å) for $[CdL^{17}Br_2].CH_3CN$

| Atom | $U_{11}$ | $U_{22}$ | $U_{33}$ | $U_{23}$ | $U_{13}$ | $U_{12}$ |
|---|---|---|---|---|---|---|
| Cd | 0.0321(4) | 0.0387(4) | 0.0317(4) | -0.0006(3) | 0.0065(3) | -0.0015(3) |
| Br(1) | 0.060(1) | 0.045(1) | 0.057(1) | 0.001(1) | 0.028(1) | -0.011(1) |
| Br(2) | 0.049(1) | 0.045(1) | 0.054(1) | 0.008(1) | 0.016(1) | -0.006(1) |
| N(2a) | 0.032(4) | 0.043(5) | 0.033(4) | 0.003(3) | 0.007(3) | -0.004(3) |
| N(1a) | 0.040(5) | 0.032(4) | 0.033(4) | 0.001(3) | 0.009(4) | 0.002(3) |
| C(1a) | 0.034(5) | 0.068(7) | 0.035(6) | 0.011(5) | 0.006(4) | 0.017(5) |
| C(2a) | 0.040(6) | 0.042(5) | 0.027(5) | 0.001(4) | -0.003(4) | -0.004(5) |
| C(3a) | 0.035(5) | 0.053(6) | 0.033(5) | 0.003(5) | -0.003(4) | 0.000(5) |
| C(4a) | 0.048(6) | 0.051(7) | 0.046(6) | 0.002(5) | -0.001(5) | -0.013(5) |
| C(5a) | 0.062(7) | 0.047(6) | 0.046(7) | -0.003(5) | -0.003(6) | -0.014(6) |
| C(6a) | 0.053(6) | 0.046(6) | 0.031(6) | -0.002(5) | -0.006(5) | 0.002(5) |
| C(7a) | 0.046(6) | 0.045(6) | 0.023(5) | -0.004(5) | -0.001(4) | -0.010(5) |
| C(8a) | 0.044(6) | 0.048(6) | 0.031(5) | -0.004(4) | 0.014(4) | 0.001(5) |
| C(9a) | 0.022(5) | 0.066(7) | 0.059(7) | -0.006(5) | 0.016(5) | 0.001(4) |
| C(10a) | 0.039(7) | 0.075(10) | 0.046(8) | -0.013(7) | -0.001(6) | 0.015(6) |

table A6.3 continued

| | | | | | | |
|---|---|---|---|---|---|---|
| C(11) | 0.048(6) | 0.059(7) | 0.058(7) | 0.005(6) | -0.001(5) | 0.007(5) |
| N(2b) | 0.035(5) | 0.036(4) | 0.038(5) | 0.001(4) | 0.004(4) | 0.001(4) |
| N(1b) | 0.043(5) | 0.052(5) | 0.033(4) | 0.004(4) | 0.005(4) | -0.006(4) |
| C(1b) | 0.044(6) | 0.042(6) | 0.042(6) | 0.002(5) | 0.013(5) | 0.009(5) |
| C(2b) | 0.051(6) | 0.043(6) | 0.036(6) | -0.001(5) | 0.021(5) | 0.001(5) |
| C(3b) | 0.081(8) | 0.048(7) | 0.063(7) | 0.001(6) | 0.041(6) | -0.001(6) |
| C(4b) | 0.112(11) | 0.043(7) | 0.093(10) | -0.014(7) | 0.052(9) | -0.005(7) |
| C(5b) | 0.096(10) | 0.062(8) | 0.088(10) | -0.043(7) | 0.031(8) | -0.021(7) |
| C(6b) | 0.071(8) | 0.070(8) | 0.060(8) | -0.024(6) | 0.023(6) | -0.010(7) |
| C(7b) | 0.051(6) | 0.052(7) | 0.046(6) | -0.011(5) | 0.031(5) | -0.017(5) |
| C(8b) | 0.046(6) | 0.062(7) | 0.036(6) | -0.015(5) | 0.015(5) | -0.012(5) |
| C(9b) | 0.042(6) | 0.072(7) | 0.054(7) | -0.018(6) | 0.011(5) | -0.019(5) |
| C(10b) | 0.035(7) | 0.053(8) | 0.063(9) | -0.005(7) | 0.011(6) | 0.003(6) |
| C(1s) | 0.080(8) | 0.070(8) | 0.049(7) | -0.006(6) | 0.015(6) | 0.003(6) |
| C(2s) | 0.101(10) | 0.069(8) | 0.050(7) | -0.011(7) | 0.024(7) | -0.023(7) |
| N(1s) | 0.151(11) | 0.123(10) | 0.066(7) | 0.015(8) | -0.016(7) | -0.030(9) |

Table A6.4 Bond lengths ( Å) for $[CdL^{17}Br_2].CH_3CN$

| | | | | | |
|---|---|---|---|---|---|
| Cd | -Br(1) | 2.793(1) | Cd | -Br(2) | 2.695(1) |
| Cd | -N(2a) | 2.450(6) | Cd | -N(1a) | 2.370(7) |
| Cd | -N(2b) | 2.440(7) | Cd | -N(1b) | 2.370(6) |
| N(2a) | -C(1a) | 1.469(12) | N(2a) | -C(2a) | 1.430(11) |
| N(2a) | -H(2e) | 0.834(7) | N(1a) | -C(8a) | 1.517(10) |
| N(1a) | -C(9a) | 1.493(11) | N(1a) | -H(1e) | 1.074(7) |
| C(1a) | -C(1b) | 1.512(12) | C(2a) | -C(3a) | 1.384(13) |
| C(2a) | -C(7a) | 1.398(14) | C(3a) | -C(4a) | 1.388(13) |
| C(4a) | -C(5a) | 1.379(16) | C(5a) | -C(6a) | 1.360(15) |
| C(6a) | -C(7a) | 1.369(13) | C(7a) | -C(8a) | 1.514(13) |
| C(9a) | -C(10a) | 1.558(13) | C(9a) | -C(10y) | 1.543(24) |
| C(10a) | -C(11) | 1.540(16) | C(10y) | -C(11) | 1.57(3) |
| C(11) | -C(10b) | 1.574(14) | C(11) | -C(10x) | 1.54(3) |
| N(2b) | -C(1b) | 1.480(10) | N(2b) | -C(2b) | 1.425(11) |
| N(2b) | -H(2f) | 1.102(7) | N(1b) | -C(8b) | 1.508(13) |
| N(1b) | -C(9b) | 1.469(11) | N(1b) | -H(1f) | 0.978(7) |
| C(2b) | -C(3b) | 1.390(13) | C(2b) | -C(7b) | 1.406(12) |
| C(3b) | -C(4b) | 1.404(15) | C(4b) | -C(5b) | 1.337(17) |
| C(5b) | -C(6b) | 1.388(16) | C(6b) | -C(7b) | 1.390(14) |
| C(7b) | -C(8b) | 1.494(13) | C(9b) | -C(10b) | 1.531(17) |
| C(9b) | -C(10x) | 1.56(3) | C(1s) | -C(2s) | 1.445(14) |
| C(2s) | -N(1s) | 1.106(15) | | | |

table A6.3 continued

| | | | | | | |
|---|---|---|---|---|---|---|
| C(11) | 0.048(6) | 0.059(7) | 0.058(7) | 0.005(6) | -0.001(5) | 0.007(5) |
| N(2b) | 0.035(5) | 0.036(4) | 0.038(5) | 0.001(4) | 0.004(4) | 0.001(4) |
| N(1b) | 0.043(5) | 0.052(5) | 0.033(4) | 0.004(4) | 0.005(4) | -0.006(4) |
| C(1b) | 0.044(6) | 0.042(6) | 0.042(6) | 0.002(5) | 0.013(5) | 0.009(5) |
| C(2b) | 0.051(6) | 0.043(6) | 0.036(6) | -0.001(5) | 0.021(5) | 0.001(5) |
| C(3b) | 0.081(8) | 0.048(7) | 0.063(7) | 0.001(6) | 0.041(6) | -0.001(6) |
| C(4b) | 0.112(11) | 0.043(7) | 0.093(10) | -0.014(7) | 0.052(9) | -0.005(7) |
| C(5b) | 0.096(10) | 0.062(8) | 0.088(10) | -0.043(7) | 0.031(8) | -0.021(7) |
| C(6b) | 0.071(8) | 0.070(8) | 0.060(8) | -0.024(6) | 0.023(6) | -0.010(7) |
| C(7b) | 0.051(6) | 0.052(7) | 0.046(6) | -0.011(5) | 0.031(5) | -0.017(5) |
| C(8b) | 0.046(6) | 0.062(7) | 0.036(6) | -0.015(5) | 0.015(5) | -0.012(5) |
| C(9b) | 0.042(6) | 0.072(7) | 0.054(7) | -0.018(6) | 0.011(5) | -0.019(5) |
| C(10b) | 0.035(7) | 0.053(8) | 0.063(9) | -0.005(7) | 0.011(6) | 0.003(6) |
| C(1a) | 0.080(8) | 0.070(8) | 0.049(7) | -0.006(6) | 0.015(6) | 0.003(6) |
| C(2a) | 0.101(10) | 0.069(8) | 0.050(7) | -0.011(7) | 0.024(7) | -0.023(7) |
| N(1a) | 0.151(11) | 0.123(10) | 0.066(7) | 0.015(8) | -0.016(7) | -0.030(9) |

Table A6.4 Bond lengths ( Å) for $[CdL^{17}Br_2].CH_3CN$

| | | | | | |
|---|---|---|---|---|---|
| Cd | -Br(1) | 2.793(1) | Cd | -Br(2) | 2.695(1) |
| Cd | -N(2a) | 2.450(6) | Cd | -N(1a) | 2.370(7) |
| Cd | -N(2b) | 2.440(7) | Cd | -N(1b) | 2.370(6) |
| N(2a) | -C(1a) | 1.469(12) | N(2a) | -C(2a) | 1.430(11) |
| N(2a) | -H(2e) | 0.834(7) | N(1a) | -C(8a) | 1.517(10) |
| N(1a) | -C(9a) | 1.493(11) | N(1a) | -H(1e) | 1.074(7) |
| C(1a) | -C(1b) | 1.512(12) | C(2a) | -C(3a) | 1.384(13) |
| C(2a) | -C(7a) | 1.398(14) | C(3a) | -C(4a) | 1.388(13) |
| C(4a) | -C(5a) | 1.379(16) | C(5a) | -C(6a) | 1.360(15) |
| C(6a) | -C(7a) | 1.369(13) | C(7a) | -C(8a) | 1.514(13) |
| C(9a) | -C(10a) | 1.558(13) | C(9a) | -C(10y) | 1.543(24) |
| C(10a) | -C(11) | 1.540(16) | C(10y) | -C(11) | 1.57(3) |
| C(11) | -C(10b) | 1.574(14) | C(11) | -C(10x) | 1.54(3) |
| N(2b) | -C(1b) | 1.480(10) | N(2b) | -C(2b) | 1.425(11) |
| N(2b) | -H(2f) | 1.102(7) | N(1b) | -C(8b) | 1.508(13) |
| N(1b) | -C(9b) | 1.469(11) | N(1b) | -H(1f) | 0.978(7) |
| C(2b) | -C(3b) | 1.390(13) | C(2b) | -C(7b) | 1.406(12) |
| C(3b) | -C(4b) | 1.404(15) | C(4b) | -C(5b) | 1.337(17) |
| C(5b) | -C(6b) | 1.388(16) | C(6b) | -C(7b) | 1.390(14) |
| C(7b) | -C(8b) | 1.494(13) | C(9b) | -C(10b) | 1.531(17) |
| C(9b) | -C(10x) | 1.56(3) | C(1s) | -C(2s) | 1.445(14) |
| C(2s) | -N(1s) | 1.106(15) | | | |

Table A6.5 Bond angles (°) for $[CdL^{17}Br_2].CH_3CN$

| | | | | | |
|---|---|---|---|---|---|
| Br(2) -Cd | -Br(1) | 175.8(1) | N(2a) -Cd | -Br(1) | 88.0(2) |
| N(2a) -Cd | -Br(2) | 89.0(2) | N(1a) -Cd | -Br(1) | 85.2(2) |
| N(1a) -Cd | -Br(2) | 91.8(2) | N(1a) -Cd | -N(2a) | 86.3(2) |
| N(2b) -Cd | -Br(1) | 93.9(2) | N(2b) -Cd | -Br(2) | 88.1(2) |
| N(2b) -Cd | -N(2a) | 74.8(2) | N(2b) -Cd | -N(1a) | 161.1(2) |
| N(1b) -Cd | -Br(1) | 78.3(2) | N(1b) -Cd | -Br(2) | 105.6(2) |
| N(1b) -Cd | -N(2a) | 152.6(3) | N(1b) -Cd | -N(1a) | 115.5(2) |
| N(1b) -Cd | -N(2b) | 82.6(2) | C(1a) -N(2a) | -Cd | 106.6(5) |
| C(2a) -N(2a) | -Cd | 114.5(5) | C(2a) -N(2a) | -C(1a) | 118.0(7) |
| H(2e) -N(2a) | -Cd | 85.9(4) | H(2e) -N(2a) | -C(1a) | 112.7(7) |
| H(2e) -N(2a) | -C(2a) | 114.5(8) | C(8a) -N(1a) | -Cd | 106.8(5) |
| C(9a) -N(1a) | -Cd | 117.0(5) | C(9a) -N(1a) | -C(8a) | 108.2(7) |
| H(1e) -N(1a) | -Cd | 103.8(5) | H(1e) -N(1a) | -C(8a) | 95.7(5) |
| H(1e) -N(1a) | -C(9a) | 122.5(6) | C(1b) -C(1a) | -N(2a) | 111.5(7) |
| C(3a) -C(2a) | -N(2a) | 121.4(9) | C(7a) -C(2a) | -N(2a) | 118.9(8) |
| C(7a) -C(2a) | -C(3a) | 119.7(8) | C(4a) -C(3a) | -C(2a) | 120.9(9) |
| C(5a) -C(4a) | -C(3a) | 118.8(9) | C(6a) -C(5a) | -C(4a) | 119.8(9) |
| C(7a) -C(6a) | -C(5a) | 123(1) | C(6a) -C(7a) | -C(2a) | 117.9(9) |
| C(8a) -C(7a) | -C(2a) | 122.6(8) | C(8a) -C(7a) | -C(6a) | 119.5(9) |
| C(7a) -C(8a) | -N(1a) | 111.3(7) | C(10a)-C(9a) | -N(1a) | 110.7(8) |
| C(10y)-C(9a) | -N(1a) | 112(2) | C(11) -C(10a) | -C(9a) | 117.4(9) |
| C(11) -C(10y) | -C(9a) | 116(2) | C(10b)-C(11) | -C(10a) | 112.1(9) |
| C(10x)-C(11) | -C(10y) | 107(2) | C(1b) -N(2b) | -Cd | 105.7(5) |
| C(2b) -N(2b) | -Cd | 112.4(5) | C(2b) -N(2b) | -C(1b) | 117.0(7) |
| H(2f) -N(2b) | -Cd | 88.7(4) | H(2f) -N(2b) | -C(1b) | 91.2(5) |

table A6.5 continued

| | | | |
|---|---|---|---|
| H(2f) -N(2b) -C(2b) | 136.1(8) | C(8b) -N(1b) -Cd | 112.4(4) |
| C(9b) -N(1b) -Cd | 119.8(6) | C(9b) -N(1b) -C(8b) | 113.4(7) |
| H(1f) -N(1b) -Cd | 91.1(4) | H(1f) -N(1b) -C(8b) | 100.7(7) |
| H(1f) -N(1b) -C(9b) | 115.9(7) | N(2b) -C(1b) -C(1a) | 110.0(7) |
| C(3b) -C(2b) -N(2b) | 122.7(7) | C(7b) -C(2b) -N(2b) | 117.2(8) |
| C(7b) -C(2b) -C(3b) | 120.0(8) | C(4b) -C(3b) -C(2b) | 119.4(9) |
| C(5b) -C(4b) -C(3b) | 122(1) | C(6b) -C(5b) -C(4b) | 118(1) |
| C(7b) -C(6b) -C(5b) | 123.1(9) | C(6b) -C(7b) -C(2b) | 117.2(9) |
| C(8b) -C(7b) -C(2b) | 121.5(8) | C(8b) -C(7b) -C(6b) | 121.3(8) |
| C(7b) -C(8b) -N(1b) | 111.2(8) | C(10b)-C(9b) -N(1b) | 108.5(7) |
| C(10x)-C(9b) -N(1b) | 116(1) | C(9b) -C(10b)-C(11) | 114(1) |
| C(9b) -C(10x)-C(11) | 114(2) | N(1s) -C(2s) -C(1s) | 179(1) |

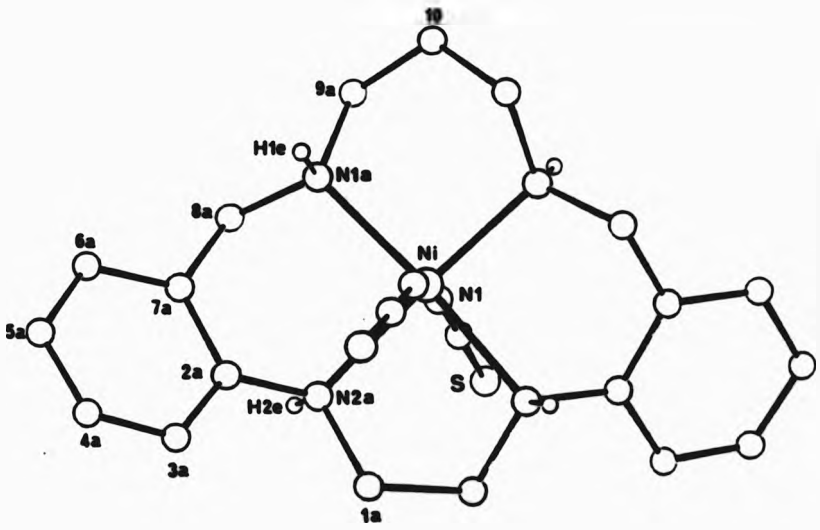


FIGURE A7 Labelled diagram of $[NiL^{15}(NCS)_2]$.

TABLE A7.1 Fractional atomic coordinates and thermal parameters ($Å^2$) for $[NiL^{15}(NCS)_2]$

| Atom | x | y | z | $U_{iso}$ or $U_{eq}$ |
|---|---|---|---|---|
| Ni | 0.00000 | 0.18383(21) | 0.25000 | 0.0406(15) |
| N(1) | 0.1436(7) | 0.1731(10) | 0.3155(6) | 0.055(8) |
| C(1) | 0.2192(9) | 0.1315(12) | 0.3351(8) | 0.046(9) |
| S(1) | 0.3222(2) | 0.0745(4) | 0.3641(3) | 0.080(3) |
| N(1a) | 0.0224(6) | 0.3267(9) | 0.1636(6) | 0.051(6) |
| N(2a) | 0.0109(6) | 0.0262(8) | 0.1622(6) | 0.041(6) |
| C(1a) | 0.0312(8) | -0.0955(12) | 0.2203(9) | 0.063(4) |
| C(2a) | 0.0731(8) | 0.0492(12) | 0.1110(8) | 0.054(4) |
| C(3a) | 0.1414(9) | -0.0466(13) | 0.1041(9) | 0.068(4) |
| C(4a) | 0.1969(9) | -0.0181(13) | 0.0504(9) | 0.065(4) |
| C(5a) | 0.1862(9) | 0.0962(14) | 0.0023(9) | 0.069(4) |
| C(6a) | 0.1194(8) | 0.1944(13) | 0.0073(8) | 0.063(4) |
| C(7a) | 0.0622(8) | 0.1674(11) | 0.0625(8) | 0.047(3) |
| C(8a) | -0.0030(9) | 0.2694(12) | 0.0695(9) | 0.057(4) |
| C(9a) | -0.0366(9) | 0.4484(13) | 0.1630(9) | 0.064(4) |
| C(10a) | 0.0000 | 0.5217(19) | 0.2500 | 0.066(6) |

TABLE A7.2 Fractional atomic coordinates for the found hydrogen atoms for $[NiL^{15}(NCS)_2]$

| Atom | x | y | z |
|---|---|---|---|
| H(3a) | 0.1512 | -0.1357 | 0.1397 |
| H(4a) | 0.2463 | -0.0858 | 0.0482 |
| H(5a) | 0.2268 | 0.1102 | -0.0419 |
| H(6a) | 0.1155 | 0.2846 | -0.0280 |
| H(8a) | 0.5742 | 0.2688 | 0.9428 |
| H(8b) | 0.4988 | 0.1640 | 0.9611 |
| H(9a) | 0.5925 | 0.0970 | 0.8455 |
| H(9b) | 0.5446 | 0.0211 | 0.9030 |
| H(10a) | 0.5468 | -0.0756 | 0.7470 |
| H(1e) | 0.0946 | 0.3551 | 0.1874 |
| H(2e) | -0.0532 | 0.0156 | 0.1060 |

TABLE A7.3 Anisotropic thermal parameters ($Å^2$) for $[NiL^{15}(NCS)_2]$

| Atom | $U_{11}$ | $U_{22}$ | $U_{33}$ | $U_{23}$ | $U_{13}$ | $U_{12}$ |
|---|---|---|---|---|---|---|
| Ni | 0.042(1) | 0.037(1) | 0.042(1) | 0.000(1) | 0.013(1) | 0.000(1) |
| N(1) | 0.061(8) | 0.058(8) | 0.047(7) | -0.002(6) | 0.010(6) | -0.002(7) |
| C(1) | 0.050(9) | 0.043(8) | 0.045(9) | -0.008(7) | 0.019(7) | -0.004(7) |
| S(1) | 0.052(2) | 0.093(3) | 0.097(3) | -0.008(3) | 0.026(2) | 0.011(2) |
| N(1a) | 0.065(7) | 0.044(6) | 0.043(6) | -0.004(6) | 0.024(5) | 0.011(6) |
| N(2a) | 0.045(6) | 0.038(6) | 0.041(6) | 0.000(5) | 0.017(5) | 0.004(5) |

TABLE A7.4 Bond lengths (Å) for [NiL$^{15}$(NCS)$_2$]

| | | | | | |
|---|---|---|---|---|---|
| Ni | -N(1) | 2.093(10) | Ni | -N(1a) | 2.075(10) |
| Ni | -N(2a) | 2.138(9) | N(1) | -C(1) | 1.170(17) |
| C(1) | -S(1) | 1.593(14) | N(1a) | -C(8a) | 1.503(16) |
| N(1a) | -C(9a) | 1.522(16) | N(2a) | -C(1a) | 1.498(15) |
| N(2a) | -C(2a) | 1.441(18) | C(1a) | -C(1a) | 1.52(3) |
| C(2a) | -C(3a) | 1.450(19) | C(2a) | -C(7a) | 1.394(17) |
| C(3a) | -C(4a) | 1.397(22) | C(4a) | -C(5a) | 1.357(19) |
| C(5a) | -C(6a) | 1.440(20) | C(6a) | -C(7a) | 1.434(20) |
| C(7a) | -C(8a) | 1.459(18) | C(9a) | -C(10a) | 1.483(16) |

TABLE A7.5 Bond angles (°) for [NiL$^{15}$(NCS)$_2$]

| | | | | | | | |
|---|---|---|---|---|---|---|---|
| N(1a) | -Ni | -N(1) | 89.2(4) | N(2a) | -Ni | -N(1) | 89.3(4) |
| N(2a) | -Ni | -N(1a) | 92.5(4) | C(1) | -N(1) | -Ni | 158.4(9) |
| S(1) | -C(1) | -N(1) | 179(1) | C(8a) | -N(1a) | -Ni | 108.5(7) |
| C(9a) | -N(1a) | -Ni | 110.3(8) | C(9a) | -N(1a) | -C(8a) | 109.9(8) |
| N(1a) | -Ni | -N(1a) | 91.7(5) | C(1a) | -N(2a) | -Ni | 105.7(7) |
| C(2a) | -N(2a) | -Ni | 115.7(7) | C(2a) | -N(2a) | -C(1a) | 114.9(9) |
| N(2a) | -Ni | -N(2a) | 83.7(5) | C(3a) | -C(2a) | -N(2a) | 123(1) |
| C(7a) | -C(2a) | -N(2a) | 117(1) | C(7a) | -C(2a) | -C(3a) | 120(1) |
| C(4a) | -C(3a) | -C(2a) | 120(1) | C(5a) | -C(4a) | -C(3a) | 121(1) |
| C(6a) | -C(5a) | -C(4a) | 121(1) | C(7a) | -C(6a) | -C(5a) | 118(1) |
| C(6a) | -C(7a) | -C(2a) | 120(1) | C(8a) | -C(7a) | -C(2a) | 122(1) |
| C(8a) | -C(7a) | -C(6a) | 118(1) | C(7a) | -C(8a) | -N(1a) | 112.2(9) |
| C(10a) | -C(9a) | -N(1a) | 110.6(9) | C(9a) | -C(10a) | -C(9a) | 120(2) |

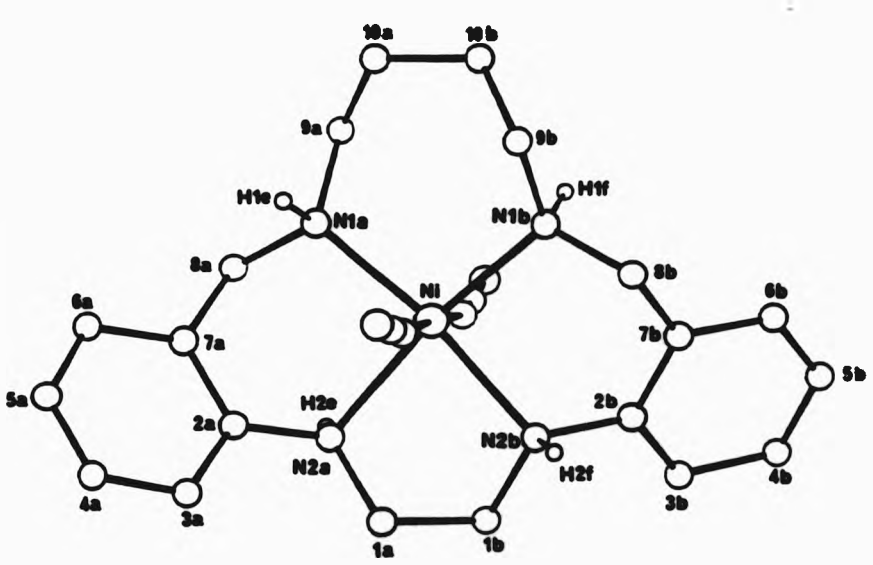


FIGURE A8 Labelled diagram of $[NiL^{16}(NCS)_2]$.

TABLE A8.1 Fractional atomic coordinates and thermal parameters (Å2) for $[NiL^{16}(NCS)_2]$

| Atom | x | y | z | $U_{iso}$ or $U_{eq}$ |
|---|---|---|---|---|
| Ni | 0.2501(1) | 0.1840(2) | 0.1839(2) | 0.052(1) |
| S(1) | 0.1799(3) | 0.5443(4) | -0.1350(5) | 0.109(3) |
| S(2) | 0.3208(3) | -0.1357(5) | 0.5440(4) | 0.107(3) |
| N(1) | 0.2267(8) | 0.3252(11) | 0.0363(12) | 0.072(7) |
| N(2) | 0.2727(8) | 0.0321(11) | 0.3272(11) | 0.070(7) |
| C(1) | 0.2084(8) | 0.4141(12) | -0.0338(13) | 0.055(8) |
| C(2) | 0.2923(8) | -0.0373(13) | 0.4162(13) | 0.059(8) |
| N(2a) | 0.1482(6) | 0.0377(9) | 0.0707(9) | 0.053(2) |
| N(1a) | 0.1324(7) | 0.2823(10) | 0.3062(11) | 0.072(3) |
| C(1a) | 0.2091(8) | -0.0755(11) | -0.0047(13) | 0.062(3) |
| C(2a) | 0.0702(8) | -0.0137(12) | 0.1593(12) | 0.061(3) |
| C(3a) | 0.0498(9) | -0.1573(14) | 0.1634(14) | 0.078(4) |
| C(4a) | -0.0304(10) | -0.1988(16) | 0.2469(15) | 0.088(4) |
| C(5a) | -0.0824(11) | -0.0957(15) | 0.3195(16) | 0.094(4) |
| C(6a) | -0.0602(10) | 0.0445(15) | 0.3179(15) | 0.085(4) |
| C(7a) | 0.0153(9) | 0.0925(13) | 0.2373(13) | 0.066(3) |
| C(8a) | 0.0355(9) | 0.2401(12) | 0.2377(14) | 0.074(4) |
| C(9a) | 0.1401(11) | 0.4379(15) | 0.3441(16) | 0.100(5) |
| C(10a) | 0.1971(13) | 0.4787(20) | 0.4798(20) | 0.125(6) |
| N(2b) | 0.3528(6) | 0.0715(9) | 0.0362(9) | 0.053(2) |
| N(1b) | 0.3663(7) | 0.3081(10) | 0.2804(10) | 0.067(3) |
| C(1b) | 0.2917(8) | -0.0027(12) | -0.0731(12) | 0.064(3) |
| C(2b) | 0.4303(8) | 0.1562(12) | -0.0133(13) | 0.062(3) |
| C(3b) | 0.4521(9) | 0.1609(13) | -0.1582(14) | 0.076(4) |
| C(4b) | 0.5295(10) | 0.2444(14) | -0.1961(17) | 0.088(4) |

TABLE A8.1 continued

| | | | | |
|---|---|---|---|---|
| C(5b) | 0.5810(11) | 0.3199(15) | -0.0967(17) | 0.096(4) |
| C(6b) | 0.5624(10) | 0.3252(15) | 0.0426(16) | 0.087(4) |
| C(7b) | 0.4850(9) | 0.2379(13) | 0.0904(14) | 0.072(4) |
| C(8b) | 0.4609(9) | 0.2364(13) | 0.2449(13) | 0.074(4) |
| C(9b) | 0.3612(11) | 0.3464(15) | 0.4406(16) | 0.097(5) |
| C(10b) | 0.3064(12) | 0.4764(17) | 0.4788(20) | 0.117(6) |

TABLE A8.2 Fractional atomic coordinates for the found hydrogen atoms for $[NiL^{16}(NCS)_2]$

| Atom | x | y | z | |
|---|---|---|---|---|
| H(2e) | 0.10345 | 0.08913 | -0.00506 | 10.0800 |
| H(1e) | 0.13772 | 0.23944 | 0.41098 | 10.0800 |
| H(2f) | 0.38291 | 0.00820 | 0.11299 | 10.0800 |
| H(1f) | 0.37862 | 0.39671 | 0.24952 | 10.0800 |

TABLE A8.3 Anisotropic thermal parameters (Å2) for $[NiL^{16}(NCS)_2]$

| Atom | $U_{11}$ | $U_{22}$ | $U_{33}$ | $U_{23}$ | $U_{13}$ | $U_{12}$ |
|---|---|---|---|---|---|---|
| Ni | 0.046(1) | 0.063(1) | 0.046(1) | 0.007(1) | -0.010(1) | 0.008(1) |
| S(1) | 0.151(4) | 0.080(3) | 0.096(3) | 0.029(2) | -0.046(3) | 0.001(3) |
| S(2) | 0.143(4) | 0.114(3) | 0.065(2) | 0.033(2) | -0.001(2) | 0.041(3) |
| N(1) | 0.085(8) | 0.049(6) | 0.082(8) | 0.018(6) | -0.009(6) | 0.008(6) |
| N(2) | 0.080(7) | 0.069(7) | 0.062(7) | 0.018(6) | -0.016(6) | 0.006(6) |
| C(1) | 0.059(8) | 0.037(7) | 0.068(8) | -0.004(6) | -0.004(6) | -0.006(6) |
| C(2) | 0.054(8) | 0.069(9) | 0.055(8) | 0.005(7) | 0.003(6) | 0.013(6) |

TABLE A8.4 Bond lengths (Å) for $[NiL^{16}(NCS)_2]$

| | | | | | |
|---|---|---|---|---|---|
| Ni | -N(1) | 2.010(11) | Ni | -N(2) | 2.054(11) |
| Ni | -N(2a) | 2.168(8) | Ni | -N(1a) | 2.136(10) |
| Ni | -N(2b) | 2.179(8) | Ni | -N(1b) | 2.125(9) |
| S(1) | -C(1) | 1.646(13) | S(2) | -C(2) | 1.611(13) |
| N(1) | -C(1) | 1.127(16) | N(2) | -C(2) | 1.126(17) |
| N(2a) | -C(1a) | 1.477(13) | N(2a) | -C(2a) | 1.464(15) |
| N(2a) | -H(2e) | 1.072(9) | N(1a) | -C(8a) | 1.505(16) |
| N(1a) | -C(9a) | 1.478(17) | N(1a) | -H(1e) | 1.090(10) |
| C(1a) | -C(1b) | 1.498(16) | C(2a) | -C(3a) | 1.381(17) |
| C(2a) | -C(7a) | 1.400(16) | C(3a) | -C(4a) | 1.426(19) |
| C(4a) | -C(5a) | 1.335(20) | C(5a) | -C(6a) | 1.353(20) |
| C(6a) | -C(7a) | 1.382(19) | C(7a) | -C(8a) | 1.414(17) |
| C(9a) | -C(10a) | 1.506(23) | C(10a) | -C(10b) | 1.491(24) |
| N(2b) | -C(1b) | 1.450(14) | N(2b) | -C(2b) | 1.431(15) |
| N(2b) | -H(2f) | 1.047(9) | N(1b) | -C(8b) | 1.476(15) |
| N(1b) | -C(9b) | 1.514(17) | N(1b) | -H(1f) | 0.920(10) |
| C(2b) | -C(3b) | 1.394(18) | C(2b) | -C(7b) | 1.399(17) |
| C(3b) | -C(4b) | 1.386(19) | C(4b) | -C(5b) | 1.322(20) |
| C(5b) | -C(6b) | 1.326(22) | C(6b) | -C(7b) | 1.439(19) |
| C(7b) | -C(8b) | 1.486(18) | C(9b) | -C(10b) | 1.443(21) |

TABLE A8.5 Bond angles (°) for $[NiL^{16}(NCS)_2]$

| | | | | | | | |
|---|---|---|---|---|---|---|---|
| N(2) | -Ni | -N(1) | 177.3(4) | N(2a) | -Ni | -N(1) | 89.9(4) |
| N(2a) | -Ni | -N(2) | 87.8(4) | N(1a) | -Ni | -N(1) | 88.8(4) |
| N(1a) | -Ni | -N(2) | 92.6(4) | N(1a) | -Ni | -N(2a) | 90.4(3) |
| N(2b) | -Ni | -N(1) | 88.3(4) | N(2b) | -Ni | -N(2) | 90.0(4) |
| N(2b) | -Ni | -N(2a) | 81.4(3) | N(2b) | -Ni | -N(1a) | 171.3(4) |
| N(1b) | -Ni | -N(1) | 91.8(4) | N(1b) | -Ni | -N(2) | 90.3(4) |
| N(1b) | -Ni | -N(2a) | 171.6(3) | N(1b) | -Ni | -N(1a) | 97.9(4) |
| N(1b) | -Ni | -N(2b) | 90.4(3) | C(1) | -N(1) | -Ni | 172(1) |
| C(2) | -N(2) | -Ni | 171(1) | N(1) | -C(1) | -S(1) | 179(1) |
| N(2) | -C(2) | -S(2) | 179.7(7) | C(1a) | -N(2a) | -Ni | 106.0(6) |
| C(2a) | -N(2a) | -Ni | 114.9(6) | C(2a) | -N(2a) | -C(1a) | 115.1(8) |
| H(2e) | -N(2a) | -Ni | 112.3(6) | H(2e) | -N(2a) | -C(1a) | 110.0(8) |
| H(2e) | -N(2a) | -C(2a) | 98.6(8) | C(8a) | -N(1a) | -Ni | 110.1(7) |
| C(9a) | -N(1a) | -Ni | 116.3(8) | C(9a) | -N(1a) | -C(8a) | 113(1) |
| H(1e) | -N(1a) | -Ni | 105.4(6) | H(1e) | -N(1a) | -C(8a) | 109.1(9) |
| H(1e) | -N(1a) | -C(9a) | 102.1(9) | C(1b) | -C(1a) | -N(2a) | 107.1(9) |
| C(3a) | -C(2a) | -N(2a) | 123(1) | C(7a) | -C(2a) | -N(2a) | 116(1) |
| C(7a) | -C(2a) | -C(3a) | 122(1) | C(4a) | -C(3a) | -C(2a) | 119(1) |
| C(5a) | -C(4a) | -C(3a) | 118(1) | C(6a) | -C(5a) | -C(4a) | 122(1) |
| C(7a) | -C(6a) | -C(5a) | 123(1) | C(6a) | -C(7a) | -C(2a) | 116(1) |
| C(8a) | -C(7a) | -C(2a) | 123(1) | C(8a) | -C(7a) | -C(6a) | 121(1) |
| C(7a) | -C(8a) | -N(1a) | 114(1) | C(10a) | -C(9a) | -N(1a) | 115(1) |
| C(10b) | -C(10a) | -C(9a) | 120(1) | C(1b) | -N(2b) | -Ni | 104.9(6) |
| C(2b) | -N(2b) | -Ni | 115.7(6) | C(2b) | -N(2b) | -C(1b) | 116.6(9) |
| H(2f) | -N(2b) | -Ni | 94.7(5) | H(2f) | -N(2b) | -C(1b) | 115.7(8) |

TABLE A8.5 continued

| | | | |
|---|---|---|---|
| H(2f) -N(2b) -C(2b) | 107.4(8) | C(8b) -N(1b) -N1 | 109.4(7) |
| C(9b) -N(1b) -N1 | 117.2(8) | C(9b) -N(1b) -C(8b) | 110(1) |
| H(1f) -N(1b) -N1 | 119.3(8) | H(1f) -N(1b) -C(8b) | 99.5(9) |
| H(1f) -N(1b) -C(9b) | 100.0(9) | N(2b) -C(1b) -C(1a) | 110.1(9) |
| C(3b) -C(2b) -N(2b) | 123(1) | C(7b) -C(2b) -N(2b) | 117(1) |
| C(7b) -C(2b) -C(3b) | 120(1) | C(4b) -C(3b) -C(2b) | 119(1) |
| C(5b) -C(4b) -C(3b) | 121(1) | C(6b) -C(5b) -C(4b) | 124(1) |
| C(7b) -C(6b) -C(5b) | 118(1) | C(6b) -C(7b) -C(2b) | 118(1) |
| C(8b) -C(7b) -C(2b) | 120(1) | C(8b) -C(7b) -C(6b) | 122(1) |
| C(7b) -C(8b) -N(1b) | 112(1) | C(10b)-C(9b) -N(1b) | 113(1) |
| C(9b) -C(10b)-C(10a) | 122(1) | | |

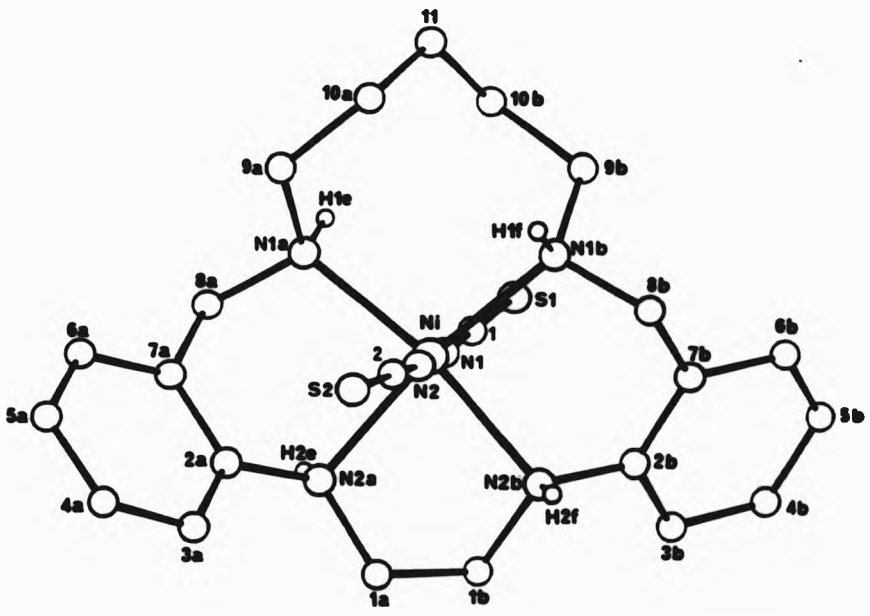


FIGURE A9 Labelled diagram of $[NiL^{17}(NCS)_2]$.

TABLE A9.1 Fractional atomic coordinates and thermal parameters ($Å^2$) for $[NiL^{17}(NCS)_2]$

| Atom | x | y | z | $U_{iso}$ or $U_{eq}$ |
|---|---|---|---|---|
| Ni | -0.24615(5) | 0.41324(9) | -0.07968(5) | 0.0414(5) |
| S(1) | -0.1956(2) | -0.0507(3) | 0.0838(2) | 0.138(2) |
| S(2) | -0.3026(1) | -0.0946(2) | -0.2306(1) | 0.064(1) |
| N(1) | -0.2308(3) | 0.1848(6) | -0.0309(3) | 0.056(4) |
| N(2) | -0.2568(4) | 0.6377(6) | -0.1283(3) | 0.052(4) |
| N(2b) | -0.1148(3) | 0.3887(6) | -0.0574(3) | 0.056(4) |
| N(2a) | -0.2715(3) | 0.3180(6) | -0.1975(3) | 0.051(3) |
| N(1b) | -0.2022(3) | 0.5327(6) | 0.0351(3) | 0.041(3) |
| N(1a) | -0.3776(3) | 0.3822(6) | -0.1138(3) | 0.046(3) |
| C(1) | -0.2161(4) | 0.0864(9) | 0.0158(4) | 0.058(4) |
| C(2) | -0.2753(4) | -0.2515(8) | -0.1690(4) | 0.041(4) |
| C(1a) | -0.1926(4) | 0.3349(9) | -0.2032(4) | 0.067(5) |
| C(2a) | -0.3472(5) | 0.3847(7) | -0.2661(4) | 0.051(4) |
| C(3a) | -0.3467(5) | 0.4642(9) | -0.3305(4) | 0.070(5) |
| C(4a) | -0.4231(7) | 0.5275(10) | -0.3923(4) | 0.078(6) |
| C(5a) | -0.4970(7) | 0.5076(10) | -0.3897(5) | 0.075(6) |
| C(6a) | -0.4977(5) | 0.4279(9) | -0.3245(4) | 0.062(5) |
| C(7a) | -0.4222(5) | 0.3667(7) | -0.2613(4) | 0.049(4) |
| C(8a) | -0.4228(4) | 0.2868(8) | -0.1900(4) | 0.050(4) |
| C(9a) | -0.4326(4) | 0.5188(8) | -0.1151(4) | 0.057(4) |
| C(10a) | -0.3992(5) | 0.6142(9) | -0.0379(4) | 0.067(5) |
| C(1b) | -0.1196(4) | 0.2818(8) | -0.1221(4) | 0.067(5) |
| C(2b) | -0.0532(4) | 0.3505(8) | 0.0248(4) | 0.053(4) |
| C(3b) | 0.0031(5) | 0.2214(9) | 0.0433(5) | 0.069(5) |
| C(4b) | 0.0611(5) | 0.1918(10) | 0.1246(6) | 0.077(6) |

TABLE A9.1 continued

| | | | | |
|---|---|---|---|---|
| C(5b) | 0.0638(5) | 0.2862(11) | 0.1866(6) | 0.073(6) |
| C(6b) | 0.0074(4) | 0.4137(10) | 0.1687(4) | 0.060(5) |
| C(7b) | -0.0519(4) | 0.4452(8) | 0.0873(4) | 0.053(4) |
| C(8b) | -0.1126(4) | 0.5850(8) | 0.0672(4) | 0.047(4) |
| C(9b) | -0.2143(4) | 0.4699(9) | 0.1040(4) | 0.055(4) |
| C(10b) | -0.3039(4) | 0.4119(9) | 0.0795(4) | 0.056(4) |
| C(11) | -0.3749(5) | 0.5362(9) | 0.0435(4) | 0.067(5) |

TABLE A9.2 Fractional atomic coordinates for the found hydrogen atoms for $[NiL^{17}(NCS)_2]$

| Atom | x | y | z |
|---|---|---|---|
| H(2f) | -0.09440 | 0.52380 | -0.05790 |
| H(1f) | -0.22970 | 0.65530 | 0.01540 |
| H(2e) | -0.28920 | 0.19370 | -0.19020 |
| H(1e) | -0.37950 | 0.33020 | -0.05020 |

TABLE A9.3 Anisotropic thermal parameters ($Å^2$) for [NiL$^{17}$(NCS)$_2$]

| Atom | $U_{11}$ | $U_{22}$ | $U_{33}$ | $U_{23}$ | $U_{13}$ | $U_{12}$ |
|---|---|---|---|---|---|---|
| Ni | 0.0473(5) | 0.0332(4) | 0.0436(5) | 0.0009(4) | 0.0219(4) | -0.0007(5) |
| S(1) | 0.225(3) | 0.066(1) | 0.122(2) | 0.044(1) | 0.118(2) | 0.052(2) |
| S(2) | 0.090(1) | 0.044(1) | 0.059(1) | 0.013(1) | 0.024(1) | 0.008(1) |
| N(1) | 0.061(4) | 0.042(3) | 0.064(4) | 0.004(3) | 0.032(3) | -0.006(3) |
| N(2) | 0.074(4) | 0.037(3) | 0.045(3) | 0.006(3) | 0.029(3) | -0.003(3) |
| N(2b) | 0.055(4) | 0.045(3) | 0.068(4) | -0.011(3) | 0.035(3) | -0.006(3) |
| N(2a) | 0.056(4) | 0.043(3) | 0.054(3) | -0.008(3) | 0.031(3) | -0.013(3) |
| N(1b) | 0.046(3) | 0.039(3) | 0.038(3) | 0.000(2) | 0.018(3) | 0.000(2) |
| N(1a) | 0.050(3) | 0.045(3) | 0.045(3) | -0.005(3) | 0.025(3) | -0.001(3) |
| C(1) | 0.070(5) | 0.040(4) | 0.064(4) | 0.000(4) | 0.039(4) | 0.006(4) |
| C(2) | 0.035(4) | 0.047(4) | 0.041(4) | -0.011(3) | 0.014(3) | -0.006(3) |
| C(1a) | 0.068(5) | 0.068(5) | 0.065(5) | -0.019(4) | 0.041(4) | -0.016(4) |
| C(2a) | 0.065(5) | 0.040(4) | 0.047(4) | -0.009(3) | 0.026(4) | -0.010(4) |
| C(3a) | 0.095(6) | 0.066(5) | 0.048(4) | -0.016(4) | 0.039(5) | -0.021(5) |
| C(4a) | 0.133(9) | 0.062(5) | 0.039(5) | -0.005(4) | 0.035(6) | -0.010(6) |

TABLE A9.3 continued

| | | | | | | |
|---|---|---|---|---|---|---|
| C(5a) | 0.106(8) | 0.064(5) | 0.055(5) | -0.005(4) | 0.027(5) | 0.016(5) |
| C(6a) | 0.079(6) | 0.058(5) | 0.050(4) | -0.011(4) | 0.020(4) | 0.007(4) |
| C(7a) | 0.062(5) | 0.036(4) | 0.049(4) | -0.011(3) | 0.021(4) | -0.007(3) |
| C(8a) | 0.046(4) | 0.049(4) | 0.055(4) | -0.002(3) | 0.023(3) | -0.005(3) |
| C(9a) | 0.053(5) | 0.065(5) | 0.053(4) | 0.002(4) | 0.022(4) | 0.016(4) |
| C(10a) | 0.068(5) | 0.078(5) | 0.054(4) | 0.002(4) | 0.029(4) | 0.039(4) |
| C(1b) | 0.055(5) | 0.062(5) | 0.083(5) | -0.033(4) | 0.042(4) | -0.013(4) |
| C(2b) | 0.045(4) | 0.048(4) | 0.066(5) | -0.006(4) | 0.022(4) | -0.007(4) |
| C(3b) | 0.053(5) | 0.046(5) | 0.106(6) | -0.001(4) | 0.030(5) | 0.002(4) |
| C(4b) | 0.056(6) | 0.053(5) | 0.124(8) | 0.011(5) | 0.025(6) | 0.011(4) |
| C(5b) | 0.051(5) | 0.080(6) | 0.088(6) | 0.036(5) | 0.006(5) | 0.011(5) |
| C(6b) | 0.049(4) | 0.072(5) | 0.059(4) | 0.007(4) | 0.012(4) | -0.004(5) |
| C(7b) | 0.044(4) | 0.050(4) | 0.065(5) | 0.005(4) | 0.021(4) | -0.004(3) |
| C(8b) | 0.046(4) | 0.046(4) | 0.050(4) | -0.011(3) | 0.022(3) | -0.002(4) |
| C(9b) | 0.052(4) | 0.069(5) | 0.045(4) | 0.006(3) | 0.022(4) | 0.000(4) |
| C(10b) | 0.058(5) | 0.069(4) | 0.041(4) | 0.012(4) | 0.027(3) | 0.006(4) |
| C(11) | 0.059(5) | 0.093(6) | 0.048(4) | 0.009(4) | 0.025(4) | 0.025(4) |

TABLE A9.4 Bond lengths (Å) for $[NiL^{17}(NCS)_2]$

| | | | | | |
|---|---|---|---|---|---|
| Ni | -N(1) | 2.072(6) | Ni | -N(2) | 2.049(5) |
| Ni | -N(2b) | 2.200(6) | Ni | -N(2a) | 2.166(6) |
| Ni | -N(1b) | 2.138(5) | Ni | -N(1a) | 2.147(6) |
| S(1) | -C(1) | 1.613(8) | S(2) | -C(2) | 1.653(7) |
| N(1) | -C(1) | 1.131(9) | N(2) | -C(2) | 1.139(8) |
| N(2b) | -C(1b) | 1.467(10) | N(2b) | -C(2b) | 1.431(8) |
| N(2b) | -H(2f) | 1.186(5) | N(2a) | -C(1a) | 1.478(11) |
| N(2a) | -C(2a) | 1.459(7) | N(2a) | -H(2e) | 1.112(5) |
| N(1b) | -C(8b) | 1.489(8) | N(1b) | -C(9b) | 1.493(10) |
| N(1b) | -H(1f) | 1.118(5) | N(1a) | -C(8a) | 1.483(7) |
| N(1a) | -C(9a) | 1.501(9) | N(1a) | -H(1e) | 1.277(6) |
| C(1a) | -C(1b) | 1.517(8) | C(2a) | -C(3a) | 1.374(12) |
| C(2a) | -C(7a) | 1.398(13) | C(3a) | -C(4a) | 1.405(11) |
| C(4a) | -C(5a) | 1.360(18) | C(5a) | -C(6a) | 1.390(13) |
| C(6a) | -C(7a) | 1.400(9) | C(7a) | -C(8a) | 1.490(11) |
| C(9a) | -C(10a) | 1.495(10) | C(10a) | -C(11) | 1.508(10) |
| C(2b) | -C(3b) | 1.403(10) | C(2b) | -C(7b) | 1.397(12) |
| C(3b) | -C(4b) | 1.388(12) | C(4b) | -C(5b) | 1.378(15) |
| C(5b) | -C(6b) | 1.394(12) | C(6b) | -C(7b) | 1.398(9) |
| C(7b) | -C(8b) | 1.516(9) | C(9b) | -C(10b) | 1.526(10) |
| C(10b) | -C(11) | 1.529(10) | | | |

TABLE A9.5 Bond angles (°) for $[Ni L^{17}(NCS)_2]$

| | | | | | | | |
|---|---|---|---|---|---|---|---|
| N(2) | -Ni | -N(1) | 177.6(3) | N(2b) | -Ni | -N(1) | 85.7(2) |
| N(2b) | -Ni | -N(2) | 91.9(2) | N(2a) | -Ni | -N(1) | 91.5(2) |
| N(2a) | -Ni | -N(2) | 87.6(2) | N(2a) | -Ni | -N(2b) | 81.1(2) |
| N(1b) | -Ni | -N(1) | 94.7(2) | N(1b) | -Ni | -N(2) | 85.8(2) |
| N(1b) | -Ni | -N(2b) | 90.3(2) | N(1b) | -Ni | -N(2a) | 168.9(2) |
| N(1a) | -Ni | -N(1) | 85.2(2) | N(1a) | -Ni | -N(2) | 97.0(2) |
| N(1a) | -Ni | -N(2b) | 166.5(2) | N(1a) | -Ni | -N(2a) | 89.2(2) |
| N(1a) | -Ni | -N(1b) | 100.4(2) | C(1) | -N(1) | -Ni | 159.6(6) |
| C(2) | -N(2) | -Ni | 166.3(4) | C(1b) | -N(2b) | -Ni | 105.3(4) |
| C(2b) | -N(2b) | -Ni | 115.7(6) | C(2b) | -N(2b) | -C(1b) | 117.0(5) |
| H(2f) | -N(2b) | -Ni | 102.6(3) | H(2f) | -N(2b) | -C(1b) | 117.9(6) |
| H(2f) | -N(2b) | -C(2b) | 97.9(4) | C(1a) | -N(2a) | -Ni | 107.0(4) |
| C(2a) | -N(2a) | -Ni | 113.8(5) | C(2a) | -N(2a) | -C(1a) | 115.2(6) |
| H(2e) | -N(2a) | -Ni | 98.8(4) | H(2e) | -N(2a) | -C(1a) | 115.9(5) |
| H(2e) | -N(2a) | -C(2a) | 105.2(5) | C(8b) | -N(1b) | -Ni | 110.5(5) |
| C(9b) | -N(1b) | -Ni | 123.9(4) | C(9b) | -N(1b) | -C(8b) | 109.3(4) |
| H(1f) | -N(1b) | -Ni | 101.8(3) | H(1f) | -N(1b) | -C(8b) | 95.0(4) |
| H(1f) | -N(1b) | -C(9b) | 112.4(5) | C(8a) | -N(1a) | -Ni | 111.7(5) |
| C(9a) | -N(1a) | -Ni | 122.4(4) | C(9a) | -N(1a) | -C(8a) | 109.7(4) |
| H(1e) | -N(1a) | -Ni | 106.2(2) | H(1e) | -N(1a) | -C(8a) | 117.3(5) |
| H(1e) | -N(1a) | -C(9a) | 87.9(5) | N(1) | -C(1) | -S(1) | 178.5(8) |
| N(2) | -C(2) | -S(2) | 178.1(6) | C(1b) | -C(1a) | -N(2a) | 107.5(7) |
| C(3a) | -C(2a) | -N(2a) | 123.8(8) | C(7a) | -C(2a) | -N(2a) | 115.2(7) |
| C(7a) | -C(2a) | -C(3a) | 121.0(6) | C(4a) | -C(3a) | -C(2a) | 119(1) |
| C(5a) | -C(4a) | -C(3a) | 120.7(9) | C(6a) | -C(5a) | -C(4a) | 120.4(7) |

TABLE A9.5 continued

| | | | |
|---|---|---|---|
| C(7a) -C(6a) -C(5a) | 119.9(9) | C(6a) -C(7a) -C(2a) | 118.9(7) |
| C(8a) -C(7a) -C(2a) | 121.4(5) | C(8a) -C(7a) -C(6a) | 119.7(8) |
| C(7a) -C(8a) -N(1a) | 112.2(5) | C(10a)-C(9a) -N(1a) | 115.5(5) |
| C(11) -C(10a)-C(9a) | 121.7(6) | C(1a) -C(1b) -N(2b) | 108.9(6) |
| C(3b) -C(2b) -N(2b) | 122.1(7) | C(7b) -C(2b) -N(2b) | 117.5(6) |
| C(7b) -C(2b) -C(3b) | 120.4(6) | C(4b) -C(3b) -C(2b) | 118.8(9) |
| C(5b) -C(4b) -C(3b) | 121.2(8) | C(6b) -C(5b) -C(4b) | 120.3(7) |
| C(7b) -C(6b) -C(5b) | 119.5(8) | C(6b) -C(7b) -C(2b) | 119.8(7) |
| C(8b) -C(7b) -C(2b) | 120.3(5) | C(8b) -C(7b) -C(6b) | 119.8(7) |
| C(7b) -C(8b) -N(1b) | 112.7(5) | C(10b)-C(9b) -N(1b) | 114.8(5) |
| C(11) -C(10b)-C(9b) | 117.1(6) | C(10b)-C(11) -C(10a) | 120.9(8) |

TITLE SYNTHESIS AND STRUCTURAL STUDIES OF SOME METAL COMPLEXES OF TETRAAZA MACROCYCLIC LIGANDS

AUTHOR Philip John BAILLIE

DEGREE Ph.D

AWARDING BODY University of North London

DATE 1993

THESIS NUMBER DX180675